

Predicting the flavour and SUSY flavour structure from Grand Unified Theories

Inauguraldissertation

zur

Erlangung der Würde eines Doktors der Philosophie

vorgelegt der

Philosophisch-Naturwissenschaftlichen Fakultät
der Universität Basel

von

Constantin Alexander Sluka

aus Österreich

Basel, 2016

Originaldokument gespeichert auf dem Dokumentenserver der Universität Basel
edoc.unibas.ch



Dieses Werk ist lizenziert unter einer Creative Commons Namensnennung - Weitergabe unter gleichen Bedingungen 4.0 International Lizenz

Genehmigt von der Philosophisch-Naturwissenschaftlichen Fakultät

auf Antrag von

Prof. Dr. Stefan Antusch, Prof. Dr. Borut Bajc

Basel, den 19.4.2016

Prof. Dr. Jörg Schibler
Dekan

Abstract

Grand Unified Theories (GUTs) offer an attractive framework for flavour models, since they feature relations between quarks and leptons. Combining them with Supersymmetry (SUSY) and flavour symmetries, we derive predictions for the flavour and SUSY flavour structure from various GUT models and discuss how the double missing partner mechanism (DMPM) solution to the doublet-triplet splitting problem can be combined with predictions for GUT scale quark-lepton Yukawa coupling relations.

We construct two predictive SUSY $SU(5)$ GUT models with an A_4 flavour symmetry, that feature realistic quark-lepton Yukawa coupling ratios and mixing angle relations. These GUT scale predictions arise after GUT symmetry breaking from a novel combination of group theoretical Clebsch-Gordan factors, and we carefully construct additional shaping symmetries and renormalisable messenger sectors to protect the models' predictions from dangerous corrections. The major difference between both models are their respective predictions of a normal and inverse neutrino mass ordering. We perform Markov Chain Monte Carlo analyses, fit to experimental data, and discuss how the models can be tested by present and future experiments.

To combine predictive GUT scale quark-lepton Yukawa coupling ratios with the DMPM in SUSY $SU(5)$, we introduce a second GUT breaking Higgs field in the adjoint representation. Two explicit flavour models with different predictions for the GUT scale Yukawa sector are presented, including shaping symmetries and renormalisable messenger sectors, and combined with the DMPM. We calculate the effective masses of the colour triplets mediating proton decay and find that they can be made sufficiently heavy.

In SUSY theories, the one-loop SUSY threshold corrections are of particular importance in investigating GUT scale quark-lepton mass relations and thus link a given GUT flavour model to the sparticle spectrum. We calculate the one-loop SUSY threshold corrections of the full MSSM Yukawa coupling matrices in the electroweak-unbroken phase and introduce a new software tool **SusyTC** as a major extension to the Mathematica package **REAP**. Finally we find predictions for the CMSSM parameters and sparticle masses from the GUT scale Yukawa coupling ratios used in the flavour models of this thesis.

This thesis is based on the author's work partly published in [1–5] conducted from April 2012 until December 2015 at the Department of Physics of the University of Basel, under the supervision of Prof. Dr. Stefan Antusch.

- [1] S. ANTUSCH, C. GROSS, V. MAURER, and C. SLUKA, $\theta_{13}^{PMNS} = \theta_C / \sqrt{2}$ from GUTs, *Nucl. Phys.* **B866**, 255 (2013), arXiv: 1205.1051.
- [2] S. ANTUSCH, C. GROSS, V. MAURER, and C. SLUKA, A flavour GUT model with $\theta_{13}^{PMNS} \simeq \theta_C / \sqrt{2}$, *Nucl. Phys.* **B877**, 772 (2013), arXiv: 1305.6612.
- [3] S. ANTUSCH, C. GROSS, V. MAURER, and C. SLUKA, Inverse neutrino mass hierarchy in a flavour GUT model, *Nucl. Phys.* **B879**, 19 (2014), arXiv: 1306.3984.
- [4] S. ANTUSCH, I. DE MEDEIROS VARZIELAS, V. MAURER, C. SLUKA, and M. SPINRATH, Towards predictive flavour models in SUSY $SU(5)$ GUTs with doublet-triplet splitting, *JHEP* **1409**, 141 (2014), arXiv: 1405.6962.
- [5] S. ANTUSCH and C. SLUKA, Predicting the Sparticle Spectrum from GUTs via SUSY Threshold Corrections with *SusyTC*, (2015), arXiv: 1512.06727.

Acknowledgements

The last four years have been an amazing time of my life, and I would like to say Thank You to all friends and collaborators who contributed to my great experience with professional advice and/or joint leisure activities.

Stefan Antusch has been a great thesis advisor, who encouraged and supported me in numerous discussions. With Vinzenz Maurer I had the luck to have an excellent programmer and researcher as collaborator, it was both very enjoyable and very efficient to work with him. It was also a pleasure to work with Christian Gross and Martin Spinrath. In particular I want to thank Martin for introducing me to Stefan and the exciting research field of flavour models. Ivo de Medeiros Varzielas not only was a great collaborator, his cheerfulness also made it very entertaining to work with him.

I learned a lot about GUTs and proton decay from discussion with Borut Bajc and his lectures at the ICTP, and I would like to thank him for agreeing on being member of my PhD committee.

My first contact with theoretical particle physics was as a summer student at CERN. For this fantastic opportunity I would like to thank Peter Girtler, Dietmar Kuhn, and Andreas Salzburger.

I also thank Eros Cazzato, David Emmanuel-Costa, Thomas Hahn, Sven Heinemeyer, Stefano Orani, and Sebastian Paßehr for useful discussions.

For many nice moments in and outside of the office I would like to thank all former and active members of the Antusch group: Stefan Antusch, Eros Cazzato, Francesco Cefala, Ivo de Medeiros Varzielas, Oliver Fischer, Christian Gross, Christian Hohl, Giti Khavari, Mansoor-ur-Rehman, Vinzenz Maurer, David Nolde, and Stefano Orani. It has always been a pleasure to spend time with you. I am grateful for the company of my friends: Christoph and Lukas, Christian, Dominik, and Liza, Daniel, Janine, Jessica, Karen, Milica, Phine, and Santiago, Nessie, Anna and Sonia. And for my amazing family: Alissa, Basti, Isi, Julia, and Sixi.

My parents Jasna and Wilhelm have encouraged my passion for science and exploration from the very first moment I was able to ask questions. I am deeply grateful for their constant support and love.

A special Thank You to Flo, who makes my life more beautiful.

Table of Contents

I	Introduction	1
II	Theoretical Framework	5
2	The Standard Model of Particle Physics	6
2.1	Gauge interactions and field content	6
2.2	The Brout-Englert-Higgs mechanism	8
2.3	Fermion masses and the CKM-Matrix	10
2.4	Open questions in the Standard Model	13
3	Massive neutrinos	17
3.1	Neutrino masses and the seesaw mechanisms	17
3.2	The PMNS-Matrix	19
3.3	Neutrino mass models & flavour model building	24
4	Grand Unified Theories	27
4.1	The Georgi-Glashow $SU(5)$ model	27
4.2	Proton decay in $SU(5)$	32
4.3	Pati-Salam unification and $SO(10)$	34
4.4	GUT scale Yukawa coupling ratios	36
5	Supersymmetry	39
5.1	The Wess-Zumino model	39
5.2	Superspace and Superfields	42
5.3	Supersymmetry breaking	48
5.4	The Minimal Supersymmetric Standard Model	52
5.5	Supersymmetric $SU(5)$ GUTs	57

III	SUSY Flavour GUT models	61
6	$\theta_{13}^{\text{PMNS}} \approx \theta_C \sin \theta_{23}^{\text{PMNS}}$ from GUTs	62
6.1	A numerical expression for $\theta_{13}^{\text{PMNS}}$ in terms of θ_C	62
6.2	Conditions for mixing angles	64
6.3	Conditions from relations between Y_d and Y_e	65
6.4	Corrections to $\theta_{13}^{\text{PMNS}} \approx \theta_C \sin \theta_{23}^{\text{PMNS}}$	69
6.5	The underlying neutrino mixing pattern in the light of $\theta_{13}^{\text{PMNS}} \approx \theta_C \sin \theta_{23}^{\text{PMNS}}$	73
7	A SUSY flavour GUT model with $\theta_{13}^{\text{PMNS}} \approx \theta_C \sin \theta_{23}^{\text{PMNS}}$	75
7.1	Outline of the model	75
7.2	The model	77
7.3	Flavon alignment	80
7.4	Phenomenology	82
8	A SUSY flavour GUT model with inverse neutrino mass ordering	90
8.1	Constructing an inverted neutrino hierarchy	90
8.2	The model	92
8.3	Flavon alignment	94
8.4	Phenomenology	96
IV	Doublet-Triplet splitting in SUSY Flavour GUT models	103
9	Towards predictive SUSY flavour $SU(5)$ models with DT splitting	104
9.1	The missing partner and double missing partner mechanisms	104
9.2	Combining predictive flavour GUT models and DMPM	108
9.3	Grand unification and the effective triplet mass	114
9.4	SUSY Flavour GUT models with DMPM	117
9.5	Proton Decay	126
V	Supersymmetric threshold corrections	131
10	Predicting the Sparticle Spectrum from GUTs with SusyTC	132
10.1	The REAP extension SusyTC	132
10.2	SUSY threshold corrections & numerical procedure	134
10.3	A brief introduction to SusyTC	140
10.4	The Sparticle Spectrum predicted from CG factors	141

VI	Summary	155
	Appendices	161
A	Brief review on group theory	162
	A.1 The special unitary group $SU(N)$	162
	A.2 The discrete group A_4	164
	A.3 Generalised CP transformations	166
B	Sparticle Mass and Mixing Matrices	169
C	Markov Chain Monte Carlo techniques	171
D	Appendices to the flavour GUT models	175
	D.1 Appendix to chapter 7	175
	D.2 Appendix to chapter 8	180
	D.3 Appendix to the first model of chapter 9	187
	D.4 Appendix to the second model of chapter 9	192
E	The β-functions in the seesaw type-I extension of the MSSM	195
	E.1 One-Loop β -functions	195
	E.2 Two-Loop β -functions	197
F	Self-energies and one-loop tadpoles including inter-generational mixing	208
G	SusyTC documentation	215
	Bibliography	223
	Curriculum Vitae	246

PART I

Introduction

CHAPTER 1

Introduction

The discovery of neutrino oscillations and thus of at least two non-zero neutrino mass eigenstates rendered the Standard Model (SM) of Particle Physics incomplete and was the first gaze on physics Beyond the Standard Model (BSM). Besides this apparent insufficiency of the SM, there are several other motivations for BSM physics.

For example, the SM lacks an explanation for the hierarchies between particle masses, which span a range of six orders of magnitude. Also the quark mixing angles differ by up to three orders of magnitudes. Taking neutrinos into consideration, one finds one small lepton mixing angle, while two lepton mixing angles are large and including the lightest non-vanishing neutrino mass, the range of particle masses covers twelve orders of magnitude, as illustrated in figure 1.1.

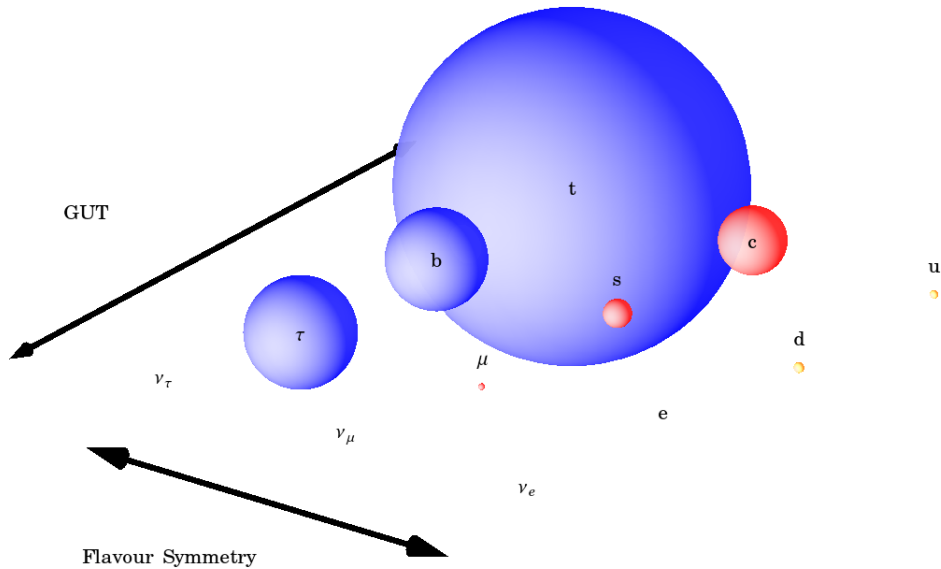


Figure 1.1: True to scale illustration of particle masses, where particles are oversimplified depicted as spheres of equal density and their masses scale with the third power of their radius. Of course, in fact elementary particles are point-like objects.

In the SM the particle masses and mixing angles are free parameters and the seesaw mechanisms explaining small neutrino masses also have to fix the lepton mixing angles by hand. The number of flavour related parameters and their striking hierarchies within and between different families constitutes the so called *flavour problem* of Particle Physics. One attractive solution is the idea of flavour symmetries, which can unify particles of different families. When a flavour symmetry is spontaneously broken, predictions for the Yukawa matrices emerge from vacuum expectation values (vevs) of dynamical fields and it is possible to explain the different flavour structures.

Another BSM concept towards a more fundamental theory of Elementary Particle Physics are Grand Unified Theories (GUTs). They unify the SM gauge group into a single simple gauge group at higher energies than those accessible to SM physics. And they unify SM fermions within a family into joint representations of the GUT gauge group. Thus they can make predictions for relations between e.g. quark and lepton masses of the same generation, making GUTs an attractive framework to address the flavour problem.

Two challenges arise when the SM is embedded into GUTs. Firstly, the SM gauge couplings do not unify and secondly too rapid proton decay mediated by heavy vector bosons is predicted. Both are avoided with the introduction of Supersymmetry (SUSY). With a relatively low mass scale of sparticles, the gauge couplings successfully unify and the mass of the additional vector bosons is high enough to suppress proton decay sufficiently. Additionally, low energy SUSY is a solution to the hierarchy problem by explaining a naturally low Electroweak scale and the lightest sparticle is a candidate for dark matter.

The focus of this thesis are *SUSY flavour GUT models*, which are BSM theories that combine the attractive ideas of SUSY, GUTs, and flavour symmetries. Particularly interesting subjects in SUSY flavour GUT models are the interdependencies between the various sectors of the models, as outlined in figure 1.2. Predictions obtained from the

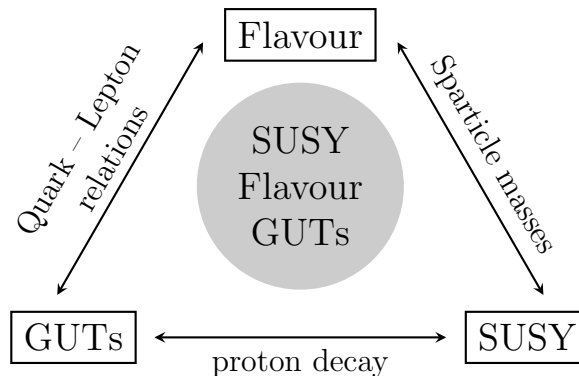


Figure 1.2: SUSY flavour GUT models feature an interplay between three “different” sectors of BSM physics.

(spontaneously broken) flavour symmetry are valid at the GUT scale. To test those predictions at lower energies the Renormalisation Group Equations (RGEs) have to be solved. Since, when heavy degrees of freedom are integrated out, SUSY and GUT breaking effects

play an important role in the precise solution of the RGEs, there is a variety of predictions emerging from SUSY, GUTs, and flavour symmetries which influence each other.

The presentation of the author's research is divided into three parts. In part III we focus on the construction of predictive SUSY flavour GUT models with realistic quark-lepton mass ratios and mixing angles relations, sketched as the left edge in the triangle of figure 1.2. In chapter 6 we present four simple conditions for unified models to predict the observed relation between the Cabibbo angle and the small 1-3 lepton mixing angle. These conditions are then realised in a SUSY flavour GUT model in chapter 7, where we carefully construct additional discrete symmetries and a renormalisable messenger sector to protect the model from dangerous effective operators. A second SUSY flavour GUT model, similar to the first but with an inverse neutrino mass ordering, is constructed in chapter 8. Both models are fitted to experimental data and we perform Markov Chain Monte Carlo analyses. Among others we predict the unmeasured neutrino CP phases and discuss how the models can be tested by future experiments.

Part IV discusses the problem of doublet-triplet splitting and the related question of proton decay in SUSY $SU(5)$, as shown as the lower edge of figure 1.2. We introduce a second GUT breaking Higgs field in the adjoint representation, which allows the adjoints to carry charges under additional discrete symmetries. We present two example models combining the double missing partner mechanism with viable GUT scale predictions for the quark-lepton Yukawa coupling ratios. We calculate the effective masses of the colour triplets mediating proton decay and find that in both models proton decay is sufficiently suppressed.

The final part V is focused on the important effects of SUSY threshold corrections on the investigation of flavour GUT models. The size of these corrections depends on the details of the SUSY sector and the sparticle masses, which we illustrate on the right edge of figure 1.2. We calculate the full one-loop SUSY threshold corrections to the MSSM Yukawa coupling matrices and introduce a new software tool `SusyTC` as an extension to the Mathematica package `REAP`. Finally we investigate the predictions of an example GUT model with realistic quark-lepton Yukawa coupling ratios for the CMSSM soft-breaking parameters and sparticle masses.

The appendices A and C contain brief reviews of group theory and Markov Chain Monte Carlo techniques used in this thesis, respectively. Appendices B, E, F, and G contain extensive formulae and equations used in chapter 10, as well as the documentation for `SusyTC`. Appendix D contains additional information for the flavour models of this thesis, such as details on additional symmetries and charges of the models' fields and the messenger sectors.

In the next part II the theoretical framework for the main parts of this thesis are reviewed and our notations and conventions are introduced. Chapter 2 introduces the SM, chapter 3 reviews massive neutrinos, in chapter 4 we discuss GUTs, and in chapter 5 SUSY is reviewed.

PART II

Theoretical Framework

CHAPTER 2

The Standard Model of Particle Physics

In the mid-20th century the effort to develop a thorough understanding of the various phenomena of Elementary Particle Physics led to the construction of the Standard Model (SM) of Particle Physics [6–9]. To its great successes belong the correct predictions of the neutral current (the existence of the Z^0 vector boson), the existence of the top quark, and the existence of a fundamental scalar boson as a result of the Brout-Englert-Higgs mechanism [10, 11], known as Higgs boson. Despite these major achievements, there are many motivations suggesting the SM is incomplete and expected to be embedded into a more fundamental theory.

This chapter is devoted to an introduction to the SM, setting the background formalism, notation, and conventions necessary for the remainder of this thesis. Finally some of the open questions in the SM are addressed, motivating physics Beyond the Standard Model (BSM) and the main part of this thesis.

2.1 Gauge interactions and field content

The SM is a chiral, renormalisable gauge quantum field theory with the gauge group given by $G_{\text{SM}} = SU(3)_C \times SU(2)_L \times U(1)_Y$, a direct product of the gauge group of Quantum Chromodynamics (QCD) $SU(3)_C$, where the C refers to *colour*, and of the Electroweak (EW) theory $SU(2)_L \times U(1)_Y$, with L for *left* and Y denoting hypercharge. Because of the local invariance under G_{SM} , massless spin one fields emerge, which are identified with the force carriers of the SM. These gauge bosons are named gluons (G_μ^a) for QCD, W_μ^a for $SU(2)_L$ and B_μ for $U(1)_Y$. Since $U(1)_Y$ is an Abelian group, B_μ does not carry hypercharge, whereas G_μ^a and W_μ^a transform in the adjoint representations of $SU(3)_C$ and $SU(2)_L$, respectively.¹

The matter fields of the SM are fermions with spin $\frac{1}{2}$. They split into quarks, which transform in the fundamental representation of $SU(3)_C$, and leptons, which are colour singlets. The left- and right-handed components of the SM fermions transform differently

¹A brief review on group theory can be found in Appendix A.

Gauge bosons			
	G_μ		$(\mathbf{8}, \mathbf{1})_0$
	W_μ		$(\mathbf{1}, \mathbf{3})_0$
	B_μ		$(\mathbf{1}, \mathbf{1})_0$
Matter fields			
$Q_1 = \begin{pmatrix} u_L \\ d_L \end{pmatrix}$	$Q_2 = \begin{pmatrix} c_L \\ s_L \end{pmatrix}$	$Q_3 = \begin{pmatrix} t_L \\ b_L \end{pmatrix}$	$(\mathbf{3}, \mathbf{2})_{\frac{1}{6}}$
u_R	c_R	t_R	$(\mathbf{3}, \mathbf{1})_{\frac{2}{3}}$
d_R	s_R	b_R	$(\mathbf{3}, \mathbf{1})_{-\frac{1}{3}}$
$L_1 = \begin{pmatrix} \nu_{eL} \\ e_L \end{pmatrix}$	$L_2 = \begin{pmatrix} \nu_{\mu L} \\ \mu_L \end{pmatrix}$	$L_3 = \begin{pmatrix} \nu_{\tau L} \\ \tau_L \end{pmatrix}$	$(\mathbf{1}, \mathbf{2})_{-\frac{1}{2}}$
e_R	μ_R	τ_R	$(\mathbf{1}, \mathbf{1})_{-1}$
Higgs field			
	ϕ		$(\mathbf{1}, \mathbf{2})_{\frac{1}{2}}$

Table 2.1: Field content of the SM with the corresponding G_{SM} representations and hypercharge Q_Y listed as $(SU(3)_C, SU(2)_L)_{Q_Y}$

under the SM gauge group: The left-handed fermions transform in the fundamental representation of $SU(2)_L$, while the right-handed fermions are $SU(2)_L$ singlets. The matter fields are thus an $SU(2)_L$ doublet Q containing the left-handed quark fields u_L and d_L , an $SU(2)_L$ doublet L containing the left-handed electron and neutrino, e_L and ν_L , respectively, the right-handed quark fields u_R and d_R , and a right-handed electron field e_R .² These particles appear in three copies, also called families, in nature, which have exactly identical couplings to the gauge bosons. The different quark and lepton species are denoted flavours.

Next to gauge bosons and fermions, the SM also contains a fundamental, complex spin 0 field. This so called Higgs field is an $SU(2)_L$ doublet and plays a crucial role in the Brout-Englert-Higgs mechanism, described in the next section. All fields of the SM are listed in table 2.1 together with their quantum numbers under G_{SM} . Using natural units $\hbar = c = 1$ and a mostly minus convention for the Minkowski metric

$$\eta_{\mu\nu} = \text{diag}(+1, -1, -1, -1), \quad (2.1)$$

the most general renormalisable Lagrange density with this field content is given by³:

$$\mathcal{L}_{\text{SM}} = -\frac{1}{4}G_{\mu\nu}^a G^{\mu\nu a} - \frac{g_3^2 \theta_{QCD}}{64\pi^2} \epsilon_{\mu\nu\lambda\rho} G^{\lambda\rho a} G^{\mu\nu a} - \frac{1}{4}W_{\mu\nu}^A W^{\mu\nu A} - \frac{1}{4}B_{\mu\nu} B^{\mu\nu}$$

²There are no right-handed neutrinos in the SM. We discuss the extension of the SM by right-handed neutrino fields in the next chapter.

³Note that we use the two-component Weyl spinor representation for the fermion fields. An extensive review including conversion formulae to four-component representations can be found in [12].

$$\begin{aligned}
& + iQ_i^\dagger \bar{\sigma}^\mu D_\mu Q_i + iu_{R_i}^\dagger \bar{\sigma}^\mu D_\mu u_{R_i} + id_{R_i}^\dagger \bar{\sigma}^\mu D_\mu d_{R_i} \\
& + iL_i^\dagger \bar{\sigma}^\mu D_\mu L_i + ie_{R_i}^\dagger \bar{\sigma}^\mu D_\mu e_{R_i} \\
& + (D_\mu \phi)^\dagger D^\mu \phi - V(\phi^\dagger \phi) \\
& - Y_{u_{ij}} Q_i \cdot \phi u_{R_j}^\dagger + Y_{d_{ij}} Q_i \cdot \tilde{\phi} d_{R_j}^\dagger + Y_{e_{ij}} L_i \cdot \tilde{\phi} e_{R_j}^\dagger + h.c. ,
\end{aligned} \tag{2.2}$$

where implicitly sums over the $SU(3)_C$, $SU(2)_L$, and family indices $a = 1 \dots 8$, $A = 1 \dots 3$, and $i = 1 \dots 3$, respectively, are understood. Since the matter fields come in three families of equal quantum numbers, they can mix and the Yukawa couplings Y_f of the fermions to the Higgs field are in general complex 3×3 matrices. The gauge field strengths are given by

$$G_{\mu\nu}^a \equiv \partial_\mu G_\nu^a - \partial_\nu G_\mu^a - g_3 f_{bc}^a G_\mu^b G_\nu^c , \tag{2.3}$$

$$W_{\mu\nu}^A \equiv \partial_\mu W_\nu^A - \partial_\nu W_\mu^A - g_2 \epsilon_{ABC} W_\mu^B W_\nu^C , \tag{2.4}$$

$$B_{\mu\nu} \equiv \partial_\mu B_\nu - \partial_\nu B_\mu , \tag{2.5}$$

where g_3 and g_2 are the gauge coupling strengths and f_{bc}^a and ϵ_{ABC} the structure constants of the gauge groups $SU(3)_C$ and $SU(2)_L$, respectively, as discussed in appendix A. The gauge covariant derivative of a field ψ is defined as

$$D_\mu \psi \equiv (\partial_\mu - ig_3 G_\mu^a T^a - ig_2 W_\mu^A \tau^A - ig' B_\mu Q_Y) \psi , \tag{2.6}$$

where g' is the gauge coupling strength of $U(1)_Y$, T^a and τ^A are the generators of the $SU(3)_C$ and $SU(2)_L$ representations of ψ , and Q_Y denotes the hypercharge of ψ . $V(\phi^\dagger \phi)$ is the scalar potential of the Higgs field (2.13). Finally we used

$$\bar{\sigma}^\mu \equiv (\mathbf{1}, -\vec{\sigma}) , \tag{2.7}$$

$$\chi \cdot \xi \equiv \epsilon^{AB} \chi_A \xi_B , \tag{2.8}$$

$$\tilde{\phi} \equiv \epsilon \phi^* , \tag{2.9}$$

with σ^i denoting the Pauli matrices

$$\sigma^1 = \begin{pmatrix} 0 & 1 \\ 1 & 0 \end{pmatrix}, \quad \sigma^2 = \begin{pmatrix} 0 & -i \\ i & 0 \end{pmatrix}, \quad \sigma^3 = \begin{pmatrix} 1 & 0 \\ 0 & -1 \end{pmatrix}, \tag{2.10}$$

and the totally antisymmetric tensors ϵ_{AB} of $SU(2)_L$ and $\epsilon_{\mu\nu\lambda\rho}$ with

$$\epsilon_{12} = -\epsilon_{21} = 1 \quad \text{and} \quad \epsilon^{0123} = -\epsilon_{0123} = 1 . \tag{2.11}$$

2.2 The Brout-Englert-Higgs mechanism

Since W^\pm and Z^0 bosons are found to be massive vector bosons in nature, the SM needs to contain a mechanism in order to explain gauge boson masses in the EW sector. The

Stückelberg formalism [13] could in principle generate massive gauge bosons, the resulting theory would be non-renormalisable, however. An elegant solution that keeps the theory renormalisable is the incorporation of the Brout-Englert-Higgs (BEH) mechanism [10, 11] into the SM, by which massive W^\pm and Z^0 emerge from the spontaneous symmetry breaking of $SU(2)_L \times U(1)_Y \rightarrow U(1)_{\text{em}}$:

The scalar potential of the complex Higgs field

$$\phi = \begin{pmatrix} \phi^+ \\ \phi^0 \end{pmatrix} \quad (2.12)$$

is given by

$$V(\phi^\dagger\phi) = \mu^2\phi^\dagger\phi + \lambda(\phi^\dagger\phi)^2. \quad (2.13)$$

The BEH mechanism assumes $\mu^2 < 0$ and thus the minimum of the Higgs potential does not coincide with vanishing field value of ϕ . Rather, the Higgs field obtains a non-vanishing vacuum expectation value (vev)

$$\langle\phi\rangle = \frac{1}{\sqrt{2}} \begin{pmatrix} 0 \\ v \end{pmatrix}. \quad (2.14)$$

This ground state is not invariant under $SU(2)_L \times U(1)_Y$, but it respects an $U(1)_{\text{em}}$ symmetry, which is identified with the gauge group of electromagnetism. The electric charge is given by

$$Q_e = \tau^3 + Q_Y. \quad (2.15)$$

Expanding ϕ around its vev one can perform a gauge transformation, such that three degrees of freedom are absorbed by the gauge fields, which get mass terms in doing so, while one real massive scalar, the Higgs boson h , remains in the particle spectrum. The new gauge bosons are linear combination of the gauge bosons in the unbroken theory. They are given by

$$W_\mu^\pm = \frac{1}{\sqrt{2}} (W_\mu^1 \mp W_\mu^2), \quad (2.16)$$

$$\begin{pmatrix} Z_\mu^0 \\ A_\mu \end{pmatrix} = \begin{pmatrix} \cos\theta_W & -\sin\theta_W \\ \sin\theta_W & \cos\theta_W \end{pmatrix} \begin{pmatrix} W_\mu^3 \\ B_\mu \end{pmatrix}, \quad (2.17)$$

where A_μ is the massless photon field and the weak mixing angle θ_W is defined by

$$\sin^2\theta_W = \frac{g'^2}{g_2^2 + g'^2} = 0.23155(5) \quad [14]. \quad (2.18)$$

The masses of the gauge bosons are given in terms of gauge couplings and the vev as

$$M_{W^\pm} = \frac{1}{2} g_2 v \quad \text{and} \quad M_{Z^0} = \frac{1}{2} \sqrt{g_2^2 + g'^2} v. \quad (2.19)$$

Experimentally the masses of the weak gauge bosons are known to be [14]

$$M_{W^\pm} = (80.385 \pm 0.015) \text{ GeV} \quad \text{and} \quad M_{Z^0} = (91.1876 \pm 0.0021) \text{ GeV}. \quad (2.20)$$

The value of $v \approx 246$ GeV can be obtained from these measurements. Finally, the mass of the Higgs boson was found to be [14]

$$m_h = (125.7 \pm 0.4) \text{ GeV} . \quad (2.21)$$

2.3 Fermion masses and the Cabibbo-Kobayashi-Maskawa-Matrix

Besides the breaking of electroweak symmetry, the non-vanishing vev of the Higgs field also leads to the appearance of fermion mass matrices

$$M_{u_{ij}} = \frac{v}{\sqrt{2}} Y_{u_{ij}} , \quad M_{d_{ij}} = \frac{v}{\sqrt{2}} Y_{d_{ij}} , \quad \text{and} \quad M_{e_{ij}} = \frac{v}{\sqrt{2}} Y_{e_{ij}} . \quad (2.22)$$

The 3×3 mass matrices M_f can be diagonalised by a singular value decomposition (SVD)

$$\left(U_L^{(f)} \right)^T M_f \left(U_R^{(f)} \right)^* = \text{diag} \left(m_1^{(f)} , m_2^{(f)} , m_3^{(f)} \right) , \quad (2.23)$$

where $U_L^{(f)}$ and $U_R^{(f)}$ are unitary 3×3 matrices⁴ and $m_i^{(f)}$ are the three singular values of M_f . In the SM six unitary matrices are introduced to rotate the quarks and charged leptons from the *flavour basis* to the *mass basis*

$$\begin{aligned} u_L &\rightarrow U_L^{(u)} u_L , & d_L &\rightarrow U_L^{(d)} d_L , & e_L &\rightarrow U_L^{(e)} e_L , \\ u_R &\rightarrow U_R^{(u)} u_R , & d_R &\rightarrow U_R^{(d)} d_R , & e_R &\rightarrow U_R^{(e)} e_R . \end{aligned} \quad (2.24)$$

Neutrinos are massless in the SM, therefore in the transformation to the mass basis the neutrino fields are rotated in correspondence with the charged lepton field

$$\nu_L \rightarrow U_L^{(e)} \nu_L . \quad (2.25)$$

With the exception of the couplings to the charged gauge bosons W_μ^\pm , all interaction terms in the SM are flavour diagonal and are thus left invariant by the transformation of (2.24). For the coupling to W_μ^\pm , however, the transformation to the mass basis leads to the emergence of the unitary Cabibbo-Kobayashi-Maskawa (CKM)-Matrix [15, 16]

$$V_{\text{CKM}} \equiv \left(U_L^{(u)} \right)^\dagger U_L^{(d)} \quad (2.26)$$

in the interaction Lagrange density of the charged current

$$\mathcal{L}_{\text{cc}} = \frac{g_2}{\sqrt{2}} \left(u_L^\dagger V_{\text{CKM}} \bar{\sigma}^\mu W_\mu^+ d_L + \nu_L^\dagger \bar{\sigma}^\mu W_\mu^+ e_L \right) + h.c. . \quad (2.27)$$

⁴Note that the matrices $U_L^{(f)}$ and $U_R^{(f)}$ are not uniquely determined by (2.23), since the matrices $\left(U_L^{(f)} \text{diag}(e^{i\gamma_1}, e^{i\gamma_2}, e^{i\gamma_3}) \right)^T$ and $\left(U_R^{(f)} \text{diag}(e^{i\gamma_1}, e^{i\gamma_2}, e^{i\gamma_3}) \right)^*$ also diagonalise M_f .

A 3×3 unitary matrix has in general nine real parameters, whereas a 3×3 orthogonal matrix has three real parameters. The additional six real parameters in the unitary case can therefore be identified as complex phases. One can thus parametrise a general 3×3 unitary matrix by [17]

$$V = U_{23}U_{13}U_{12}P, \quad (2.28)$$

with

$$\begin{aligned} U_{23} &= \begin{pmatrix} 1 & 0 & 0 \\ 0 & c_{23} & s_{23}e^{-i\delta_{23}} \\ 0 & -s_{23}e^{i\delta_{23}} & c_{23} \end{pmatrix}, & U_{13} &= \begin{pmatrix} c_{13} & 0 & s_{13}e^{-i\delta_{13}} \\ 0 & 1 & 0 \\ -s_{13}e^{i\delta_{13}} & 0 & c_{13} \end{pmatrix}, \\ U_{12} &= \begin{pmatrix} c_{12} & s_{12}e^{-i\delta_{12}} & 0 \\ -s_{12}e^{i\delta_{12}} & c_{12} & 0 \\ 0 & 0 & 1 \end{pmatrix}, & \text{and } P &= \begin{pmatrix} e^{i\gamma_1} & 0 & 0 \\ 0 & e^{i\gamma_2} & 0 \\ 0 & 0 & e^{i\gamma_3} \end{pmatrix}, \end{aligned} \quad (2.29)$$

where s_{ij} and c_{ij} denote $\sin \theta_{ij}$ and $\cos \theta_{ij}$, respectively. For the CKM matrix

$$V_{\text{CKM}} = U_{23}^{\text{CKM}}U_{13}^{\text{CKM}}U_{12}^{\text{CKM}}P^{\text{CKM}} \quad (2.30)$$

the mixing angle θ_{12}^{CKM} is given a special name and is referred to as *Cabibbo angle* θ_C . Taking advantage of the freedom in the SVD to multiply the unitary matrices $U_L^{(u)}$ and $U_L^{(d)}$ by diagonal phase matrices, complex phases of V_{CKM} can be absorbed in the phases of the quark fields. Although there are six quark fields at hand, because the full SM Lagrangian is invariant under a global rotation of all quarks by a common phase, only five complex phases of V_{CKM} can be absorbed. With the new unitary matrices

$$\begin{aligned} U_L^{(u)} &\rightarrow U_L^{(u)} \text{diag} \left(1, e^{i\delta_{12}^{\text{CKM}}}, e^{i(\delta_{12}^{\text{CKM}} + \delta_{23}^{\text{CKM}})} \right) \\ \text{and } U_L^{(d)} &\rightarrow U_L^{(d)} (P^{\text{CKM}})^{-1} \text{diag} \left(1, e^{i\delta_{12}^{\text{CKM}}}, e^{i(\delta_{12}^{\text{CKM}} + \delta_{23}^{\text{CKM}})} \right) \end{aligned} \quad (2.31)$$

the CKM matrix is brought into the Particle Data Group (PDG) standard parametrisation [14]

$$V_{\text{CKM}} = \begin{pmatrix} c_{12}c_{13} & s_{12}c_{13} & s_{13}e^{-i\delta} \\ -c_{23}s_{12} - s_{23}s_{13}c_{12}e^{i\delta} & c_{23}c_{12} - s_{23}s_{13}s_{12}e^{i\delta} & s_{23}c_{13} \\ s_{23}s_{12} - c_{23}s_{13}c_{12}e^{i\delta} & -s_{23}c_{12} - c_{23}s_{13}s_{12}e^{i\delta} & c_{23}c_{13} \end{pmatrix}, \quad (2.32)$$

where for the sake of readability the superscript CKM has been dropped on all parameters. The CP violating phase δ^{CKM} is given in terms of [17]

$$\delta^{\text{CKM}} = \delta_{13}^{\text{CKM}} - \delta_{12}^{\text{CKM}} - \delta_{23}^{\text{CKM}}. \quad (2.33)$$

The experimental values reported by the PDG are given as [14]

$$\begin{aligned} \theta_{12}^{\text{CKM}} &= 13.02^\circ \pm 0.036^\circ, & \theta_{13}^{\text{CKM}} &= 0.204^\circ \pm 0.0099^\circ, \\ \theta_{23}^{\text{CKM}} &= 2.37^\circ \pm 0.071^\circ, & \delta^{\text{CKM}} &= 71.7^\circ \pm 3.1^\circ. \end{aligned} \quad (2.34)$$

Finally, the masses of the fermions are reported. The masses of the electron and muon are most precisely determined from atomic physics experiments, causing the uncertainty of the precise value of the atomic mass unit u in MeV to be the dominant contribution to the mass uncertainty of m_e and m_μ [18]

$$\begin{aligned} m_e &= (0.510998928 \pm 0.000000011) \text{ MeV} , \\ m_\mu &= (105.6583715 \pm 0.0000035) \text{ MeV} . \end{aligned} \quad (2.35)$$

The mass of the tau lepton is obtained from experiments measuring the production cross section $e^-e^+ \rightarrow \tau^-\tau^+$ [14]

$$m_\tau = (1776.82 \pm 0.16) \text{ MeV} . \quad (2.36)$$

Free quarks are not observed in nature, rendering the quark mass determination a very difficult endeavour. Due to the absence of a physical observable, quark masses have to be reported in a mass independent renormalisation scheme, such as $\overline{\text{MS}}$ at a certain renormalisation scale. The masses of the light quarks u , d , and s are determined from lattice QCD [19] and chiral perturbation theory [20,21]. The PDG reports the light quark masses in $\overline{\text{MS}}$ at a renormalisation scale $\mu = 2 \text{ GeV}$ [14]

$$m_u = 2.3_{-0.5}^{+0.7} \text{ MeV} , \quad m_d = 4.8_{-0.3}^{+0.5} \text{ MeV} , \quad m_s = (95 \pm 5) \text{ MeV} . \quad (2.37)$$

Note that chiral perturbation theory determines quark mass ratios rather than absolute quantities and needs additional input from e.g. lattice theory to obtain specific quark masses. Therefore often the reported light quark mass ratios⁵ are used

$$\frac{m_s}{m_d} = 18.9 \pm 0.8 \quad [22] \quad \text{and} \quad \frac{m_s}{\frac{1}{2}(m_u + m_d)} = 27.5 \pm 1.0 \quad [14]. \quad (2.38)$$

The masses of the heavy quarks are obtained from measured $q\bar{q}$ production cross sections and in the case of bottom and charm, lattice simulations and heavy quark effective theory [23] of the D and B mesons. For b and c the heavy quark masses are given as $\overline{\text{MS}}$ mass at a renormalisation scale equal to their respective quark mass [14]

$$\begin{aligned} m_c(m_c) &= (1.275 \pm 0.025) \text{ GeV} , \\ m_b(m_b) &= (4.18 \pm 0.03) \text{ GeV} . \end{aligned} \quad (2.39)$$

Because of its very heavy mass the top quark has the unique feature among all quarks to decay before it can form $t\bar{t}$ bound states, allowing to determine its pole mass [14]

$$m_t = (173.21 \pm 0.51 \pm 0.71) \text{ GeV} , \quad (2.40)$$

in analogy with the determination of the τ pole mass.

⁵In pure QCD these mass ratios are independent from the renormalisation scale in the $\overline{\text{MS}}$ scheme and are therefore reported at $\mu = 2 \text{ GeV}$. In the full SM they are scale dependent, however.

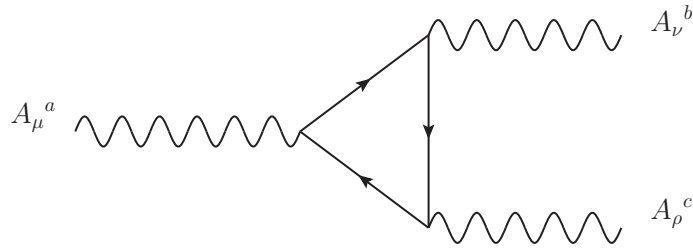


Figure 2.1: Triangle diagram with chiral fermions in the loop and three external gauge bosons, possibly leading to an anomaly. In general the gauge bosons need not to be of the same gauge group.

2.4 Open questions in the Standard Model

We close this chapter with a brief discussion of various open problems and deficiencies of the Standard Model. The following chapters will bring widely expected solutions to these open problems into focus and introduce several Beyond the Standard Model extension of Particle Physics. The last concern in the following list motivates the main parts of this thesis.

Neutrino masses The SM predicts vanishing masses of neutrinos. This is in contradiction with the observation of neutrino oscillations and therefore the strongest indication that BSM physics is needed to understand the phenomena of Particle Physics. Chapter 3 is devoted to massive neutrinos and neutrino mixing.

$U(1)_{\text{em}}$ Charge quantisation For the $SU(3)_C$ and $SU(2)_L$ subgroups of the SM gauge group, the interaction between gauge bosons and fermions is defined purely by group theory and the gauge coupling strengths g_3 and g_2 . This guarantees universality, e.g. all $SU(2)_L$ doublets couple the same way to the gauge bosons W_μ^a . In contrast, there is no such mechanism guaranteeing $U(1)_Y$ hypercharge universality. Within the SM there is no theoretical reason, but solely experimental observation, that Q_Y is quantised and distributed to the SM matter fields as listed in table 2.1. Chapter 4 discusses Grand Unified Theories (GUTs), where the $U(1)_Y$ emerges from spontaneous breaking of a more fundamental gauge group. The group theoretical universal coupling of the more fundamental gauge group is then inherited by the SM $U(1)_Y$, leading finally to $U(1)_{\text{em}}$ charge quantisation.

Anomaly cancellation Anomalies appear in chiral gauge theories, when a symmetry of the Lagrangian is not conserved by higher order loop terms [24, 25]. Triangle diagrams with three external gauge bosons as depicted in figure 2.1 can contribute to the anomaly of a symmetry. In order for the gauge theory to stay anomaly free, the anomaly coefficients

$$\mathcal{A}^{abc} \equiv \text{Tr} (T^a \{T^b, T^c\}) \quad (2.41)$$

need to vanish [26], where T^a , T^b , and T^c denote generators of the respective gauge group. Looking closer at one example with one external $U(1)_Y$ gauge boson and two external $SU(2)_L$ gauge bosons, (2.41) reduces to the trace over the hypercharges

$$\mathcal{A}^{Ybc} = \frac{\delta^{bc}}{2} \text{Tr} Q_Y = \frac{3\delta^{bc}}{2} \left(3 \cdot \left(\frac{1}{6} + \frac{2}{3} - \frac{1}{3} \right) - \frac{1}{2} - 1 \right) = 0. \quad (2.42)$$

As in (2.42) all other anomaly coefficients in the SM vanish. The crucial point is the cancellation of lepton and quark contributions. Similar to the open question of $U(1)_Y$ charge quantisation, there is no theoretical reason for the leptons and quarks to carry precisely the right hypercharges for the anomaly coefficients to vanish and thereby rendering the SM anomaly free. In GUTs leptons and quarks are unified in joint representations of the GUT gauge group, which in certain cases guarantees anomaly cancellation automatically.

Naturalness problem I - The hierarchy problem As the only scalar field in the SM, the Higgs boson is subject to much larger radiative corrections than the SM fermion fields. Whereas the radiative corrections to fermion masses are logarithmically divergent

$$\delta m_f \sim m_0 \log \left(\frac{\Lambda^2}{m_0^2} \right), \quad (2.43)$$

the corresponding radiative corrections to the Higgs boson mass due to a fermion loop is quadratically divergent

$$\delta m_h^2 \sim |y_f|^2 \Lambda^2, \quad (2.44)$$

where we used a momentum cutoff regularisation of the divergent loop corrections.

Since the Higgs mass is known to be around 126 GeV, an enormous amount of fine tuning between the bare mass parameter and the counterterm has to appear in the renormalisation, otherwise the Higgs mass would be expected to be at a much higher energy scale associated with new physics, e.g. the Planck scale. Another way to view the unnaturalness of small m_h is due to the fact that δm_h^2 is independent of m_h^2 itself. Setting $m_h = 0$ does therefore not restore a symmetry of the Lagrange density and the smallness of m_h fails to satisfy t'Hooft's naturalness criterion [27]. Chapter 5 discusses Supersymmetry (SUSY), which introduces a bosonic partner to each fermion. Including the bosonic partner in the radiative corrections, the quadratic divergence of m_h vanishes to all order in perturbation theory. Additionally, some discrepancy between predictions of GUTs and phenomenology can be resolved when supersymmetric GUTs are studied.

The flavour problem There are in total nineteen parameters in the Standard Model Lagrange density (2.2) when using the freedom to absorb some phases of the CKM Matrix into the quark fields as discussed in 2.3. The majority of those, thirteen parameters, belong to the flavour sector of the SM, parametrising nine fermion masses, three mixing angles and the CKM phase. Including extensions of the SM to incorporate massive neutrinos,

as discussed in chapter 3, into the parameter counting, the number of flavour related parameters is even increased. As was shown in figure 1.1, looking at the values of the particles' masses, one encounters huge hierarchies, within single families, but also when comparing the masses of different families. The CKM mixing angles are small, but it will be seen in the next chapter, that some of the neutrino mixing angles are very large. The SM lacks an explanation of these patterns and hierarchies, and includes all flavour parameters fixed simply as measured from experiments. Expecting a more elegant explanation from a fundamental theory, one can build flavour models with discrete symmetries to describe relations among the measured flavour observables. In part III of this thesis, two such flavour models are constructed within the framework of supersymmetry and GUTs, and their predictions are discussed in detail.

At the end of this chapter three open problems of the Standard Model are listed, that lie outside the scope of this thesis. For the sake of completeness they are presented here nevertheless.

Naturalness problem II - The strong CP problem Although being a total derivative, the CP violating θ_{QCD} term in the SM Lagrange density can not be dismissed due to instanton effects [28]. When the quark mass matrices are diagonalised, due to a chiral anomaly the value of θ_{QCD} is changed [29]

$$\bar{\theta} = \theta_{QCD} + \text{Arg Det} (M_u M_d) . \quad (2.45)$$

Although one could expect $\bar{\theta}$ to be of order $\mathcal{O}(1)$, from measurements of the neutron electric dipole moment it is known [14]

$$|\bar{\theta}| < 10^{-10} . \quad (2.46)$$

The strong CP problem is the question for an explanation of small $\bar{\theta}$. One possible solution is to extend the SM by a spontaneously broken $U(1)_{PQ}$ Peccei-Quinn symmetry [30] and effectively replaces $\bar{\theta}$ by the pseudo-Nambu-Goldstone boson of $U(1)_{PQ}$, the axion [31]. Another possible solution is spontaneous breaking of CP symmetry, such that $\theta_{QCD} = 0$ in the QCD sector, whereas $\text{Arg Det} (M_u M_d) = 0$ is enforced by flavour models [32].

Dark Matter Observations of rotation curves of galaxies [33], anisotropies in the Cosmic Microwave Background (CMB) [34, 35], and gravitational lensing of the bullet cluster [36] signalise the existence of Dark Matter (DM). Due to gravitational lensing surveys it is known that the majority of DM has to be composed out of non-baryonic matter [37], thus a BSM explanation is required. Possible DM candidates are heavy sterile neutrinos, axions, and the lightest supersymmetric particle in SUSY [38–40].

Naturalness problem III - The cosmological constant problem From the Particle Physics point of view, it is always possible to add a constant term into the SM Lagrange density, without altering any prediction of the theory. Such a term corresponds to the

energy of the vacuum and it does become important in cosmology, where it is known as cosmological constant ρ_{cc} or dark energy to explain the observed accelerating expansion of the universe [41]. The value of the cosmological constant is [14]

$$\rho_{cc} \approx (2.2 \text{ meV})^4 . \quad (2.47)$$

The SM is incapable of explaining any value of ρ_{cc} , but even when attempting an analysis on dimensional grounds one expects contributions from quantum loop effects

$$\rho \sim m^4 , \quad (2.48)$$

which could be cancelled by new physics at scales larger than at least TeV, leading to an estimate of ρ_{cc} that is at least 60 orders of magnitude larger than observed. So far, no satisfying solution to the cosmological constant problem has been proposed and it remains an open question.

CHAPTER 3

Massive neutrinos

In the process of developing the Standard Model of Particle Physics, it was assumed that neutrinos are massless particles. In fact, the SM only contains left-handed neutrino fields, included in the $SU(2)_L$ doublets L_i . With the observation of neutrino oscillations [42–46], the presumption of massless neutrinos has been falsified and one is compelled to extend the SM to account for very small neutrino masses. Excitingly, there are still open questions and unmeasured observables in Neutrino Physics, such that no definite neutrino mass generation mechanism exists.

This chapter introduces lepton mixing as general consequence of massive neutrinos and discusses some of the suggested SM extensions for neutrino masses. Finally a first brief introduction towards flavour model building is presented. The content of this chapter is based on [47–49].

3.1 Neutrino masses and the seesaw mechanisms

Besides observations of neutrino oscillations there is no evidence for neutrino masses from other types of experiments. Measurements of β -decay set only an upper bound for the mass of the electron-type anti-neutrino [50]

$$m_{\bar{\nu}_e} < 2.05 \text{ eV} . \quad (3.1)$$

Anisotropies in the CMB and large-scale clustering of galaxies constrain the energy density of neutrinos Ω_ν and lead to an upper bound for the sum of light neutrino masses [35]

$$\sum_{\nu} m_{\nu} < 0.23 \text{ eV} . \quad (3.2)$$

These masses are substantially smaller than the masses of quarks and charged leptons, thus the flavour problem described in 2.4 got more severe with the discovery of non-vanishing neutrino masses.

There are two straightforward options for incorporating neutrino masses into the SM. One is to simply extend the particle content of the SM by right-handed neutrino fields ν_{R_i} ,

which transform as total singlets under the gauge group of the SM. Then the Lagrange density is extended by a new Yukawa coupling

$$\mathcal{L}_\nu = i\nu_{R_i}^\dagger \bar{\sigma}^\mu \partial_\mu \nu_{R_i} - \left(Y_{\nu_{ij}} L_i \cdot \phi \nu_{R_j}^\dagger + h.c. \right), \quad (3.3)$$

which generates a Dirac mass when the Higgs field ϕ obtains its vev (2.14), just as quark and charged lepton masses emerge when the electroweak symmetry gets broken. The number N of right-handed neutrinos is left undetermined and Y_ν can be any general complex $3 \times N$ matrix. Since this option requires Yukawa coupling of $\mathcal{O}(10^{-12})$ to explain $\mathcal{O}(\text{eV})$ neutrino masses, the problem of naturalness remains unsolved.

Because the ν_{R_i} are gauge singlets, additionally to (3.3) the Lagrange density can include a Majorana mass term

$$\mathcal{L} = \mathcal{L}_\nu - \frac{1}{2} M_{\nu_{ij}} \nu_{R_i} \nu_{R_j} + h.c., \quad (3.4)$$

when one dismisses the Lepton number conservation of the original SM.

The second straightforward suggestion to generate massive neutrinos results from the abandonment of renormalisability of the SM. Then the SM is extended by the effective dimension five Weinberg operator [51]

$$\mathcal{L}_\kappa = \frac{1}{2} \kappa_{ij} (L_i \cdot \phi) (L_j \cdot \phi) + h.c., \quad (3.5)$$

which gives rise to a Majorana mass term

$$\mathcal{L}_\nu = \frac{v^2}{4} \kappa_{ij} \nu_{L_i} \nu_{L_j} + h.c. \quad (3.6)$$

after EW symmetry is broken.

Particle Physics knows the non-renormalisable four-fermion Fermi theory of beta-decay, which emerges from the renormalisable SM as effective theory when the heavy W^\pm boson are integrated out. Repeating this successful idea for non-renormalisable neutrino operators gives rise to the seesaw mechanisms: The Weinberg operator (3.5) is obtained as effective operator by integrating out heavy degrees of freedom. With the resulting neutrino masses being inverse proportional to the mass of the heavy fields, the seesaw mechanism are attractive solutions to explain the smallness of neutrino masses without the necessity of unnatural small couplings.

There are three different types of seesaw mechanisms, depending on what type of heavy degrees of freedom are introduced in order to generate (3.5). In this thesis we will exclusively make use of type-I seesaw [52], which is based on new heavy right-handed neutrino fields ν_{R_i} and the SM Lagrange density is extended as in (3.4). When the heavy right-handed neutrinos are integrated out, the Weinberg operator emerges effectively and the neutrino Majorana mass is given by

$$m_\nu = -\frac{v^2}{2} Y_\nu M_\nu^{-1} Y_\nu^T, \quad (3.7)$$

when the SM Higgs field ϕ obtains its vev. Type-I seesaw is an attractive extension of the SM, since the gauge-singlets ν_{R_i} can naturally have large Majorana masses, leading to an explanation of the smallness of neutrino masses. When the SM is embedded into an $SO(10)$ GUT, a right-handed neutrino ν_{R_i} is automatically included in the spectrum, as will be discussed in the next chapter.

Other seesaw mechanisms are obtained from heavy scalar $SU(2)_L$ triplets (type-II [53]) or from fermion $SU(2)_L$ triplets (type-III [54]). Another mechanism for neutrino mass generation is the double seesaw mechanism [55], where the right-handed neutrinos of the seesaw type-I are originally massless and the heavy mass M_ν is itself an effective mass originating from another instance of the seesaw mechanism with sterile neutrinos ν_{S_i} , which do not couple to the SM doublets L_i . Finally there is the possibility to explain small neutrino masses as loop corrections to vanishing tree-level masses [56], but such models do also need new particles in addition to the SM particles to run inside the loop and can be made arbitrarily complex.

3.2 The Pontecorvo-Maki-Nakagawa-Sakata Matrix

In the SM the neutrinos were assumed to be massless and rotated like the charged leptons (2.25) when transforming from the flavour basis to the mass basis. Massive neutrinos, however, require to diagonalise the neutrino mass matrix as well. If neutrinos have a Dirac mass, the mass matrix can be diagonalised by a singular value decomposition as for the quarks and charged leptons (2.23). For Majorana neutrinos, however, m_ν is a complex symmetric matrix, and therefore has to be diagonalised by a Takagi decomposition (TD)

$$U_{(\nu)}^T m_\nu U_{(\nu)} = \text{diag}(m_1, m_2, m_3) , \quad (3.8)$$

where $U_{(\nu)}$ is an unitary 3×3 matrix and m_i are the three singular values of the complex symmetric matrix m_ν . As for SVD, $U_{(\nu)}$ is not uniquely defined by (3.8). In SVD the unitary matrices are defined up to a diagonal phase matrix, which in TD is in general reduced to a sign ambiguity

$$U_{(\nu)} \rightarrow U_{(\nu)} \text{diag}(e^{i\gamma_1}, e^{i\gamma_2}, e^{i\gamma_3}) , \quad (3.9)$$

with $\gamma_i = 0, \pi$. Only if the corresponding singular value m_i is vanishing, γ_i can be arbitrary.

With (2.24) the rotations to the mass basis in the lepton sector are

$$e_L \rightarrow U_L^{(e)} e_L , \quad e_R \rightarrow U_R^{(e)} e_R , \quad \text{and} \quad \nu_L \rightarrow U_{(\nu)} \nu_L . \quad (3.10)$$

The coupling of leptons to the neutral current is flavour diagonal as for quarks. In the coupling to the charged current the transformations (3.10) lead to the emergence of the unitary Pontecorvo-Maki-Nakagawa-Sakata (PMNS)-Matrix [42, 57]

$$V_{\text{PMNS}} \equiv \left(U_L^{(e)} \right)^\dagger U_{(\nu)} \quad (3.11)$$

in

$$\mathcal{L}_{cc} = \frac{g_2}{\sqrt{2}} \left(u_L^\dagger V_{\text{CKM}} \bar{\sigma}^\mu W_\mu^+ d_L + e_L^\dagger V_{\text{PMNS}} \bar{\sigma}^\mu W_\mu^- \nu_L \right) + h.c. . \quad (3.12)$$

As for the CKM-Matrix (2.3), at first the PMNS-Matrix can be parametrised in terms of (2.29) with three real angles and six phases as

$$V_{\text{PMNS}} = U_{23}^{\text{PMNS}} U_{13}^{\text{PMNS}} U_{12}^{\text{PMNS}} P^{\text{PMNS}} . \quad (3.13)$$

Three phases can be absorbed in the charged lepton fields using the freedom of $U_L^{(e)}$ as

$$U_L^{(e)} \rightarrow U_L^{(e)} \text{diag} \left(e^{i\gamma_1^{\text{PMNS}}}, e^{i(\gamma_1^{\text{PMNS}} + \delta_{12}^{\text{PMNS}})}, e^{i(\gamma_1^{\text{PMNS}} + \delta_{12}^{\text{PMNS}} + \delta_{23}^{\text{PMNS}})} \right) . \quad (3.14)$$

This brings V_{PMNS} into its standard parametrisation

$$V_{\text{PMNS}} = \begin{pmatrix} c_{12}c_{13} & s_{12}c_{13} & s_{13}e^{-i\delta} \\ -c_{23}s_{12} - s_{23}s_{13}c_{12}e^{i\delta} & c_{23}c_{12} - s_{23}s_{13}s_{12}e^{i\delta} & s_{23}c_{13} \\ s_{23}s_{12} - c_{23}s_{13}c_{12}e^{i\delta} & -s_{23}c_{12} - c_{23}s_{13}s_{12}e^{i\delta} & c_{23}c_{13} \end{pmatrix} P_\alpha , \quad (3.15)$$

where for readability the superscript PMNS has been dropped. P_α is a diagonal phase matrix containing the two *Majorana phases* α_1 and α_2

$$P_\alpha = \text{diag} \left(1, e^{i\frac{\alpha_1^{\text{PMNS}}}{2}}, e^{i\frac{\alpha_2^{\text{PMNS}}}{2}} \right) . \quad (3.16)$$

The three physical phases of V_{PMNS} are given in terms of the parametrisation (3.13) as¹

$$\delta^{\text{PMNS}} = \delta_{13}^{\text{PMNS}} - \delta_{12}^{\text{PMNS}} - \delta_{23}^{\text{PMNS}} , \quad (3.17a)$$

$$\frac{\alpha_1^{\text{PMNS}}}{2} = \gamma_2^{\text{PMNS}} - \gamma_1^{\text{PMNS}} - \delta_{12}^{\text{PMNS}} , \quad (3.17b)$$

$$\frac{\alpha_2^{\text{PMNS}}}{2} = \gamma_3^{\text{PMNS}} - \gamma_1^{\text{PMNS}} - \delta_{12}^{\text{PMNS}} - \delta_{23}^{\text{PMNS}} . \quad (3.17c)$$

In the case that neutrinos are Dirac particles, m_ν is diagonalised by a SVD and the PMNS-Matrix is analogously to the CKM-Matrix obtained, i.e. the Majorana phases are unphysical.

Neutrino oscillations arise due to the fact that neutrinos are created and observed via charged current interactions as flavour eigenstates $|\nu_\alpha\rangle$, which are superpositions of mass eigenstates² $|\nu_i\rangle$

$$|\nu_\alpha\rangle = U_{\alpha i}^* |\nu_i\rangle . \quad (3.18)$$

¹In the literature one also finds the convention of $P_\alpha = \text{diag} \left(e^{-i\frac{\phi_1}{2}}, e^{-i\frac{\phi_2}{2}}, 1 \right)$, in which case the Majorana phases are given as $\frac{\phi_1^{\text{PMNS}}}{2} = \gamma_3^{\text{PMNS}} - \gamma_1^{\text{PMNS}} - \delta_{12}^{\text{PMNS}} - \delta_{23}^{\text{PMNS}}$ and $\frac{\phi_2^{\text{PMNS}}}{2} = \gamma_3^{\text{PMNS}} - \gamma_2^{\text{PMNS}} - \delta_{23}^{\text{PMNS}}$, respectively, whereas the Dirac phase is unchanged from (3.17a).

²Note that in contrast to the field rotation in (3.10) the complex conjugate $U_{\alpha i}^*$ appears in the transformation of states, because in standard convention of quantum field theory a quantum field contains the creation operator for an anti-particle state $|\bar{\psi}\rangle = \psi|0\rangle$.

If one is interested in oscillations of the three *active* light neutrinos of the SM, U is identified with V_{PMNS} . More generally however, U can also describe oscillations into sterile neutrinos.

The different mass eigenstates in a neutrino beam evolve differently and the probability of detecting a specific neutrino flavour eigenstate is thus time-dependent. Since neutrinos are ultra relativistic particles, the time-dependence is exchanged for a dependence on the distance L between the places of origin and detection. Due to weak current interactions of ν_e with electrons in matter, oscillations of ν_e also depend on the electron density n_e [58].

In vacuum the probability for a flavour eigenstate $|\nu_\alpha\rangle$ to oscillate into $|\nu_\beta\rangle$ is given by [43, 59, 60]

$$P(\nu_\alpha \rightarrow \nu_\beta) = \sum_i |U_{\alpha i}|^2 |U_{\beta i}|^2 + \sum_{i>j} U_{\alpha i}^* U_{\beta i} U_{\alpha j} U_{\beta j}^* e^{-i \frac{\Delta m_{ij}^2 L}{2E}}, \quad (3.19)$$

which is independent of the Majorana phases. This probability furthermore does not depend on the absolute neutrino masses, but rather depends on the differences of the squared masses

$$\Delta m_{ij}^2 = m_i^2 - m_j^2. \quad (3.20)$$

Thus it is impossible to inquire an overall scale of neutrino masses from vacuum neutrino oscillation experiments. If

$$|\Delta m_{ij}^2 L| \ll 4\pi E, \quad (3.21)$$

the oscillation due to Δm_{ij}^2 are negligible, since the distance between neutrino source and detection is much smaller than the oscillation length

$$L_{ij}^{\text{osc}} \equiv \frac{4\pi E}{|\Delta m_{ij}^2|}. \quad (3.22)$$

When the uncertainty of the size ΔL or energy ΔE for neutrino production or detection are much larger than L_{ij}^{osc} , the neutrino oscillations due to Δm_{ij}^2 get averaged [61].

In the case of three oscillating neutrinos, conventionally one labels the neutrino mass states such that

$$0 < \Delta m_{21}^2, \quad \Delta m_{21}^2 < |\Delta m_{32}^2|, \quad \Delta m_{21}^2 < |\Delta m_{31}^2|. \quad (3.23)$$

Then there are two options for the remaining neutrino mass m_3 , denoted as *normal ordering* (NO) and *inverse ordering* (IO), respectively

$$\begin{aligned} m_1 &< m_2 < m_3 & \text{(NO)}, \\ m_3 &< m_1 < m_2 & \text{(IO)}. \end{aligned} \quad (3.24)$$

Experiments have not yet succeeded to distinguish between these mass orderings. A global fit of neutrino oscillation measurements finds [62]

$$\begin{aligned} \Delta m_{21}^2 &= 7.50_{-0.17}^{+0.19} \cdot 10^{-5} \text{ eV}^2, \\ \Delta m_{31}^2 \text{ (NO)} &= +2.457_{-0.047}^{+0.047} \cdot 10^{-3} \text{ eV}^2, \\ \Delta m_{32}^2 \text{ (IO)} &= -2.449_{-0.047}^{+0.048} \cdot 10^{-3} \text{ eV}^2. \end{aligned} \quad (3.25)$$

Because of $\Delta m_{21}^2 \ll |\Delta m_{31(32)}^2|$ and distinct neutrino energies for specific oscillation experiments, one can find separate regimes of experiments, where a single mass squared splitting dominates. The observed solar $\nu_e \rightarrow \nu_{\mu,\tau}$ oscillations are related to Δm_{21}^2 , whereas the larger of the two mass squared splittings Δm_{31}^2 and Δm_{32}^2 , is related to atmospheric $\nu_\mu \rightarrow \nu_\tau$ oscillations. Therefore one often refers to these mass splittings as

$$\Delta m_{sol}^2 = \Delta m_{21}^2, \quad \Delta m_{atm}^2 = \begin{cases} \Delta m_{31}^2 & (\text{NO}) \\ \Delta m_{32}^2 & (\text{IO}) \end{cases}. \quad (3.26)$$

The experimental values of the lepton mixing angles are given by [62]

$$\theta_{12}^{\text{PMNS}} = 33.48^\circ \begin{smallmatrix} +0.78^\circ \\ -0.75^\circ \end{smallmatrix} \quad \text{and} \quad \theta_{13}^{\text{PMNS}} = 8.50^\circ \begin{smallmatrix} +0.20^\circ \\ -0.21^\circ \end{smallmatrix}. \quad (3.27)$$

The global best-fit value of $\theta_{23}^{\text{PMNS}}$ depends on whether a normal or an inverse mass ordering is assumed as prior

$$\theta_{23}^{\text{PMNS}} = \begin{cases} 42.3^\circ \begin{smallmatrix} +3.0^\circ \\ -1.6^\circ \end{smallmatrix} & (\text{NO}) \\ 49.5^\circ \begin{smallmatrix} +1.5^\circ \\ -2.2^\circ \end{smallmatrix} & (\text{IO}) \end{cases}. \quad (3.28)$$

With small $\theta_{13}^{\text{PMNS}}$, solar and atmospheric neutrino oscillations can be understood to be dominantly two-flavour oscillations, where $\theta_{12}^{\text{PMNS}}$ is identified as *solar mixing angle* θ_{sol} and atmospheric neutrino oscillations are related to the *atmospheric mixing angle* $\theta_{atm} \equiv \theta_{23}^{\text{PMNS}}$. Oscillation experiments measuring the survival rate of $\bar{\nu}_e$ from nuclear reactors are most sensitive to corrections due to non-vanishing $\theta_{13}^{\text{PMNS}}$, which is therefore sometimes referred to as *reactor mixing angle*.

While large solar and atmospheric mixing angles were established in the early 2000s [45], until 2011, when a small but non-vanishing $\theta_{13}^{\text{PMNS}}$ was discovered [46], it was speculated that $\theta_{13}^{\text{PMNS}} = 0$. Two famous structures for V_{PMNS} had been suggested: Bimaximal (BM) mixing [63] features vanishing $\theta_{13}^{\text{PMNS}}$ and maximal $\theta_{12}^{\text{PMNS}} = \theta_{23}^{\text{PMNS}} = 45^\circ$

$$V_{\text{BM}} = \begin{pmatrix} \frac{1}{\sqrt{2}} & \frac{1}{\sqrt{2}} & 0 \\ -\frac{1}{2} & \frac{1}{2} & \frac{1}{\sqrt{2}} \\ \frac{1}{2} & -\frac{1}{2} & \frac{1}{\sqrt{2}} \end{pmatrix}. \quad (3.29)$$

Like in the bimaximal case, tri-bimaximal (TBM) mixing [64] has $\theta_{13}^{\text{PMNS}} = 0$ and maximal $\theta_{23}^{\text{PMNS}} = 45^\circ$, however the solar mixing angle is given by $\theta_{12}^{\text{PMNS}} \simeq 35.3^\circ$

$$V_{\text{TBM}} = \begin{pmatrix} \sqrt{\frac{2}{3}} & \frac{1}{\sqrt{3}} & 0 \\ -\frac{1}{\sqrt{6}} & \frac{1}{\sqrt{3}} & \frac{1}{\sqrt{2}} \\ \frac{1}{\sqrt{6}} & -\frac{1}{\sqrt{3}} & \frac{1}{\sqrt{2}} \end{pmatrix}. \quad (3.30)$$

Although this structures for V_{PMNS} are ruled out by data due to the discovery of non-vanishing $\theta_{13}^{\text{PMNS}}$, they are prominently used as candidates for the neutrino mixing matrix $U_{(\nu)}$ in neutrino mass model building, when the small non-vanishing $\theta_{13}^{\text{PMNS}}$ results from

$(U_L^{(e)})^\dagger$, as so-called *charged lepton correction* to the neutrino mixing angle $\theta_{13}^\nu = 0$. Assuming “small” charged lepton mixing angles and θ_{13}^ν , respectively, one can perform a small angle expansion of (3.11) to find [65]

$$s_{23}^{\text{PMNS}} e^{-i\delta_{23}^{\text{PMNS}}} \approx s_{23}^\nu e^{-i\delta_{23}^\nu} - \theta_{23}^e c_{23}^\nu e^{-i\delta_{23}^e}, \quad (3.31a)$$

$$\theta_{13}^{\text{PMNS}} e^{-i\delta_{13}^{\text{PMNS}}} \approx \theta_{13}^\nu e^{-i\delta_{13}^\nu} - \theta_{13}^e c_{23}^\nu e^{-i\delta_{13}^e} - \theta_{12}^e e^{-i\delta_{12}^e} (s_{23}^\nu e^{-i\delta_{23}^\nu} - \theta_{23}^e c_{23}^\nu e^{-i\delta_{23}^e}), \quad (3.31b)$$

$$s_{12}^{\text{PMNS}} e^{-i\delta_{12}^{\text{PMNS}}} \approx s_{12}^\nu e^{-i\delta_{12}^\nu} + \theta_{13}^e c_{12}^\nu s_{23}^\nu e^{i(\delta_{23}^\nu - \delta_{13}^e)} - \theta_{12}^e c_{23}^\nu c_{12}^\nu e^{-i\delta_{12}^e}, \quad (3.31c)$$

in leading order of θ_{13}^ν . The higher order term proportional to $\theta_{12}^e \theta_{23}^e$ is shown in (3.31b), since it demonstrates that (3.31b) can be rewritten as

$$\theta_{13}^{\text{PMNS}} e^{-i\delta_{13}^{\text{PMNS}}} \approx \theta_{13}^\nu e^{-i\delta_{13}^\nu} - \theta_{13}^e c_{23}^\nu e^{-i\delta_{13}^e} - \theta_{12}^e s_{23}^{\text{PMNS}} e^{-i(\delta_{12}^e + \delta_{23}^{\text{PMNS}})}. \quad (3.32)$$

An especially interesting case is when θ_{13}^ν and θ_{13}^e vanish, and one can derive from (3.32) the interesting relation

$$\theta_{13}^{\text{PMNS}} \approx \theta_{12}^e s_{23}^{\text{PMNS}}, \quad (3.33)$$

highlighting that $\theta_{13}^{\text{PMNS}}$ can result purely from charged lepton corrections. If one furthermore assumes $\theta_{23}^e \ll \theta_{12}^e$, one obtains from (3.31), using (3.17a), the *lepton mixing sum rule* [65–67]

$$s_{12}^\nu \approx s_{12}^{\text{PMNS}} - \theta_{13}^{\text{PMNS}} c_{12}^{\text{PMNS}} \cot \theta_{23}^{\text{PMNS}} \cos \delta^{\text{PMNS}}, \quad (3.34)$$

to leading order in $\theta_{13}^{\text{PMNS}}$. (3.33) and (3.34) will be in the center of the discussion in chapter 6 and motivate much of the work in part III.

We now turn to a discussion of the phases in V_{PMNS} . It was already mentioned that the neutrino oscillation probability (3.19) does not depend on the Majorana phases. In neutrino oscillations, CP violation can be parametrised by the Jarlskog invariant J defined by [68]

$$\text{Im} (U_{\alpha i}^* U_{\beta i} U_{\alpha j} U_{\beta j}^*) \equiv J \sum_{k,\gamma} \epsilon_{\alpha\beta\gamma} \epsilon_{ijk}, \quad (3.35)$$

which is independent of the phase convention for U . Note that CP violation can only be observed in flavour violating oscillation measurements $\nu_\alpha \neq \nu_\beta$. For oscillations of three light neutrinos $U = V_{\text{PMNS}}$ one obtains

$$J = c_{13}^2 s_{13} c_{12} s_{12} c_{23} s_{23} \sin \delta, \quad (3.36)$$

where again the superscripts PMNS have been dropped for readability. It follows that CP violation is only observable in vacuum neutrino oscillations if all lepton mixing angles are non-vanishing. Therefore only the recent detection of non-vanishing $\theta_{13}^{\text{PMNS}}$ opened the possibility to discover CP violation in neutrino oscillation experiments. Today global fits report hints towards a value of [62]

$$\delta^{\text{PMNS}} = \begin{cases} 306^\circ \begin{smallmatrix} +39^\circ \\ -70^\circ \end{smallmatrix} & \text{(NO)} \\ 254^\circ \begin{smallmatrix} +63^\circ \\ -62^\circ \end{smallmatrix} & \text{(IO)} \end{cases}. \quad (3.37)$$

For the studies and numerical fits in this thesis, the value of δ^{PMNS} has been kept an open parameter, however. A future measurement of δ^{PMNS} can be expected from the long baseline neutrino oscillation experiment DUNE [69], which will also be able to measure the sign of Δm_{31}^2 and determine the neutrino mass ordering.

We conclude this section with a brief discussion of the Majorana phases α_1^{PMNS} and α_2^{PMNS} . In comparison to a Dirac mass matrix, which can be diagonalised by a SVD, a Majorana mass matrix has to be diagonalised by a TD, and therefore the Majorana phases are physical and can not be absorbed by neutrino fields. Whether neutrino mass is of Dirac or Majorana type, can be distinguished by neutrinoless double beta decay ($2\beta_{0\nu}$) [70]: In such processes two nucleons simultaneously experience beta decay. If neutrinos have a Majorana mass, instead of two antineutrinos and two charged leptons with continuous spectrum, the antineutrino emitted by one W boson can be absorbed as neutrino by the second W , leading to a final state of $2\beta_{0\nu}$ with two monochromatic charged leptons. The rate of this process is proportional to the effective Majorana mass

$$\langle m_{\beta\beta} \rangle = \left| \sum_i U_{ei}^2 m_i \right| = c_{12}^2 c_{13}^2 m_1 + s_{12}^2 c_{13}^2 e^{i\alpha_1} m_2 + s_{13}^2 e^{i(\alpha_2 - 2\delta)} m_3, \quad (3.38)$$

where the superscript PMNS was dropped for readability. Because the mixing angles and mass squared splittings are known from oscillation experiments, a measurement of $\langle m_{\beta\beta} \rangle$ could, additionally to answering the Majorana or Dirac mass question, bring insights into CP violation due to Majorana phases and into the question of whether neutrino masses follow normal mass ordering, inverse mass ordering, or are nearly degenerate.³ A careful average of various $2\beta_{0\nu}$ experiments leads to a conservative upper bound [72]

$$\langle m_{\beta\beta} \rangle < 0.46 \text{ eV}. \quad (3.39)$$

3.3 Neutrino mass models & flavour model building

We close this chapter with a discussion of neutrino mass models, whose aim is to explain simple structures of V_{PMNS} , such as tri-bimaximal mixing, from discrete symmetries. In a basis where the charged lepton Yukawa coupling matrix is diagonal one can phrase the neutrino mass matrix m_ν from (3.8) as [73]

$$m_\nu = V_{\text{PMNS}}^* \text{diag}(m_1, m_2, m_3) V_{\text{PMNS}}^\dagger = m_1 \Phi_1^* \Phi_1^\dagger + m_2 \Phi_2^* \Phi_2^\dagger + m_3 \Phi_3^* \Phi_3^\dagger, \quad (3.40)$$

where Φ_i are the columns of V_{PMNS} . For a simple mixing structure such as TBM, these vectors are

$$\Phi_1 = \frac{1}{\sqrt{6}} \begin{pmatrix} -2 \\ 1 \\ 1 \end{pmatrix}, \quad \Phi_2 = \frac{1}{\sqrt{3}} \begin{pmatrix} 1 \\ 1 \\ 1 \end{pmatrix}, \quad \Phi_3 = \frac{1}{\sqrt{2}} \begin{pmatrix} 0 \\ 1 \\ -1 \end{pmatrix}. \quad (3.41)$$

³Note that other BSM lepton number violating mechanism can lead to $2\beta_{0\nu}$ as well. It was shown however, that regardless of the underlying mechanism of $2\beta_{0\nu}$, neutrinos feature Majorana masses in all cases, due to a ‘‘black-box’’ theorem [71].

When the small neutrino masses result from a type-I seesaw with diagonal heavy right-handed neutrino mass matrix M_ν , the columns of the neutrino Yukawa matrix Y_ν are proportional to the columns Φ_i

$$m_\nu = -\frac{v^2}{2} Y_\nu M_\nu^{-1} Y_\nu^T = -\frac{v^2}{2} \left(\frac{\epsilon_1^2}{M_1} \Phi_1 \Phi_1^T + \frac{\epsilon_2^2}{M_2} \Phi_2 \Phi_2^T + \frac{\epsilon_3^2}{M_3} \Phi_3 \Phi_3^T \right), \quad (3.42)$$

where ϵ_i parametrise small couplings. If the lightest neutrino is massless, the first column Φ_1 can be dropped and one is left with so-called *Constrained Sequential Dominance* (CSD) [17, 66], where the neutrino Yukawa and mass matrices are given by

$$Y_\nu = \begin{pmatrix} \epsilon_2 & 0 \\ \epsilon_2 & \epsilon_3 \\ \epsilon_2 & -\epsilon_3 \end{pmatrix}, \quad M_\nu = \begin{pmatrix} M_2 & 0 \\ 0 & M_3 \end{pmatrix}. \quad (3.43)$$

The resulting neutrino masses and lepton mixing feature NO and TBM. An inverse neutrino mass ordering and bimaximal mixing can be obtained with a Dirac pair of two heavy right-handed neutrinos, such that M_ν is off-diagonal, and a neutrino Yukawa coupling matrix given by [74]

$$Y_\nu = \begin{pmatrix} a & 0 \\ 0 & b \\ 0 & c \end{pmatrix}, \quad M_\nu = \begin{pmatrix} 0 & M \\ M & 0 \end{pmatrix}. \quad (3.44)$$

We will revisit these two configurations of the neutrino sector in chapters 7 and 8, when we present two SUSY flavour GUT models in part III of this thesis.

The general idea of flavour models originates in the attempt to explain hierarchical Yukawa couplings and mixing angles from a spontaneously broken Abelian flavour symmetry $U(1)_{\text{FN}}$ [75]. Each generation of matter fields carries a different charge under $U(1)_{\text{FN}}$, thereby requiring varying numbers of insertions of the flavour symmetry breaking *flavon* fields Φ , in order to form (non-renormalisable) neutral Yukawa operators. When the flavour symmetry is spontaneously broken, the Yukawa couplings emerge from the flavon vevs

$$Y \sim \left(\frac{\langle \Phi \rangle}{\Lambda} \right)^n, \quad (3.45)$$

where Λ is a high energy scale. Thus flavour models replace Yukawa couplings by vevs of dynamical fields. In order to explain not only the hierarchy of Yukawa couplings, but also special structures (like in (3.43)), non-Abelian flavour symmetries are necessary. Because there are three generations, non-Abelian groups which feature a triplet representation are prominent candidates for flavour symmetries. In CSD the flavons are also triplets and their vevs are aligned such that

$$\langle \Phi_2 \rangle \sim \begin{pmatrix} 1 \\ 1 \\ 1 \end{pmatrix} \quad \text{and} \quad \langle \Phi_3 \rangle \sim \begin{pmatrix} 0 \\ 1 \\ -1 \end{pmatrix}. \quad (3.46)$$

A complete flavour model will not only build the neutrino Yukawa matrix from flavons, but the rows or columns of all Yukawa matrices will be obtained from vevs of flavons. To this end a flavour model must also include a suitable potential which guarantees the desired alignment of flavon vevs in flavour space.

There are several choices for symmetry groups G that can be used to successfully construct flavour models. One example is the discrete group A_4 (cf. [76–78] and appendix A). In part III two predictive flavour GUT models are presented, using a supersymmetric $SU(5)$ GUT and A_4 flavour symmetry.

CHAPTER 4

Grand Unified Theories

Ignoring the evidence of massive neutrinos for the moment, the Standard Model is remarkably successful in describing particle physics phenomena. Yet there are some deficiencies such as the unexplained charge quantisation of $U(1)_{\text{em}}$ or the “miraculous” anomaly cancellation. Arguably, the fact that the SM features three gauge couplings and five distinct representations of matter fields may be viewed as the SM being too elaborate. A very attractive solution to these questions at hand is the unification of SM forces and representations, respectively. If the SM gauge groups are embedded into one single gauge group, such a theory of unification is denoted *Grand Unified Theory* (GUT). Since GUTs also enable quark and lepton unification, they are an appealing BSM setting to tackle the flavour problem.

In this chapter we review the theoretical framework of $SU(5)$ GUTs [79] and proton decay, necessary for the understanding of the main part of this thesis, based loosely on [80–82]. The subject of supersymmetric GUTs will be discussed in the next chapter. In the final section of this chapter we briefly discuss the appearance of group-theoretical Clebsch-Gordan factors in predictions for GUT scale Yukawa coupling matrices [83].

4.1 The Georgi-Glashow $SU(5)$ model

Any GUT gauge group must contain the SM gauge group as subgroup. Since $SU(3)_C \times SU(2)_L \times U(1)_Y$ has rank four, any GUT gauge group must be at least of rank four as well. The simple group $SU(5)$ is of rank four and remarkably allows to fit all SM fields into $SU(5)$ representations, without having to introduce new matter fields.

In order to discuss how the SM gauge group is embedded into $SU(5)$, one first must reassure that the SM gauge couplings do indeed unify at a higher energy scale. To this end the $U(1)_Y$ gauge coupling g' needs to be normalised to match the normalisation of the non-Abelian $SU(N)$ gauge groups. As discussed in appendix A, the $SU(N)$ generators are normalised as

$$\text{Tr } T^a T^b = \frac{1}{2} \delta^{ab} . \quad (4.1)$$

The fundamental representation of $SU(5)$ decomposes into the SM gauge group representations as¹

$$\mathbf{5} = (\mathbf{3}, \mathbf{1})_{-\frac{1}{3}} + (\mathbf{1}, \mathbf{2})_{\frac{1}{2}}. \quad (4.2)$$

One can therefore identify $\mathbf{5}$ with d_R and the charge-conjugated lepton-doublet L^c . The trace over the $U(1)_Y$ hypercharges within $\mathbf{5}$ is thus given by

$$\text{Tr } Q_Y^2 = \frac{5}{6}, \quad (4.3)$$

from which one can determine the GUT normalisation of hypercharge to be

$$Q_Y = \sqrt{\frac{5}{3}} Q_{Y^{\text{GUT}}} \quad \text{and} \quad g' = \sqrt{\frac{3}{5}} g_1. \quad (4.4)$$

One can now study the renormalisation group equations (RGEs) for the gauge couplings g_1 , g_2 , and g_3 , which at the one-loop level are

$$\mu \frac{d}{d\mu} g_a = \frac{g_a^3}{16\pi^2} b_a, \quad (4.5)$$

with $b_1 = \frac{41}{10}$, $b_2 = -\frac{19}{6}$, and $b_3 = -7$ for SM field content [86]. If the three gauge couplings unite into one gauge coupling g_5 at high energy, one could replace the SM gauge group with the GUT gauge group. Starting from the experimental values for the gauge couplings at M_Z and evolving them to higher energy, one finds however that the gauge coupling unification condition

$$g_5 \equiv g_1 = g_2 = g_3 \quad (4.6)$$

is never sufficiently satisfied. As will be discussed in the next section, this problem is solved when supersymmetry is introduced. For the moment we consider the energy scale of approximately 10^{15} GeV, where the discrepancy of gauge coupling unification is the smallest, as unification scale $M_{GUT} \sim 10^{15}$ GeV, and continue with the field content of the Georgi-Glashow $SU(5)$ model [79].

The irreducible $SU(5)$ representations $\bar{\mathbf{5}}$, $\mathbf{10}$, and $\mathbf{24}$ decompose under the SM gauge group as

$$\begin{aligned} \bar{\mathbf{5}} &= (\bar{\mathbf{3}}, \mathbf{1})_{\frac{1}{3}} + (\mathbf{1}, \mathbf{2})_{-\frac{1}{2}}, \\ \mathbf{10} &= (\mathbf{3}, \mathbf{2})_{\frac{1}{6}} + (\bar{\mathbf{3}}, \mathbf{1})_{-\frac{2}{3}} + (\mathbf{1}, \mathbf{1})_1, \\ \mathbf{24} &= (\mathbf{8}, \mathbf{1})_0 + (\mathbf{3}, \mathbf{2})_{-\frac{5}{6}} + (\bar{\mathbf{3}}, \mathbf{2})_{\frac{5}{6}} + (\mathbf{1}, \mathbf{3})_0 + (\mathbf{1}, \mathbf{1})_0. \end{aligned} \quad (4.7)$$

¹Throughout this thesis, all decompositions of $SU(N)$ and $SO(N)$ representations have been obtained with [84] (see also [85]).

Thus for each generation one can embed the three charge-conjugated down type quark fields d_R^\dagger and the lepton-doublet² L into a joint field \mathcal{F} transforming as $\bar{\mathbf{5}}$

$$\mathcal{F} = \begin{pmatrix} d_{RR}^\dagger \\ d_{RB}^\dagger \\ d_{RG}^\dagger \\ e \\ -\nu \end{pmatrix}, \quad (4.8)$$

where R , B , and G denote the three colors of QCD. The remaining matter fields fit into the antisymmetric $\mathbf{10}$ as charged-conjugated u_R^\dagger and e_R^\dagger , and quark doublet Q

$$\mathcal{T} = \frac{1}{\sqrt{2}} \begin{pmatrix} 0 & -u_{RG}^\dagger & u_{RB}^\dagger & -u_{LR} & -d_{LR} \\ u_{RG}^\dagger & 0 & -u_{RR}^\dagger & -u_{LB} & -d_{LB} \\ -u_{RB}^\dagger & u_{RR}^\dagger & 0 & -u_{LG} & -d_{LG} \\ u_{LR} & u_{LB} & u_{LG} & 0 & -e_R^\dagger \\ d_{LR} & d_{LB} & d_{LG} & e_R^\dagger & 0 \end{pmatrix}. \quad (4.9)$$

Right-handed neutrinos can be added as singlet fields, such that neutrino masses can arise via the see-saw type-I mechanism. It is now easy to understand the origin of $U(1)_{\text{em}}$ charge quantisation: When $SU(5)$ gets broken into the SM subgroup, the $U(1)_Y$ generator arises from the diagonal $SU(5)$ generator³

$$T_0 = \sqrt{\frac{3}{5}} \text{diag} \left(-\frac{1}{3}, -\frac{1}{3}, -\frac{1}{3}, \frac{1}{2}, \frac{1}{2} \right), \quad (4.10)$$

and the Q_Y hypercharges of the SM matter fields emerge from the embedding (4.7) of the SM representation into $SU(5)$ representations. The electric charge operator is

$$Q_e = T_3 + \sqrt{\frac{5}{3}} T_0 = \text{diag} \left(-\frac{1}{3}, -\frac{1}{3}, -\frac{1}{3}, 1, 0 \right), \quad (4.11)$$

which explains the fractional electric charge of quarks from the fact that quarks come in three colours and $SU(5)$ generators are traceless. Overall the peculiar $U(1)_Y$ hypercharge assignment of the SM fields in table 2.1 is strikingly explained when the SM is embedded into $SU(5)$.

Note that the Georgi-Glashow model is anomaly free, since the contributions from \mathcal{F} and \mathcal{T} to the anomaly coefficients cancel.

The gauge bosons G_μ , W_μ , and B_μ are contained in the adjoint $\mathbf{24}$. Finally $\mathbf{24}$ also contains twelve additional gauge fields in $(\mathbf{3}, \mathbf{2})_{-\frac{5}{6}}$ and $(\bar{\mathbf{3}}, \mathbf{2})_{\frac{5}{6}}$, which do not correspond to any existing SM field. These new *leptoquark* gauge bosons are named X and Y , respectively,

²Note that $\bar{\mathbf{5}}$ contains the $SU(2)$ conjugate ϵL , which explains the sign of ν in (4.8).

³The $SU(3)_C$ generators are embedded into the 3×3 upper-left block and the $SU(2)_L$ generators into the 2×2 lower-right block of the $SU(5)$ generators.

and carry $SU(2)$ and $SU(3)$ indices. The Higgs boson ϕ is supplemented by a new coloured scalar Higgs triplet $T^{(5)}$ and embedded into a fundamental H_5

$$H_5 = \begin{pmatrix} T_R^{(5)} \\ T_B^{(5)} \\ T_G^{(5)} \\ \phi^+ \\ \phi^0 \end{pmatrix}. \quad (4.12)$$

To spontaneously break $SU(5)$ down to the SM subgroup, one introduces a Higgs field H_{24} transforming in the adjoint representation $\mathbf{24}$, which obtains a vev aligned along the hypercharge direction

$$\langle H_{24} \rangle = V \text{diag} \left(1, 1, 1, -\frac{3}{2}, -\frac{3}{2} \right). \quad (4.13)$$

Equation (4.13) is obtained as global minimum of the most general renormalisable potential for the adjoint⁴

$$V(H_{24}) = -\frac{m_{24}^2}{2} \text{Tr} H_{24}^2 + \frac{\lambda_{24}}{4} (\text{Tr} H_{24}^2)^2 + \frac{\lambda'_{24}}{4} \text{Tr} H_{24}^4, \quad (4.14)$$

when the parameters satisfy $m_{24}, \lambda'_{24} > 0$, and $\lambda_{24} > -\frac{7}{30} \lambda'_{24}$. Because $\langle H_{24} \rangle$ commutes with the $SU(5)$ generators of the SM subgroup, the SM gauge group remains unbroken, while the X and Y gauge bosons acquire a heavy mass due to the BEH mechanism

$$M_X^2 = M_Y^2 = \frac{25}{8} g_5^2 V^2. \quad (4.15)$$

One identifies M_X with the mass scale of GUT unification $M_{\text{GUT}} \equiv M_X$. Expanding H_{24} around its vev one finds that twelve degrees of freedom are would-be Goldstone bosons and absorbed by the massive gauge fields X and Y . The remaining degrees of freedom are transforming as one $SU(3)_C$ octet $O^{(24)}$, one $SU(2)_L$ triplet $T^{(24)}$, and one total singlet $S^{(24)}$, with masses

$$m_{O^{(24)}}^2 = \frac{5}{8} \lambda'_{24} V^2, \quad m_{T^{(24)}}^2 = \frac{5}{2} \lambda'_{24} V^2, \quad m_{S^{(24)}}^2 = m_{24}^2. \quad (4.16)$$

The full scalar potential also includes the Higgs boson H_5 and (4.14) is extended to

$$\begin{aligned} V(H_{24}, H_5^\dagger H_5) &= V(H_{24}) - \mu_5^2 (H_5^\dagger H_5) + \lambda_5 (H_5^\dagger H_5)^2 \\ &\quad + \lambda' H_5^\dagger H_5 \text{Tr} H_{24}^2 + \lambda'' H_5^\dagger H_{24}^2 H_5. \end{aligned} \quad (4.17)$$

⁴For simplicity we assume that H_{24} carries charge 1 under an additional \mathbb{Z}_2 symmetry, which however is not a necessary condition for the potential V to obtain (4.13).

With $\mu_5, m_{24} > 0$, $\lambda'_{24} > 0 > \lambda''$, $\lambda_{24} < -\frac{7}{30}\lambda'_{24}$, $\lambda' > -\frac{3}{10}\lambda''$, and $\lambda_5 > (\lambda' + \frac{3}{10}\lambda'') \frac{\mu_5^2}{m_{24}^2}$ the potential (4.17) is minimised by $\langle H_{24} \rangle$ and the non-vanishing vev

$$\langle H_5 \rangle = \frac{1}{\sqrt{2}} \begin{pmatrix} 0 \\ 0 \\ 0 \\ 0 \\ v \end{pmatrix}, \quad (4.18)$$

which spontaneously breaks the Electroweak symmetry to $U(1)_{\text{em}}$.⁵ The two vevs $\langle H_{24} \rangle$ and $\langle H_5 \rangle$ thus spontaneously break $SU(5) \rightarrow SU(3)_C \times U(1)_{\text{em}}$. The masses of the coloured triplet $T^{(5)}$ and the SM Higgs boson h are given by

$$m_{T^{(5)}}^2 = -\frac{5}{4}\lambda''V^2 \quad \text{and} \quad m_h^2 = \lambda_5v^2. \quad (4.19)$$

In the next section it will be discussed that the coloured triplet $T^{(5)}$ mediates proton decay, which leads to a lower bound of $m_{T^{(5)}} \gtrsim 10^{12}$ GeV. The Higgs mass on the other hand is $m_h \sim 125$ GeV, leading to the so-called *doublet-triplet splitting* (DTS) problem. It is related to the hierarchy problem and can be accounted for by a fine-tuning of the potential's parameters λ' and λ'' , as can be seen for example from the solution

$$v^2 = \frac{\mu_5^2 - (\frac{30}{4}\lambda' + \frac{9}{4}\lambda'')V^2}{\lambda_5}. \quad (4.20)$$

In SUSY $SU(5)$ the DTS problem is tightened due to new proton decay mediating operators involving sparticles. We will return to the DTS problem in section 5.5 and chapter 9.

We close this section with a discussion of the Yukawa sector of the Georgi-Glashow model. There are two $SU(5)$ invariant Yukawa operators

$$\mathcal{L}_Y = -Y_5 \mathcal{T}_{ij} \mathcal{F}^i (H_5^*)^j - Y_{10} \epsilon^{ijklm} \mathcal{T}_{ij} \mathcal{T}_{kl} (H_5)_m + h.c., \quad (4.21)$$

where i, j, \dots, m denote $SU(5)$ indices and we have suppressed flavour indices for readability. When $SU(5)$ gets broken (4.21) decomposes into the SM Yukawa interactions

$$\mathcal{L}_Y = -4Y_{10} Q \cdot \phi u_R^\dagger + \frac{1}{\sqrt{2}} Y_5 Q \cdot \tilde{\phi} d_R^\dagger + \frac{1}{\sqrt{2}} Y_5^T L \cdot \tilde{\phi} e_R^\dagger + h.c., \quad (4.22)$$

and new Yukawa interactions between the coloured triplet $T^{(5)}$ and the matter fields

$$\mathcal{L}_{Y_{T^{(5)}}} = -\frac{1}{\sqrt{2}} Y_5 \left(Q \cdot L - u_R^\dagger d_R^\dagger \right) T^{(5)*} - 2Y_{10} \left(2u_R^\dagger e_R^\dagger - Q \cdot Q \right) T^{(5)} + h.c.. \quad (4.23)$$

Comparison with (2.2) gives the following $SU(5)$ GUT scale predictions for the Yukawa matrices

$$Y_d = Y_e^T, \quad Y_u = Y_u^T. \quad (4.24)$$

⁵ $\langle H_5 \rangle$ also leads to negligibly small shifts of $\mathcal{O}(v/V)$ in the heavy masses of (4.16).

The GUT scale relation $Y_d = Y_e^T$ is however refuted by the observed quark and lepton masses, when an RG analysis to M_{GUT} is performed. This problem can be solved by adding a new Higgs field H_{45} transforming as **45** [87]. Under the SM gauge group **45** decomposes as

$$\mathbf{45} = (\mathbf{3}, \mathbf{1})_{-\frac{1}{3}} + (\mathbf{1}, \mathbf{2})_{\frac{1}{2}} + (\bar{\mathbf{3}}, \mathbf{1})_{\frac{4}{3}} + (\bar{\mathbf{3}}, \mathbf{2})_{-\frac{7}{6}} + (\mathbf{3}, \mathbf{3})_{-\frac{1}{3}} + (\bar{\mathbf{6}}, \mathbf{1})_{-\frac{1}{3}} + (\mathbf{8}, \mathbf{2})_{\frac{1}{2}}, \quad (4.25)$$

therefore the SM Higgs field ϕ can be embedded in H_{45} . Writing $SU(5)$ tensor indices explicitly, H_{45} is given by $(H_{45})_k^{ij} = -(H_{45})_k^{ji}$ with vanishing trace $(H_{45})_i^i = 0$. When H_{45} obtains a vev, $SU(3)_C$ must not be broken and because of the traceless condition the vev is given by

$$\langle (H_{45})_k^{i5} \rangle = v (\delta_k^i - 4\delta^{i4}\delta^{k4}) \quad i, k = 1, \dots, 4, \quad (4.26)$$

such that the term giving mass to the charged leptons compensates for the number of colours. Invoking new global symmetries, one can construct a Lagrange density such that H_{45} couples exclusively to the second family

$$\mathcal{L}_Y \supset -y_s (\mathcal{T}_2)_{ij} \mathcal{F}_2^k (H_{45}^*)_{k}^{ij}, \quad (4.27)$$

whereas the remaining matter fields couple to H_5 .⁶ The resulting GUT scale Yukawa coupling ratios are known as the Georgi-Jarlskog (GJ) relations [87]

$$y_\mu = 3y_s, \quad y_e = \frac{1}{3}y_d, \quad (4.28)$$

where the second relation also requires vanishing 1-1 element of Y_5 . We will discuss later, that the GJ relations are also challenged by the data today. In section 4.4 we will review other predictions for GUT scale Yukawa coupling ratios, when higher-dimensional operators involving the adjoint are constructed.

The crucial point is that within the framework of GUTs predictions for quark and lepton mass ratios are constructed, setting the stage for flavour models.

4.2 Proton decay in $SU(5)$

The unification of quarks and leptons into joint representations inevitably enables baryon and lepton number violating operators and thus predicts proton decay. Figure 4.1 shows how exchange of the heavy gauge bosons X and Y leads to baryon number violating operators, which can mediate proton decay, like for example $p \rightarrow e^+ + \pi^0$, as shown in figure 4.2. In the effective theory where the heavy gauge bosons are integrated out, dimension 6 proton decay operators emerge proportional to the $SU(5)$ gauge coupling g_5 and M_{GUT} [82]

$$\mathcal{L}_{\mathcal{B}} = \frac{g_5^2}{2M_{\text{GUT}}^2} \left(u_R^\dagger \bar{\sigma} Q \cdot e_R^\dagger \bar{\sigma} Q + u_R^\dagger \bar{\sigma} Q \cdot d_R^\dagger \bar{\sigma} L \right). \quad (4.29)$$

⁶Because of the additional shaping symmetries, in flavour GUT models several H_5 's might be required.

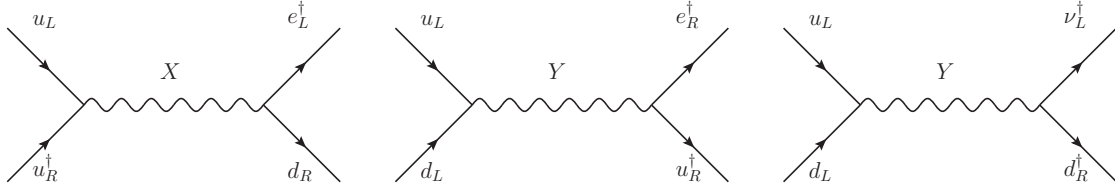


Figure 4.1: Baryon number violating operators mediating proton decay due to heavy gauge boson exchange.

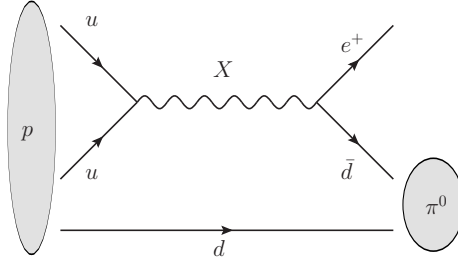


Figure 4.2: Feynman diagram for the proton decay $p \rightarrow e^+ \pi^0$ mediated by the heavy gauge boson X .

The amplitude for proton decay depends on the RG evolution and the quark and lepton mixing matrices. Based on dimensional analysis there is a model-independent estimate for the proton decay rate

$$\Gamma_p \approx \alpha_5^2 \frac{m_p^5}{M_{\text{GUT}}^4}, \quad (4.30)$$

where $\alpha_5 \equiv \frac{g_5^2}{4\pi^2}$ and $m_p \sim 938$ MeV is the proton mass. The most stringent bound on the proton lifetime is $\tau(p \rightarrow e^+ + \pi^0) > 8 \cdot 10^{33}$ years [14], which yields a lower bound for the GUT scale of

$$M_{\text{GUT}} \gtrsim 10^{16} \text{ GeV}, \quad (4.31)$$

for $\alpha_5 \approx \frac{1}{25}$. The too high proton decay rate predicted by the unification scale $M_{\text{GUT}} = 10^{15}$ GeV is another problem that can be elegantly solved in SUSY $SU(5)$, where the unification scale can easily be above 10^{16} GeV, as discussed in 5.5 and 9.3.

Besides the heavy X and Y bosons, also the colour triplet $T^{(5)}$ can mediate proton decay via the Yukawa couplings to quarks and leptons shown in (4.23) and figure 4.3. Like for the heavy gauge boson mediated proton decay, the decay rate is flavour model dependent. Again an estimate based on dimensional grounds is [82]

$$\Gamma_p \approx |y_u y_d|^2 \frac{m_p^5}{m_{T^{(5)}}^4}, \quad (4.32)$$

where y_u and y_d are the Yukawa couplings of the first generation quarks. The lower bound for the mass of the coloured triplet is then given by

$$m_{T^{(5)}} > 5 \cdot 10^{11} \text{ GeV}, \quad (4.33)$$

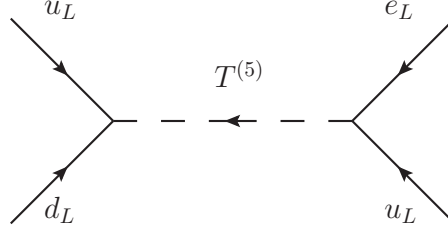


Figure 4.3: Example for a baryon violating operator mediating proton decay through a heavy coloured triplet.

with $y_u y_d \approx 4 \cdot 10^{-10}$. Thus we have identified the root of the doublet-triplet splitting problem, in order to prevent too rapid proton decay the triplet in H_5 has to be many orders of magnitude heavier than the doublet, whose mass is at the electroweak scale.

4.3 Pati-Salam unification and $SO(10)$

The main part of this thesis is dedicated to SUSY flavour models in $SU(5)$ grand unification. We therefore only briefly discuss unification in Pati-Salam (PS) [88] and $SO(10)$ [89] gauge groups in this section.

The Pati-Salam gauge group is $SU(4)_C \times SU(2)_L \times SU(2)_R$ with the underlying idea to identify leptons as fourth colour of $SU(4)_C$. The SM matter content can be embedded into two representations \mathcal{Q}_L and \mathcal{Q}_R transforming as $(\mathbf{4}, \mathbf{2}, \mathbf{1})$ and $(\bar{\mathbf{4}}, \mathbf{1}, \mathbf{2})$, respectively. Under the SM gauge group they decompose as

$$\begin{aligned} (\mathbf{4}, \mathbf{2}, \mathbf{1}) &= (\mathbf{3}, \mathbf{2})_{\frac{1}{6}} + (\mathbf{1}, \mathbf{2})_{-\frac{1}{2}} \\ (\bar{\mathbf{4}}, \mathbf{1}, \mathbf{2}) &= (\bar{\mathbf{3}}, \mathbf{1})_{\frac{1}{3}} + (\mathbf{3}, \mathbf{1})_{-\frac{2}{3}} + (\mathbf{1}, \mathbf{1})_1 + (\mathbf{1}, \mathbf{1})_0 . \end{aligned} \quad (4.34)$$

Therefore the SM $SU(2)_L$ doublets Q and L are embedded into \mathcal{Q}_L and the charge-conjugated fields u_R^\dagger , d_R^\dagger , and e_R^\dagger are embedded into \mathcal{Q}_R . The multiplet \mathcal{Q}_R is completed with a SM singlet field, which can be identified with the charge-conjugate of a heavy right-handed neutrino ν_R^\dagger . Thus massive neutrinos arise as prediction from PS unification. The SM Higgs doublet is contained in \mathcal{H} , transforming as

$$(\mathbf{1}, \mathbf{2}, \mathbf{2}) = (\mathbf{1}, \mathbf{2})_{\frac{1}{2}} + (\mathbf{1}, \mathbf{2})_{-\frac{1}{2}} . \quad (4.35)$$

The most general renormalisable Yukawa interaction Lagrange density in PS is thus

$$\mathcal{L}_{Y_{PS}} = -Y_{PS} \mathcal{Q}_L \mathcal{H} \mathcal{Q}_R . \quad (4.36)$$

When the PS gauge group is broken to the SM, this gives rise to the (very bad) GUT scale predictions

$$Y_u = Y_d = Y_e = Y_\nu . \quad (4.37)$$

These GUT scale relations can be improved. The GJ relations for example are obtained with a new Higgs field transforming as

$$\begin{aligned} (\mathbf{15}, \mathbf{2}, \mathbf{2}) &= (\mathbf{1}, \mathbf{2})_{\frac{1}{2}} + (\mathbf{1}, \mathbf{2})_{-\frac{1}{2}} + (\mathbf{3}, \mathbf{2})_{\frac{7}{6}} + (\mathbf{3}, \mathbf{2})_{\frac{1}{6}} \\ &\quad + (\bar{\mathbf{3}}, \mathbf{2})_{-\frac{7}{6}} + (\bar{\mathbf{3}}, \mathbf{2})_{-\frac{1}{6}} + (\mathbf{8}, \mathbf{2})_{\frac{1}{2}} + (\mathbf{8}, \mathbf{2})_{-\frac{1}{2}} , \end{aligned} \quad (4.38)$$

since the $SU(4)_C$ adjoint $\mathbf{15}$ is traceless and the leptons compensate for the number of three colours, when $SU(4)_C$ is broken to $SU(3)_C$. Another method to obtain better GUT scale Yukawa coupling ratios is to introduce non-renormalisable operators, as outlined in the next section.

Pati-Salam is a partial unified theory and has three distinct gauge couplings⁷, opposite to complete gauge coupling unification in a grand unified theory. It is possible, however, to embed PS into a simple GUT gauge group $SO(10)$ [89]. All SM matter fields of one generation plus one right-handed neutrino fit into a single field \mathcal{Q}_{16} , transforming in the 16-dimensional spinor representation of $SO(10)$

$$\begin{aligned} \mathbf{16} &= (\mathbf{4}, \mathbf{2}, \mathbf{1}) + (\bar{\mathbf{4}}, \mathbf{1}, \mathbf{2}) \\ &= (\mathbf{3}, \mathbf{2})_{\frac{1}{6}} + (\mathbf{1}, \mathbf{2})_{-\frac{1}{2}} + (\bar{\mathbf{3}}, \mathbf{1})_{\frac{1}{3}} + (\mathbf{3}, \mathbf{1})_{-\frac{2}{3}} + (\mathbf{1}, \mathbf{1})_1 + (\mathbf{1}, \mathbf{1})_0 , \end{aligned} \quad (4.39)$$

where the first row shows the decomposition into the PS and the second row into the SM gauge group. With all matter fields contained in one single GUT representation, $SO(10)$ has the benefit of being anomaly free without the requirement of any cancellation between different fields. The SM Higgs field is contained in \mathcal{H}_{10} , transforming as

$$\begin{aligned} \mathbf{10} &= (\mathbf{1}, \mathbf{2}, \mathbf{2}) + (\mathbf{6}, \mathbf{1}, \mathbf{1}) \\ &= (\mathbf{1}, \mathbf{2})_{\frac{1}{2}} + (\mathbf{1}, \mathbf{2})_{-\frac{1}{2}} + (\mathbf{3}, \mathbf{1})_{-\frac{1}{3}} + (\bar{\mathbf{3}}, \mathbf{1})_{\frac{1}{3}} . \end{aligned} \quad (4.40)$$

In $SO(10)$ the most general renormalisable Yukawa coupling interaction is then simply given by

$$\mathcal{L}_{Y_{SO(10)}} = -Y_{SO(10)} \mathcal{Q}_{16} \mathcal{H}_{10} \mathcal{Q}_{16} , \quad (4.41)$$

with symmetric $Y_{SO(10)}$. This also yields the GUT scale relations (4.37) with the additional prediction of symmetric Yukawa matrices. Again, also in $SO(10)$ GUT model building one can construct GJ relations by a Higgs transforming in

$$\mathbf{126} = (\mathbf{15}, \mathbf{2}, \mathbf{2}) + (\mathbf{6}, \mathbf{1}, \mathbf{1}) + (\mathbf{10}, \mathbf{1}, \mathbf{3}) + (\bar{\mathbf{10}}, \mathbf{3}, \mathbf{1}) , \quad (4.42)$$

which contains the $(\mathbf{15}, \mathbf{2}, \mathbf{2})$ of PS for the GJ relations. Due to the high dimensionality of $\mathbf{126}$ we refrain from showing the SM decomposition.

PS is not the only subgroup of $SO(10)$ which contains the SM gauge group. $SO(10)$ can also be broken into $SU(5) \times U(1)_X$, therefore Georgi-Glashow $SU(5)$ as well as so-called *flipped* $SU(5)$ [90] can be embedded into $SO(10)$. The breaking mechanisms of $SO(10) \rightarrow SU(4)_C \times SU(2)_L \times SU(2)_R \rightarrow SU(3)_C \times SU(2)_L \times U(1)$ and $SO(10) \rightarrow$

⁷Two if one requires left-right symmetry.

$SU(5) \times U(1)_X \rightarrow SU(3)_C \times SU(2)_L \times U(1)$ are rather complicated and involve several GUT-breaking Higgs fields. Since the flavour models in the main part of this thesis are $SU(5)$ GUTs, the details of $SO(10)$ and subsequently PS breaking are of no relevance for this thesis and therefore not discussed.

4.4 GUT scale Yukawa coupling ratios

The $SU(5)$ and PS predictions of $Y_e = Y_d^T$ and $Y_e = Y_d = Y_u$, respectively, are highly disfavoured by experimental results, when the RG evolution of the particle masses (or rather their Yukawa couplings) to the GUT scale is studied.⁸ A convenient test whether GUT predictions for the first two families are consistent with the experimental data is provided by the - RG invariant and SUSY threshold correction invariant⁹ - double ratio [91]

$$\left| \frac{y_\mu y_d}{y_s y_e} \right| \approx 10.7_{-0.8}^{+1.8}. \quad (4.43)$$

Thus also the GJ relations (4.28) are in tension with experimental observations, since they yield a double ratio of 9 and thus deviate from the constraint (4.43) by more than two sigma.

The problem of poor GUT scale predictions can be solved when the Yukawa couplings are effective higher-dimensional operators, containing a GUT breaking Higgs field. When the GUT gauge group gets spontaneously broken to the SM, new GUT scale Yukawa coupling ratios arise due to the appearance of group theoretical Clebsch-Gordan (CG) factors [83].

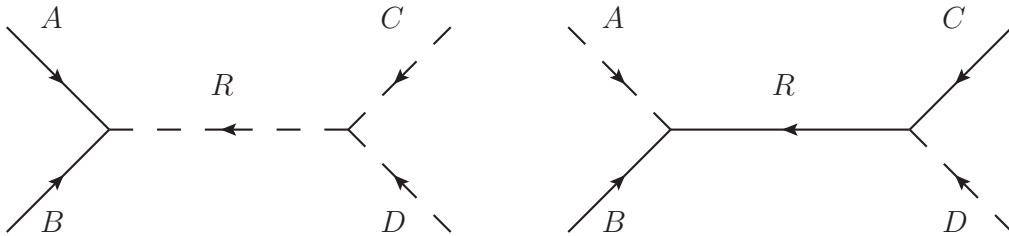


Figure 4.4: Feynman diagrams with heavy messenger fields R give rise to the effective dimension 5 operators $ABCD$, thereby new GUT-scale predictions for the Yukawa coupling ratios arise from group-theoretical CG factors.

Generally, in a higher-dimensional operator involving GUT non-singlet fields there are several possibilities how the GUT group indices are contracted to form a gauge singlet, yielding a non predictive, arbitrary linear combination of multiple CG factors. For example in $SU(5)$ GUTs the dimension five operator $\mathcal{FT}(H_5)^* H_{24}$ yields a linear combination of the GUT scale Yukawa couplings ratios 1 and -3 . In order to restore predictivity in a

⁸SUSY threshold effects in RG analyses are discussed in section 5.4 and chapter 10.

⁹As long as the first two families of sfermions are almost degenerate in mass, as commonly assumed.

specific flavour GUT model, one therefore must introduce heavy *messenger fields* in GUT non-singlet representations, which *UV complete* the model at high energy and single out a specific GUT index contraction. This guarantees that only an unique effective operator with defined CG factor is constructed in the effective theory, when the heavy messenger field is integrated out. Figure 4.4 shows the two Feynman diagrams yielding predictive effective dimension five operators. In table 4.1 some examples are shown for the case of an $SU(5)$ GUT. If for example the effective operator $\mathcal{FT}(H_5)^*H_{24}$ is obtained via a messenger

AB	CD	R	$(Y_e)_{ji}/(Y_d)_{ij}$
\mathcal{FT}	$H_5^* H_{24}$	$\bar{\mathbf{5}}$	1
\mathcal{FT}	$H_5^* H_{24}$	$\overline{\mathbf{45}}$	-3
$H_{24}\mathcal{F}$	$\mathcal{T}H_{45}^*$	$\mathbf{45}$	$-\frac{1}{2}$
$H_{24}\mathcal{F}$	$\mathcal{T}H_5^*$	$\mathbf{5}$	$-\frac{3}{2}$
$H_{24}\mathcal{T}$	$\mathcal{F}H_5^*$	$\overline{\mathbf{10}}$	6

Table 4.1: CG factors for the dimension five effective operators from figure 4.4. The upper part corresponds to the left diagram, the lower one to the right one. See the main text for details.

field Φ_R transforming as $\overline{\mathbf{45}}$

$$\mathcal{L} \supset -\lambda\mathcal{FT}\Phi_R - mH_5^*H_{24}\Phi_R^* - m_{\Phi_R}^2\Phi_R\Phi_R^*, \quad (4.44)$$

the unique CG factor -3 arises as prediction for the GUT scale Yukawa coupling ratios. If one would use instead a messenger field transforming as $\bar{\mathbf{5}}$, one would obtain the CG factor 1.

In table 4.1 we have also listed the $SU(5)$ CG factors $-\frac{1}{2}$, $-\frac{3}{2}$, and 6, since they are of special importance in the main part of this thesis. The full list of possible CG factors c_i in $SU(5)$ is given by [83]

$$c_i \in \left\{-\frac{1}{2}, 1, \pm\frac{3}{2}, -3, \frac{9}{2}, 6, 9, -18\right\}. \quad (4.45)$$

In PS partial unification one also finds CG factors for the Yukawa coupling ratios $(Y_e)_{ij}/(Y_d)_{ij}$, as well as $(Y_u)_{ij}/(Y_d)_{ij}$ from higher-dimensional operators. An extensive list of CG predictions from dimension 5 and dimension 6 operators in PS embedded in $SO(10)$ is found in [83] (see also [92]). We will be only interested in the relations between Y_e and Y_d in PS, for which for example the CG factors

$$c_i \in \left\{\frac{3}{4}, 1, 2, -3, 9\right\} \quad (4.46)$$

are available.

In a recent paper [93] further new CG factors were obtained, by replacing the masses of the messengers fields with vevs from non-singlet fields. These new CG factors for Y_e/Y_d are given by

$$c_i \in \begin{cases} \{-\frac{2}{3}, \frac{1}{6}\} & \text{in SU(5) ,} \\ \{-\frac{1}{3}, 0, \frac{3}{2}\} & \text{in PS .} \end{cases} \quad (4.47)$$

Utilising CG factors for quark and lepton Yukawa coupling ratios will be an essential concept in the flavour GUT models of this thesis.

CHAPTER 5

Supersymmetry

The Georgi-Glashow $SU(5)$ model beautifully unifies the SM matter fields into the joint representation \mathcal{F} and \mathcal{T} , enabling the construction of predictions for quark - lepton Yukawa coupling ratios. There are two problems however: Firstly the SM gauge couplings never unite satisfactory, and secondly there is the prediction of too rapid proton decay due to heavy gauge boson mediation. Remarkably, both problems can be solved at once with the introduction of supersymmetry (SUSY).

In a nutshell, SUSY is a symmetry transforming fermions into bosons and vice versa. The minimal supersymmetric Standard Model (MSSM) predicts the existence of a scalar particle for each SM fermion and a Majorana fermion for each gauge boson of the SM. When these additional supersymmetric partners (sparticles) of the SM particles have not too heavy masses, the MSSM gauge couplings successfully unify at a GUT scale high enough to sufficiently suppress proton decay. Additionally SUSY provides a solution to the hierarchy problem and a candidate particle for dark matter.

In this chapter $\mathcal{N} = 1$ supersymmetry and SUSY $SU(5)$ are reviewed, following the presentations of [81, 94–99].

5.1 The Wess-Zumino model

The simplest supersymmetric quantum field theory with minimal field content is given by the Wess-Zumino (WZ) model [100]. A supersymmetric theory must contain the same number of fermionic and bosonic degrees of freedom (d.o.f.). In four-dimensional spacetime the smallest fermionic representation is a two-component Weyl spinor ψ . On-shell, ψ satisfies the Dirac equation $i\bar{\sigma}^\mu\partial_\mu\psi = m\psi^\dagger$, which eliminates two of ψ 's four real d.o.f. A complex scalar field ϕ is thus enough to balance the number of fermionic and bosonic d.o.f. on-shell. The *superpartners* ψ and ϕ form a *chiral supermultiplet*. Finally, to match the fermionic d.o.f. also off-shell, an *auxiliary* complex scalar field F with two non-physical

d.o.f. is additionally introduced. The Wess-Zumino Lagrange density of ψ , ϕ , and F is

$$\begin{aligned} \mathcal{L}_{WZ} = & i\psi^\dagger \bar{\sigma}^\mu \partial_\mu \psi + \partial_\mu \phi \partial^\mu \phi^* \\ & - \frac{1}{2} (m\psi\psi + m^* \psi^\dagger \psi^\dagger) - \frac{1}{4} (y\phi\psi\psi + y^* \phi^* \psi^\dagger \psi^\dagger) \\ & + FF^* + F \left(m\phi + \frac{y}{2} \phi^2 \right) + F^* \left(m^* \phi^* + \frac{y^*}{2} \phi^{*2} \right). \end{aligned} \quad (5.1)$$

There is no kinetic term for the auxiliary field F , since it does not propagate a physical d.o.f. It can thus be integrated out yielding the scalar potential

$$V_{WZ}(\phi\phi^*) = FF^* = m^2 \phi\phi^* + \left(\frac{my^*}{2} \phi\phi^{*2} + \frac{my}{2} \phi^* \phi^2 \right) + \frac{yy^*}{4} (\phi\phi^*)^2. \quad (5.2)$$

\mathcal{L}_{WZ} is invariant under the supersymmetry transformation

$$\begin{aligned} \delta\phi &= \epsilon\psi, & \delta\phi^* &= \epsilon^\dagger \psi^\dagger, \\ \delta\psi &= -i\sigma^\mu \epsilon^\dagger \partial_\mu \phi + \epsilon F, & \delta\psi^\dagger &= i\epsilon\sigma^\mu \partial_\mu \phi^* + \epsilon^\dagger F^*, \\ \delta F &= -i\epsilon^\dagger \bar{\sigma}^\mu \partial_\mu \psi, & \delta F^* &= i\partial_\mu \psi^\dagger \bar{\sigma}^\mu \epsilon, \end{aligned} \quad (5.3)$$

where ϵ is a two-component spinor, anti-commuting, and the infinitesimal supersymmetry transformation parameter.¹ The mass dimension of ϵ is $-\frac{1}{2}$. Requiring invariance under (5.3) is the reason why the couplings for all terms in \mathcal{L}_{WZ} and V_{WZ} are given only by the two parameters m and y .

Using a Wess-Zumino chiral multiplet, one can now present in a simplified manner how SUSY yields a solution to the hierarchy problem. Taking m in (5.1) to be due to the Higgs vev $m \rightarrow \frac{\lambda}{\sqrt{2}}(v+h)$ one finds the couplings

$$-\frac{\lambda}{2\sqrt{2}} (h\psi\psi + h\psi^\dagger \psi^\dagger), \quad -\frac{\lambda^2}{2} h^2 \phi\phi^*, \quad \text{and} \quad -\lambda^2 v h \phi\phi^*, \quad (5.4)$$

between the real scalar Higgs boson h and the WZ component fields ψ and ϕ . The Higgs self-energy contribution from the fermion loops shown in figure 5.1 is quadratically divergent

$$\Pi_{hh}^{(f)}(0) = (-1)\lambda^2 \int \frac{d^4k}{(2\pi)^4} \frac{1}{k^2 - m^2} + \frac{2m^2}{(k^2 - m^2)^2}, \quad (5.5)$$

and independent of the Higgs mass m_h . We know that if the SM is embedded into a GUT, there are particles with $m \sim M_{\text{GUT}}$ in the spectrum, which yields the hierarchy problem²: There must be a fine-tuning in the renormalisation of the quadratic divergence

¹We limit our discussion to the case of global SUSY, where ϵ is independent of x^μ .

²The hierarchy problem is not specific to GUTs but appears whenever new (non-supersymmetric) physics at high scales is introduced.

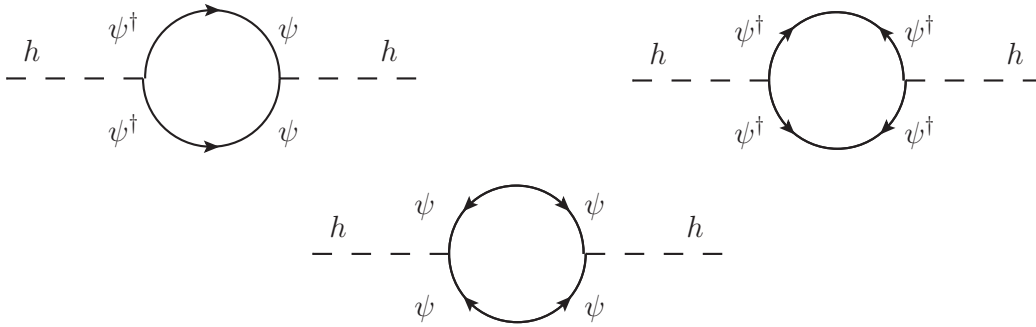


Figure 5.1: The Feynman diagrams contributing to the Higgs self-energy via a fermion loop. Note that for Weyl fermions the arrows on the propagators do not correspond to charge or momentum (see e.g. [12]).



Figure 5.2: The Feynman diagrams contributing to the Higgs self-energy via the scalar superpartner ϕ .

of 1 in 10^{28} since $m_h \sim \mathcal{O}(100 \text{ GeV})$. In supersymmetry, however, the contribution to the Higgs self-energy from the superpartner ϕ loops in figure 5.2 give

$$\Pi_{hh}^{(b)}(0) = \lambda^2 \int \frac{d^4k}{(2\pi)^4} \frac{1}{k^2 - m^2} + \frac{2m^2}{(k^2 - m^2)^2}, \quad (5.6)$$

and thus precisely cancels the fermionic contributions. This is true to all orders in perturbation theory.

There is no evidence for scalar particles with the same masses as the SM fermions, therefore SUSY has to be broken. In order to keep the cancellation of the quadratic divergence, only *soft* SUSY breaking terms are allowed. For example a small mass squared difference δ between ψ and ϕ yields

$$\Pi_{hh}^{(b)}(0) \simeq \lambda^2 \int \frac{d^4k}{(2\pi)^4} \frac{1}{k^2 - m^2} + \frac{2m^2}{(k^2 - m^2)^2} + \frac{2\delta^2}{(k^2 - m^2)^2}, \quad (5.7)$$

such that only a logarithmic divergence of $\mathcal{O}\left(\delta^2 \log \frac{m^2}{\mu^2}\right)$ remains. Supersymmetry breaking will be discussed in 5.3.

We close this section by a discussion of gauge supermultiplets. The superpartner of a gauge boson A_μ^a is a two-component spin $\frac{1}{2}$ *gaugino* λ^a . Like for the WZ supermultiplet, one introduces a real auxiliary scalar field D^a to manifest SUSY off-shell.³ All components

³We give the expressions in *Wess-Zumino gauge* [101].

of the gauge supermultiplet transform in the same representation of the gauge group. The Lagrange density for the gauge supermultiplet is given by

$$\mathcal{L}_{\text{gauge}} = -\frac{1}{4}F_{\mu\nu}^a F^{\mu\nu a} + i\lambda^{a\dagger}\bar{\sigma}^m u D_\mu \lambda^a + \frac{1}{2}D^a D^a, \quad (5.8)$$

with the gauge covariant derivative for the gaugino

$$D_\mu \lambda^a = \partial_\mu \lambda^a + g f^a_{bc} A_\mu^b \lambda^c. \quad (5.9)$$

The SUSY transformations are given by

$$\begin{aligned} \delta A_\mu^a &= -\frac{1}{\sqrt{2}} (\epsilon^\dagger \bar{\sigma}_\mu \lambda^a + \lambda^{a\dagger} \bar{\sigma}_\mu \epsilon), \\ \delta \lambda^a &= \frac{i}{2\sqrt{2}} \sigma^\mu \bar{\sigma}^\nu \epsilon F_{\mu\nu}^a + \frac{1}{\sqrt{2}} \epsilon D^a, \\ \delta D^a &= \frac{i}{\sqrt{2}} (-\epsilon^\dagger \bar{\sigma}^\mu D_\mu \lambda^a + D_\mu \lambda^{a\dagger} \bar{\sigma}^\mu \epsilon). \end{aligned} \quad (5.10)$$

Finally the coupling of the WZ supermultiplet to the gauge supermultiplet is given by the additional terms

$$-\sqrt{2}g(\phi^* T^a \psi) \lambda^a, \quad -\sqrt{2}g\lambda^{a\dagger} (\psi^\dagger T^a \phi), \quad g(\phi^* T^a \phi) D^a, \quad (5.11)$$

where additionally in (5.3) the ordinary derivatives have to be replaced by gauge covariant ones and the transformations δF and δF^* get extra terms $+\sqrt{2}g(T^a \phi)\epsilon^\dagger \lambda^{a\dagger}$ and $+\sqrt{2}g\lambda^a \epsilon(T^a \phi^*)$, respectively. The auxiliary field D^a can be integrated out and the scalar potential gets a D -term contribution in addition to the F -term (5.2)

$$V(\phi, \phi^*) = FF^* + \frac{1}{2}D^a D^a. \quad (5.12)$$

Note that $V(\phi, \phi^*)$ is strictly non-negative. In section 5.3 it will be shown that in SUSY theories the vacuum energy is always zero.

5.2 Superspace and Superfields

A simple formalism for supersymmetric theories can be achieved by introducing superspace [102]. In addition to the spacetime coordinate x^μ , superspace is spanned by two anti-commuting two-component spinors θ and θ^\dagger . The mass dimension of θ and θ^\dagger is $-\frac{1}{2}$. Superfields are functions of x^μ , θ , and θ^\dagger and unite the component fields of a supermultiplet. Because θ and θ^\dagger are Grassmann variables, an expansion of a general superfield in θ and θ^\dagger terminates

$$\begin{aligned} S(x^\mu, \theta, \theta^\dagger) &= \phi + \theta\xi + \theta^\dagger \chi^\dagger + \theta\theta F \\ &\quad + \theta^\dagger \theta^\dagger \rho + \theta^\dagger \bar{\sigma}^\mu \theta V_\mu + \theta^\dagger \theta^\dagger \theta \eta + \theta\theta\theta^\dagger \zeta^\dagger + \theta\theta\theta^\dagger \theta^\dagger \delta, \end{aligned} \quad (5.13)$$

where ϕ , F , ρ , δ are complex scalar fields, V_μ is a complex vector boson, and ξ , χ^\dagger , η , and ζ^\dagger are two-component Weyl fermions. Thus, the number of bosonic and fermionic d.o.f. match.

In analogy with the gauge covariant derivative D_μ one introduces the *chiral covariant derivatives* D_α and $D_{\dot{\alpha}}^\dagger$ in superspace, which are SUSY covariant

$$D_\alpha = \frac{\partial}{\partial\theta^\alpha} - i(\sigma^\mu\theta^\dagger)_\alpha \partial_\mu, \quad D_{\dot{\alpha}}^\dagger = \frac{\partial}{\partial\theta^{\dagger\dot{\alpha}}} + i(\theta\sigma^\mu)_{\dot{\alpha}} \partial_\mu. \quad (5.14)$$

One can now prescribe constraints on a general superfield S to reduce the total number of 32 degrees of freedom to the small number of d.o.f. in the WZ supermultiplet. Imposing

$$D_{\dot{\alpha}}^\dagger\Phi = 0 \quad (5.15)$$

yields a *left-chiral* superfield

$$\begin{aligned} \Phi(x^\mu, \theta, \theta^\dagger) &= \phi(x) + \sqrt{2}\theta\psi(x) + \theta\theta F(x) \\ &+ i\theta^\dagger\bar{\sigma}^\mu\theta\partial_\mu\phi(x) + \frac{1}{4}\theta\theta\theta^\dagger\theta^\dagger\partial_\mu\partial^\mu\phi(x) - \frac{i}{\sqrt{2}}\theta\theta\theta^\dagger\bar{\sigma}^\mu\partial_\mu\psi(x), \end{aligned} \quad (5.16)$$

which contains the component fields of the WZ supermultiplet. Its complex conjugate Φ^* satisfying $D_\alpha\Phi^* = 0$ is named *right-chiral*. Chiral superfields have mass dimension one. Starting from several left-chiral superfields Φ_i one can build a new left-chiral superfield from a holomorphic⁴ function $\mathcal{W}(\Phi_i)$.

Imposing

$$V = V^* \quad (5.17)$$

yields a *vector* superfield

$$\begin{aligned} V(x^\mu, \theta, \theta^\dagger) &= \phi(x) + \theta\xi(x) + \theta^\dagger\xi^\dagger(x) + \theta\theta F(x) + \theta^\dagger\theta^\dagger F^*(x) \\ &+ \theta^\dagger\bar{\sigma}^\mu\theta V_\mu(x) + \theta^\dagger\theta^\dagger\theta\eta(x) + \theta\theta\theta^\dagger\eta^\dagger(x) + \theta\theta\theta^\dagger\theta^\dagger\delta(x), \end{aligned} \quad (5.18)$$

where ϕ , δ , and A_μ are now real fields. One can construct a vector superfield from chiral fields by e.g. $\Phi + \Phi^*$ and $\Phi^*\Phi$.

Whenever V is the vector superfield to a gauge symmetry it transforms as

$$e^{2gV} \rightarrow e^{-2ig\Lambda^*} e^{2gV} e^{2ig\Lambda}, \quad (5.19)$$

where $V \equiv V^a T^a$, $\Lambda \equiv \Lambda^a T^a$, T^a are the generators of the gauge group, and Λ^a is a chiral superfield and the *supergauge* transformation parameter. Ordinary gauge transformation are obtained as special case when Λ is restricted to its scalar component. The chiral superfields transform under the supergauge symmetry as

$$\Phi \rightarrow e^{-2ig\Lambda}\Phi, \quad \Phi^* \rightarrow e^{2ig\Lambda^*}\Phi^*. \quad (5.20)$$

⁴Here holomorphic refers to the complex scalar component fields ϕ_i of Φ_i .

For an Abelian gauge symmetry the supergauge transformation for V simplifies to

$$V \rightarrow V + i(\Lambda - \Lambda^*) . \quad (5.21)$$

One can now use this freedom to make a suitable supergauge transformation and bring (5.18) into Wess-Zumino gauge

$$V(x^\mu, \theta, \theta^\dagger) = \theta^\dagger \bar{\sigma}_\mu \theta A_\mu(x) + \theta^\dagger \theta^\dagger \theta \lambda(x) + \theta \theta \theta^\dagger \lambda^\dagger(x) + \frac{1}{2} \theta \theta \theta^\dagger \theta^\dagger D(x) . \quad (5.22)$$

In WZ gauge it is easily recognised that V is dimensionless, justifying the e^V terms above. It is very useful to note that due to the Grassmann characteristics of θ and θ^\dagger the expansion series of e^V terminates

$$\begin{aligned} e^{2gV} &= 1 + 2gV + 2g^2V^2 \\ &= 1 + 2g \left(\theta \sigma^\mu \theta^\dagger A_\mu + \theta \theta \theta^\dagger \lambda^\dagger + \theta^\dagger \theta^\dagger \theta \lambda + \frac{1}{2} \theta \theta \theta^\dagger \theta^\dagger D \right) + g^2 \theta \theta \theta^\dagger \theta^\dagger A_\mu A^\mu . \end{aligned} \quad (5.23)$$

One can construct chiral spinorial field strength superfields

$$W_\alpha = -\frac{1}{4} D^\dagger D^\dagger e^{-2gV} D_\alpha e^{2gV} , \quad W_\alpha^\dagger = -\frac{1}{4} D D e^{2gV} D_\alpha^\dagger e^{-2gV} , \quad (5.24)$$

which transform as

$$W_\alpha \rightarrow e^{-2ig\Lambda} W_\alpha e^{2ig\Lambda} , \quad W_\alpha^\dagger \rightarrow e^{2ig\Lambda^\dagger} W_\alpha^\dagger e^{-2ig\Lambda^\dagger} , \quad (5.25)$$

under supergauge transformations.

In superspace formalism the Lagrange density is obtained from integrating a vector superfield over the Grassmann coordinates θ and θ^\dagger

$$\mathcal{L} = [V]_D \equiv \int d^2\theta \int d^2\theta^\dagger V(x^\mu, \theta, \theta^\dagger) = \frac{1}{2} D + \dots , \quad (5.26)$$

which is supersymmetric invariant since the D -term transforms into a total derivative under SUSY transformations (5.10) and \dots represents a total derivative term which is of no importance in \mathcal{L} . Another SUSY invariant term is the F -term of a chiral superfield gauge singlet, which also transforms into a total derivative under SUSY (5.3)

$$[\Phi]_F \equiv \int d^2\theta \Phi(x^\mu, \theta, \theta^\dagger) = F . \quad (5.27)$$

The Lagrange density can then be built from

$$\mathcal{L} = [\Phi]_F + h.c. \quad (5.28)$$

A general supersymmetric Lagrange density can thus be built out of chiral and vector superfields as

$$\mathcal{L}_{\text{SUSY}} = \left[K (\Phi_i^* e^{2gV} \Phi_j) + 2\kappa V \right]_D + \left(\left[\frac{1}{4} f_{ab} (\Phi_i) W^a W^b + \mathcal{W} (\Phi_i) \right]_F + h.c. \right), \quad (5.29)$$

where i, j denote generation indices, a, b are indices of the adjoint representation of the gauge group, and we introduced the following quantities:

Kähler potential K of left-chiral, right-chiral, and vector superfields. K is real and has mass dimension two. In the renormalisable case it is simply given by $\Phi_i^* e^{2gV} \Phi_i = \Phi^* \Phi + 2g \Phi^* V \Phi + 2g^2 \Phi^* V^2 \Phi$ and it's D -term yields the kinetic energy terms of the matter fields

$$\mathcal{L}_K = (D_\mu \phi_i)^\dagger D^\mu \phi_i + i \psi_i^\dagger \bar{\sigma}^\mu D_\mu \psi_i + F_i F_i^* - \sqrt{2} g (\phi^* T^a \psi \lambda^a + h.c.) + g (\phi^* T^a \phi) D^a. \quad (5.30)$$

In global SUSY the Kähler potential is invariant under the transformation

$$K \rightarrow K + F(\Phi_i) + F^*(\Phi_i^*), \quad (5.31)$$

with F a holomorphic function of Φ_i . All holomorphic and antiholomorphic functions can therefore be removed from the Kähler potential.

Fayet-Iliopoulos (FI) term $2\kappa[V]_D$ [103] in the case of an Abelian gauge group, since the D -term of a gauge singlet V is gauge invariant.

$$\mathcal{L}_{FI} = \kappa D. \quad (5.32)$$

The FI term does not exist for vector bosons of non-Abelian gauge groups.

gauge kinetic function f_{ab} , a dimensionless chiral superfield and holomorphic function of chiral superfields. In renormalisable theories f_{ab} is simply given by $\delta_{ab} + \frac{ig_a \theta_a}{8\pi^2} \delta_{ab}$, such that the F -terms yield the usual gauge kinetic energy plus in the case of a non-Abelian gauge symmetry a potentially topologically non-trivial θ term

$$\mathcal{L}_{\text{gauge}} = -\frac{1}{4} F_{\mu\nu}^a F^{\mu\nu a} - \frac{g_a^2 \theta}{64\pi^2} \epsilon_{\mu\nu\lambda\rho} F^{\lambda\rho a} F^{\mu\nu a} + i \lambda^a \sigma^\mu D_\mu \lambda^{a\dagger} + \frac{1}{2} D^a D^a. \quad (5.33)$$

superpotential \mathcal{W} , a holomorphic function of left-chiral superfields. It has mass dimension three and for renormalisable Lagrange densities it is given by

$$\mathcal{W}(\Phi_i) = L_i \Phi_i + \frac{1}{2} M_{ij} \Phi_i \Phi_j + \frac{1}{6} Y_{ijk} \Phi_i \Phi_j \Phi_k, \quad (5.34)$$

where the first term vanishes for non gauge singlet superfields Φ_i . The F -term $[\mathcal{W}(\Phi_i)]_F + h.c.$ yields mass terms and Yukawa couplings

$$\begin{aligned} \mathcal{L} &= \mathcal{W}^i F_i - \frac{1}{2} \mathcal{W}^{ij} \psi_i \psi_j + h.c. \\ &= \left(L_i + M_{ij} \phi_j + \frac{1}{2} Y_{ijk} \phi_j \phi_k \right) F_i - \frac{1}{2} (M_{ij} + Y_{ijk} \phi_k) \psi_i \psi_j + h.c., \end{aligned} \quad (5.35)$$

where the notation

$$\mathcal{W}_i \equiv \left. \frac{\partial \mathcal{W}}{\partial \Phi^i} \right|_{\theta=\theta^\dagger=0}, \quad \mathcal{W}_{ij} \equiv \left. \frac{\partial^2 \mathcal{W}}{\partial \Phi^i \partial \Phi^j} \right|_{\theta=\theta^\dagger=0} \quad (5.36)$$

was introduced which indicates that we set $\theta = \theta^\dagger = 0$ after differentiation, such that only the scalar components remain. Similarly we define \mathcal{W}^{*i} and \mathcal{W}^{*ij} for the conjugate superpotential $\mathcal{W}^*(\Phi^*)$.

Like mentioned above, the auxiliary fields F_i and D^a do not propagate a physical d.o.f. and can be integrated out to yield the scalar potential

$$V(\phi, \phi^*) = \mathcal{W}_i \mathcal{W}^{*i} + \frac{1}{2} \sum_a |g_a \phi^\dagger T^a \phi + \kappa^a|^2, \quad (5.37)$$

where for non-Abelian gauge symmetries $\kappa^a = 0$.

For non-renormalisable SUSY theories it is convenient to introduce supergraphs [104] (see e.g. [97, 105] for a review). When heavy particles are integrated out from a renormalisable theory, a non-renormalisable Kähler potential and a non-renormalisable superpotential emerge in the effective theory, as shown in figure 5.3. After the heavy superfields Φ_n are integrated out, the terms

$$\frac{Y_{ijn} Y_{kln}}{M_{nn}} \Phi_i \Phi_j \Phi_k \Phi_l \quad \text{and} \quad \frac{Y_{ijn} Y_{kln}^*}{M_{nn}^2} \Phi_i \Phi_j \Phi_k^* \Phi_l^* \quad (5.38)$$

appear in the superpotential and Kähler potential, respectively. Note that one can easily obtain the effective Kähler potential by cutting a propagator in the supergraph of an effective superpotential term in half, “flip” one side to the charge-conjugated expression and stitch the resulting parts together. From the Kähler potential one can define the Kähler metric⁵

$$K_i^j \equiv \left. \frac{\partial^2}{\partial \Phi_i \partial \Phi_j^*} \right|_{\theta=\theta^\dagger=0}, \quad (5.39)$$

⁵Here we use the convention that lower indices correspond to derivatives with respect to left-chiral superfields and upper indices to derivatives with respect to their complex conjugated (right-chiral) superfields, e.g. $(K_i^j)^* = K_j^i$.

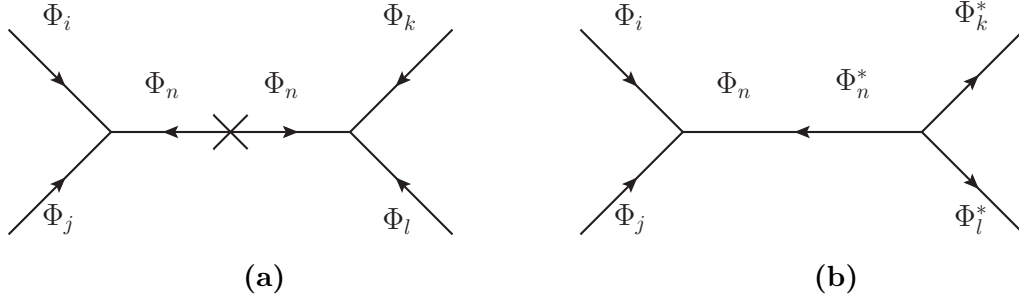


Figure 5.3: Supergraphs for non-renormalisable superpotential (a) and non-renormalisable Kähler potential (b).

with the inverse $(K^{-1})_j^i$ satisfying $(K^{-1})_j^i K_j^k = \delta_j^k$. Mathematically this means that the chiral fields are defined on a Kähler manifold and one can calculate the connection

$$\Gamma_{ij}^k = (K^{-1})_n^k K_{ij}^n, \quad (5.40)$$

and Riemann curvature tensor

$$R_{ik}^{jl} = K_{ik}^{jl} - (K^{-1})_m^n K_{ik}^m K_n^{jl}, \quad (5.41)$$

where

$$K_{ij}^k \equiv \frac{\partial^3}{\partial \Phi_i \partial \Phi_j \partial \Phi_k^*} \Big|_{\theta=\theta^\dagger=0}, \quad \text{and } K_{ij}^{kl} \equiv \frac{\partial^4}{\partial \Phi_i \partial \Phi_j \partial \Phi_k^* \partial \Phi_l^*} \Big|_{\theta=\theta^\dagger=0}. \quad (5.42)$$

The on-shell Lagrange density for the matter component fields after integrating out the auxiliary fields F and D^a can then be expressed as

$$\begin{aligned} \mathcal{L}_{\text{matter}} &= K_i^j D_\mu \phi_i (D^\mu \phi_j)^* + i K_i^j \psi_j^\dagger \bar{\sigma}^\mu D_\mu \psi_i \\ &\quad - \frac{1}{2} (\mathcal{W}_{ij} \psi_i \psi_j - \Gamma_{ij}^k \mathcal{W}_k \psi_i \psi_j + h.c.) \\ &\quad + \frac{1}{4} R_{ik}^{jl} \psi_i \psi_k \psi_j^\dagger \psi_l^\dagger \\ &\quad - (K^{-1})_j^i \mathcal{W}_i \mathcal{W}^{*j} - \frac{1}{2} \sum_a \left| g_a \phi_i^\dagger T^a K^i + \kappa^a \right|^2, \end{aligned} \quad (5.43)$$

where the covariant derivative of the fermion fields includes the connection

$$D_\mu \psi = \partial_\mu \psi - ig V_\mu^a T^a \psi + \Gamma_{ij}^i \partial_\mu \phi_j \psi_k, \quad (5.44)$$

and we introduced

$$K^i \equiv \frac{\partial K}{\partial \Phi_i^*} \Big|_{\theta=\theta^\dagger=0}. \quad (5.45)$$

For non-trivial Kähler metric $K_i^j \neq \delta_i^j$ the kinetic terms in (5.43) have to be brought into canonical form via *canonical normalisation* (CN) [106]. The CN procedure transforms the superfields $\Phi \rightarrow P_\Phi^{-1} \Phi$ such that K_i^j is diagonalised and rescaled [107, 108]

$$P_\Phi^\dagger K P_\Phi = \mathbf{1}, \quad (5.46)$$

where the most general form of P_Φ is given by

$$P_\Phi = U_\Phi^\dagger \left(\sqrt{K^{\text{diag}}} \right)^{-1} \tilde{U}, \quad \text{with} \quad U_\Phi K U_\Phi^\dagger = K^{\text{diag}}. \quad (5.47)$$

The unitary matrix \tilde{U} can be chosen arbitrarily and allows to set P_Φ hermitean. Rescaling the superfields in CN also affects masses and Yukawa couplings in the effective superpotential. In flavour models Yukawa couplings emerge from non-renormalisable operators when flavon fields obtain their vevs. Therefore, in SUSY flavour models, the effective superpotential for the Yukawa couplings will always adjoin an effective Kähler potential as described below (5.38). Explicit SUSY flavour models thus have to either guarantee that the CN effects are negligible ($K_i^j \approx \delta_i^j$ in the effective theory) or otherwise the sizeable CN corrections need to be carefully included into the model's predictions [107, 108].

We close this section by briefly discussing R -symmetries. A global $U(1)_R$ symmetry is defined by the transformation of the anti-commuting coordinates θ and θ^\dagger

$$\theta \rightarrow e^{i\alpha_R} \theta, \quad \text{and} \quad \theta^\dagger \rightarrow e^{-i\alpha_R} \theta^\dagger. \quad (5.48)$$

The Lagrange density can be invariant under $U(1)_R$ when R -charges R_Φ are assigned to each superfield. A general superfield $S(x^\mu, \theta, \theta^\dagger)$ transforms as

$$S(x^\mu, \theta, \theta^\dagger) \rightarrow e^{i\alpha R_\Phi} S(x^\mu, e^{-i\alpha} \theta, e^{i\alpha} \theta^\dagger). \quad (5.49)$$

The components of a chiral superfield Φ transform with R -charges $R(\phi) = R_\Phi$, $R(\psi) = R_\Phi - 1$, and $R(F) = R_\Phi - 2$. To build an $U(1)_R$ invariant Lagrange density the superpotential must carry R -charge $R(\mathcal{W}) = 2$, thus the form of the most general superpotential (5.34) gets constrained. A vector superfield V always has R -charge zero, therefore the corresponding (gauge-independent) R -charges of its component fields are $R(A_\mu) = 0$, $R(\lambda) = 1$, and $R(D) = 0$. A gaugino mass term $-\frac{1}{2} M \lambda^a \lambda^a$ has R -charge two and therefore not only breaks SUSY, but also $U(1)_R$. Discrete \mathbb{Z}^n are also candidates for R -symmetries, with R -parity \mathbb{Z}_R^2 conventionally assigned to the superfields in such a way that SM particles have R -parity $+1$ and sparticles have R -parity -1 . If R -parity is an unbroken symmetry of nature, the lightest supersymmetric particle (LSP) is stable and therefore a promising candidate for Dark Matter.

5.3 Supersymmetry breaking

As discussed at the beginning of this chapter, supersymmetry has to be a broken symmetry of nature, since there is no evidence for the existence of the the charged leptons' superpartners. There are two ways SUSY can be broken: spontaneously via non-vanishing vevs and explicitly. We start the discussion with spontaneous SUSY breaking and look at the SUSY transformations of the component fields of a general vev. Because of Lorentz invariance, only scalar fields can have non-vanishing vevs, fermion fields and field derivatives must

vanish. From Eqs. (5.3) and (5.10) it follows

$$\begin{aligned} \delta\langle\phi_i\rangle &= 0, & \delta\langle\psi_i\rangle &\sim \epsilon\langle F_i\rangle, & \delta\langle F_i\rangle &= 0, \\ \delta\langle A_\mu^a\rangle &= 0, & \delta\langle\lambda^a\rangle &\sim \epsilon\langle D^a\rangle, & \delta\langle D^a\rangle &= 0. \end{aligned} \quad (5.50)$$

Therefore a vev is only SUSY invariant if and only if $\langle F_i\rangle = 0$ and $\langle D^a\rangle = 0$. Consequently, from (5.12), a supersymmetric vacuum has zero energy.⁶ In order to break SUSY spontaneously one needs to assure that either $\langle F_i\rangle \neq 0$ or $\langle D\rangle \neq 0$ via an *F-term SUSY breaking* or *D-term SUSY breaking* mechanism, respectively.

F-term SUSY breaking requires that the global minimum of the scalar potential develops a vev such that $\langle F_i\rangle = 0$ can not be simultaneously satisfied for all F_i . Thus the superpotential for *F-term SUSY breaking* needs to contain a linear term of a gauge singlet $\mathcal{W} \supset L_i\Phi_i$ since otherwise $F_i^* = -\mathcal{W}_i$ has always a vanishing solution with $\langle\phi_i\rangle = 0$. The simplest *F-term breaking* mechanism of interacting superfields is given by the O’Raifeartaigh model [109]

$$\mathcal{W}_{\text{O’Raifeartaigh}} = m\Phi_2\Phi_3 + \lambda\Phi_1(\Phi_3^2 - \mu^2), \quad (5.51)$$

with real m , λ , and μ . The *F*-terms are given by

$$F_1 = -\lambda(\phi_3^* - \mu^2), \quad F_2 = -m\phi_3^*, \quad \text{and } F_3 = -m\phi_2^* - \lambda\phi_1^*\phi_3^*. \quad (5.52)$$

Since $F_1 = 0$ and $F_2 = 0$ are impossibly simultaneously satisfied, one *F-term* has to obtain a vev and SUSY is spontaneously broken.

D-term SUSY breaking emerges from a non-vanishing vev of a *D-term* component of a vector superfield, which has to be a gauge singlet due to gauge invariance of the Lagrange density. The simplest model for *D-term SUSY breaking* is due to Fayet-Iliopoulos [103]

$$V_{\text{FI}}(\phi, \phi^*) = \frac{1}{2}(\kappa + gq|\phi|^2)^2. \quad (5.53)$$

If $\kappa q > 0$ no vev of ϕ can achieve vanishing scalar potential, the minimum of V is given by $\frac{1}{2}\kappa^2$ at $\langle\phi\rangle = 0$, therefore the *D-term* is given by

$$D = -\kappa, \quad (5.54)$$

and SUSY is spontaneously broken.

That SUSY is broken by non-vanishing vevs of the auxiliary *F* and *D* component fields can also be noticed from the fact that $\langle F\rangle$ and $\langle D\rangle$ induce mass terms for the scalar particles and therefore introduce a mass splitting between scalar and fermion components. A general sum rule for the masses of fermions and bosons can be derived from the mass matrices of scalars

$$M_S^2 = \begin{pmatrix} \mathcal{W}^{*ik}\mathcal{W}_{kj} + D^{ai}D_j^a + D_j^{ai}D^a & \mathcal{W}^{*ijk}\mathcal{W}_k + D^{ai}D^{aj} \\ \mathcal{W}_{ijk}\mathcal{W}^{*k} + D_i^aD_j^a & \mathcal{W}_{ik}\mathcal{W}^{*kj} + D_i^aD^{aj} + D_i^{aj}D^a \end{pmatrix} \quad (5.55)$$

⁶More technical this can be derived by the $\mathcal{N} = 1$ SUSY algebra $\{Q_\alpha, Q_\beta^\dagger\} = 2\sigma_{\alpha\beta}^\mu P_\mu$, $\{Q_\alpha, Q_\beta\} = \{Q_\alpha^\dagger, Q_\beta^\dagger\} = 0$, where the generators of SUSY transformation Q and Q^\dagger are Weyl spinors and the Hamiltonian is given by $H = P_0 = \frac{1}{4}(\{Q_1, Q_1^\dagger\} + \{Q_2, Q_2^\dagger\})$.

where we defined $D_i^a = \left. \frac{\partial}{\partial \Phi_i} D^a \right|_{\theta=\theta^\dagger=0}$, the mass matrix of fermions

$$M_F = \begin{pmatrix} \mathcal{W}_{ij} & -\sqrt{2}D_i^a \\ -\sqrt{2}D_j^a & 0 \end{pmatrix}, \quad (5.56)$$

and the mass matrix of massive vector bosons emerging from some non-vanishing vev $\langle \phi_i \rangle$ and the BEH-mechanism

$$M_V^{2ab} = (D_i^a D^{bi} + D^{ai} D_i^b). \quad (5.57)$$

The result is the so-called *supertrace* [110]

$$\text{STr}(M^2) = \sum_{J=0}^1 (-1)^{2J} (2J+1) M_J^2 = -2g^a \text{Tr}(T^a \langle D^a \rangle), \quad (5.58)$$

which holds in spontaneously broken and unbroken SUSY, and the RHS vanishes for non-anomalous $U(1)$ such as the $U(1)_Y$ in the MSSM. Analogous to Goldstone's theorem for bosonic symmetries, the spontaneous breaking of global SUSY yields the *Goldstino* [103, 111], a massless Majorana fermion, which is proportional to the fermionic partners of the auxiliary fields obtaining a vev⁷

$$\psi^G \sim \langle F_i \rangle \psi_i + \frac{1}{\sqrt{2}} \langle D^a \rangle \lambda^a. \quad (5.59)$$

Phenomenological constraints such as the supertrace (e.g. $2m_e^2 = m_{e_1}^2 + m_{e_2}^2$ for vanishing lepton flavour mixing) or the fact that an $U(1)_Y$ FI term would spontaneously break $SU(3)_C$ or $U(1)_{\text{em}}$ necessitate SUSY breaking in a hidden sector, rather than superfields of known SM particles. For this purpose it is useful to investigate soft explicit SUSY breaking first. A SUSY breaking term in the Lagrange density is named *soft* if it is at most logarithmically divergent and therefore does not reintroduce the hierarchy problem. A necessary but not sufficient condition is that soft terms must not have mass dimension larger than three [112]. To all orders in perturbation theory, a general soft-breaking Lagrange density is given by [113]

$$\begin{aligned} \mathcal{L}_{\text{soft}} = & -\frac{1}{2} M_a \lambda^a \lambda^a + h.c. - m_{ij}^2 \phi_i^* \phi_j \\ & - \left(h_i \phi_i + \frac{1}{2} b_{ij} \phi_i \phi_j + \frac{1}{6} a_{ijk} \phi_i \phi_j \phi_k + h.c. \right). \end{aligned} \quad (5.60)$$

It contains Majorana mass terms for the gauginos λ^a , trilinear, bilinear, and linear terms for the scalar fields ϕ_i as well as a hermitean mass squared matrix m_{ij}^2 for $\phi_i^* \phi_j$. Of course

⁷In general this can be shown from the supercurrent formalism, here it suffices to notice that $(\langle F_i \rangle, \langle D^a \rangle / \sqrt{2})^T$ is an eigenvector of M_F with eigenvalue 0.

$\mathcal{L}_{\text{soft}}$ has to be gauge invariant, thus all terms have to be allowed by gauge symmetry and the linear terms are only present for gauge singlets ϕ_i . Whether or not the terms in

$$\mathcal{L}_{\text{soft/hard}} = -\frac{1}{2}c^{ijk}\phi_i^*\phi_j\phi_k - \frac{1}{2}m_{F_{ij}}\psi_i\psi_j - M^a\lambda^a\psi_a + h.c. \quad (5.61)$$

are soft depends on whether or not the theory contains a chiral superfield transforming as gauge singlet. If such a gauge singlet ϕ_i exist, these terms can contract to linearly divergent tadpole diagrams and thus spoil the solution to the hierarchy problem (see e.g. [98, 114]).

The explicit soft-breaking Lagrange density introduces many new parameters and in general the soft-breaking parameter space will be constrained by phenomenology, such as the absence of large flavour mixing and CP-violating processes in nature. Such constraints can be enforced when the soft-breaking parameters result from spontaneous SUSY breaking in a *hidden* sector, which is only weakly coupled to the *observable* sector containing the SM particles. Gravity, being the weakest force known and coupling universally to all particles, is a promising candidate for mediating SUSY breaking between those sectors [115].

Allowing for gravity requires *supergravity* (SUGRA), the theory of local supersymmetry. As a theory of gravity SUGRA contains the graviton, a massless spin two boson obtained from linearising the Einstein-Hilbert action. The superpartner of the graviton is a massless spin $\frac{3}{2}$ fermion, the *gravitino*. As a generalisation of the BEH-mechanism, when SUGRA is spontaneously broken the gravitino absorbs the goldstino and obtains a mass $m_{3/2}$ due to the *super-Higgs* mechanism [116]. The supertrace is then generalised to

$$\text{STr}(M^2) = \sum_{J=0}^{\frac{3}{2}} (-1)^{2J} (2J+1) M_J^2 = 2(N-1)m_{3/2}^2 - 2g^a \text{Tr}(T^a \langle D^a \rangle) , \quad (5.62)$$

with N being the number of chiral superfields in the theory. The sparticle masses are thus expected to be heavier than the SM particles and are therefore no longer in conflict with phenomenology.

Instead of constructing the SUSY breaking hidden sector explicitly, one usually assumes that the superpotential splits into an observable and a hidden part $\mathcal{W} = \mathcal{W}_{\text{obs}} + \mathcal{W}_{\text{hid}}$, a minimal Kähler potential, and a minimal gauge kinetic function. Then, when SUSY is broken in the hidden sector, universal soft-breaking parameters $m_{1/2}$, m_0 , A_0 , and B_0 emerge for the soft-breaking masses $m_0^2 |\phi_i|^2$, trilinear couplings $A_0 Y_{ijk} \phi_i \phi_j \phi_k$, and bilinear couplings $B_0 M_{ij} \phi_i \phi_j$ of (5.60) [117], where Y_{ijk} and M_{ij} are parameters in the superpotential (5.34). The assumption of these universal boundary conditions at a high unification scale (usually M_{pl} or M_{GUT}) is known as *mSUGRA* or *Constrained MSSM* (CMSSM).

Other common SUSY breaking mechanism are *Gauge Mediated SUSY Breaking* [118], where gauge non-singlet superfields act as messengers between hidden and observable sector and SUSY soft-breaking terms are generated from loops. Another scenario is *Anomaly Mediated SUSY Breaking* [119], which assumes that the hidden sector is localised on a separate brane than the observable sector in an extra dimension. SUSY breaking is mediated

by the superconformal anomaly and the soft-breaking terms are generated via loops⁸.

In conclusion, while the details of an explicit SUSY breaking mechanism are quite involved and beyond the scope of this thesis, well motivated by mSUGRA we can impose universal CMSSM boundary conditions for the soft-breaking Lagrange density (5.60) at a high scale. In chapter 10 we will analyse SUSY threshold corrections from a CMSSM SUSY scenario.

5.4 The Minimal Supersymmetric Standard Model

In this section we extend the successful Standard Model by SUSY and introduce the minimal supersymmetric Standard Model (MSSM) [120]. First one must assign superpartners to each SM particle and define the MSSM superfield content. The SM fermions are embedded into chiral superfields. The superpartners are named like the fermion components but with an ‘s’ prepended. Since the superpotential of the MSSM has to be a holomorphic function of left-chiral superfields, one resorts to the left-handed conjugates of the right-handed SM fermions. Of concern is the SM Higgs field. As seen in (2.2) the conjugated Higgs field $\tilde{\phi}$ couples to down-type quarks and charged leptons, which would require a non-holomorphic term in the superpotential. Also, the fermionic superpartner of the Higgs, the *Higgsino*, spoils the anomaly freedom of the SM. Both issues can be solved at once with the introduction of a second Higgs superfield of opposite $U(1)_Y$ hypercharge, such that the anomaly coefficients cancel and Yukawa couplings of the down-type quarks and charged leptons can originate from holomorphic terms. The vector bosons of the SM are accompanied with gauginos and embedded into vector superfields. The gauginos are named gluinos, Winos, Zino, and Bino. The supersymmetric version of table 2.1, the superfield content of the MSSM, is thus as given in table 5.1.

As a renormalisable quantum field theory, the Kähler potential and the gauge kinetic function of the MSSM are trivial. The most general superpotential allowed by the MSSM gauge group would permit baryon and lepton number violating terms, which would induce too rapid proton decay and are ruled out by observations. One therefore requires the MSSM to be invariant under *matter parity* [121, 122]

$$P_M = (-1)^{3(B-L)} , \quad (5.63)$$

where B and L are the baryon and lepton numbers of a superfield, respectively.⁹ The MSSM superpotential is thus given by

$$\mathcal{W}_{\text{MSSM}} = Y_{e_{ij}} H_d \cdot L_i E_j^c + Y_{d_{ij}} H_d \cdot Q_i D_j^c - Y_{u_{ij}} H_u \cdot Q_i U_j^c + \mu H_u \cdot H_d , \quad (5.64)$$

where we use the *SUSY Les Houches Accord* (SLHA) convention [123]. The first three terms yield the SM Yukawa coupling terms, Higgsino-sfermion-fermion interactions, and

⁸Since the resulting sfermion masses are tachyonic, an universal shift by m_0 needs to be introduced by hand nevertheless.

⁹Matter parity is equivalent to R -parity, where each particle of spin j is assigned $P_R = (-1)^{3(B-L)+2j}$. Thus all SM particles have even R -parity, all sparticles odd.

Superfield	SM field	Superpartner	Quantum Numbers	
Vector superfields				
G	G_μ	\tilde{G}	$(\mathbf{8}, \mathbf{1})_0$	+1
W	W_μ	\tilde{W}	$(\mathbf{1}, \mathbf{3})_0$	+1
B	B_μ	\tilde{B}	$(\mathbf{1}, \mathbf{1})_0$	+1
Matter superfields				
Q	$Q_L = \begin{pmatrix} u_L \\ d_L \end{pmatrix}$	$\tilde{Q} = \begin{pmatrix} \tilde{u}_L \\ \tilde{d}_L \end{pmatrix}$	$(\mathbf{3}, \mathbf{2})_{\frac{1}{6}}$	-1
U^c	u_R^\dagger	\tilde{u}_R^*	$(\bar{\mathbf{3}}, \mathbf{1})_{-\frac{2}{3}}$	-1
D^c	d_R^\dagger	\tilde{d}_R^*	$(\bar{\mathbf{3}}, \mathbf{1})_{\frac{1}{3}}$	-1
L	$L_L = \begin{pmatrix} \nu_L \\ e_L \end{pmatrix}$	$\tilde{L} = \begin{pmatrix} \tilde{\nu}_L \\ \tilde{e}_L \end{pmatrix}$	$(\mathbf{1}, \mathbf{2})_{-\frac{1}{2}}$	-1
E^c	e_R^\dagger	\tilde{e}_R^*	$(\mathbf{1}, \mathbf{1})_1$	-1
Higgs superfields				
H_u	$h_u = \begin{pmatrix} h_u^+ \\ h_u^0 \end{pmatrix}$	$\tilde{h}_u = \begin{pmatrix} \tilde{h}_u^+ \\ \tilde{h}_u^0 \end{pmatrix}$	$(\mathbf{1}, \mathbf{2})_{\frac{1}{2}}$	+1
H_d	$h_d = \begin{pmatrix} h_d^0 \\ h_d^- \end{pmatrix}$	$\tilde{h}_d = \begin{pmatrix} \tilde{h}_d^0 \\ \tilde{h}_d^- \end{pmatrix}$	$(\mathbf{1}, \mathbf{2})_{-\frac{1}{2}}$	+1

Table 5.1: Superfield content of the MSSM with their SM fields and superpartners. All matter superfields come in three flavours, the superpartners to the SM fields are indicated by a tilde. Besides the MSSM gauge group quantum numbers we list the matter parity P_M .

(scalar)⁴ terms. The μ -term is important to the breaking of EW symmetry, as discussed below. Together with the other terms of the superpotential it yields Higgs-sfermion-sfermion interactions.

The soft-breaking Lagrange density of the MSSM is given by

$$\begin{aligned}
-\mathcal{L}_{\text{soft}} = & \frac{1}{2} \left(M_1 \tilde{B} \tilde{B} + M_2 \tilde{W} \tilde{W} + M_3 \tilde{G} \tilde{G} \right) + h.c. \\
& + T_{e_{ij}} h_d \cdot \tilde{L}_i \tilde{e}_{R_j}^* + T_{d_{ij}} h_d \cdot \tilde{Q}_i \tilde{d}_{R_j}^* - T_{u_{ij}} h_u \cdot \tilde{Q}_i \tilde{u}_{R_j}^* + h.c. \\
& + \tilde{Q}_i^\dagger m_{\tilde{Q}_{ij}}^2 \tilde{Q}_j + \tilde{L}_i^\dagger m_{\tilde{L}_{ij}}^2 \tilde{L}_j + \tilde{u}_{R_i} m_{\tilde{u}_{ij}}^2 \tilde{u}_{R_j}^* + \tilde{d}_{R_i} m_{\tilde{d}_{ij}}^2 \tilde{d}_{R_j}^* + \tilde{e}_{R_i} m_{\tilde{e}_{ij}}^2 \tilde{e}_{R_j}^* \\
& + m_{h_u}^2 |h_u|^2 + m_{h_d}^2 |h_d|^2 + (m_3^2 h_u \cdot h_d + h.c.) .
\end{aligned} \tag{5.65}$$

In addition to the 19 parameters of the SM, the MSSM adds the complex parameters μ , m_3 , complex trilinear couplings T_e , T_d , and T_u , hermitean matrices $m_{\tilde{f}}^2$, complex gaugino masses M_1 , M_2 , and M_3 , and real mass parameters $m_{h_u}^2$ and $m_{h_d}^2$. The total number of parameters in the MSSM is therefore 124.

For vanishing μ and m_3^2 the MSSM would be invariant under a global $U(1)_{\text{PQ}}$. Treating those parameters as spurions, the MSSM $U(1)_{\text{PQ}}$ charges are given as in table 5.2. Thus by

Superfield / Spurion	H_u	H_d	Q	U^c	D^c	L	E^c	μ	m_3^2
$U(1)_{\text{PQ}}$	1	1	$-\frac{1}{2}$	$-\frac{1}{2}$	$-\frac{1}{2}$	$-\frac{1}{2}$	$-\frac{1}{2}$	-2	-2

Table 5.2: Non vanishing $U(1)_{\text{PQ}}$ charges of the MSSM superfields and spurions μ and m_3 .

a Peccei-Quinn transformation of the superfields one can choose to work in a basis where the phase of m_3^2 is zero [124] (see also [98,125]). Similarly, while the soft-breaking Lagrange density is invariant under R -parity, it explicitly breaks a global $U(1)_R$. By treating gaugino masses, trilinear couplings, and m_3^2 as spurions, one can set e.g. one of the gaugino phases zero [124] (see e.g. [98]).

Let us have a look at the (s)particle spectrum of the MSSM, starting with the Higgs bosons. Unlike in the SM, the quartic Higgs coupling of the MSSM Higgs potential is not a free parameter, but determined by the gauge couplings through the D -terms. The MSSM Higgs potential is

$$V_{\text{H}} = (m_{h_d}^2 + |\mu|^2) |h_d|^2 + (m_{h_u}^2 + |\mu|^2) |h_u|^2 + (m_3^2 h_u \cdot h_d + h.c.) + \frac{1}{8} (g'^2 + g_2^2) (|h_u|^2 - |h_d|^2)^2 + \frac{g_2^2}{2} |h_u^* h_d|^2 . \quad (5.66)$$

In order for EW symmetry to be spontaneously broken, the Higgs bosons h_u and h_d acquire the vevs

$$\langle h_d \rangle = \frac{1}{\sqrt{2}} \begin{pmatrix} v_1 \\ 0 \end{pmatrix} \quad \text{and} \quad \langle h_u \rangle = \frac{1}{\sqrt{2}} \begin{pmatrix} 0 \\ v_2 \end{pmatrix} , \quad (5.67)$$

with $v_1^2 + v_2^2 = v^2 \approx 246$ GeV. The ratio between v_2 and v_1 is denoted

$$\tan \beta \equiv \frac{v_2}{v_1} . \quad (5.68)$$

Requiring that the vevs (5.67) do minimise the Higgs potential allows to express $|\mu|^2$ and m_3^2 on tree-level in terms of

$$|\mu|^2 = \frac{1}{2} (\tan(2\beta) (m_{h_u}^2 \tan \beta - m_{h_d}^2 \cot \beta) - M_Z^2) , \\ m_3^2 = \frac{1}{2} (\tan(2\beta) (m_{h_u}^2 - m_{h_d}^2) - M_Z^2 \sin(2\beta)) , \quad (5.69)$$

whereas the phase of μ is left free. Another requirement for EW symmetry breaking is a negative mass square for h_u or h_d , yielding

$$m_3^4 > (m_{h_u}^2 + |\mu|^2) (m_{h_d}^2 + |\mu|^2) . \quad (5.70)$$

With mSUGRA boundary conditions $m_{h_u}^2 = m_{h_d}^2$ at a high scale, the RGEs typically yield small or negative values of $m_{h_u}^2$ at the EW scale, such that (5.70) is satisfied in what is known as *radiative EW symmetry breaking*. Expanding h_u and h_d around their vevs (see e.g. [125])

$$h_d = \frac{1}{\sqrt{2}} \begin{pmatrix} v_1 + s_1 + ip_1 \\ h_1^- \end{pmatrix} \quad \text{and} \quad h_u = \frac{1}{\sqrt{2}} \begin{pmatrix} h_2^+ \\ v_2 + s_s + ip_2 \end{pmatrix} e^{i\xi}, \quad (5.71)$$

where ξ is a relative phase between h_d and h_u , one obtains mass matrices

$$M_{sspp} = \begin{pmatrix} M_{ss} & M_{sp} \\ M_{sp}^\dagger & M_{pp} \end{pmatrix} \quad \text{and} \quad M_{h^+h^-}, \quad (5.72)$$

with

$$M_{sp} = \begin{pmatrix} 0 & m_3^2 \sin \xi \\ m_3^2 \sin \xi & 0 \end{pmatrix}. \quad (5.73)$$

Minimising the Higgs potential is equivalent to vanishing tadpole coefficients for s_1 , s_2 , p_1 , and p_2 . In chapter 10 we resort to the one-loop tadpole equations in order to obtain the one-loop analogue of (5.69). For the tree-level potential the tadpole coefficient of p_1 requires a vanishing phase ξ . Therefore, in general on tree-level and in the CP-conserving case¹⁰ where $\xi = 0$ to all orders in perturbation theory, M_{sspp} is block diagonal and the mass eigenstates have well-defined CP quantum numbers

$$\begin{aligned} \begin{pmatrix} H \\ h \end{pmatrix} &= \begin{pmatrix} \cos \alpha & \sin \alpha \\ -\sin \alpha & \cos \alpha \end{pmatrix} \begin{pmatrix} s_1 \\ s_2 \end{pmatrix}, \\ \begin{pmatrix} A \\ G^0 \end{pmatrix} &= \begin{pmatrix} \sin \beta_n & \cos \beta_n \\ -\cos \beta_n & \sin \beta_n \end{pmatrix} \begin{pmatrix} p_1 \\ p_2 \end{pmatrix}, \\ \begin{pmatrix} H^\pm \\ G^\pm \end{pmatrix} &= \begin{pmatrix} \sin \beta_c & \cos \beta_c \\ -\cos \beta_c & \sin \beta_c \end{pmatrix} \begin{pmatrix} h_1^\pm \\ h_2^\pm \end{pmatrix}, \end{aligned} \quad (5.74)$$

with $h_1^+ \equiv (h_1^-)^*$ and equivalently for h_2^- . There are two CP even Higgs bosons h , H in the real MSSM, where conventionally $m_h < m_H$. A is an CP odd Higgs boson and G^0 , G^\pm are the three Goldstone bosons that give massive Z and W^\pm bosons. Note that on tree-level the requirement of vanishing tadpole coefficients yields $\beta_n = \beta_c = \beta$. The tree-level Higgs masses are given by

$$\begin{aligned} m_A^2 &= \frac{2m_3^2}{\sin(2\beta)}, \\ m_{H^\pm}^2 &= m_A^2 + M_W^2, \\ m_{h,H}^2 &= \frac{1}{2} \left(m_A^2 + M_Z^2 \mp \sqrt{(m_A^2 - M_Z^2)^2 + 4M_Z^2 m_A^2 \sin^2(2\beta)} \right). \end{aligned} \quad (5.75)$$

¹⁰We will denote the CP-conserving MSSM as *real* MSSM and the CP-violating MSSM as *complex*.

In the CP violating case, the three mass eigenstates h_1 , h_2 , and h_3 are obtained from

$$\begin{pmatrix} h_1 \\ h_2 \\ h_3 \end{pmatrix} = S \begin{pmatrix} s_1 \\ s_2 \\ p_1 \\ p_2 \end{pmatrix}, \quad (5.76)$$

with S a 3×4 matrix satisfying $S^\dagger S = \mathbb{1}_4$ and $m_{h_1} < m_{h_2} < m_{h_3}$ (see e.g. [123]). The mass of the lightest Higgs boson m_h (or m_{h_1}) is strongly affected by loop corrections [126]. Precise calculations of these loop corrections are very elaborate, in chapter 10 a two-loop Higgs mass calculation will be performed with the published software `FeynHiggs` [125, 127–129].

Turning to the sparticles, the mass eigenstates of gauginos and Higgsinos are four *neutralinos* χ_i^0 from \tilde{B} , \tilde{W}^0 , \tilde{h}_u^0 , and \tilde{h}_d^0 and two *charginos* χ_i^\pm from \tilde{W}^\pm , \tilde{h}_u^\pm , and \tilde{h}_d^\pm . Their mixing matrices are given in appendix B. The superpartners of the SM fermions are six up-type squarks, six down-type squarks, six charged sleptons, and three sneutrinos. In general they mix to form mass eigenstates, with the 6×6 (3×3) mass and mixing matrices given in appendix B as well.

We close this section with three remarks:

Supersymmetric seesaw In order to extend the MSSM by a type-I seesaw mechanism one introduces a left-handed chiral superfield N^c as gauge singlet and adds the superpotential terms

$$\mathcal{W}_{\text{seesaw}} = Y_{\nu_{ij}} H_u \cdot L_i N_j^c + \frac{1}{2} M_{n_{ij}} N_i^c N_j^c. \quad (5.77)$$

The soft-breaking Lagrange density is extended by

$$\mathcal{L}_{\text{soft}} \supset -\tilde{\nu}_{R_i}^* m_{\tilde{\nu}_{ij}}^2 \tilde{\nu}_{R_j}. \quad (5.78)$$

Supersymmetric threshold corrections The SM is an effective theory of the MSSM. When solving the MSSM RGEs, the MSSM is commonly matched to the SM at a renormalisation scale chosen to represent an average mass M_{SUSY} of the sparticles. Conventionally it is set to the geometric mean of the stop quark masses $Q \equiv \sqrt{\tilde{m}_{t_1} \tilde{m}_{t_2}}$, where the loop-corrected result for the light Higgs mass is numerically stable against small changes of the renormalisation scale [130]. The SUSY scale has to be larger than M_Z and typical values are assumed to be around 1 TeV.

On tree-level, down-type quarks and charged leptons only couple to the Higgs field h_d . On one-loop level however, there are also couplings to h_u . These loops yield $\tan \beta$ -enhanced threshold corrections to Yukawa couplings when the MSSM is matched to the SM and the sparticles are intergrated out [131, 132]. Thus, although loop-suppressed, they can have significant magnitude for sizeable $\tan \beta$ and are of importance for the prediction of quark-lepton mass ratios [133]. A full calculation of SUSY threshold corrections will be presented in chapter 10.

Charge and colour breaking vacua Besides the Higgs fields h_u and h_d , the MSSM scalar potential also contains sfermion fields. In principle those fields can obtain non-vanishing vevs as well, thereby breaking $SU(3)_C$ and $U(1)_{\text{em}}$ spontaneously. The existence of such dangerous charge and colour breaking (CCB) minima in the scalar potential is linked to the violation of bounds for the soft-breaking trilinear couplings [134, 135], e.g.

$$|T_{ij}|^2 \leq \left(m_{L_{ii}}^2 + m_{R_{jj}}^2 + m_{h_f}^2 + |\mu|^2 \right) \begin{cases} (y_i^2 + y_j^2) & i \neq j \\ 3y_i^2 & i = j \end{cases}, \quad (5.79)$$

where m_L , m_R , and m_{h_f} denote the soft-breaking mass parameters of the scalar fields associated with the trilinear coupling T in the basis of diagonal Yukawa matrices.

Additionally, the scalar potential might feature directions in field space which are unbounded from below (UFB). For the tree-level scalar potential these yield constraints [134]

$$\begin{aligned} m_{h_u}^2 + m_{h_d}^2 + 2|\mu|^2 &> 2m_3^2, \\ m_{h_u}^2 + |\mu|^2 + m_{\tilde{L}_i}^2 &> \frac{m_3^4}{m_{h_d}^2 + |\mu|^2 - m_{\tilde{L}_i}^2}, \\ m_{h_u}^2 + m_{\tilde{L}_i}^2 &> 0. \end{aligned} \quad (5.80)$$

Note that the first equation is always satisfied when $|\mu|$ is calculated from the requirement (5.69) of successful EW symmetry breaking. If any of the CCB or UFB constraints are violated for a particular MSSM parameter point, the decay rate of our physical vacuum into the deeper unphysical one can still be so small, that our vacuum's lifetime exceeds the age of the universe by orders of magnitude. This will be discussed further in chapter 10. Finally we note that the tree-level scalar potential receives radiative corrections and UFB directions will become bounded from below eventually, thereby turning into CCB vacua.

5.5 Supersymmetric $SU(5)$ GUTs

As shown in figure 5.4, the field content of the MSSM yields an unification of the gauge couplings at $M_{\text{GUT}} \approx 2 \cdot 10^{16}$ GeV, where the α_i are defined analogous to the QED fine-structure constant $\alpha_i \equiv \frac{g_i^2}{4\pi}$ and the one-loop β function coefficients for the gauge couplings in the MSSM are $b_1 = \frac{33}{5}$, $b_2 = 1$, and $b_3 = -3$ [86, 136]. This motivates the embedding of the MSSM gauge group into a GUT gauge group like $SU(5)$. Note that the gauge couplings do not unify entirely, rather at M_{GUT} small differences¹¹ do remain, but those can be attributed to threshold effects from heavy GUT-scale particles, such as the $SU(3)_C$ octet $O^{(24)}$, $SU(2)_L$ triplet $T^{(24)}$, $SU(3)_C$ triplets $T^{(5)}$, $\bar{T}^{(5)}$, and heavy gauge bosons X and Y in an $SU(5)$ GUT [137]. In the last line we have already assumed that the field content of the Georgi-Glashow $SU(5)$ from section 4.1 is accompanied with superpartners

¹¹Conventionally M_{GUT} is defined by the unification $\alpha_1(M_{\text{GUT}}) = \alpha_2(M_{\text{GUT}})$.

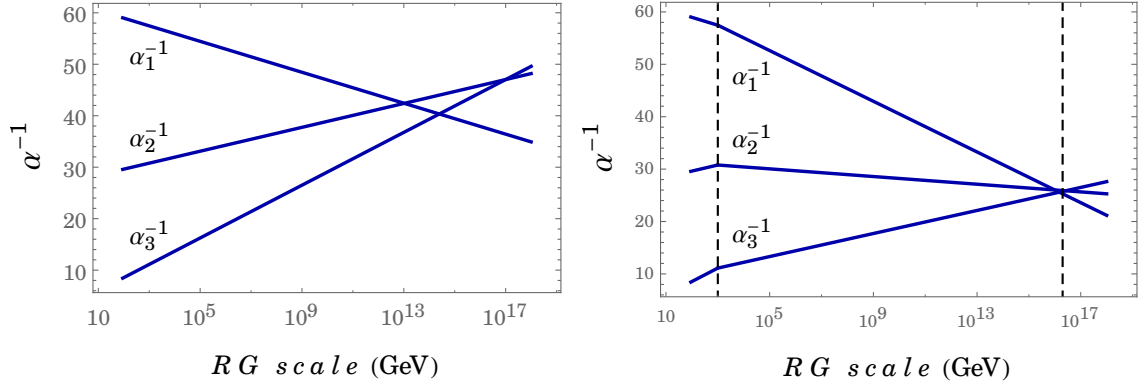


Figure 5.4: One-loop RG evolution of the inverse gauge couplings α_i^{-1} in the SM (left) and MSSM (right), assuming a common SUSY scale $M_{\text{SUSY}} = 10^3$ GeV. The dashed lines indicate $M_{\text{SUSY}} = 10^3$ GeV and $M_{\text{GUT}} \approx 2 \cdot 10^{16}$ GeV.

and embedded into superfields. Because $M_{\text{SUSY}} \ll M_{\text{GUT}}$ we almost never have the need to write $SU(5)$ superfields in scalar and fermion components notation. Thus we use the same notation for the superfields as introduced for the corresponding non-SUSY $SU(5)$ multiplet, e.g.

$$\mathcal{F} \supset D^c, L \quad \text{and} \quad \mathcal{T} \supset Q, U^c, E^c . \quad (5.81)$$

Because of the two Higgs fields in the MSSM, another $SU(5)$ Higgs multiplet \bar{H}_5 , transforming as $\bar{\mathbf{5}}$, is introduced

$$H_5 \supset H_u, T^{(5)} \quad \text{and} \quad \bar{H}_5 \supset H_d, \bar{T}^{(5)} . \quad (5.82)$$

The embedding of the MSSM superfields into $SU(5)$ multiplets, or equivalently the ‘‘supersymmetrisation’’ of the Georgi-Glashow $SU(5)$ model, is denoted *minimal SUSY $SU(5)$* [138]. The superpotential for this model is given by

$$\mathcal{W} = M_{24} \text{Tr} H_{24}^2 + \lambda_{24} \text{Tr} H_{24}^3 + (\mu_5 + \lambda H_{24}) H_5 \bar{H}_5 + Y_5 \mathcal{F} \mathcal{T} \bar{H}_5 + \epsilon_5 Y_{10} \mathcal{T} \mathcal{T} H_5 , \quad (5.83)$$

where flavour and $SU(5)$ indices have been suppressed. When $SU(5)$ gets broken the colour octet $O^{(24)}$, $SU(2)_L$ triplet $T^{(24)}$, and gauge singlet $S^{(24)}$ obtain masses

$$m_{O^{(24)}} = m_{T^{(24)}} = \frac{15}{4} \lambda_{24} V \quad \text{and} \quad m_{S^{(24)}} = \frac{3}{4} \lambda_{24} V . \quad (5.84)$$

In addition to the MSSM superpotential, there are also terms coupling matter superfields to the colour Higgs triplets

$$\mathcal{W}_T = \frac{1}{\sqrt{2}} Y_5 (Q \cdot L - U^c D^c) \bar{T}^{(5)} + 2Y_{10} (2U^c E^c - Q \cdot Q) T^{(5)} , \quad (5.85)$$

which leads to dangerous dimension five baryon number violating operators [122, 139–143] (see also [82])

$$\mathcal{W}_{\mathcal{B}} = \frac{\sqrt{2}}{M_T} (Y_5 Q \cdot L) (Y_{10} Q \cdot Q) + \frac{2\sqrt{2}}{M_T} (Y_5 U^c D^c) (Y_{10} U^c E^c) . \quad (5.86)$$

These operators have to be “dressed” with gluinos, charginos, or neutralinos to become a dimension six proton decay operator, as shown in figure 5.5 for an example. The resulting

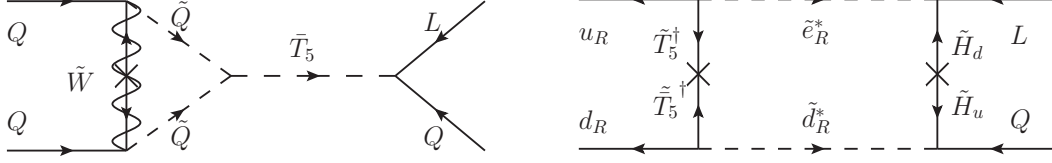


Figure 5.5: Examples for dressed LLLL and RRRR contributions to proton decay mediated by the colour triplets T_5 and \bar{T}_5 . Note that flavour indices are suppressed.

dimension six operators are suppressed by $\frac{1}{M_{\text{SUSY}}M_T}$ in contrast to the $\frac{1}{M_T^2}$ suppression of non-supersymmetric dimension six proton decay. Thus the lower bound on the proton lifetime yields a heavy lower limit for the triplet mass [82, 143],

$$M_T \gtrsim 10^{17} \text{ GeV} . \quad (5.87)$$

A $SU(5)$ GUT model with a heavy Higgs triplet mass of this scale suffers from two problems:

Firstly, there is the problem of doublet-triplet splitting. When $SU(5)$ is broken, the μ -term for the Higgs doublets and the mass of the colour triplets are given by

$$\mathcal{W} \supset \left(\mu_5 - \frac{3\lambda}{2} V \right) H_u \cdot H_d + (\mu_5 + \lambda V) T^{(5)} \bar{T}^{(5)} . \quad (5.88)$$

Via fine-tuning of λ , a strong hierarchy between doublet and triplet masses can be achieved. In predictive flavour models, however, employing CG factors via higher dimensional Yukawa coupling operators involving H_{24} , as discussed in section 4.4, will forbid terms like $\lambda H_{24} H_5 \bar{H}_5$ due to discrete symmetries and a fine-tuning solution to DTS will be no longer feasible. Besides fine-tuning, the DTS problem can be solved via the *missing partner mechanism* (MPM) [144]. We review MPM in part IV of this thesis in chapter 9, where we present our results for combining predictive SUSY $SU(5)$ flavour models with DTS.

Secondly, the contribution of the colour Higgs triplets to the RGEs of the gauge couplings spoil the successful unification unless $M_T \lesssim 10^{15}$ GeV [145]. Giving up the condition of renormalisability for the superpotential

$$\mathcal{W} \supset M_{24} \text{Tr} H_{24}^2 + \lambda_{24} \text{Tr} H_{24}^3 + \frac{a}{M_{\text{pl}}} (\text{Tr} H_{24}^2)^2 + \frac{b}{M_{\text{pl}}} \text{Tr} H_{24}^4 + (\mu_5 + \lambda H_{24}) H_5 \bar{H}_5 , \quad (5.89)$$

the masses of $O^{(24)}$ and $T^{(24)}$ split which shifts the upper bound for M_T to higher values [146]

$$M_T = M_T^0 \left(\frac{m_{T^{(24)}}}{m_{O^{(24)}}} \right)^{\frac{5}{2}} , \quad (5.90)$$

where M_T^0 denotes the triplet mass in the renormalisable minimal $SU(5)$. Building non-renormalisable operators by coupling H_{24} to Yukawa operators in general allows to fit the

observed quark-lepton mass ratios, at the cost of losing predictability. In chapter 9 in the main part of this thesis we will discuss how DTS, a sufficiently heavy triplet mass M_T , and gauge coupling unification can be achieved in predictive SUSY flavour GUT models.

Finally we note that the constraint $M_{\text{GUT}} \gtrsim 10^{16}$ GeV from dimension six proton decay (4.31) is satisfied in minimal SUSY $SU(5)$.

PART III

SUSY Flavour GUT models

CHAPTER 6

$\theta_{13}^{\text{PMNS}} \approx \theta_C \sin \theta_{23}^{\text{PMNS}}$ from GUTs

Grand Unified Theories offer a promising setting to predict quark - lepton mass ratios. As was discussed in 4.4, when down-type quark Yukawa matrix and charged lepton Yukawa matrix are generated from the same set of GUT operators, the resulting entries are linked and differ only by group theoretical Clebsch-Gordan factors. This connection is not limited to quark and lepton masses, however, but also links quark and lepton mixing angles. In this chapter we present our results of [1] and discuss simple conditions such that the large value of $\theta_{13}^{\text{PMNS}}$ can be explained from $\theta_{13}^{\text{PMNS}} \approx \theta_C \sin \theta_{23}^{\text{PMNS}}$ in $SU(5)$ GUTs and PS unification.

6.1 A numerical expression for $\theta_{13}^{\text{PMNS}}$ in terms of θ_C

After neutrino oscillations were discovered and large $\theta_{12}^{\text{PMNS}}$ and $\theta_{23}^{\text{PMNS}}$ had been established, it was widely assumed $\theta_{13}^{\text{PMNS}}$ would be small or vanishing. In many GUT models small non-vanishing $\theta_{13}^{\text{PMNS}} \approx 3^\circ$ was predicted, when the Georgi-Jarlskog CG factor 3 (4.28) was used to correct the minimal $SU(5)$ prediction $Y_e = Y_d^T$ in the first two families.

In 2011 a surprisingly large $\theta_{13}^{\text{PMNS}} \approx 8.8^\circ \pm 1.0^\circ$ was measured by T2K, DoubleCHOOZ, DayaBay, and RENO [46, 147]. Following the discovery, it was noted that by replacing the Georgi-Jarlskog CG factor with the newly proposed alternatives of [83], large $\theta_{13}^{\text{PMNS}}$ could be obtained [148, 149].

$\theta_{13}^{\text{PMNS}}$ also complied with a very interesting numerical expression in terms of the Cabibbo angle $\theta_C = 13.02^\circ \pm 0.04^\circ$

$$\theta_{13}^{\text{PMNS}} \approx \frac{\theta_C}{\sqrt{2}} \approx 9.2^\circ. \quad (6.1)$$

In the meantime the lepton mixing angles have been measured with higher precision [62]

$$\theta_{12}^{\text{PMNS}} = 33.48^\circ \begin{matrix} +0.78^\circ \\ -0.75^\circ \end{matrix}, \quad \theta_{13}^{\text{PMNS}} = 8.50^\circ \begin{matrix} +0.20^\circ \\ -0.21^\circ \end{matrix}, \quad \text{and } \theta_{23}^{\text{PMNS}} = \begin{cases} 42.3^\circ \begin{matrix} +3.0^\circ \\ -1.6^\circ \end{matrix} & \text{(NO)} \\ 49.5^\circ \begin{matrix} +1.5^\circ \\ -2.2^\circ \end{matrix} & \text{(IO)} \end{cases}. \quad (6.2)$$

With these updated values the lepton mixing angles still amount to a very interesting numerical agreement of

$$\theta_{13}^{\text{PMNS}} \approx \theta_C \sin \theta_{23}^{\text{PMNS}} = 8.84^\circ \begin{smallmatrix} +0.30^\circ \\ -0.44^\circ \end{smallmatrix}, \quad (6.3)$$

in the case of the NO best fit point. Equation (6.1) follows from (6.3) as a special case when $\theta_{23}^{\text{PMNS}} = 45^\circ$.¹ The appearance of θ_C in relation (6.3) motivates the viewpoint of an underlying GUT symmetry connecting the quark and lepton sectors.

Note that even before $\theta_{13}^{\text{PMNS}}$ was measured various different approaches featuring large values of $\theta_{13}^{\text{PMNS}}$ existed in the literature. The estimate $\theta_{13}^{\text{PMNS}} = \mathcal{O}(\theta_C)$ for example can be obtained from charged lepton corrections if one merely assumes the Wolfenstein parameter $\lambda \approx \theta_C$ as expansion parameter in the charged lepton mixing matrix in so-called *Cabibbo haze* [152], or e.g. in [153]. However, in such scenarios $\theta_{13}^{\text{PMNS}}$ is not predicted, since it differs from λ by an unknown prefactor. In the context of *Quark-Lepton Complementary* (QLC) $\theta_{12}^{\text{PMNS}} + \theta_C = 45^\circ$ [154] the relation $\theta_{13}^{\text{PMNS}} = \frac{\theta_C}{\sqrt{2}}$ appeared from assuming bimaximal neutrino mixing and a lepton mixing matrix $U_L^{(e)}$ exactly equal to V_{CKM} [155]. The latter assumption, however, is not expected to hold in realistic GUTs since the mass matrices of quarks and charged leptons cannot be identical, especially regarding the masses of the first two families. The GUT scale mass ratio $\frac{m_\mu}{m_s}$ in particular is severely different from one. As mentioned before, non-universal group-theoretical CG factors are required to bring GUT predictions for quark-lepton mass ratios in accordance with observations. But with different singular values of Y_d and Y_e , it can not be expected that the charged lepton mixing matrix equals V_{CKM} .

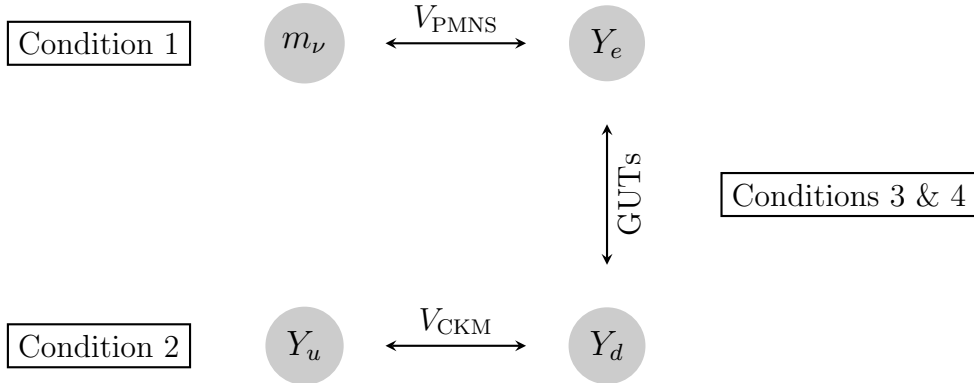


Figure 6.1: In our set-up, the relation $\theta_{13}^{\text{PMNS}} \approx \theta_C \sin \theta_{23}^{\text{PMNS}}$ is obtained by linking the charged lepton and quark sectors via GUTs, demanding four constraints on the mixing angles and GUT structure, as discussed in the main text.

In contrast, we will not require bimaximal mixing in the neutrino sector nor identical $U_L^{(e)}$ and V_{CKM} . In the light of the new CG factors available in model building, our strategy

¹In 2011, global fits reported large uncertainties for $\theta_{23}^{\text{PMNS}}$, e.g. $\theta_{23}^{\text{PMNS}} = 46.1^\circ \pm 3.4^\circ$ [147] and $\theta_{23}^{\text{PMNS}} = 40.4^\circ$ with a one sigma confidence interval of $[38.6^\circ, 45.0^\circ]$ [150]. Also in 2016 there is still potential for higher precision, with e.g. a one sigma interval of $[38.6^\circ, 53.7^\circ]$ reported by the NO ν A collaboration for $\theta_{23}^{\text{PMNS}}$ [151].

is to use GUT relations plus additional conditions/constraints on the structure of $SU(5)$ GUTs and Pati-Salam models, as illustrated in figure 6.1, to establish $\theta_{12}^e \approx \theta_C$, which then induces $\theta_{13}^{\text{PMNS}} \approx \theta_C \sin \theta_{23}^{\text{PMNS}}$ via a charged lepton correction to the neutrino mixing matrix. In 6.5 we come back to a comparison between our results and the QLC relation.

In the following sections we discuss in detail four simple conditions to realise $\theta_{13}^{\text{PMNS}} \approx \theta_C \sin \theta_{23}^{\text{PMNS}}$ in GUTs. Note that, while these conditions can act as an instruction how to build predictive flavour GUT models with $\theta_{13}^{\text{PMNS}} \approx \theta_C \sin \theta_{23}^{\text{PMNS}}$, we do not claim that our strategy is the only functioning set-up. For example, while our paper [1] was finalised, [156] appeared, which also discusses strategies for obtaining $\theta_{13}^{\text{PMNS}} \approx \theta_C \sin \theta_{23}^{\text{PMNS}}$, e.g. from a shared flavon in the quark and neutrino sector of a flavour model.

6.2 Conditions for mixing angles

In the following, we will assume hierarchical Y_u, Y_d , and Y_e , which implies that the left-mixing angles $\theta_{ij}^u, \theta_{ij}^d$, and θ_{ij}^e are all comparatively small (i.e., not much larger than the Cabibbo angle θ_C) as is typical for GUT flavour models in the flavour basis.

We first revisit the charged lepton corrections (3.31)

$$s_{23}^{\text{PMNS}} e^{-i\delta_{23}^{\text{PMNS}}} \approx s_{23}^\nu e^{-i\delta_{23}^\nu} - \theta_{23}^e c_{23}^\nu e^{-i\delta_{23}^e}, \quad (6.4a)$$

$$\theta_{13}^{\text{PMNS}} e^{-i\delta_{13}^{\text{PMNS}}} \approx \theta_{13}^\nu e^{-i\delta_{13}^\nu} - \theta_{13}^e c_{23}^\nu e^{-i\delta_{13}^e} - \theta_{12}^e e^{-i\delta_{12}^e} (s_{23}^\nu e^{-i\delta_{23}^\nu} - \theta_{23}^e c_{23}^\nu e^{-i\delta_{23}^e}), \quad (6.4b)$$

$$s_{12}^{\text{PMNS}} e^{-i\delta_{12}^{\text{PMNS}}} \approx s_{12}^\nu e^{-i\delta_{12}^\nu} + \theta_{13}^e c_{12}^\nu s_{23}^\nu e^{i(\delta_{23}^\nu - \delta_{13}^e)} - \theta_{12}^e c_{23}^\nu c_{12}^\nu e^{-i\delta_{12}^e}, \quad (6.4c)$$

in leading order of θ_{13}^ν and (3.32)

$$\theta_{13}^{\text{PMNS}} e^{-i\delta_{13}^{\text{PMNS}}} \approx \theta_{13}^\nu e^{-i\delta_{13}^\nu} - \theta_{13}^e c_{23}^\nu e^{-i\delta_{13}^e} - \theta_{12}^e s_{23}^{\text{PMNS}} e^{-i(\delta_{12}^e + \delta_{23}^{\text{PMNS}})}, \quad (6.5)$$

in order to find simple conditions for obtaining a predictive GUT scenario with $\theta_{13}^{\text{PMNS}} \approx \theta_C \sin \theta_{23}^{\text{PMNS}}$. Similarly, the CKM angles θ_{ij}^{CKM} can be expressed in terms of quark mixing angles θ_{ij}^u and θ_{ij}^d by a small angle expansion of $V_{\text{CKM}} = \left(U_L^{(u)} \right)^\dagger U_L^{(d)}$ [157]

$$\theta_{23}^{\text{CKM}} e^{-i\delta_{23}^{\text{CKM}}} \approx \theta_{23}^d e^{-i\delta_{23}^d} - \theta_{23}^u e^{-i\delta_{23}^u}, \quad (6.6a)$$

$$\theta_{13}^{\text{CKM}} e^{-i\delta_{13}^{\text{CKM}}} \approx \theta_{13}^d e^{-i\delta_{13}^d} - \theta_{13}^u e^{-i\delta_{13}^u} - \theta_{12}^u e^{-i\delta_{12}^u} (\theta_{23}^d e^{-i\delta_{23}^d} - \theta_{23}^u e^{-i\delta_{23}^u}), \quad (6.6b)$$

$$\theta_{12}^{\text{CKM}} e^{-i\delta_{12}^{\text{CKM}}} \approx \theta_{12}^d e^{-i\delta_{12}^d} - \theta_{12}^u e^{-i\delta_{12}^u}. \quad (6.6c)$$

The standard PDG Dirac CP phase δ_{CKM} in V_{CKM} can be identified as [17]

$$\delta_{\text{CKM}} = \delta_{13}^{\text{CKM}} - \delta_{23}^{\text{CKM}} - \delta_{12}^{\text{CKM}}. \quad (6.7)$$

We are now ready to state first conditions towards scenarios featuring (6.3):

Condition 1: Since we want to use the charged lepton correction proportional to θ_{12}^e to establish the link to θ_C via GUTs we require, as assumed to derive (3.31) and (3.32), hierarchical Y_u , Y_d , and Y_e , and furthermore

$$\theta_{13}^\nu \approx 0, \quad \theta_{13}^e \approx 0. \quad (6.8)$$

Then the first two summands on the right side of (3.32) drop out and we obtain (3.33), independently of any phases

$$\theta_{13}^{\text{PMNS}} \approx \theta_{12}^e s_{23}^{\text{PMNS}}. \quad (6.9)$$

Condition 2: Secondly, since we want to establish a link between $\theta_{13}^{\text{PMNS}}$ and θ_C based on GUT relations between Y_d and Y_e , we require that to a good approximation

$$\theta_{12}^d \approx \theta_C. \quad (6.10)$$

This may follow from (6.6c) as a consequence of $\theta_{12}^u \ll \theta_{12}^d$, which is a typical feature of models with hierarchical Yukawa matrices where the stronger hierarchy in the up-quark sector implies the smaller mixing angles. An alternative possibility arises when one requires $\theta_{13}^u, \theta_{13}^d \approx 0$. Such cases yield the *quark mixing sum rule* [157] from (6.6) and (6.7)

$$\theta_{12}^d \approx \left| \theta_{12}^{\text{CKM}} - \frac{\theta_{13}^{\text{CKM}}}{\theta_{23}^{\text{CKM}}} e^{-i\delta^{\text{CKM}}} \right| \approx 12.0^\circ \pm 0.3^\circ. \quad (6.11)$$

6.3 Conditions from relations between Y_d and Y_e

To arrive at $\theta_{13}^{\text{PMNS}} \approx \theta_C \sin \theta_{23}^{\text{PMNS}}$, we want to employ GUT relations between the down-type quark Yukawa matrix Y_d and the charged lepton Yukawa matrix Y_e . The GUT relations emerge since the down-type quark Yukawa matrix and the charged lepton Yukawa matrix are generated from joint GUT operators, as discussed in chapter 4. This leads to the following condition:

Condition 3: To obtain predictive GUT relations, we require that all elements of the Yukawa matrices Y_d and Y_e are each dominantly generated by one single joint GUT operator. This condition can be somewhat relaxed in specific cases, for instance it would be sufficient to restrict this requirement to the distinct matrix elements which enter the relation between θ_C and θ_{12}^e . Furthermore it is possible that two operators featuring the same CG factor contribute at similar strength. In this case, the relation between the elements of Y_d and Y_e is still given by only one single CG factor. We demand the stronger requirement stated at the beginning at this point, to keep the discussion simple.

Thus, the matrix elements are closely linked by group theoretical CG factors. For hierarchical Y_d and Y_e and small mixing angles we can focus our discussion exclusively on the 1-2 submatrix of the first two families

$$Y_d = \begin{pmatrix} d & b \\ a & c \end{pmatrix} \Rightarrow \begin{cases} Y_e = \begin{pmatrix} c_d d & c_b b \\ c_a a & c_c c \end{pmatrix} & (\text{PS}) , \\ Y_e = \begin{pmatrix} c_d d & c_a a \\ c_b b & c_c c \end{pmatrix} & (SU(5) \text{ GUTs}) \end{cases} . \quad (6.12)$$

Here, c_a, c_b, c_c , and c_d are the CG factors relating the elements of Y_d and Y_e . As discussed in chapter 4, in $SU(5)$ GUTs Y_d is related to Y_e^T , whereas in Pati-Salam unified theories Y_d is related directly to Y_e . Lists of available CG factors in $SU(5)$ and PS were given in (4.45) and (4.46), respectively.

The CG factors play an important role in flavour model building: A successful model requires a consistent set of CG factors in (6.12), leading to viable mass relations for the first two families. It has been noted in [148, 149], that various combinations of phenomenologically viable CG factors exist which can lead to a comparatively large $\theta_{13}^{\text{PMNS}}$. The prediction $\theta_{13}^{\text{PMNS}} \approx \theta_C \sin \theta_{23}^{\text{PMNS}}$ only emerges from a subset of these combinations of CG factors, as we now discuss in the context of Pati-Salam unified theories and $SU(5)$ GUTs.

To obtain conditions on the CG factors, we first note that the 1-2 mixing angle of Y_d is given in leading order in a small mixing approximation by

$$\theta_{12}^d \approx \left| \frac{b}{c} \right| , \quad (6.13)$$

and the Yukawa couplings by

$$y_d \approx \left| d - \frac{a b}{c} \right| \quad \text{and} \quad y_s \approx |c| . \quad (6.14)$$

6.3.1 $\theta_{13}^{\text{PMNS}} \approx \theta_C \sin \theta_{23}^{\text{PMNS}}$ in Pati-Salam Theories

In Pati-Salam unified theories, to leading order in a small angle approximation the Yukawa couplings y_e and y_μ of the first two families are given by [148]

$$y_e \approx \left| c_d d - \frac{c_a a c_b b}{c_c c} \right| \quad \text{and} \quad y_\mu \approx |c_c c| , \quad (6.15)$$

and the 1-2 mixing angle θ_{12}^e is given by

$$\theta_{12}^e \approx \left| \frac{c_b b}{c_c c} \right| \approx \left| \frac{c_b}{c_c} \right| \theta_C , \quad (6.16)$$

where (6.10) and (6.13) were used in the last step. Finally, using (6.9) we obtain

$$\theta_{13}^{\text{PMNS}} \approx \theta_{12}^e \sin \theta_{23}^{\text{PMNS}} \approx \left| \frac{c_b}{c_c} \right| \theta_C \sin \theta_{23}^{\text{PMNS}} . \quad (6.17)$$

From here we can read off the condition on the CG factors in Pati-Salam theories:

Condition 4 (PS): In Pati-Salam unified models, and in general in unified models with a direct GUT relation between Y_d and Y_e (and not as in $SU(5)$ GUTs between Y_d and Y_e^T) we require that the CG factors for the operators generating the 2-2 element and the 1-2 element of Y_e are equal, i.e.

$$|c_b| = |c_c| . \quad (6.18)$$

In Pati-Salam unified theories, this simple additional condition is indeed sufficient and may readily be implemented in flavour models. The remaining parameters and CG factors of such a model of course have to be constructed in such a way that the phenomenological constraints on the down-type quark and charged lepton sectors are satisfied. In Pati-Salam models it turns out that in the case of vanishing 1-1 element $d = 0$, there is no set of CG factors available which simultaneously satisfies (6.18) and the double ratio (4.43)

$$\left| \frac{y_\mu y_d}{y_s y_e} \right| \approx \left| \frac{c_c^2}{c_a c_b} \right| \approx 10.7_{-0.8}^{+1.8} . \quad (6.19)$$

Therefore viable scenarios of Pati-Salam unification require non vanishing 1-1 elements in Y_d and Y_e [148] (see also [158]). Let us remark that in principle the set $c_c = c_b = 9$ and $c_a = \frac{3}{4}$ yields the double ratio 12, which is also within the one sigma confidence interval, but the GUT scale relation $y_\mu = 9y_s$ requires SUSY threshold corrections of about 50%, which exceeds typical results in realistic SUSY scenarios (see e.g. [133] and figure 10.3).

We will see next that in $SU(5)$ GUTs zero 1-1 elements of Y_d and Y_e are consistent and even favourable for obtaining the relation $\theta_{13}^{\text{PMNS}} \approx \theta_C \sin \theta_{23}^{\text{PMNS}}$.

6.3.2 $\theta_{13}^{\text{PMNS}} \approx \theta_C \sin \theta_{23}^{\text{PMNS}}$ from $SU(5)$ GUTs

In $SU(5)$ GUTs the 1-2 mixing angle θ_{12}^e is given in leading order in a small angle approximation by

$$\theta_{12}^e \approx \left| \frac{c_a a}{c_c c} \right| . \quad (6.20)$$

Employing (6.13) and condition (6.10) shows that in order to obtain a link between θ_C and θ_{12}^e we need to relate

$$\theta_C \approx \left| \frac{b}{c} \right| \quad \text{and} \quad \theta_{12}^e \approx \left| \frac{c_a a}{c_c c} \right| \quad (6.21)$$

This implies that towards establishing a simple link between $\theta_{13}^{\text{PMNS}}$ and θ_C in $SU(5)$ GUTs, we have to impose at least one further constraint on the structure of the Yukawa matrices. From (6.21) one can see that one possibility to restore a direct link between θ_C and θ_{12}^e is to enforce

$$|a| \approx |b| \quad (6.22)$$

which immediately translates into

$$\theta_{12}^e \approx \left| \frac{c_a a}{c_c c} \right| \approx \left| \frac{c_a}{c_c} \right| \theta_C , \quad (6.23)$$

and thus to a simple condition

$$|c_a| = |c_c| \quad \Rightarrow \quad \theta_{13}^{\text{PMNS}} \approx \theta_C \sin \theta_{23}^{\text{PMNS}} \quad (6.24)$$

on the CG factors in $SU(5)$ GUTs. We discuss two ways to enforce $|a| = |b|$ (or $|a| \approx |b|$ to a good approximation) in the following and give two choices for the final condition:

Condition 4.1 ($SU(5)$ GUTs): The first possibility is rather straightforward, namely that the Yukawa matrices Y_d and Y_e are symmetric in the 1-2 submatrix considered above. Although this is not a typical feature in $SU(5)$ GUTs, symmetric matrices could be a consequence of a flavour symmetry in specific models. This would imply that

$$|a| = |b| \quad \text{and} \quad |c_a| = |c_b| , \quad (6.25)$$

such that the above condition is satisfied. We note that in order to obtain realistic mass ratios, in the case of symmetric Y_d and Y_e , the 1-1 elements have to be non-vanishing and the CG factor c_d has to be chosen appropriately.

Condition 4.2 ($SU(5)$ GUTs): The second possibility is less straightforward but leads to almost exactly the same prediction. It arises when one imposes vanishing 1-1 elements of Y_d and Y_e . Then the resulting structure of the Yukawa matrices is quite predictive, since the five observables y_e, y_μ, y_d, y_s , and $\theta_{12}^d \approx \theta_C$ are determined by only three parameters $|a|, |b|$, and $|c|$ and the corresponding CG coefficients. In leading order in a small mixing angle approximation, we obtain:

$$y_s \approx |c| , \quad y_\mu \approx |c_c c| , \quad y_d \approx \left| \frac{ab}{c} \right| , \quad y_e \approx \left| \frac{c_a a c_b b}{c_c c} \right| , \quad \theta_C \approx \left| \frac{b}{c} \right| . \quad (6.26)$$

This situation has been considered in [148] and the relation

$$\theta_{12}^e \approx \frac{y_e}{y_\mu} \left| \frac{c_c}{c_b} \right| \frac{1}{\theta_C} \quad (6.27)$$

has been derived. There is an interesting phenomenological relation between the Cabibbo angle and the quark mass ratio (2.38)

$$\frac{m_s}{m_d} = 18.9 \pm 0.8 , \quad (6.28)$$

commonly known as *GST-relation*

$$\theta_C \approx \sqrt{\frac{1}{19}} \approx \sqrt{\frac{y_d}{y_s}} . \quad (6.29)$$

Historically it was first phrased in [159] as $\theta_C^2 \approx \frac{m_\pi^2}{2m_K^2}$, where m_π and m_K denote pion and kaon masses, respectively, and in [160] in the context of quark masses. Necessary

constraints for (6.29) to hold in viable flavour models are [161] approximately vanishing 1-1 element of Y_d and $|a| \approx |b|$, as can be seen from (6.26)

$$\frac{y_d}{y_s} \approx \left| \frac{ab}{c^2} \right| \approx \left| \frac{a}{b} \right| \theta_C^2. \quad (6.30)$$

Thus, although less direct than in condition 4.1, $|a| \approx |b|$ is found via vanishing 1-1 element of Y_d and the GST relation. From (6.23) the connection to θ_C , i.e. $\theta_{12}^e \approx \left| \frac{c_a}{c_c} \right| \theta_C$, is obtained, thus realising $\theta_{13}^{\text{PMNS}} \approx \theta_C \sin \theta_{23}^{\text{PMNS}}$.

Note that c_b has to be properly chosen in addition to $|c_a| = |c_c|$, to yield viable GUT scale quark-lepton mass ratios for the first two families [148, 149]. In $SU(5)$ GUTs with zero 1-1 elements in Y_d and Y_e , only one combination of CG factors listed in (4.45) results in $\theta_{13}^{\text{PMNS}} \approx \theta_C \sin \theta_{23}^{\text{PMNS}}$, while being consistent with phenomenological constraints (including $\frac{m_s}{m_d} \approx 19$), namely

$$c_c = c_a = 6, \quad c_b = -\frac{1}{2}. \quad (6.31)$$

6.4 Corrections to $\theta_{13}^{\text{PMNS}} \approx \theta_C \sin \theta_{23}^{\text{PMNS}}$

As we have discussed above, the relation $\theta_{13}^{\text{PMNS}} \approx \theta_C \sin \theta_{23}^{\text{PMNS}}$ can emerge under four simple conditions from GUTs, by charged lepton contributions to V_{PMNS} and linking θ_{12}^e to θ_C . Let us now discuss how this relation is affected by certain, unavoidable corrections, for example from RG running between the GUT scale where the prediction arises and low energies where the neutrino oscillation experiments are performed. Other corrections arise from the fact that we presented leading order results in a small mixing approximation.

Note that given a specific flavour model, the deviation from the exact relation can be calculated, and future more precise measurements of the lepton mixing angles may allow to discriminate between different models realising $\theta_{13}^{\text{PMNS}} \approx \theta_C \sin \theta_{23}^{\text{PMNS}}$.

Possible corrections are:

Corrections due to small mixing approximation: In 6.3 we omitted higher order terms in a small mixing angle expansion to keep our discussion as simple as possible. The error introduced by this simplification depends on the structure of the Yukawa matrices and on the CG factors and can easily be computed. Let us consider, for instance, the example of a $SU(5)$ GUT with zero 1-1 elements in Y_d and Y_e and CG factors as in (6.31), i.e.

$$Y_d = \begin{pmatrix} 0 & b \\ a & c \end{pmatrix}, \quad Y_e = \begin{pmatrix} 0 & 6a \\ -\frac{1}{2}b & 6c \end{pmatrix}. \quad (6.32)$$

Instead of a small angle approximation, we numerically perform an exact diagonalisation of the Yukawa matrices (6.32) and find $\theta_{12}^e = 13.8^\circ$ from a fit to the experimental values $\frac{y_e}{y_\mu}$ and θ_C . The more precise GUT scale prediction is thus

$$\text{SU}(5) \text{ with } d = 0, \quad c_c = c_a = 6, \quad c_b = -\frac{1}{2}, \quad \text{and } \theta_{12}^d = \theta_C: \quad \theta_{13}^{\text{PMNS}} \approx 9.3^\circ. \quad (6.33)$$

Corrections from $\theta_{12}^d \neq \theta_C$: In explicit flavour GUT models, condition 2 may not be exactly fulfilled. Without a specific model, this is a source of theoretical uncertainty. Within a specific model, however, such a deviation is calculable and results in a modified prediction for $\theta_{13}^{\text{PMNS}}$, which may open up the possibility to distinguish explicit flavour models with a future more precise measurement of the lepton mixing angles. As mentioned above, the quark mixing sum rule (6.11) yields $\theta_{12}^d \approx 12.0^\circ \pm 0.3^\circ \neq \theta_C$ in models where $\theta_{13}^u, \theta_{13}^d \approx 0$.

Let us study this in more detail in a Pati-Salam model with CG factors 9 and -3 , where we assume embedding in a $SO(10)$ GUT or a suitable flavour symmetry, such that the Yukawa matrices are symmetric, i.e.

$$Y_d = \begin{pmatrix} d & b \\ b & c \end{pmatrix}, \quad Y_e = \begin{pmatrix} 9d & -3b \\ -3b & -3c \end{pmatrix}. \quad (6.34)$$

As above, we perform an exact diagonalisation of the Yukawa matrices and fit to the experimental value of $\frac{y_e}{y_\mu}$ and $\theta_{12}^d = 12.0^\circ$. We obtain the prediction

$$\text{PS with } \theta_{13}^u \approx \theta_{13}^d \approx 0, a = b, c_d = 9, \text{ and } c_b = c_c = -3: \quad \theta_{13}^{\text{PMNS}} \approx 8.2^\circ. \quad (6.35)$$

Corrections due the uncertainty of $\theta_{23}^{\text{PMNS}}$: There is still a large uncertainty for the value of $\theta_{23}^{\text{PMNS}}$. The most immediate uncertainty is caused by the dependence of $\theta_{23}^{\text{PMNS}}$ on the yet undetermined mass ordering of neutrinos. But even when a specific ordering is assumed as prior, the relative uncertainty induced in the prediction for $\theta_{13}^{\text{PMNS}}$ still amounts to about 5% (3%) for normal (inverse) mass ordering. Note that [62] reports a 3σ range for $\theta_{23}^{\text{PMNS}}$ of $[38.3^\circ, 53.3^\circ]$ in the general case where no specific mass ordering is assumed. As mentioned above, the $\text{NO}\nu\text{A}$ experiments finds an one sigma interval of $[38.6^\circ, 53.7^\circ]$ for $\theta_{23}^{\text{PMNS}}$ [151]. An improved experimental accuracy for $\theta_{23}^{\text{PMNS}}$ and a measurement of the neutrino mass ordering are therefore necessary in order to predict $\theta_{13}^{\text{PMNS}}$ more precisely.

Corrections due to RG evolution: Let us now discuss the impact of RG corrections. The relation $\theta_{13}^{\text{PMNS}} \approx \theta_C \sin \theta_{23}^{\text{PMNS}}$ is defined at the GUT scale. Our strategy is to run the measured values of θ_C and $\theta_{23}^{\text{PMNS}}$ up to M_{GUT} to determine $\theta_{13}^{\text{PMNS}}|_{M_{\text{GUT}}}$, and then perform the RG running of $\theta_{13}^{\text{PMNS}}|_{M_{\text{GUT}}}$ down to the electroweak scale M_{EW} to obtain $\theta_{13}^{\text{PMNS}}|_{M_{\text{EW}}}$, the parameter measurable in experiments. For simplicity, we assume a strongly hierarchical neutrino mass spectrum with $m_1 = 0$ (NO) or $m_3 = 0$ (IO) in the MSSM. The running of θ_C is known to be tiny (see e.g. [91]) and will be neglected in the following.

Using the analytical results of [162], one can estimate

$$\Delta s_{23}^{\text{PMNS}} \equiv s_{23}^{\text{PMNS}}|_{M_{\text{EW}}} - s_{23}^{\text{PMNS}}|_{M_{\text{GUT}}} \quad (6.36)$$

in leading logarithmic approximation and in leading (zeroth) order in $\theta_{13}^{\text{PMNS}}$:

$$\Delta s_{23}^{\text{PMNS}} \approx \begin{cases} \frac{(y_\tau^{\text{SM}})^2(1 + \tan^2 \beta)}{16\pi^2} \ln \left(\frac{M_{\text{GUT}}}{M_{\text{EW}}} \right) (c_{23}^{\text{PMNS}})^2 s_{23}^{\text{PMNS}} & \text{(NO)}, \\ -\frac{(y_\tau^{\text{SM}})^2(1 + \tan^2 \beta)}{16\pi^2} \ln \left(\frac{M_{\text{GUT}}}{M_{\text{EW}}} \right) (c_{23}^{\text{PMNS}})^2 s_{23}^{\text{PMNS}} & \text{(IO)} \end{cases}. \quad (6.37)$$

For the running of $\theta_{13}^{\text{PMNS}}$, we obtain for

$$\Delta \theta_{13}^{\text{PMNS}} \equiv \theta_{13}^{\text{PMNS}} \Big|_{M_{\text{EW}}} - \theta_{13}^{\text{PMNS}} \Big|_{M_{\text{GUT}}} \quad (6.38)$$

in leading (first) order in $\theta_{13}^{\text{PMNS}}$:

$$\Delta \theta_{13}^{\text{PMNS}} \approx \begin{cases} \frac{(y_\tau^{\text{SM}})^2(1 + \tan^2 \beta)}{16\pi^2} \ln \left(\frac{M_{\text{GUT}}}{M_{\text{EW}}} \right) \\ \left(2 \frac{m_2}{m_3} \cos(\delta^{\text{PMNS}} + \alpha_1^{\text{PMNS}} - \alpha_2^{\text{PMNS}}) c_{12}^{\text{PMNS}} s_{12}^{\text{PMNS}} c_{23}^{\text{PMNS}} s_{23}^{\text{PMNS}} \right. \\ \left. + (c_{23}^{\text{PMNS}})^2 \theta_{13}^{\text{PMNS}} \right), & \text{(NO)} \\ -\frac{(y_\tau^{\text{SM}})^2(1 + \tan^2 \beta)}{16\pi^2} \ln \left(\frac{M_{\text{GUT}}}{M_{\text{EW}}} \right) (c_{23}^{\text{PMNS}})^2 \theta_{13}^{\text{PMNS}} & \text{(IO)}, \end{cases} \quad (6.39)$$

where α_1^{PMNS} and α_2^{PMNS} denote the Majorana phases introduced in (3.16). $\theta_{13}^{\text{PMNS}} \Big|_{M_{\text{EW}}}$ can now be predicted in terms of the measured values of θ_C and $\theta_{23}^{\text{PMNS}} \Big|_{M_{\text{EW}}}$ using the GUT scale relation (6.3):

$$\begin{aligned} \theta_{13}^{\text{PMNS}} \Big|_{M_{\text{EW}}} &= \theta_C s_{23}^{\text{PMNS}} \Big|_{M_{\text{GUT}}} + \Delta \theta_{13}^{\text{PMNS}} \\ &= \theta_C \left(s_{23}^{\text{PMNS}} \Big|_{M_{\text{EW}}} - \Delta s_{23}^{\text{PMNS}} \right) + \Delta \theta_{13}^{\text{PMNS}}. \end{aligned} \quad (6.40)$$

Remarkably, in the case of an inverse mass ordering the terms $\Delta \theta_{13}^{\text{PMNS}}$ and $\theta_C \Delta s_{23}^{\text{PMNS}}$ cancel each other at leading order, while for normal ordering only the term proportional to the neutrino mass ratio $\frac{m_2}{m_3}$ remains. Plugging in the experimental values of the mixing parameters and $y_\tau^{\text{SM}} \approx 0.01$ we obtain the following estimate for the effects of RG running:

$$\theta_{13}^{\text{PMNS}} \Big|_{M_{\text{EW}}} \approx \begin{cases} \theta_C s_{23}^{\text{PMNS}} \Big|_{M_{\text{EW}}} + 0.2^\circ \cos(\delta^{\text{PMNS}} + \alpha_1^{\text{PMNS}} - \alpha_2^{\text{PMNS}}) \left(\frac{\tan \beta}{50} \right)^2 & \text{(NO)}, \\ \theta_C s_{23}^{\text{PMNS}} \Big|_{M_{\text{EW}}} & \text{(IO)}. \end{cases} \quad (6.41)$$

In the IO case corrections coming from the next order terms are estimated to be about $\mathcal{O}(0.05^\circ) \left(\frac{\tan \beta}{50} \right)^2$. It is thus in general a rather good approximation to evaluate (6.3) with

the measured parameters at low energies, even more so for the case of an inverse mass ordering, where the effects due to RG evolution are negligible small.

Note that the above treatment does not include running of neutrino Yukawa couplings in type-I seesaw scenarios. Such effects contribute above the mass thresholds of heavy right-handed neutrinos. They are more model dependent and can be estimated using the analytical formulae of [163] or calculated numerically, e.g. using the Mathematica package REAP [163]. For hierarchical neutrino Yukawa matrices dominated by a large 3-3 element $Y_{\nu_{33}}$ one can obtain an estimate for the additional correction by simply replacing

$$(y_\tau^{\text{SM}})^2 (1 + \tan^2 \beta) \ln \frac{M_{\text{GUT}}}{M_{\text{EW}}} \longrightarrow Y_{\nu_{33}}^2 \ln \frac{M_{\text{GUT}}}{M_{r_3}} \quad (6.42)$$

in the above equations, where M_{r_3} is the mass of the corresponding righthanded neutrino.

Let us remark that when matching the MSSM to the SM at M_{SUSY} , effects from SUSY threshold corrections on θ_C and the lepton mixing angles are negligible to a very good approximation. A numerical calculation can be performed with `SusyTC` [5], which will be presented in chapter 10.

Corrections from canonical normalisation: Finally there can be corrections from canonical normalisation of kinetic terms from a non-trivial Kähler metric, as it emerges e.g. by integrating out heavy messenger fields in a flavour model, as discussed below (5.47). Since the effective Kähler potential in such scenarios contains terms proportional to the Yukawa couplings, it is typically dominated by third family effects. For example, in a specific flavour GUT model the effective Kähler metric might be written in leading order as e.g. [107, 108]

$$K \approx k_0 \left(\mathbb{1} + \frac{k_3}{k_0} \frac{\langle \phi_3^\dagger \rangle \langle \phi_3 \rangle}{M_3^2} \right), \quad (6.43)$$

where k_0 and k_3 are order one coefficients and ϕ_3 is a heavy messenger field of mass M_3 yielding third family Yukawa couplings of $y_3 \approx \frac{\langle \phi_3 \rangle}{M_3}$. Then, defining

$$\eta^{CN} \equiv \frac{k_3}{k_0} \frac{\langle \phi_3^\dagger \rangle \langle \phi_3 \rangle}{M_3^2} \quad (6.44)$$

results in formulae analogous to the case of the RG corrections discussed above as estimate for the CN corrections [107, 108]. This formulae are given by (6.37) and (6.39) upon the replacement

$$(y_\tau^{\text{SM}})^2 (1 + \tan^2 \beta) \ln \frac{M_{\text{GUT}}}{M_{\text{EW}}} \longrightarrow 8\pi^2 \eta^{CN}. \quad (6.45)$$

Thus, in scenarios with an inverse mass ordering the relation $\theta_{13}^{\text{PMNS}} \approx \theta_C \sin \theta_{23}^{\text{PMNS}}$ is also quite insensitive to CN corrections.

Note that while (6.45) holds in general in theories with dominant third family contributions to K , the specific form for η^{CN} (6.43) and (6.44), and whether or not η^{CN} is of significant magnitude, are highly model dependent. Whereas in some models the effect

6.5 The underlying neutrino mixing pattern in the light of

$$\theta_{13}^{\text{PMNS}} \approx \theta_C \sin \theta_{23}^{\text{PMNS}}$$

73

of CN corrections can be of the same size as RG running corrections (in the NO case) or larger, there are classes of models where CN effects are negligibly small (cf. [107]).

To summarise, in general the uncertainties for the relation $\theta_{13}^{\text{PMNS}} \approx \theta_C \sin \theta_{23}^{\text{PMNS}}$ can amount up to about $\mathcal{O}(10\%)$, which is larger than the current experimental uncertainty. However, it is important to note that within an explicit flavour GUT model, these corrections can be explicitly calculated, thereby decreasing the uncertainty drastically. With a typical theoretical uncertainty for $\theta_{13}^{\text{PMNS}}$ of roughly $\pm 0.25^\circ$ in a careful model analysis, it is thus possible to discriminate between specific flavour GUT models. In the following two chapters two predictive flavour GUT models featuring $\theta_{13}^{\text{PMNS}} \approx \theta_C \sin \theta_{23}^{\text{PMNS}}$ will be constructed and analysed.

6.5 The underlying neutrino mixing pattern in the light of $\theta_{13}^{\text{PMNS}} \approx \theta_C \sin \theta_{23}^{\text{PMNS}}$

Assuming hierarchic Yukawa matrices such that condition 1 ($\theta_{13}^\nu, \theta_{13}^e \ll \theta_C$) and $\theta_{23}^e \ll \theta_C$ are satisfied, the mixing angle θ_{12}^ν is related to $\theta_{13}^{\text{PMNS}}$ and $\theta_{12}^{\text{PMNS}}$ by the lepton mixing sum rule² (3.34) [65–67]

$$s_{12}^\nu \approx s_{12}^{\text{PMNS}} - \theta_{13}^{\text{PMNS}} c_{12}^{\text{PMNS}} \cot \theta_{23}^{\text{PMNS}} \cos \delta^{\text{PMNS}}, \quad (6.46)$$

which in the light of $\theta_{13}^{\text{PMNS}} \approx \theta_C \sin \theta_{23}^{\text{PMNS}}$ becomes

$$s_{12}^\nu \approx s_{12}^{\text{PMNS}} - \theta_C c_{23}^{\text{PMNS}} c_{12}^{\text{PMNS}} \cos \delta^{\text{PMNS}}. \quad (6.47)$$

Thus, based on a specific model for neutrino mixing, the Dirac CP phase δ^{PMNS} can be predicted.

For example, if bimaximal mixing is realised in the neutrino sector, i.e. $\theta_{12}^\nu = 45^\circ$, the lepton mixing sum rule becomes

$$\theta_{12}^{\text{PMNS}} - \theta_C c_{23}^{\text{PMNS}} \cos(\delta^{\text{PMNS}}) \approx 45^\circ. \quad (6.48)$$

Note that this differs substantially from the QLC relation $\theta_C + \theta_{12}^{\text{PMNS}} = 45^\circ$. With the experimental data for the mixing angles, (6.48) predicts a Dirac CP phase $\delta^{\text{PMNS}} \approx 180^\circ$.

As a further example, let us consider tri-bimaximal neutrino mixing, i.e. $\sin(\theta_{12}^\nu) = \frac{1}{\sqrt{3}}$, such that the lepton mixing sum rule is given by

$$\theta_{12}^{\text{PMNS}} - \theta_C c_{23}^{\text{PMNS}} \cos(\delta^{\text{PMNS}}) \approx \arcsin\left(\frac{1}{\sqrt{3}}\right). \quad (6.49)$$

Then one predicts a Dirac CP phase of

$$\delta^{\text{PMNS}} = 100.8^\circ \begin{matrix} +4.6^\circ \\ -4.7^\circ \end{matrix}. \quad (6.50)$$

²RG corrections to the lepton mixing sum rule have been discussed in [164].

Note that such values for δ^{PMNS} at the EW scale can result from specific GUT scale predictions for $\delta^{\text{PMNS}} \in \{0^\circ, \pm 90^\circ, 180^\circ\}$ in explicit flavour GUT models with discrete shaping symmetries like \mathbb{Z}_2 or \mathbb{Z}_4 in the context of spontaneous CP violation (see e.g. [165] and the flavour GUT models in the following chapters).

Finally, let us emphasise again that we do not require tri-bimaximal or bimaximal neutrino mixing to obtain the prediction $\theta_{13}^{\text{PMNS}} \approx \theta_C \sin \theta_{23}^{\text{PMNS}}$ from GUTs. The only requirement on the neutrino sector is $\theta_{13}^\nu \ll \theta_C$ in condition 1. The future long baseline neutrino oscillation experiment DUNE [69] aims to measure δ^{PMNS} and the lepton mixing sum rule can be understood to “reconstruct” the value of θ_{12}^ν via a future measurement of the Dirac CP phase, as shown in figure 6.2. Thus, using the lepton mixing sum rule (6.47), a precise measurement of $\theta_{12}^{\text{PMNS}}$, $\theta_{13}^{\text{PMNS}}$, and δ^{PMNS} may hint at a specific neutrino mixing pattern.

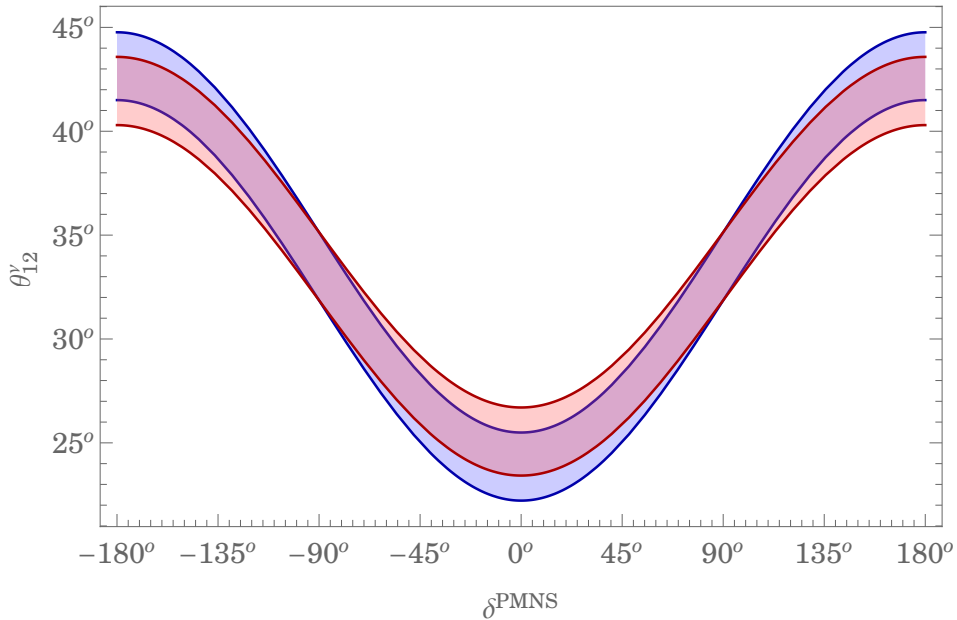


Figure 6.2: One sigma hpd intervals from a Monte Carlo simulation of the lepton mixing sum rule (6.47) in case of normal (blue) and inverse (red) neutrino mass ordering. A measurement of δ^{PMNS} allows to determine θ_{12}^ν (under the conditions $\theta_{13}^\nu, \theta_{13}^e, \theta_{23}^e \ll \theta_C$). See appendix C for a definition of hpd intervals.

CHAPTER 7

A SUSY flavour GUT model with $\theta_{13}^{\text{PMNS}} \approx \theta_C \sin \theta_{23}^{\text{PMNS}}$

In this chapter we propose a predictive supersymmetric $SU(5)$ GUT model with an A_4 flavour symmetry, supplemented by discrete shaping symmetries and an R -symmetry, which realises the relation (6.3)

$$\theta_{13}^{\text{PMNS}} \approx \theta_C \sin \theta_{23}^{\text{PMNS}}, \quad (7.1)$$

based on [2]. The neutrino sector features tri-bimaximal mixing, and (6.3) emerges from the charged lepton contribution to the lepton mixing matrix, which in turn is linked to quark mixing via specific GUT relations, as discussed in the previous chapter. In addition to $\theta_{13}^{\text{PMNS}}$, the model leads to promising quark lepton mass ratios in excellent agreement with experimental results. Our model also features spontaneous CP violation, with all quark and lepton CP phases determined from flavour symmetry breaking.

7.1 Outline of the model

Our model is constructed with the requirement to satisfy the four conditions of the previous chapter. In this section we discuss how they are implemented in our model. The desired structure of the Yukawa matrices will be achieved, as we discuss in the next section, via spontaneously breaking the flavour symmetry A_4 by vevs of flavon fields, which – due to an appropriate potential for the flavons – point in specific directions of flavour space.

Condition 1: $\theta_{13}^e, \theta_{13}^\nu \approx 0$ will be satisfied by constructing a Yukawa matrix Y_e with vanishing 1-3 element and tri-bimaximal mixing in the neutrino sector.

Condition 2: $\theta_{12}^d \approx \theta_C$ is achieved by constructing Y_d and Y_u with vanishing 1-3 elements, such that the quark mixing sum rule (6.11) is realised. Additionally, under the condition

$\theta_{13}^u, \theta_{13}^d \approx 0$, the quark unitarity triangle angle

$$\begin{aligned} \alpha &\equiv \arg \left(-\frac{V_{td}V_{tb}^*}{V_{ud}V_{ub}^*} \right) = \arg \left(-\frac{(s_{23}s_{12} - c_{23}s_{13}c_{12}e^{i\delta})c_{23}c_{13}}{c_{12}c_{13}s_{13}e^{i\delta}} \right) \\ &\approx \arg \left(1 - \frac{\theta_{23}\theta_{12}}{\theta_{13}} e^{-i\delta} \right), \end{aligned} \quad (7.2)$$

where the subscript CKM was suppressed for higher readability, is given by a *phase sum rule* [157]

$$\alpha \approx \arg \left(\frac{\theta_{12}^d}{\theta_{12}^u} e^{i(\delta_{12}^d - \delta_{12}^u)} \right) = \delta_{12}^d - \delta_{12}^u. \quad (7.3)$$

Equations (6.6) and (6.7) were used to derive (7.3) from (7.2). Thus, a right-angled quark unitarity triangle with $\alpha \approx 90^\circ$ can be achieved by constructing Y_d with purely imaginary 1-2 element and Y_u with purely real 1-2 element, yielding $\delta_{12}^d = 90^\circ$ and $\delta_{12}^u = 0^\circ$, respectively, when all other elements in the 1-2 submatrices are real. There are two more expressions that can be obtained from (6.6) and (6.7) with $\theta_{13}^u, \theta_{13}^d \approx 0$ [157]

$$\theta_{12}^u \approx \frac{\theta_{13}^{\text{CKM}}}{\theta_{23}^{\text{CKM}}}, \quad \frac{\theta_{13}^{\text{CKM}}\theta_{12}^{\text{CKM}}}{\theta_{23}^{\text{CKM}}} e^{-i\delta^{\text{CKM}}} \approx -\theta_{12}^u \left(\theta_{12}^d e^{-i(\delta_{12}^d - \delta_{12}^u)} - \theta_{12}^u \right). \quad (7.4)$$

From (6.11) and (7.4), the experimental value $\delta^{\text{CKM}} = 71.1^\circ \pm 3.1^\circ$ yields

$$\delta_{12}^d - \delta_{12}^u = 86.1^\circ \pm 3.3^\circ. \quad (7.5)$$

Note that the experimental value of α is given by $\alpha = 85.4^\circ \pm_{-3.8^\circ}^{+3.9^\circ}$. Thus our set-up implies a realistic value for δ_{CKM} , by a single purely imaginary 2-2 entry in Y_d .

Due to the $SU(5)$ relation the 2-2 element of Y_e is purely imaginary as well, and the CP violation is carried from the quark to the lepton mixing sector, yielding a Dirac CP phase $\delta^{\text{PMNS}} \approx 90^\circ$. Thus, from the discussion in 6.5 and the lepton mixing sum rule (6.47), the neutrino sector must feature tri-bimaximal mixing. In our model we therefore employ type-I seesaw and *Constrained Sequential Dominance* (3.43), as described in 3.3. Our model will also include a charged lepton mixing θ_{23}^e , which can generate a deviation of $\theta_{23}^{\text{PMNS}}$ from maximal mixing.

Note that the feature of purely imaginary Yukawa matrix elements can be achieved by a suitable flavon alignment potential as well, such that CP symmetry is broken only spontaneously due to CP-violating vevs of flavon fields.

Condition 3: All relevant elements of Y_e and Y_d will be generated by single GUT-operators in order to construct predictive quark-lepton relations.

Condition 4: In the setting of an $SU(5)$ GUT, we construct Y_d and Y_e with vanishing 1-1 elements. As mentioned in the previous chapter, we therefore must use GUT operators

that yield the CG factors $c_{12} = 6$, $c_{21} = -\frac{1}{2}$, and $c_{22} = 6$ (where c_{ij} is the CG factor of the i - j element of Y_e).

Note that, since the CG factors play a crucial role for the phenomenological viability of the model, it is essential that we not only provide an effective model at the GUT scale, but that we also specify the messenger sector, which when integrated out realises only single GUT operators with predictive CG factors, as discussed in 4.4.

We pursue the following procedure to construct a model with the features described above:

- In our model the rows respectively columns of the Yukawa matrices are generated as vevs of flavon fields, which are triplets of the flavour symmetry group A_4 .

In order to obtain the desired structure of the Yukawa matrices, we first find a suitable set of effective operators for the matter sector, appropriate vevs for the flavon fields and a viable alignment potential generating these vevs.

- The next step is to identify the *shaping symmetry* of the thus specified superpotential. As shaping symmetry we denote \mathbb{Z}_n and $U(1)$ symmetries, required in addition to A_4 , to forbid terms which would spoil the desired features. Note that, since one can always redefine several \mathbb{Z}_n symmetries by linear combinations into another set of \mathbb{Z}_n s, the resulting shaping symmetry is not unique.
- Now we turn to the *UV completion* of the effective superpotential and find a suitable set of messenger fields, that, when integrated out, can generate all effective operators. Usually, one has a sizeable freedom of choice in doing so, both from using different representations for the messengers and from using different “topologies” for the supergraph diagrams. An important constraint on the messenger sector is, however, that it must guarantee the correct CG factors for the effective operators of Y_e , see 4.4.
- Finally, with the flavon, matter, Higgs, and messenger field content at hand, and the given shaping symmetry, one has to check whether the most general superpotential contains any additional effective operators, which spoil the desired features of the Yukawa matrices. If this is the case, one has to modify some choice made in one of the previous steps, be it the flavon alignment, the structure of the effective superpotential or the set of messenger fields. Ultimately, a consistent flavour model is developed, by successively going through the previous steps and gradually improving the different sectors, until no such dangerous operators are present.

7.2 The model

We now present our model in detail. The matter content of SUSY $SU(5)$ is embedded into one A_4 triplet \mathcal{F} , which thus contains all three families D_i^c and L_i , and into three A_4 -invariant singlets \mathcal{T}_i , one for each family. Additionally, we introduce two right-handed neutrinos N_1^c and N_2^c as invariant singlets under A_4 and $SU(5)$. The Higgs sector contains

flavon φ_i :	ϕ_2	ϕ_3	ϕ_{ab}	ϕ_{N_1}	ϕ_{N_2}	ξ_{12}	ξ_{23}	ξ_M	χ
$\frac{\langle \varphi_i \rangle}{\Lambda}$:	$\epsilon_2 \begin{pmatrix} 0 \\ 1 \\ 0 \end{pmatrix}$	$\epsilon_3 \begin{pmatrix} 0 \\ 0 \\ 1 \end{pmatrix}$	$\epsilon_{ab} \begin{pmatrix} c_{ab} \\ -i s_{ab} \\ 0 \end{pmatrix}$	$\epsilon_{N_1} \begin{pmatrix} 0 \\ 1 \\ -1 \end{pmatrix}$	$\epsilon_{N_2} \begin{pmatrix} 1 \\ 1 \\ 1 \end{pmatrix}$	ϵ_{12}	ϵ_{23}	ϵ_M	ϵ_χ

Table 7.1: The vevs of the flavon superfields. The ϵ_i are all assumed to be real numbers. We abbreviated $c_{ab} \equiv \cos(\theta_{ab})$ and $s_{ab} \equiv \sin(\theta_{ab})$. The scale Λ is a placeholder for the individual messenger mass suppression. See the next section for a detailed discussion of the flavon alignment.

the H_{24} , responsible for the spontaneous breaking of $SU(5)$, and the superfields H_5 , \bar{H}_5 , H_{45} , and \bar{H}_{45} lead to electroweak symmetry breaking.¹

The flavon fields are five A_4 triplets called ϕ_i , three A_4 invariant singlets called ξ_i , and one A_4 non-invariant singlet in the $\mathbf{1}'$ representation called χ . They break the flavour symmetry by their vevs as given in table 7.1. In the next section we discuss the superpotential responsible for the spontaneous breaking of A_4 which yields the desired flavon vevs in flavour space. A brief review of A_4 group theory is presented in appendix A.

The scale Λ is a placeholder for the messenger mass suppression specific to the operator which generates the entry, row, or column of the Yukawa matrices (7.10) and (7.12), where the ϵ_i appears. A full list of all operators, including the messenger fields, which generate the effective superpotential, is given in appendix D. There we also present the supergraphs yielding the effective operators, such that the suppression of the effective operators by their particular messenger masses and couplings can be read off.

The effective superpotential in the matter sector is given by

$$\mathcal{W}_{\text{eff}} = \mathcal{W}_{Y_\nu} + \mathcal{W}_{M_R} + \mathcal{W}_{Y_d} + \mathcal{W}_{Y_u} , \quad (7.6)$$

with

$$\mathcal{W}_{Y_\nu} = H_5 \mathcal{F} (N_1^c \phi_{N_1} + N_2^c \phi_{N_2}) , \quad (7.7a)$$

$$\mathcal{W}_{M_R} = \xi_M^2 \left((N_1^c)^2 \phi_{N_1}^2 + (N_2^c)^2 \phi_{N_2}^2 \right) , \quad (7.7b)$$

$$\begin{aligned} \mathcal{W}_{Y_d} = & [\mathcal{T}_1 \bar{H}_{45}]_{45} [\mathcal{F} H_{24}]_{\bar{45}} \phi_2 + [\mathcal{T}_2 H_{24}]_{10} [\mathcal{F} \bar{H}_5]_{\bar{10}} \phi_{ab} \\ & + [\mathcal{T}_3 \bar{H}_5]_{\bar{5}} [\mathcal{F} H_{24}]_{\bar{5}} \phi_3 + [\mathcal{T}_3 H_{24}]_{10} [\mathcal{F} \bar{H}_5]_{\bar{10}} \chi \phi_2 , \end{aligned} \quad (7.7c)$$

$$\mathcal{W}_{Y_u} = H_5 \left(\mathcal{T}_3^2 + \mathcal{T}_2^2 \phi_{ab}^2 + \mathcal{T}_1^2 (\phi_2^2)^2 + \mathcal{T}_2 \mathcal{T}_3 \xi_{23} + \mathcal{T}_1 \mathcal{T}_2 \xi_{12}^5 \right) , \quad (7.7d)$$

where $[XY]_R$ denotes the contraction of the fields X and Y to an $SU(5)$ tensor in the representation \mathbf{R} , indicating which representation the messenger field, which was integrated out to obtain the effective operator, had. In our model, the CG factors 6, $-\frac{1}{2}$, and $-\frac{3}{2}$

¹We note that while we will explicitly construct the GUT matter sector and the flavour symmetry breaking sector, the details of the (GUT) Higgs sector are beyond the scope of this flavour model. We will come back to this question in chapter 9.

arise from contractions mediated by messengers transforming as **10**, **45**, and **5** under $SU(5)$, coupling to \bar{H}_5 and \bar{H}_{45} , respectively, as can be seen in table 4.1. Since we need these specific contractions for our model to work, it is essential that we also construct the messenger sector. The full set of messenger fields, together with their charges, is shown in appendix D.

Note that for the sake of brevity, we do not explicitly write down the appropriate suppression by powers of the relevant mass scales Λ (which are different for each operator) in (7.7), and we also suppress the couplings in front of each term.

In order to parametrise the resulting Yukawa matrices, we define the quantities

$$\tilde{\epsilon}_i \equiv \frac{\langle H_{24} \rangle}{\Lambda} \epsilon_i \quad \text{and} \quad \hat{\epsilon}_\chi \equiv \frac{\langle H_{24} \rangle \langle \phi_2 \rangle}{\Lambda^2} \epsilon_\chi, \quad (7.8)$$

where again Λ is a placeholder for the individual messenger mass.

After GUT and flavour symmetry breaking, the superpotential for the Yukawa matrices and right-handed neutrino mass matrix (5.64) and (5.77) is given by

$$\mathcal{W} = Y_{e_{ij}} H_d \cdot L_i E_j^c + Y_{d_{ij}} H_d \cdot Q_i D_j^c - Y_{u_{ij}} H_u \cdot Q_i U_j^c + Y_{\nu_{ij}} H_u \cdot L_i N_j^c + \frac{1}{2} M_{n_{ij}} N_i^c N_j^c, \quad (7.9)$$

with the Yukawa matrices of the quarks and charged leptons given by

$$Y_d = \begin{pmatrix} 0 & \tilde{\epsilon}_2 & 0 \\ \tilde{\epsilon}_{ab} c_{ab} & -i\tilde{\epsilon}_{ab} s_{ab} & 0 \\ 0 & \omega \hat{\epsilon}_\chi & \tilde{\epsilon}_3 \end{pmatrix}, \quad Y_e = \begin{pmatrix} 0 & 6\tilde{\epsilon}_{ab} c_{ab} & 0 \\ -\frac{1}{2}\tilde{\epsilon}_2 & -i6\tilde{\epsilon}_{ab} s_{ab} & 6\omega \hat{\epsilon}_\chi \\ 0 & 0 & -\frac{3}{2}\tilde{\epsilon}_3 \end{pmatrix}, \quad Y_u = \begin{pmatrix} \epsilon_2^4 & \epsilon_{12}^5 & 0 \\ \epsilon_{12}^5 & \epsilon_{ab}^2 & \epsilon_{23} \\ 0 & \epsilon_{23} & y_t \end{pmatrix}, \quad (7.10)$$

up to subleading corrections from higher-dimensional operators or canonical normalisation. With the messenger sector of the model specified in appendix D both corrections can be neglected. The rows and columns of the down-type quark and charged lepton Yukawa matrices, respectively, are built from flavon vevs. The phase

$$\omega \equiv e^{\frac{2\pi i}{3}} \quad (7.11)$$

comes from the fact that the flavon field χ transforms as one-dimensional $\mathbf{1}'$ representation of A_4 . The hierarchy in Y_u is generated by the different powers of flavon vevs in each entry.

The neutrino Yukawa matrix respectively the mass matrix of the heavy neutrinos are given by (3.43)

$$Y_\nu = \begin{pmatrix} 0 & \epsilon_{N_2} \\ \epsilon_{N_1} & \epsilon_{N_2} \\ -\epsilon_{N_1} & \epsilon_{N_2} \end{pmatrix}, \quad M_R = \begin{pmatrix} M_{R_1} & 0 \\ 0 & M_{R_2} \end{pmatrix}. \quad (7.12)$$

The mass matrix of the light neutrinos is obtained from the type-I seesaw formula (3.7)

$$m_\nu = -\frac{v_u^2}{2} \begin{pmatrix} A & A & A \\ A & A+B & A-B \\ A & A-B & A+B \end{pmatrix}, \quad \text{with} \quad A \equiv \frac{\epsilon_{N_2}^2}{M_{R_2}}, \quad B \equiv \frac{\epsilon_{N_1}^2}{M_{R_1}}, \quad (7.13)$$

which implies tri-bimaximal mixing in the neutrino sector. Note that, since m_ν depends only on the two parameters A and B , we are free to fix two of the four parameters which enter Y_ν and M_R , as discussed below in (7.27).

7.3 Flavon alignment

Here we present the mechanism responsible for the vacuum alignment of the A_4 -triplet flavons ϕ_i , the A_4 -invariant flavons ξ_i , and the flavon χ in the $\mathbf{1}'$ representation of A_4 . For a brief review of A_4 group theory, see appendix A.

The scalar potential for the flavon fields is obtained from the F -term contributions of the *driving fields* S_i , D_i , A_i , and O_i , which have $U(1)_R$ charge 2. Under the A_4 flavour symmetry they transform as singlets, with the exception of A , D' , and D'' , which transform as $\mathbf{3}$, $\mathbf{1}'$, and $\mathbf{1}''$, respectively. In the supersymmetric vacuum the F -terms are required to vanish, which forces the scalar components of the flavon fields to obtain the desired vevs. All flavons and driving fields are listed in the lower part of table D.1 in the appendix, together with their charges under the imposed symmetries. Note that the S -fields are all singlets with respect to all symmetries (apart from $U(1)_R$ symmetry) and hence are interchangeable.

After the messenger fields are integrated out, the effective superpotential responsible for the vacuum alignment of the flavon field vevs, as listed in table 7.1, is given by

$$\mathcal{W}_{\text{flavon}} = \mathcal{W}_{\perp} + \mathcal{W}_{N_1 N_2} + \mathcal{W}_{ab} + \mathcal{W}_{\chi} + \mathcal{W}_M + \mathcal{W}_{12}, \quad (7.14)$$

with²

$$\begin{aligned} \mathcal{W}_{\perp} = & S_2 ((\phi_2^2)^3 - M_2^2) + S_3 (\phi_3^2 - M_3^2) \\ & + A_2 (\phi_2 \star \phi_2) + A_3 (\phi_3 \star \phi_3) + O_{2,3} (\phi_2 \phi_3), \end{aligned} \quad (7.15a)$$

$$\begin{aligned} \mathcal{W}_{N_1 N_2} = & S_{N_1} ((\phi_{N_1} \star \phi_{N_1})^2 \phi_{N_1}^2 - M_{N_1}^2) + D_{N_1} (\phi_{N_1} \star \phi_{N_1}) \phi_{N_1} + O_{N_1; N_2} (\phi_{N_1} \phi_{N_2}) \\ & + S_{N_2} ((\phi_{N_2}^2)^3 - M_{N_2}^2) + D'_{N_2} (\phi_{N_2}^2)_{1''} + D''_{N_2} (\phi_{N_2}^2)_{1'} , \end{aligned} \quad (7.15b)$$

$$\begin{aligned} \mathcal{W}_{ab} = & S_{ab} ((\phi_{ab} \star \phi_{ab})^2 \xi_{23}^2 - M_{ab}^2) + D_{ab}^{\alpha} (\phi_{ab}^2 + \lambda_{ab} \xi_{23}^2) + D_{ab}^{\beta} (\phi_{ab} \star \phi_{ab}) \phi_{ab} \\ & + D_{ab}^{\gamma} ((\phi_{ab}^2)_{1'} (\phi_{ab}^2)_{1''} + k_{ab} (\phi_{ab} \star \phi_{ab})^2) , \end{aligned} \quad (7.15c)$$

$$\mathcal{W}_{\chi} = S_{\chi} (\chi^6 - M_{\chi}^2) , \quad (7.15d)$$

$$\mathcal{W}_M = S_M (\xi_M^6 - M_M^2) , \quad (7.15e)$$

$$\mathcal{W}_{12} = S_{12} (\xi_{12}^6 - M_{12}^2) , \quad (7.15f)$$

where “ \star ” denotes the symmetric product of two A_4 triplets (see appendix A) and the brackets $(\dots)_{1'}$ and $(\dots)_{1''}$ indicate that the fields are contracted to the $\mathbf{1}'$ and $\mathbf{1}''$ representation of A_4 , respectively.

The constants M^2 are real due to invariance under CP symmetry.³ Then the terms of the type

$$S(\varphi^n - M^2) \quad (7.16)$$

²As we did for the matter superpotential, we omit the appropriate suppressions by powers of the messenger masses.

³Note that we checked the CP invariance of our superpotentials using the *generalised CP* transformation applicable to models with the discrete flavour group A_4 [166]. See appendix A for a brief review.

restrict the phases of the flavon vevs to specific discrete values. In particular, among the discrete vacua for the phases there are the possibilities of 0° and 180° for n even and $M^2 > 0$, which we assume everywhere in (7.15). Thus it is possible to obtain the desired purely imaginary 2-2 elements in Y_e and Y_d and CP is broken spontaneously by the vev of ϕ_{ab} . The real vevs of χ , ξ_M , and ξ_{12} are then obtained, up to a discrete choice, as in table 7.1. Let us discuss the alignment of the remaining flavon fields in detail.

\mathcal{W}_\perp : Denoting the components of the triplets ϕ_2 and ϕ_3 with x_1, x_2, x_3 , and y_1, y_2, y_3 , respectively, the terms containing the triplet driving fields, e.g.

$$A_2(\phi_2 \star \phi_2) = A_2 \begin{pmatrix} x_2 x_3 \\ x_3 x_1 \\ x_1 x_2 \end{pmatrix}, \quad (7.17)$$

force two of each $\langle \phi_i \rangle$'s components to vanish. The term containing the A_4 singlet

$$O_{2;3}(\phi_2 \phi_3) = O_{2;3}(x_1 y_1 + x_2 y_2 + x_3 y_3) \quad (7.18)$$

forces $\langle \phi_2 \rangle$ and $\langle \phi_3 \rangle$ to be orthogonal. The phase and magnitude of the vevs is then fixed by the S terms as discussed above

$$S_2 \left((x_1^2 + x_2^2 + x_3^2)^3 - M_2^2 \right), \quad S_3 \left((y_1^2 + y_2^2 + y_3^2) - M_3^2 \right), \quad (7.19)$$

such that \mathcal{W}_\perp has a supersymmetric minimum at the points $\langle \phi_2 \rangle$ and $\langle \phi_3 \rangle$ specified in table 7.1.

$\mathcal{W}_{N_1 N_2}$: The vev $\langle \phi_{N_2} \rangle$ is fixed by the second line of $\mathcal{W}_{N_1 N_2}$. The two terms

$$D'_{N_2}(\phi_{N_2}^2)_{1''} + D''_{N_2}(\phi_{N_2}^2)_{1'} = D'_{N_2}(x_1^2 + \omega x_2^2 + \omega^2 x_3^2) + D''_{N_2}(x_1^2 + \omega^2 x_2^2 + \omega x_3^2) \quad (7.20)$$

force $x_1^2 = x_2^2 = x_3^2$, and the S_{N_2} term again fixes phase and magnitude such that $\langle \phi_{N_2} \rangle \propto (1, 1, 1)^T$. The vev $\langle \phi_{N_1} \rangle$ is constrained by

$$D_{N_1}(\phi_{N_1} \star \phi_{N_1})\phi_{N_1} = 3 D_{N_1} y_1 y_2 y_3, \quad (7.21)$$

which requires the vanishing of one component, and the orthogonality condition between $\langle \phi_{N_1} \rangle$ and $\langle \phi_{N_2} \rangle$, which results from setting the F -term of $O_{N_1; N_2}$ to zero. Then, with phase and magnitude set by the F -term of S_{N_1} , one obtains $\langle \phi_{N_1} \rangle \propto (0, 1, -1)^T$ as in table 7.1.

\mathcal{W}_{ab} : Here, the S -term determines the magnitude and the overall phase of the product $\langle \phi_{ab} \rangle \langle \xi_{23} \rangle$. The individual magnitudes and the relative phase between $\langle \phi_{ab} \rangle$ and $\langle \xi_{23} \rangle$ are determined by

$$D_{ab}^\alpha (\phi_{ab}^2 + \lambda_{ab} \xi_{23}^2). \quad (7.22)$$

One of the components of $\langle \phi_{ab} \rangle$ is required to vanish by the term with the driving field D_{ab}^β , analogously to (7.21). With the overall phase and norm of $\langle \phi_{ab} \rangle$ fixed, the relative

magnitude $\tan \theta_{ab} \equiv \left| \frac{a}{b} \right|$ and phase φ of the two non-vanishing components a and b are constrained by

$$D_{ab}^\gamma \left((\phi_{ab}^2)_{1'} (\phi_{ab}^2)_{1''} + k_{ab} (\phi_{ab} \star \phi_{ab})^2 \right) = D_{ab}^\gamma (a^4 + b^4 + (k_{ab} - 1)a^2b^2) . \quad (7.23)$$

Setting the F -term of D_{ab}^γ to zero, one obtains

$$\frac{a^2}{b^2} + \frac{b^2}{a^2} = (1 - k_{ab}) . \quad (7.24)$$

Depending on the value of k_{ab} there are three distinct solutions for a and b

$$\begin{aligned} -1 \leq k_{ab} \leq 3 : & \quad \tan \theta_{ab} = 1 & \quad k_{ab} = 1 - 2 \cos(2\varphi) \\ k_{ab} < -1 : & \quad \varphi \in \{0, \pi\} & \quad k_{ab} = -1 - 4 \cot^2(2\theta_{ab}) \\ k_{ab} > 3 : & \quad \varphi = \pm \frac{\pi}{2} & \quad k_{ab} = 3 + 4 \cot^2(2\theta_{ab}) \end{aligned} \quad (7.25)$$

Thus, with an appropriate choice of k_{ab} , the potential has a minimum at the points $\langle \phi_{ab} \rangle$ and $\langle \xi_{23} \rangle$ given in table 7.1.

7.4 Phenomenology

In this section we perform a fit of the model's GUT scale parameters to experimental data given at the low energy scale of the $\overline{\text{MS}}$ top mass $m_t(m_t)$. Towards this end, the RG running from M_{GUT} to $m_t(m_t)$ has to be performed, including SUSY threshold effects at M_{SUSY} where the MSSM is matched to the SM. Here we discuss the numerical procedure of our analysis and present the results.

7.4.1 Numerical procedure

The fit is performed in the following way: Using the one-loop MSSM RGEs of the Mathematica package REAP [163], we run the parameters in the MSSM from M_{GUT} to a conjectured SUSY scale $M_{\text{SUSY}} = 1$ TeV. REAP automatically integrates out the heavy, right-handed neutrinos at their respective mass scales and calculates the effective mass matrix of the light neutrinos from the see-saw formula (3.7).

In our analysis we include the $\tan \beta$ -enhanced SUSY threshold corrections at M_{SUSY} in the basis where Y_u is diagonal, with the approximate matching relations given by [132]

$$Y_d^{\text{SM}} = (\mathbb{1} + \text{diag}(\eta_{Q_{12}}, \eta_{Q_{12}}, \eta_{Q_3})) Y_d^{\text{MSSM}} \cos \beta , \quad (7.26a)$$

$$Y_u^{\text{SM}} = Y_u^{\text{MSSM}} \sin \beta , \quad (7.26b)$$

$$Y_e^{\text{SM}} = Y_e^{\text{MSSM}} \cos \beta , \quad (7.26c)$$

where the η_i are proportional to $\tan \beta$ and can be calculated from the sparticle spectrum, see chapter 10. Since we do not specify a certain SUSY scenario, in our analysis they are treated as free parameters. The SUSY threshold corrections for the first two families are

assumed to be equal due to approximately equal down and strange squark masses, which is typical in scenarios with CMSSM soft-breaking. We do not explicitly include SUSY threshold corrections for the charged leptons, since, because GUTs only predict ratios of quark and charged lepton masses, to a good approximation they can be absorbed in the quark corrections $\eta_{Q_{12}}$ and η_{Q_3} . We set $\tan\beta = 40$ to allow for substantial threshold effects, as required for the CG factors 6 and $-\frac{3}{2}$ appearing in our model (cf. [83]).

Then the Yukawa matrices are evolved from M_{SUSY} to $m_t(m_t)$, using the one-loop SM RGEs in REAP. Finally all observables are calculated and compared to the experimental values.

There are 14 free parameters in our model which we fit: $\tilde{\epsilon}_2, \tilde{\epsilon}_3, \tilde{\epsilon}_{ab}, \theta_{ab}, \hat{\epsilon}_\chi, \eta_{Q_{12}},$ and η_{Q_3} for the down-quark and charged-lepton sector and $y_t, \epsilon_{ab}, \epsilon_2, \epsilon_{12},$ and ϵ_{23} for the up-quark sector. In the neutrino sector we choose to fix the masses of the right-handed neutrinos

$$Y_\nu = \begin{pmatrix} 0 & \epsilon_{N_2} \\ \epsilon_{N_1} & \epsilon_{N_2} \\ -\epsilon_{N_1} & \epsilon_{N_2} \end{pmatrix}, \quad M_R = 2 \cdot 10^{10} \text{ GeV} \cdot \begin{pmatrix} 1 & 0 \\ 0 & 10 \end{pmatrix}, \quad (7.27)$$

so that the mass matrix of the light neutrinos depends on the parameters $\epsilon_{N_1}, \epsilon_{N_2}$. The choice of the right-handed neutrino masses does not significantly affect the fit as long as we are in the regime where the neutrino Yukawa couplings are $\ll 1$.

We fit these 14 parameters to 18 measured observables: 9 fermion masses, 3 quark and 3 lepton mixing angles, the quark mixing phase, and the two neutrino mass-squared differences. We report the results from our analysis in [2], where we used the quark and charged lepton masses given in [167] at $m_t(m_t)$, the winter 2013 results of the UTfit collaboration for the quark mixing sector [168], and the 2013 1.1 lepton mixing data of the NuFIT collaboration [169] for the fit. At the end of the chapter we add a discussion in the light of newly available data. Note that, although the masses of the charged leptons are given in [167] to high precision, in our analysis we set their uncertainty to one percent, which is roughly the accuracy of the one-loop calculation used here.

Having four more observables than parameters implies that our model is capable of predicting four out of these observables. Therefore, including the yet unknown Dirac CP phase δ^{PMNS} and the single physical Majorana phase φ_2^{PMNS} of the PMNS matrix in case of a massless lightest neutrino and normal mass hierarchy, our model makes 6 predictions.

7.4.2 Results

Following the procedure described above, we find a best fit for the parameters with a $\chi^2 = 8.1$. Having 14 parameters and 18 fitted observables this translates to a reduced χ^2 of $\chi^2/\text{d.o.f.} = 2.0$. We present the results for the parameters in table 7.2.⁴

We perform a Markov Chain Monte Carlo (MCMC) analysis, using a Metropolis algorithm, to determine Bayesian highest posterior density (hpd) intervals as (one sigma

⁴Note that there is a sign ambiguity for the parameters ϵ_2 and ϵ_{ab} , which enter the Yukawa matrix of the up-type quarks at quartic and quadratic order. In our analysis we fix these parameters to be positive.

unless stated otherwise) uncertainty for our results. See appendix C for a brief review of MCMC and Bayesian hpd intervals. Since in a realistic supersymmetry breaking scenario the SUSY threshold corrections for large $\tan \beta$ typically do not exceed about 50% (see e.g. [133]), we implement a prior in the MCMC analysis to restrict the SUSY threshold parameters $\eta_{Q_{12}}$ and η_{Q_3} to values between -0.5 and 0.5 .

Parameter	Best fit value	Uncertainty
$\tilde{\epsilon}_2$ in 10^{-4}	6.83	$+0.10$ -0.07
$\tilde{\epsilon}_3$ in 10^{-1}	2.16	± 0.04
$\tilde{\epsilon}_{ab}$ in 10^{-3}	-3.09	$+0.03$ -0.04
θ_{ab}	1.319	$+0.005$ -0.003
$\hat{\epsilon}_\chi$ in 10^{-2}	-1.27	$+0.21$ -0.26
$\eta_{Q_{12}}$ in 10^{-1}	3.31	$+1.45$ -3.50
η_{Q_3} in 10^{-1}	1.93	$+0.49$ -0.38
ϵ_2 in 10^{-2}	$\left\{ \begin{array}{l} 5.27 \\ 6.07 \end{array} \right.$	$\left\{ \begin{array}{l} +0.34 \\ -0.36 \\ +0.17 \\ -0.26 \end{array} \right.$
ϵ_{ab} in 10^{-2}	4.46	$+0.75$ -0.19
ϵ_{12} in 10^{-1}	-1.65	± 0.05
ϵ_{23} in 10^{-2}	1.78	$+0.73$ -0.22
y_t in 10^{-1}	5.29	$+0.29$ -0.25
ϵ_{N_1} in 10^{-3}	2.91	± 0.05
ϵ_{N_2} in 10^{-3}	3.12	± 0.06

Table 7.2: Best fit results of the parameters with $\chi^2/\text{d.o.f.} = 2.0$. We give one sigma highest posterior density intervals as uncertainty. The two modes for ϵ_2 can be understood as the two solutions of the (leading order) equation $y_u \approx \left| Y_{u_{11}} - \frac{Y_{u_{12}}^2}{Y_{u_{22}}} \right|$, where $Y_{u_{11}} = \epsilon_2^4$.

The corresponding best fit values of the observables at $m_t(m_t) = (162.9 \pm 2.8)$ GeV are shown in table 7.3. Since we used the “ \sin^2 ” of the lepton mixing angles as experimental input for the fit, we also present the values of the lepton mixing parameters in degree in table 7.4, for convenience. Correlations among the lepton mixing angles and the Dirac CP phase of the MCMC analysis results are plotted in figure 7.1.

We now discuss how the results shown in table 7.3 and figure 7.1 can be understood from analytic formulae and the Yukawa matrices presented in 7.2.

Let us start with the prediction for the ratio of m_s and m_d . From our fit, we obtain

$$\frac{m_s}{m_d} = 18.95_{-0.24}^{+0.33}, \quad (7.28)$$

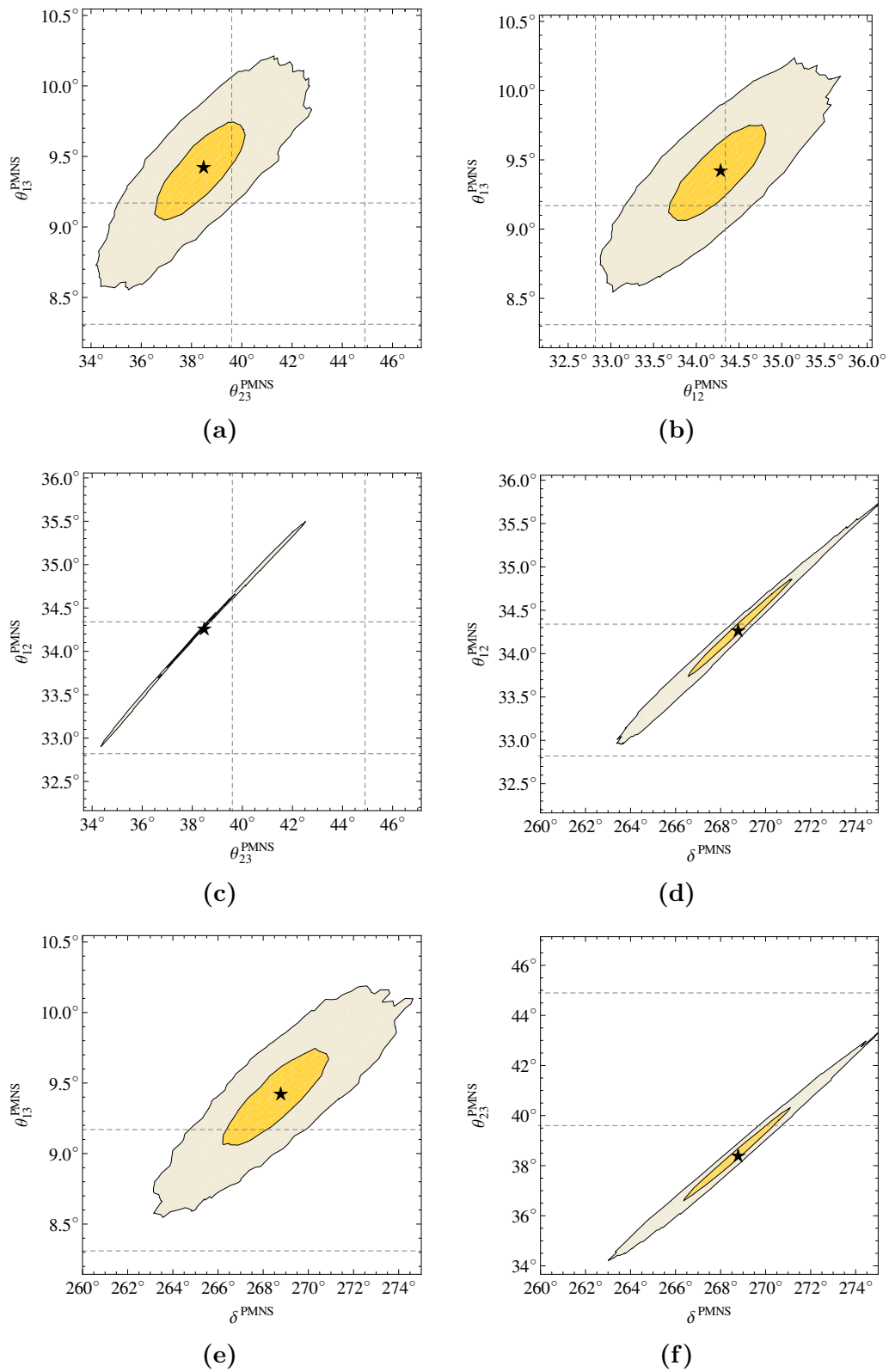


Figure 7.1: Correlations among the lepton mixing angles and the Dirac CP phase. The black star marks the best fit value, the yellow and grey regions give the one and three sigma hpd regions obtained from the MCMC analysis, respectively. The dashed grey lines indicate the one sigma intervals for the measured observables.

Observable	Value at $m_t(m_t)$	Best fit result	Uncertainty
m_u in MeV	1.22 $^{+0.48}_{-0.40}$	1.22	$^{+0.49}_{-0.40}$
m_c in GeV	0.59 ± 0.08	0.59	± 0.08
m_t in GeV	162.9 ± 2.8	162.89	$^{+2.62}_{-2.36}$
m_d in MeV	2.76 $^{+1.19}_{-1.14}$	2.73	$^{+0.30}_{-0.70}$
m_s in MeV	52 ± 15	51.66	$^{+5.60}_{-13.68}$
m_b in GeV	2.75 ± 0.09	2.75	± 0.09
m_e in MeV	0.485 $\pm 1\%$	0.483	± 0.005
m_μ in MeV	102.46 $\pm 1\%$	102.83	$^{+1.01}_{-0.98}$
m_τ in MeV	1742 $\pm 1\%$	1741.75	$^{+17.38}_{-17.10}$
$\sin \theta_C$	0.2254 ± 0.0007	0.2255	± 0.0007
$\sin \theta_{23}^{\text{CKM}}$	0.0421 ± 0.0006	0.0422	± 0.0006
$\sin \theta_{13}^{\text{CKM}}$	0.0036 ± 0.0001	0.0036	± 0.0001
δ^{CKM} in $^\circ$	69.2 ± 3.1	65.65	$^{+1.78}_{-0.53}$
$\sin^2 \theta_{12}^{\text{PMNS}}$	0.306 ± 0.012	0.317	± 0.006
$\sin^2 \theta_{23}^{\text{PMNS}}$	0.437 $^{+0.061}_{-0.031}$	0.387	$^{+0.017}_{-0.023}$
$\sin^2 \theta_{13}^{\text{PMNS}}$	0.0231 $^{+0.0023}_{-0.0022}$	0.0269	$^{+0.0011}_{-0.0015}$
δ^{PMNS} in $^\circ$	-	268.79	$^{+1.32}_{-1.72}$
φ_2^{PMNS} in $^\circ$	-	297.34	$^{+8.66}_{-10.01}$
Δm_{12}^2 in 10^{-5} eV^2	7.45 $^{+0.19}_{-0.16}$	7.45	$^{+0.18}_{-0.17}$
Δm_{31}^2 in 10^{-3} eV^2	2.421 $^{+0.022}_{-0.023}$	2.421	$^{+0.022}_{-0.023}$

Table 7.3: Experimental values, best fit results, and uncertainties of the observables at $m_t(m_t)$. We give one sigma highest posterior density intervals as uncertainty. Note that although the masses of the charged leptons are known far more precise than listed here, we set an 1% uncertainty for the experimental values, which is roughly the accuracy of the one loop calculation used here.

which is in excellent agreement with (2.38)

$$\frac{m_s}{m_d} = 18.9 \pm 0.8, \quad (7.29)$$

obtained from experiments [22]. This can be understood from our choice of CG factors,

Observable		Value at $m_t(m_t)$	Best fit result	Uncertainty
$\theta_{12}^{\text{PMNS}}$	in $^\circ$	33.57 $\begin{smallmatrix} +0.77 \\ -0.75 \end{smallmatrix}$	34.29	$\begin{smallmatrix} +0.35 \\ -0.39 \end{smallmatrix}$
$\theta_{23}^{\text{PMNS}}$	in $^\circ$	41.4 $\begin{smallmatrix} +3.5 \\ -1.8 \end{smallmatrix}$	38.49	$\begin{smallmatrix} +1.11 \\ -1.26 \end{smallmatrix}$
$\theta_{13}^{\text{PMNS}}$	in $^\circ$	8.75 $\begin{smallmatrix} +0.42 \\ -0.44 \end{smallmatrix}$	9.43	$\begin{smallmatrix} +0.20 \\ -0.25 \end{smallmatrix}$

Table 7.4: Experimental values [169] and best fit results for the lepton mixing angles at $m_t(m_t)$, given here in degree for convenience.

since in leading order in a small angle approximation they relate the ratio of electron and muon masses to the ratio of down and strange quark masses

$$\frac{m_s}{m_d} \approx \left| \frac{c_{12}c_{21}}{c_{22}^2} \right| \frac{m_\mu}{m_e}, \quad (7.30)$$

as can be seen from (6.19) and (6.26). Although this is just a leading-order estimate, it illustrates well that in order to obtain a viable ratio $\frac{m_s}{m_d}$, a suitable set of CG factors is mandatory. In our model, the CG factors $c_{12} = c_{22} = 6$ and $c_{21} = -\frac{1}{2}$ are in a remarkably good agreement with the experimental data, whereas the often used CG factors $c_{12} = c_{21} = 1$ and $c_{22} = 3$, leading to the GJ relations, would result in $\frac{m_s}{m_d} = 25.27$, when considering the 1-2 blocks of Y_e and Y_d with zero 1-1 elements and fitting to the experimental values of θ_C , m_e , and m_μ . Additionally, these CG factors would also not satisfy condition 4 of chapter 6 ($c_{12} = c_{22}$) and therefore predict a too small $\theta_{13}^{\text{PMNS}}$.

The correlations between the lepton mixing parameters, presented in figure 7.1, can also be understood from the lepton mixing sum rule (3.34)

$$\theta_{12}^{\text{PMNS}} \approx \theta_{12}^\nu + \theta_{13}^{\text{PMNS}} \cot \theta_{23}^{\text{PMNS}} \cos \delta^{\text{PMNS}}, \quad (7.31)$$

and the relation⁵

$$\theta_{13}^{\text{PMNS}} \approx \theta_C \sin \theta_{23}^{\text{PMNS}}. \quad (7.32)$$

The latter relation directly explains the correlation between $\theta_{13}^{\text{PMNS}}$ and $\theta_{23}^{\text{PMNS}}$ in figure 7.1a. The correlation between $\theta_{23}^{\text{PMNS}}$ and $\theta_{12}^{\text{PMNS}}$ follows from the lepton mixing sum rule: Larger values of $\theta_{23}^{\text{PMNS}}$ have smaller values of $\cot \theta_{23}^{\text{PMNS}}$. For more than 90% of the MCMC results $\cos \delta^{\text{PMNS}}$ is negative. Therefore the values of $\theta_{12}^{\text{PMNS}}$ rise with increasing values of $\theta_{23}^{\text{PMNS}}$ as can be seen in figure 7.1c. The correlation between $\theta_{12}^{\text{PMNS}}$ and $\theta_{13}^{\text{PMNS}}$ is opposite to what one would naively expect from the lepton mixing sum rule. However one also needs to consider the relation $\theta_{13}^{\text{PMNS}} \approx \theta_C \sin \theta_{23}^{\text{PMNS}}$, which, when plugged into the lepton mixing sum rule leads to

$$\theta_{12}^{\text{PMNS}} \approx \theta_{12}^\nu - \theta_C \sqrt{1 - \frac{(\theta_{13}^{\text{PMNS}})^2}{\theta_C^2}} |\cos \delta^{\text{PMNS}}|, \quad (7.33)$$

⁵More precisely, our model features a slightly larger $\theta_{12}^e \gtrsim \theta_C$, see (6.27) and [148]. This explains the tendency towards larger values of $\theta_{13}^{\text{PMNS}}$.

where the negative sign of $\cos \delta^{\text{PMNS}}$ is written explicitly. This explains the rising of $\theta_{12}^{\text{PMNS}}$ with increasing $\theta_{13}^{\text{PMNS}}$ seen in figure 7.1b. The correlation in figure 7.1d is again obvious from the lepton mixing sum rule. Naively one would not expect correlations between δ^{PMNS} and the lepton mixing angles $\theta_{13}^{\text{PMNS}}$ and $\theta_{23}^{\text{PMNS}}$, respectively. The correlations seen in figures 7.1e and 7.1f however follow indirectly from the other correlations discussed above.

7.4.3 Discussion of the results

We close this chapter with a discussion of the various predictions of our model and how the model potentially can be falsified with future experiments.

- Our best fit values $\theta_{13}^{\text{PMNS}} = 9.44_{-0.25}^{+0.20}$ and $\theta_{23}^{\text{PMNS}} = 38.49_{-1.26}^{+1.11}$ lie within their respective 2σ intervals reported in [169]. The correlation between $\theta_{13}^{\text{PMNS}}$ and $\theta_{23}^{\text{PMNS}}$ in figure 7.1a shows that our model favours slightly smaller values of $\theta_{23}^{\text{PMNS}}$ and slightly larger values of $\theta_{13}^{\text{PMNS}}$ than in [169], whereas the most recent global fit results [62], given in (6.2), have a tendency in the opposite direction. Note however, that the uncertainty of the individual measurements is still comparatively large, such as for instance $\theta_{13}^{\text{PMNS}} = 8.29_{-0.72}^{+0.85}$ reported by the RENO collaboration [170] and the one sigma interval of $[38.6^\circ, 53.7^\circ]$ reported by the NO ν A collaboration for $\theta_{23}^{\text{PMNS}}$ [151]. The latest result from DayaBay on the other hand is $\theta_{13}^{\text{PMNS}} = 8.42_{-0.25}^{+0.26}$ [171]. Therefore, a more precise determination of $\theta_{13}^{\text{PMNS}}$ and $\theta_{23}^{\text{PMNS}}$ is needed to test our model in the future.
- For the yet unmeasured Dirac CP phase of the PMNS matrix we predict

$$\delta^{\text{PMNS}} = 268.79_{-1.72}^{+1.32}, \quad (7.34)$$

which is in agreement with the results from recent global fits (3.37) $\delta^{\text{PMNS}} = 306_{-70}^{+39}$.

- From the prediction of δ^{PMNS} follows that the $\cos \delta^{\text{PMNS}}$ term in the lepton mixing sum rule leads to a negative correction to the TBM prediction of 35.3° for the solar mixing angle. We find $\theta_{12}^{\text{PMNS}} = 34.29_{-0.40}^{+0.35}$, which is within the one sigma interval of [169] and just 0.03° outside of the one sigma interval reported in the recent global fit [62]. Like for $\theta_{13}^{\text{PMNS}}$, figure 7.1c suggests slightly smaller values for $\theta_{23}^{\text{PMNS}}$ than currently reported.
- In the quark sector, our model predicts a CKM phase of $\delta^{\text{CKM}} = 65.65_{-0.53}^{+1.78}$, which is a slight discrepancy to the experimental value of $69.2^\circ \pm 3.1^\circ$. With future, more precise measurements of δ^{CKM} our model thus could be falsified. As already discussed in (7.28), the model predicts $\frac{m_s}{m_d} = 18.95_{-0.24}^{+0.33}$, which is currently in excellent agreement with experiments, but will be tested further in the future.
- Finally, we discuss our prediction for the Majorana phase

$$\varphi_2^{\text{PMNS}} = 297.34_{-10.01}^{+8.66}, \quad (7.35)$$

which is extremely difficult to be tested, due to the normal ordering of neutrino masses. The effective Majorana mass parameter (3.38), which is determined in neutrino-less double beta decay experiments, is given by

$$\langle m_{\beta\beta} \rangle = \left| (V_{e2}^{\text{PMNS}})^2 \sqrt{\Delta m_{21}^2} + (V_{e3}^{\text{PMNS}})^2 \sqrt{\Delta m_{31}^2} \right| = (2.31_{-0.09}^{+0.12}) \cdot 10^{-3} \text{ eV} , \quad (7.36)$$

which is far below the sensitivity of current experiments. Of course, a discovery of neutrino-less double beta decay or of an inverse neutrino mass ordering would falsify our model. Note however, that if a non-vanishing mass for the lightest neutrino ν_1 would be discovered, our model could simply be rearranged – with an appropriate adjustment of shaping symmetries and messenger sector – by adding a third heavy right-handed neutrino and corresponding flavon field.

To conclude this chapter, we have successfully constructed a first SUSY flavour GUT model featuring $\theta_{13}^{\text{PMNS}} \approx \theta_C \sin \theta_{23}^{\text{PMNS}}$. Let us remark at this point, we do not consider our model as *the* final model, rather it should be viewed as *class* of models, yielding realistic quark-lepton mass ratios and mixing angles relations. For example, the set of shaping symmetries and messenger fields can be understood as proof of principle, instead of being an one-of-a-kind realisation of our model's features.

A complete SUSY flavour GUT model will have to include a successful SUSY breaking mechanism, a viable GUT Higgs sector, and a discussion on proton decay, among others. Some of this questions will be approached in chapters 9 and 10, where we discuss a solution to the doublet-triplet splitting problem in the context of flavour GUT models and present detailed calculations of the SUSY threshold corrections, which have been simply approximated as model parameters in this chapter.

CHAPTER 8

A SUSY flavour GUT model with inverse neutrino mass ordering

It is interesting to note that the vast majority of SUSY GUT models in the literature (see e.g. [172]) feature a normal neutrino mass ordering, whereas only few such models predict an inverted neutrino mass ordering. In this chapter we present our work [3] and construct a predictive and relatively simple SUSY $SU(5) \times A_4$ flavour GUT model, in which an inverse neutrino mass hierarchy is realised without fine-tuning of parameters. We follow the general procedure outlined in chapter 7 and both models share some of their properties, in particular the relation

$$\theta_{13}^{\text{PMNS}} \approx \theta_C \sin \theta_{23}^{\text{PMNS}}, \quad (8.1)$$

by following the conditions of chapter 6. Other shared features are the novel CG factors $-\frac{1}{2}$, 6, and $-\frac{3}{2}$ to obtain viable quark-lepton mass ratios, and spontaneous CP-symmetry breaking by CP-violating vevs of flavon fields leading to $\alpha \approx 90^\circ$ in the quark unitarity triangle.

Besides these shared features, there are also important differences, mainly due to the different neutrino sector. These differences not only change the predictions in the lepton sector, but also in the quark sector, and will allow to discriminate between the two models using the results of present and future experiments.

8.1 Constructing an inverted neutrino hierarchy

If the neutrino mass ordering would be measured to be inverse, it would imply that at least two of the neutrino masses, namely m_1 and m_2 , are almost degenerate, i.e. with mass splittings much smaller than the mass eigenvalues. Often, in order to realise such a small neutrino mass splitting, an effective “special” lepton number symmetry like $L_e - L_\mu - L_\tau$ [173] or more generally some $U(1)$ flavour symmetry is appealed to, yielding a mass matrix

for the light neutrinos of the form

$$m_\nu \sim \begin{pmatrix} 0 & \star & \star \\ \star & 0 & 0 \\ \star & 0 & 0 \end{pmatrix}. \quad (8.2)$$

Such symmetries have been used to construct GUT models (e.g. [174, 175]), but realising an inverse mass ordering often turns out to be more involved than realising a normal one.

As discussed in 3.3, a promising approach for explaining an inverse mass ordering is to consider a (mostly) off-diagonal mass matrix M_R for two of the right-handed neutrinos, e.g.

$$M_R = \hat{M}_R \begin{pmatrix} \varepsilon & 1 \\ 1 & 0 \end{pmatrix}, \quad (8.3)$$

so that the two right-handed neutrinos form a (quasi-)Dirac pair with (almost) degenerate Majorana masses. The small entry ε in the 1-1 position of M_R lifts the degeneracy of the right-handed neutrino masses and is in turn also responsible for the small mass splitting between the light neutrino masses m_1 and m_2 , as seen below. With a neutrino Yukawa coupling matrix given by (3.44)

$$Y_\nu = \begin{pmatrix} a & 0 \\ 0 & b \\ 0 & c \end{pmatrix}, \quad (8.4)$$

the seesaw formula (3.7) yields the light neutrino mass matrix

$$m_\nu = \begin{pmatrix} 0 & B & C \\ B & 0 & 0 \\ C & 0 & 0 \end{pmatrix} + \alpha \begin{pmatrix} 0 & 0 & 0 \\ 0 & B & C \\ 0 & C & C^2/B \end{pmatrix}, \quad (8.5)$$

with

$$B \equiv -b \frac{a v_u^2}{2\hat{M}_R}, \quad C \equiv -c \frac{a v_u^2}{2\hat{M}_R}, \quad \text{and } \alpha \equiv -\varepsilon \frac{b}{a}. \quad (8.6)$$

The first part leads to two light neutrinos ν_1, ν_2 with exactly degenerate masses [173], while the second part can be considered as a small perturbation which induces the solar mass splitting Δm_{12}^2 . Here we consider only two right-handed neutrinos, thus the mass of the lightest neutrino is zero, $m_3 = 0$, and our model features a *strong inverse neutrino mass hierarchy*, although strictly speaking the hierarchy is only between m_3 and $m_1 \approx m_2$.

Implementation in flavour models: In order to construct a flavour model which realises an inverse neutrino mass hierarchy, we thus need to have the columns of the neutrino Yukawa matrix (8.4) be generated by vevs of flavon fields, which are triplets under a non-Abelian discrete flavour symmetry group like A_4 . Additionally, the right-handed neutrinos need to be charged under the model's shaping symmetry such that the desired mass matrix

(8.5) is obtained. In 8.3 we present an alignment superpotential which enforces flavon fields to obtain vevs pointing in the specific directions

$$\begin{pmatrix} a \\ 0 \\ 0 \end{pmatrix} \quad \text{and} \quad \begin{pmatrix} 0 \\ b \\ c \end{pmatrix} \quad (8.7)$$

in flavour space.

Mixing angles and the Dirac CP phase: One can calculate the non-vanishing neutrino masses m_i and the mixing angles θ_{ij}^ν in leading order in α

$$-\Delta m_{32}^2 = m_2^2 \approx B^2 + C^2, \quad (8.8a)$$

$$\Delta m_{21}^2 = m_2^2 - m_1^2 \approx 2\alpha \frac{(B^2 + C^2)^{3/2}}{|B|}, \quad (8.8b)$$

$$\tan \theta_{12}^\nu \approx \left| 1 - \frac{\alpha}{2} \frac{\sqrt{B^2 + C^2}}{|B|} \right| \approx \left| 1 + \frac{1}{4} \frac{\Delta m_{\text{sol}}^2}{\Delta m_{\text{atm}}^2} \right|, \quad (8.8c)$$

$$\tan \theta_{23}^\nu = \left| \frac{C}{B} \right|, \quad (8.8d)$$

$$\theta_{13}^\nu = 0, \quad (8.8e)$$

where all parameters were assumed to be real. The small mass splitting between ν_1 and ν_2 thus directly results from the correction α , whose smallness can be naturally explained as being due to a higher-dimensional operator, such that no unnatural cancellation of a priori unrelated parameters is necessary.

Looking at the neutrino mixing angles, we find that θ_{23}^ν is a free parameter. On the other hand, the deviation from $\tan \theta_{12}^\nu = 1$ is smaller than 10^{-2} , which amounts to a negligibly small deviation from maximal $\theta_{12}^\nu = 45^\circ$, and the 1-3 mixing in the neutrino sector is fixed to zero. Thus, it is in accordance with condition 1 of chapter 6 and it opens up the possibility to explain $\theta_{13}^{\text{PMNS}} \approx \theta_C \sin \theta_{23}^{\text{PMNS}}$ via charged lepton corrections and suitable CG factors in GUTs. As discussed in 6.5, via the lepton mixing sum rule (6.47) maximal θ_{12}^ν and the observed value of $\theta_{12}^{\text{PMNS}}$ require a Dirac CP phase of $\delta^{\text{PMNS}} = 180^\circ$. Note that all necessary assumptions of chapter 6 like $\theta_{13}^e \approx \theta_{23}^e \approx 0$, and a Dirac CP phase of $\delta^{\text{PMNS}} = 180^\circ$ will be built-in features of our model, as we discuss in the following section.

8.2 The model

As in the previous chapter, we embed the three families of the MSSM matter superfields D_i^c and L_i into one A_4 triplet \mathcal{F} , transforming as $\mathbf{5}$ of $SU(5)$, and the remaining matter superfields into three A_4 -invariant singlets \mathcal{T}_i , one for each family, which transform as $\mathbf{10}$ under $SU(5)$. We introduce two right-handed neutrinos N_1^c and N_2^c as singlets under $SU(5)$

and A_4 . Spontaneous breaking of electroweak symmetry is due to the usual Higgs fields H_5 and \bar{H}_5 , and newly introduced Higgs fields H_{45} and \bar{H}_{45} . The Higgs field \bar{H}_{45} , transforming as $\overline{\mathbf{45}}$ under $SU(5)$, is necessary to obtain the CG factor $-\frac{1}{2}$. Finally there is the GUT breaking Higgs field H_{24} , transforming as $\mathbf{24}$ under $SU(5)$, in the model¹.

We now discuss the desired Yukawa matrices of our model, which emerge after $SU(5)$ gets spontaneously broken. The rows respectively columns of the Yukawa matrices are formed by specific vevs of flavon fields, which we present in table 8.1. There are five flavon superfields ϕ_i transforming as triplet under A_4 and three A_4 -invariant singlets ξ_i . The symbol Λ is again to be understood as placeholder for suppression by messenger

flavon φ_i :	ϕ_1	ϕ_2	ϕ_3	ϕ_{ab}	ϕ_{bc}	ξ_{12}	ξ_{23}	ξ_M
$\frac{\langle \varphi_i \rangle}{\Lambda}$:	$\epsilon_1 \begin{pmatrix} 1 \\ 0 \\ 0 \end{pmatrix}$	$\epsilon_2 \begin{pmatrix} 0 \\ -i \\ 0 \end{pmatrix}$	$\epsilon_3 \begin{pmatrix} 0 \\ 0 \\ 1 \end{pmatrix}$	$\epsilon_{ab} \begin{pmatrix} c_{ab} \\ s_{ab} \\ 0 \end{pmatrix}$	$\epsilon_{bc} \begin{pmatrix} 0 \\ c_{bc} \\ s_{bc} \end{pmatrix}$	ϵ_{12}	ϵ_{23}	ϵ_M

Table 8.1: The vevs of the flavon fields. The ϵ_i are all assumed to be real numbers. The flavon alignment yielding this specific directions in flavour space is discussed in the next section. We abbreviated $c_{ab} \equiv \cos(\theta_{ab})$ and $s_{ab} \equiv \sin(\theta_{ab})$ and analogously for θ_{bc} .

mass scales, keeping in mind that in fact each effective operator is in general suppressed by different messenger masses, as can be seen from the supergraphs in appendix D. As discussed in the next section, the parameters ϵ_i are all real.

The effective superpotential for the matter sector is given by

$$\mathcal{W} = \mathcal{W}_{Y_\nu} + \mathcal{W}_{M_R} + \mathcal{W}_{Y_d} + \mathcal{W}_{Y_u} , \quad (8.9)$$

with

$$\mathcal{W}_{Y_\nu} = (H_5 \mathcal{F}) (N_1^c \phi_1 + N_2^c \phi_{bc}) , \quad (8.10a)$$

$$\mathcal{W}_{M_R} = \xi_M^4 (N_1^c N_2^c + \phi_{bc}^2 (N_1^c)^2) , \quad (8.10b)$$

$$\mathcal{W}_{Y_d} = [\mathcal{T}_1 \bar{H}_{45}]_{45} [\mathcal{F} H_{24}]_{\overline{45}} \phi_2 + [\mathcal{T}_2 H_{24}]_{10} [\mathcal{F} \bar{H}_5]_{\overline{10}} \phi_{ab} + [\mathcal{T}_3 \bar{H}_5]_5 [\mathcal{F} H_{24}]_{\overline{5}} \phi_3 , \quad (8.10c)$$

$$\mathcal{W}_{Y_u} = H_5 \left(\mathcal{T}_3^2 + \mathcal{T}_2^2 \phi_{ab}^2 + \mathcal{T}_1^2 (\phi_2^2)^2 + \mathcal{T}_2 \mathcal{T}_3 \xi_{23} + \mathcal{T}_1 \mathcal{T}_2 \xi_{12}^5 \right) , \quad (8.10d)$$

where again we omitted real order one coefficients and messenger mass scales Λ for the sake of brevity. After GUT- and flavour symmetry breaking the desired neutrino Yukawa matrix and right-handed neutrino mass matrix, which, as discussed above, lead to a strong inverse neutrino mass hierarchy in a natural way, are obtained from \mathcal{W}_{Y_ν} and \mathcal{W}_{M_R} . The parameters \hat{M}_R and ε in (8.5) are then given in terms of ϵ_{bc} and ϵ_M . Finally, the Yukawa

¹Again we note, that we restrict our discussion to the matter and flavon sector, whereas the details of the (GUT) Higgs superpotential are beyond the scope of this flavour model. This question will be discussed in chapter 9.

matrices of the quarks and charged leptons are given by

$$Y_d = \begin{pmatrix} 0 & -i\tilde{\epsilon}_2 & 0 \\ \tilde{\epsilon}_{ab}c_{ab} & \tilde{\epsilon}_{ab}s_{ab} & 0 \\ 0 & 0 & \tilde{\epsilon}_3 \end{pmatrix}, \quad Y_e = \begin{pmatrix} 0 & 6\tilde{\epsilon}_{ab}c_{ab} & 0 \\ i\frac{1}{2}\tilde{\epsilon}_2 & 6\tilde{\epsilon}_{ab}s_{ab} & 0 \\ 0 & 0 & -\frac{3}{2}\tilde{\epsilon}_3 \end{pmatrix}, \quad Y_u = \begin{pmatrix} \epsilon_2^4 & \epsilon_{12}^5 & 0 \\ \epsilon_{12}^5 & \epsilon_{ab}^2 & \epsilon_{23} \\ 0 & \epsilon_{23} & y_t \end{pmatrix}, \quad (8.11)$$

where we defined

$$\tilde{\epsilon}_i \equiv \frac{\langle H_{24} \rangle}{\Lambda} \epsilon_i \quad (8.12)$$

for convenience. Note that Y_d and Y_u fulfil the necessary conditions $\theta_{13}^u, \theta_{13}^d \approx 0$ for the quark mixing and phase sum rule, respectively, such that $\theta_{12}^d \approx \theta_C$ and a right-angled quark unitarity triangle is obtained.

As discussed in 7.1, in order to construct a viable and predictive flavour GUT model, it is necessary to identify a shaping symmetry and a set of messenger fields, that, when integrated out, gives rise to the effective superpotential (8.10). Specifically, no effective operators must exist which spoil the features of our Yukawa matrices, e.g. by generating unwanted CG factors or relevant corrections to the desired structure of the Yukawa matrices (8.4), (8.11), and of the right-handed neutrino mass matrix (8.5). In appendix D we therefore present the model's shaping symmetry and messenger fields, and explicitly construct the renormalisable superpotential which yields (8.10) after the messenger fields are integrated out. With this messenger sector at hand, sub-leading corrections from e.g. higher-dimensional operators or from canonical normalisation can be neglected.

8.3 Flavon alignment

In this section we present the flavon alignment superpotential, which enforces the flavon vevs into the specific directions in flavour space shown in table 8.1. We introduce the driving fields S_i , D_i , O_i , and O'_i , which are all singlets under $SU(5)$ and – with the exception of O'_i , which transform as $\mathbf{1}'$ under A_4 – invariant singlets $\mathbf{1}$ under A_4 . In appendix D, all flavon and driving superfields are listed in the lower part of table D.3, together with their charges under the imposed symmetries. The effective flavon alignment superpotential is given by

$$\mathcal{W}_{\text{flavon}} = \mathcal{W}_{\phi_i} + \mathcal{W}_{ab} + \mathcal{W}_{bc} + \mathcal{W}_M + \mathcal{W}_{12}, \quad (8.13)$$

where

$$\mathcal{W}_{\phi_i} = S_2 \left((\phi_2^2)^3 + M_2^2 \right) + \sum_{i \in \{1,3\}} S_i (\phi_i^2 - M_i^2) + \sum_{\substack{i,j=1 \\ j>i}}^3 (O'_{ij} (\phi_i \phi_j)_{1''} + O_{ij} (\phi_i \phi_j)), \quad (8.14a)$$

$$\begin{aligned} \mathcal{W}_{ab} = & S_{ab} \left((\phi_{ab} \star \phi_{ab})^2 \xi_{23}^2 - M_{ab}^2 \right) + D_{ab}^\alpha (\phi_{ab}^2 + \lambda_{ab} \xi_{23}^2) \\ & + D_{ab}^\beta (\phi_{ab} \star \phi_{ab}) \phi_{ab} + D_{ab}^\gamma \left((\phi_{ab}^2)_{1'} (\phi_{ab}^2)_{1''} + k_{ab} (\phi_{ab} \star \phi_{ab})^2 \right), \end{aligned} \quad (8.14b)$$

$$\mathcal{W}_{bc} = S_{bc} \left((\phi_{bc} \star \phi_{bc})^2 \phi_{bc}^2 - M_{bc}^2 \right) + D_{bc}^\beta (\phi_{bc} \star \phi_{bc}) \phi_{bc} + D_{bc}^\gamma \left((\phi_{bc}^2)_{1'} (\phi_{bc}^2)_{1''} + k_{bc} (\phi_{bc} \star \phi_{bc})^2 \right) , \quad (8.14c)$$

$$\mathcal{W}_M = S_M \left(\xi_M^6 - M_M^2 \right) , \quad (8.14d)$$

$$\mathcal{W}_{12} = S_{12} \left(\xi_{12}^6 - M_{12}^2 \right) . \quad (8.14e)$$

Since CP symmetry is assumed to be broken only spontaneously, the constants k_i and M_i are real. In addition we assume $M_i^2 > 0$ everywhere. The terms \mathcal{W}_{12} and \mathcal{W}_M lead to vevs with discrete phases as discussed in 7.3, of which we select the real phases. The alignment superpotential \mathcal{W}_{ab} is the same as in chapter 7, i.e. the term containing S_{ab} determines the magnitude and a discrete global phase of the product of ϕ_{ab} and ξ_{23} , whereas the individual magnitudes are fixed by the F -term of D_{ab}^α . The term with the driving superfield D_{ab}^β sets one of the components of $\langle \phi_{ab} \rangle$ to zero and the relative magnitude or the relative phase is finally enforced as in (7.25) by the value of k_{ab} . Similarly, replacing $a, b \rightarrow b, c$ and $k_{ab} \rightarrow k_{bc}$, respectively, the vev of the flavon superfield ϕ_{bc} , which appears in the neutrino Yukawa matrix (8.4), is obtained. Let us now discuss the remaining flavon vevs in detail.

\mathcal{W}_{ϕ_i} : Let us denote the components of ϕ_i with x_1, x_2 , and x_3 , and the components of ϕ_j with y_1, y_2 , and y_3 . The F -term equations corresponding to $O_{i;j}$ and $O'_{i;j}$ then take the form

$$x_1 y_1 + x_2 y_2 + x_3 y_3 = 0 , \quad (8.15a)$$

and

$$x_1 y_1 + \omega x_2 y_2 + \omega^2 x_3 y_3 = 0 , \quad (8.15b)$$

respectively, where for each pair $O_{i;j}$ and $O'_{i;j}$ there is one such system of equations. There are two classes of solutions to the system (8.15), namely

$$x_1 y_1 = x_2 y_2 = x_3 y_3 = 0 , \quad (8.16a)$$

and

$$x_1 y_1 = \gamma , \quad x_2 y_2 = \omega \gamma , \quad x_3 y_3 = \omega^2 \gamma , \quad (8.16b)$$

where γ is a complex constant $\gamma \neq 0$. There is no consistent solution for ϕ_1, ϕ_2 , and ϕ_3 that satisfies (8.16a) for one pair $O_{i;j}$ and $O'_{i;j}$ and (8.16b) for another pair. The only solutions to all three equation pairs are thus either all of type (8.16a) or all of type (8.16b). They are given by

$$\phi_1 \propto \begin{pmatrix} 1 \\ 0 \\ 0 \end{pmatrix} , \quad \phi_2 \propto \begin{pmatrix} 0 \\ 1 \\ 0 \end{pmatrix} , \quad \phi_3 \propto \begin{pmatrix} 0 \\ 0 \\ 1 \end{pmatrix} , \quad (8.17a)$$

or permutations thereof, and

$$\phi_i \propto \begin{pmatrix} 1 \\ \sqrt{\omega} \\ \omega \end{pmatrix}, \quad \text{for } i = 1, 2, 3. \quad (8.17b)$$

Which solution is realised depends on the terms containing the driving superfields S_i . Since for solution (8.17b) the invariant ϕ_i^2 vanishes for all ϕ_i , in our superpotential (8.14a) only solution (8.17a) is generated. Again, their phases take on discrete values and we select an imaginary vev for ϕ_2 and real vevs for ϕ_1 and ϕ_3 , as shown in table 8.1.

8.4 Phenomenology

We now turn to a discussion of the model's phenomenology. There are 14 free parameters: $\tilde{\epsilon}_2, \tilde{\epsilon}_3, \tilde{\epsilon}_{ab}, \theta_{ab}, \eta_{Q_{12}},$ and η_{Q_3} parametrise the Yukawa matrices Y_d and Y_e . The parameters $y_t, \epsilon_{ab}, \epsilon_2, \epsilon_{12},$ and ϵ_{23} enter Y_u , where, since ϵ_{ab} and ϵ_2 do only appear at quadratic and quartic order, respectively, we restrict them to positive values. As shown in (8.5), the effective mass matrix of the light neutrinos depends only on three parameters after the heavy right-handed neutrinos are integrated out. It is thus possible to fix two out of the five parameters in the neutrino sector: While we use $\epsilon_1, \epsilon_{bc},$ and θ_{bc} to fit the GUT scale Yukawa neutrino matrix Y_ν , we set the parameters of M_R to $\hat{M}_R = 2 \cdot 10^{10}$ GeV and $\varepsilon = 10^{-2}$. Again, for neutrino Yukawa couplings much smaller than one, which implies that Y_ν is irrelevant in the RGEs, our choice of M_R does not affect the fit. The neutrino sector is therefore given by

$$Y_\nu = \begin{pmatrix} \epsilon_1 & 0 \\ 0 & \epsilon_{bc} \cos \theta_{bc} \\ 0 & \epsilon_{bc} \sin \theta_{bc} \end{pmatrix}, \quad M_R = 2 \cdot 10^{10} \text{ GeV} \cdot \begin{pmatrix} 10^{-2} & 1 \\ 1 & 0 \end{pmatrix}. \quad (8.18)$$

We follow the same numerical procedure as described in 7.4.1 and again set $\tan \beta = 40$ due to the need of $\tan \beta$ -enhanced SUSY threshold corrections in order for the models's CG factors to be viable. Once again the SUSY threshold corrections at $M_{\text{SUSY}} = 1$ TeV are included by the approximate matching relations (7.26) as model parameters assuming degenerate first and second family sfermion masses.

Analogous to our model in chapter 7, we here report our results from [3], where we used 2013 data [167–169] for the experimental values at the low energy scale $m_t(m_t)$. We will discuss our results in the light of newly available data at the end of the chapter.

Note that with a strong inverse neutrino mass hierarchy and massless ν_3 , the single physical Majorana phase predicted by our model is given by

$$\phi^{\text{PMNS}} = \phi_2^{\text{PMNS}} - \phi_1^{\text{PMNS}}. \quad (8.19)$$

With the prediction of the Dirac CP phase δ^{PMNS} and from fitting 14 parameters to 18 measured observables, it follows that our model makes six predictions.

8.4.1 Results

We find a best fit point with a total $\chi^2 = 4.6$. The reduced χ^2 is thus $\chi^2/\text{d.o.f.} = 1.1$. Compared to $\chi^2/\text{d.o.f.} = 2.0$ in the fit of the normal hierarchy model of chapter 7, we thus obtain an even better agreement with the measured observables. In table 8.2 we present the best fit values of our parameters, together with uncertainties obtained as one sigma hpd intervals from a MCMC analysis using a Metropolis algorithm. Note that again we enforce a prior on the SUSY threshold correction parameters to restrict their absolute values $|\eta_i| < 0.5$, justified by the typical size of SUSY threshold corrections in common SUSY breaking scenarios.

Parameter	Best fit value	Uncertainty
$\tilde{\epsilon}_2$ in 10^{-4}	6.71	+0.08 -0.07
$\tilde{\epsilon}_3$ in 10^{-1}	2.23	± 0.03
$\tilde{\epsilon}_{ab}$ in 10^{-3}	3.03	± 0.03
θ_{ab}	1.314	+0.004 -0.003
$\eta_{Q_{12}}$ in 10^{-1}	3.36	+1.35 -2.50
η_{Q_3} in 10^{-1}	1.64	+0.44 -0.37
ϵ_2 in 10^{-2}	$\begin{cases} 5.22 \\ 6.04 \end{cases}$	$\begin{cases} +0.34 \\ -0.37 \\ +0.18 \\ -0.23 \end{cases}$
ϵ_{ab} in 10^{-2}	4.45	+0.53 -0.18
ϵ_{12} in 10^{-1}	-1.64	+0.05 -0.04
ϵ_{23} in 10^{-2}	1.76	+0.49 -0.16
y_t in 10^{-1}	5.30	+0.35 -0.27
ϵ_1 in 10^{-3}	3.21	+0.11 -0.09
ϵ_{bc} in 10^{-3}	-5.12	+0.11 -0.15
θ_{bc}	0.71	± 0.02

Table 8.2: Best fit results of the model's parameters with $\chi^2/\text{d.o.f.} = 1.1$. The uncertainties are given as one sigma hpd intervals. Again, the two modes for ϵ_2 can be understood as the two solutions of the (leading order) equation $y_u \approx \left| Y_{u_{11}} - \frac{Y_{u_{12}}^2}{Y_{u_{22}}} \right|$, where $Y_{u_{11}} = \epsilon_2^4$.

In tables 8.3 and 8.4 the best fit values of the observables at $m_t(m_t)$ are shown. Correlations among the lepton mixing angles in the MCMC analysis are shown in figure 8.1. Like in 7.4.2, they can be understood in terms of the lepton mixing sum rule $\theta_{12}^{\text{PMNS}} \approx \theta_{12}^\nu + \theta_{13}^{\text{PMNS}} \cot \theta_{23}^{\text{PMNS}} \cos \delta^{\text{PMNS}}$ and $\theta_{13}^{\text{PMNS}} \approx \theta_C \sin \theta_{23}^{\text{PMNS}}$. The noticeable difference in the shape of figures 7.1c and 8.1c is due to the different values of δ^{PMNS} . Whereas

$\cos \delta^{\text{PMNS}}$ almost vanishes in 7.4.2, leading to $\theta_{12}^{\text{PMNS}}$ given almost exclusively in terms of θ_{12}^ν , the value of $\delta^{\text{PMNS}} = 180^\circ$ in the inverse hierarchy model maximises the contribution of $\theta_{23}^{\text{PMNS}}$ to $\theta_{12}^{\text{PMNS}}$, leading to a large deviation of $\theta_{12}^{\text{PMNS}}$ from $\theta_{23}^\nu = 45^\circ$ and explaining the larger hpd regions in figure 8.1c.

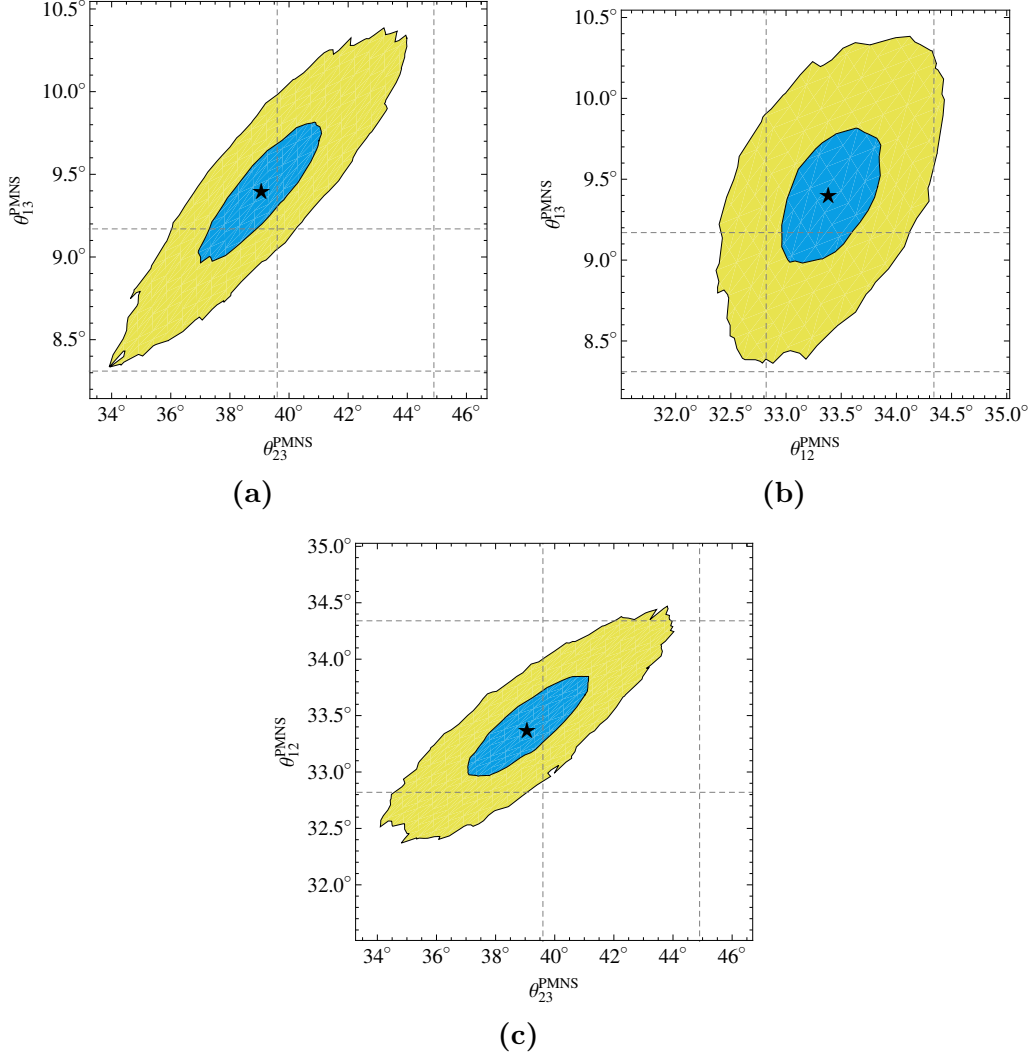


Figure 8.1: Correlations among the lepton mixing angles. The black star marks the best fit value. The blue and golden regions give the one sigma and three sigma hpd regions obtained from the MCMC analysis, respectively. The dashed grey lines indicate the one sigma intervals for the measured observables.

As for the normal hierarchy model in chapter 7, we obtain an excellent prediction for

$$\frac{m_s}{m_d} = 18.55_{-0.24}^{+0.26}, \quad (8.20)$$

due to the specific CG factors in our model.

Observable	Value at $m_t(m_t)$	Best fit result	Uncertainty
m_u in MeV	1.22 $^{+0.48}_{-0.40}$	1.22	$^{+0.50}_{-0.39}$
m_c in GeV	0.59 ± 0.08	0.59	$^{+0.07}_{-0.09}$
m_t in GeV	162.9 ± 2.8	162.91	$^{+3.35}_{-2.44}$
m_d in MeV	2.76 $^{+1.19}_{-1.14}$	2.73	$^{+0.25}_{-0.54}$
m_s in MeV	52 ± 15	50.70	$^{+4.86}_{-9.72}$
m_b in GeV	2.75 ± 0.09	2.75	± 0.09
m_e in MeV	0.485 $\pm 1\%$	0.483	± 0.005
m_μ in MeV	102.46 $\pm 1\%$	102.87	$^{+1.04}_{-0.91}$
m_τ in MeV	1742 $\pm 1\%$	1741.99	$^{+16.84}_{-17.70}$
$\sin \theta_C$	0.2254 ± 0.0007	0.2255	± 0.0007
$\sin \theta_{23}^{\text{CKM}}$	0.0421 ± 0.0006	0.0421	± 0.0006
$\sin \theta_{13}^{\text{CKM}}$	0.0036 ± 0.0001	0.0036	± 0.0001
δ^{CKM} in $^\circ$	69.2 ± 3.1	69.27	$^{+0.91}_{-0.69}$
$\sin^2 \theta_{12}^{\text{PMNS}}$	0.306 ± 0.012	0.303	± 0.005
$\sin^2 \theta_{23}^{\text{PMNS}}$	0.437 $^{+0.061}_{-0.031}$	0.397	$^{+0.023}_{-0.022}$
$\sin^2 \theta_{13}^{\text{PMNS}}$	0.0231 $^{+0.0023}_{-0.0022}$	0.0267	$^{+0.0016}_{-0.0015}$
δ^{PMNS} in $^\circ$	-	180	-
φ^{PMNS} in $^\circ$	-	180	-
Δm_{12}^2 in 10^{-5} eV 2	7.45 $^{+0.19}_{-0.16}$	7.45	$^{+0.18}_{-0.17}$
Δm_{32}^2 in 10^{-3} eV 2	-2.410 $^{+0.062}_{-0.063}$	-2.410	$^{+0.062}_{-0.064}$

Table 8.3: Experimental values, best fit results, and uncertainties of the observables at $m_t(m_t)$. We give one sigma highest posterior density intervals as uncertainty. δ^{PMNS} and φ^{PMNS} are exactly 180° , since Y_ν is real and the phase of $Y_{e_{21}}$ can be absorbed by the right-handed electron field. Note that although the masses of the charged leptons are known far more precise than listed here, we set an 1% uncertainty for the experimental values, which is roughly the accuracy of the one loop calculation used here.

The sign of the larger neutrino mass splitting Δm_{3i}^2 will be in the focus of the next round of neutrino oscillation experiments and will allow to distinguish between inverse and normal neutrino mass ordering. Furthermore, neutrino-less double beta decay experiments

Observable		Value at $m_t(m_t)$	Best fit result	Uncertainty
$\theta_{12}^{\text{PMNS}}$	in $^\circ$	33.57 $^{+0.77}_{-0.75}$	33.38	$^{+0.30}_{-0.28}$
$\theta_{23}^{\text{PMNS}}$	in $^\circ$	41.4 $^{+3.5}_{-1.8}$	39.06	$^{+1.33}_{-1.32}$
$\theta_{13}^{\text{PMNS}}$	in $^\circ$	8.75 $^{+0.42}_{-0.44}$	9.41	$^{+0.28}_{-0.27}$

Table 8.4: Experimental values [169] and best fit results for the lepton mixing angles at $m_t(m_t)$, given here in degree for convenience.

will soon be able to test predictions from inverse neutrino mass ordering models. Our model predicts an effective Majorana mass parameter (3.38) of

$$\begin{aligned} \langle m_{\beta\beta} \rangle &= \left| (V_{e1}^{\text{PMNS}})^2 \sqrt{-\Delta m_{32}^2 - \Delta m_{21}^2} + (V_{e2}^{\text{PMNS}})^2 \sqrt{-\Delta m_{32}^2} \right| \\ &= (1.83_{-0.06}^{+0.05}) \cdot 10^{-2} \text{ eV} . \end{aligned} \quad (8.21)$$

This is in reach of future experiments, such as nEXO (see e.g. [176]) and AMoRE [177].

8.4.2 Discussion

In the following we turn to a detailed discussion of the fit results of our model, including comments regarding the more recent data for lepton mixing angles [62].

- Our model predicts the PMNS phases of

$$\delta^{\text{PMNS}} = 180^\circ \quad \text{and} \quad \varphi^{\text{PMNS}} = 180^\circ . \quad (8.22)$$

Since Y_ν is real and the phase of the 2-1 element of Y_e can be absorbed by the right-handed electron field E_1^c , the PMNS phases are fixed at the GUT scale and do not evolve under the RGEs. Our model's best fit value for the Dirac CP phases is marginally outside the one sigma interval of the recently reported hints towards $\delta^{\text{PMNS}} = 254^\circ \text{ }^{+63^\circ}_{-62^\circ}$ from global fits assuming a inverse neutrino mass ordering (3.37). A future precise measurement of δ^{PMNS} could decide whether our model agrees with the data or not.

- As for the normal hierarchy model in chapter 7, our inverse mass hierarchy model also features a best fit value $\theta_{13}^{\text{PMNS}} = 9.41^\circ \text{ }^{+0.28^\circ}_{-0.27^\circ}$ slightly larger than the reported experimental value in [169], and a best fit value $\theta_{23}^{\text{PMNS}} = 39.06^\circ \text{ }^{+1.33^\circ}_{-1.32^\circ}$ slightly smaller than reported in [169]. Both best fit points are within their respective two sigma intervals, however.

In the light of the recent global fit [62], the most drastic difference lies in the reported value for $\theta_{23}^{\text{PMNS}}$, which, when an inverse neutrino mass ordering is assumed as prior, lies in the second octant $\theta_{23}^{\text{PMNS}} = 49.5^\circ \text{ }^{+1.5^\circ}_{-2.2^\circ}$, whereas the 2013 data [169] reported a best fit point in the first octant for both, normal and inverse mass orderings. If future measurements of $\theta_{23}^{\text{PMNS}}$ would confirm a value larger than 45° , it effectively would

refute the relation $\theta_{13}^{\text{PMNS}} \approx \theta_C \sin \theta_{23}^{\text{PMNS}}$, especially since in the case of an inverse mass hierarchy this relation is highly insensitive to corrections from RG running or canonical normalisation, as discussed in 6.4. Large corrections would be necessary however, to cure the bad contribution of $\sin \theta_{23}^{\text{PMNS}} > \frac{1}{\sqrt{2}}$.

Let us remark at this point, that precise measurements of $\theta_{23}^{\text{PMNS}}$ are still work in progress, e.g. by the NO ν A collaboration, which reports an one sigma interval of $[38.6^\circ, 53.7^\circ]$ [151]. The subject whether $\theta_{23}^{\text{PMNS}}$ lies in the first or second octant therefore remains an important open question and in the future global fits might report $\theta_{23}^{\text{PMNS}} < 45^\circ$ again.

Future improvements on the determination of $\theta_{23}^{\text{PMNS}}$ and $\theta_{13}^{\text{PMNS}}$ thus have the capability to falsify our model, or to strengthen the relation $\theta_{13}^{\text{PMNS}} \approx \theta_C \sin \theta_{23}^{\text{PMNS}}$ with higher precision.

- Finally, our model finds a best fit point $\theta_{12}^{\text{PMNS}} = 33.38^\circ_{-0.28^\circ}^{+0.30^\circ}$, which lies within the one sigma range of the experimental values as reported in the 2013 [169] and 2015 data [62].

8.4.3 Phenomenological differences to the model of chapter 7

Let us close this chapter by discussing the differences between the SUSY flavour GUT models of [2] presented in chapter 7 and the model of [3] discussed in this chapter. There are five major differences between these models, summarised in table 8.5.

	NH	IH
Δm_{3i}^2	$2.421_{-0.023}^{+0.022} \cdot 10^{-3} \text{ eV}^2$	$-2.410_{-0.064}^{+0.062} \cdot 10^{-3} \text{ eV}^2$
$\langle m_{\beta\beta} \rangle$	$2.31_{-0.09}^{+0.12} \cdot 10^{-3} \text{ eV}$	$1.83_{-0.06}^{+0.05} \cdot 10^{-2} \text{ eV}$
δ^{PMNS}	$268.79^\circ_{-1.72^\circ}^{+1.32^\circ}$	180°
$\theta_{12}^{\text{PMNS}}$	$34.29^\circ_{-0.39^\circ}^{+0.35^\circ}$	$33.38^\circ_{-0.28^\circ}^{+0.30^\circ}$
δ^{CKM}	$65.65^\circ_{-0.53^\circ}^{+1.78^\circ}$	$69.27^\circ_{-0.69^\circ}^{+0.91^\circ}$

Table 8.5: Major differences in the best fit results between the two SUSY flavour GUT models of [2] (NH) and [3] (IH).

The sign of the larger neutrino mass splitting Δm_{32}^2 (IH) respectively Δm_{31}^2 (NH) is the defining characteristic of normal vs inverse hierarchy models. Its measurement is in the focus of upcoming long baseline neutrino experiments, e.g. at DUNE [69]. Similarly, the different magnitudes of the effective Majorana mass $\langle m_{\beta\beta} \rangle$ for neutrinoless double beta decay are a typical distinction between normal and inverse neutrino mass ordering.

The observed large value of $\theta_{13}^{\text{PMNS}}$ opens up the possibility of measuring the Dirac CP phase δ^{PMNS} in long-baseline neutrino oscillation experiments. Therefore our two SUSY flavour GUT models can also clearly be distinguished via their respective predictions of δ^{PMNS} , whose measurement is also a scientific goal of the DUNE experiment [69].

The lepton mixing angles in both models share the same characteristic correlations and the differences between the best fit values turn out to be less than one degree. Since future more precise measurements of $\theta_{13}^{\text{PMNS}}$ and $\theta_{23}^{\text{PMNS}}$ will support or disprove our models in equal measure, they are not expected to distinguish our two models. A future 50 – 70 km baseline reactor experiment though could measure $\theta_{12}^{\text{PMNS}}$ with high precision [178], allowing to discriminate between the respective predictions of $\theta_{12}^{\text{PMNS}}$ in the normal and inverse mass ordering models. Note however that the fit results for $\theta_{12}^{\text{PMNS}}$ depend on the experimental ranges for $\theta_{13}^{\text{PMNS}}$ and $\theta_{23}^{\text{PMNS}}$ via the lepton mixing sum rule.

Finally let us note the remarkable fact that our models, although mainly distinct by their neutrino sector, can furthermore be distinguished in the quark sector by their predictions for the CKM phase.

PART IV

Doublet-Triplet splitting in SUSY Flavour GUT models

CHAPTER 9

Towards predictive SUSY flavour $SU(5)$ models with doublet-triplet splitting

Grand Unified Theories offer an attractive framework for flavour models, since they link the quark and lepton sectors of the MSSM. As discussed in chapters 4 and 5, they however also feature potentially wrong predictions for proton decay. In the previous chapters we presented two predictive SUSY flavour $SU(5)$ GUT models, which successfully explain the observed hierarchies of fermion masses and mixing angles. But in addition to correct predictions for the flavour observables, a complete SUSY flavour GUT model also has to include a viable mechanism for GUT symmetry breaking, including sufficient suppression of proton decay without unacceptably large fine-tuning.

In this chapter we present our results of [4] and introduce a novel version of the *double missing partner mechanism* (DMPM) solution to the doublet-triplet splitting problem, which can be combined with predictive models for the GUT scale quark-lepton Yukawa coupling ratios. Two explicit flavour models with different GUT scale predictions are presented, including shaping symmetries and renormalisable messenger sectors.

9.1 The missing partner and double missing partner mechanisms

Since we are considering SUSY $SU(5)$ GUTs, the GUT scale of about 10^{16} GeV is large enough to sufficiently suppress proton decay from dimension six GUT operators, as discussed in 5.5. There we also discussed the doublet-triplet splitting problem arising from requiring sufficiently heavy Higgs colour triplets $T^{(5)}$ and $\bar{T}^{(5)}$, which mediate dimension five proton decay, whereas the MSSM Higgs doublets have to remain light.

In $SU(5)$ GUTs, one proposed solution to the DTS problem is the *missing partner mechanism* (MPM) [144] or its improved version, the *double missing partner mechanism* (DMPM) [179], which we will review briefly below.¹ These solutions have been applied in

¹In theories of extra dimensions, another solution exists, see e.g. [180].

GUT models, but they either predict the unrealistic quark-lepton Yukawa relation $Y_e = Y_d^T$ (e.g. [181]), the experimentally disfavoured combination of the Georgi-Jarlskog relations (4.28) (as e.g. in [182]), or they rely on linear combinations of GUT Yukawa operators (e.g. [183]), which again implies the loss of predictivity.

On the other hand, there exists a large number of GUT models which focus on the flavour sector, but do not include the (GUT) Higgs potential. It is therefore an interesting question to ask how the DTS problem can be resolved in predictive SUSY flavour GUT models, given the present rather precise experimental data on the fermion masses and mixing angles.

As successfully constructed in our two SUYS flavour GUT models of the previous chapters, we employ new Clebsch-Gordan factors emerging from higher-dimensional operators containing a GUT breaking Higgs field in the adjoint representation, to arrive at experimentally favoured GUT scale Yukawa coupling ratios. In this chapter we present how this approach can be combined with a novel DMPM version for solving the DTS problem.

Let us now review the missing partner mechanisms. Note that throughout this section, for illustrative purposes, we consider that the bounds on proton decay rates require the effective mass of the colour triplets (5.87) to be of at least $M_T^{\text{dim}=5} \approx 10^{17}$ GeV [82, 143], while the effective mass suppressing dimension six proton decay mediated by the colour triplets (4.33) is required to be $M_T^{\text{dim}=6} \gtrsim 10^{12}$ GeV [82].

9.1.1 The missing partner mechanism

The basic idea of the MPM is the introduction of two new superfields Z_{50} and \bar{Z}_{50} in $\mathbf{50}$ and $\bar{\mathbf{50}}$ representations of $SU(5)$. The decomposition of $\mathbf{50}$ under the SM gauge group is given by

$$\mathbf{50} = (\mathbf{1}, \mathbf{1})_{-2} + (\mathbf{3}, \mathbf{1})_{-\frac{1}{3}} + (\bar{\mathbf{3}}, \mathbf{2})_{-\frac{7}{6}} + (\mathbf{6}, \mathbf{1})_{\frac{4}{3}} + (\bar{\mathbf{6}}, \mathbf{3})_{-\frac{1}{3}} + (\mathbf{8}, \mathbf{2})_{\frac{1}{2}}, \quad (9.1)$$

which does not contain an $SU(2)_L$ doublet, but it includes an $SU(3)_C$ triplet. Thus, using the $\mathbf{50}$ s as messenger fields to generate an effective mass term for H_5 and \bar{H}_5 keeps the electroweak doublets massless, while the colour triplets acquire masses of the order of the GUT scale.

Note that $\mathbf{50}$ is not in the $SU(5)$ tensor product

$$\mathbf{24} \times \mathbf{5} = \mathbf{5} + \mathbf{45} + \mathbf{70}. \quad (9.2)$$

Thus, instead of $\mathbf{24}$, the MPM contains a GUT breaking Higgs field H_{75} transforming as $\mathbf{75}$ of $SU(5)$ [184, 185], since

$$\mathbf{75} \times \mathbf{5} = \mathbf{45} + \mathbf{50} + \mathbf{280}. \quad (9.3)$$

The superpotential for the MPM is given by²

$$\mathcal{W}_{\text{MPM}} = \bar{H}_5 H_{75} Z_{50} + \bar{Z}_{50} H_{75} H_5 + M_{50} Z_{50} \bar{Z}_{50}. \quad (9.4)$$

²For readability we omit $SU(5)$ indices and most order one coefficients in the superpotentials, except where they are relevant to the discussion.

Note that, because of

$$\mathbf{75} \subset \mathbf{24} \times \mathbf{24} , \quad (9.5)$$

H_{75} can be replaced by the effective combination $\frac{H_{24}^2}{\Lambda}$ in non-renormalisable theories, where Λ denotes a general mass suppression [181], see also 9.2.2.

With the triplet mass contribution from $\langle H_{75} \rangle$ denoted by V , the mass matrices of the Higgs fields H_5 , \bar{H}_5 and Z_{50} , \bar{Z}_{50} are given by

$$m_D = 0 , \quad m_T = \begin{pmatrix} 0 & V \\ V & M_{50} \end{pmatrix} , \quad (9.6)$$

for the doublet and triplet components D and T of H_5 and Z_{50} , respectively. The dangerous terms for dimension five proton decay are obtained from the Yukawa couplings (5.83)

$$\mathcal{W}_{\text{Yuk}} = \mathcal{T}_i \mathcal{F}_j \bar{H}_5 + \mathcal{T}_i \mathcal{T}_j H_5 . \quad (9.7)$$

To calculate the effective dimension five proton decay operators, all Higgs triplets from all $\mathbf{5}$, $\mathbf{50}$, and their respective conjugate representations have to be integrated out, but only the triplets in H_5 and \bar{H}_5 couple to matter. We denote the triplet mass eigenvalues with \tilde{M}_1 and \tilde{M}_2 , and the corresponding mass eigenstates as \tilde{T}_1 and \tilde{T}_2 , respectively. The triplets that couple to matter are given by the combinations

$$T^{(5)} = \sum_i U_{1i}^* \tilde{T}_i , \quad \bar{T}^{(5)} = \sum_i V_{1i} \tilde{T}_i , \quad (9.8)$$

where U and V are unitary matrices defined by $m_T = U m_T^{\text{diag}} V^\dagger$. Integrating out the triplet mass eigenstates \tilde{T}_i leads to the effective dimension five operator for proton decay, which is proportional to the inverse of the *effective triplet mass*

$$(M_T^{\text{dim}=5})^{-1} \equiv U_{1i}^* \left(m_T^{\text{diag}} \right)_{ij}^{-1} V_{1j} = U_{1i}^* \left(m_T^{\text{diag}} \right)_{ij}^{-1} V_{j1}^T = (m_T^{-1})_{11} . \quad (9.9)$$

The Kähler potential for the MPM triplet superfields is given by

$$K_T = T^{(5)} T^{(5)*} + \bar{T}^{(5)} \bar{T}^{(5)*} + T^{(50)} T^{(50)*} + \bar{T}^{(50)} \bar{T}^{(50)*} . \quad (9.10)$$

When the heavy colour triplet mass eigenstates are also integrated out in K_T , effective dimension six Kähler operators emerge from inserting their equations of motion. Then the Lagrange density obtained from the D -term of the effective Kähler potential contains baryon number violating four fermion operators, proportional to

$$(M_T^{\text{dim}=6})^{-2} \equiv V_{1i} \left(m_T^{\text{diag}} \right)_{ij}^{-1} U_{jk}^\dagger U_{km} \left(m_T^{\text{diag}} \right)_{ml}^{-1} V_{l1}^\dagger = \left(m_T^{-1} m_T^{\dagger-1} \right)_{11} \quad (9.11)$$

from $T^{(r)} T^{(r)*}$ and to

$$(M_T^{\text{dim}=6})^{-2} \equiv \left(m_T^{\dagger-1} m_T^{-1} \right)_{11} \quad (9.12)$$

from $\bar{T}^{(r)}\bar{T}^{(r)*}$. With the mass matrix m_T given in (9.6), the effective triplet mass is thus³

$$M_T^{\text{dim}=5} = (m_T^{-1})_{11}^{-1} = -\frac{V^2}{M_{50}}, \quad (9.13)$$

while the suppression of dimension six proton decay is given by

$$(M_T^{\text{dim}=6})^2 = (M_{\bar{T}}^{\text{dim}=6})^2 = \left(m_T^{-1}m_T^{\dagger-1}\right)_{11}^{-1} = \frac{|V|^4}{|M_{50}|^2 + |V|^2}. \quad (9.14)$$

Note that with a GUT scale value of $V \approx 10^{16}$ GeV and M_{50} below the Planck scale, the dimension six proton decay is suppressed sufficiently with values of $M_T^{\text{dim}=6}$ between 10^{13} and 10^{16} GeV.

The splitting between doublet and triplet masses is achieved since the doublets obtain no mass term. Using $M_T^{\text{dim}=5} \gtrsim 10^{17}$ GeV one obtains an upper bound for $M_{50} \lesssim 10^{15}$ GeV. Having the large representations **50** and $\overline{\mathbf{50}}$ enter the RGEs at such a low energy scale, however, leads to the breakdown of perturbativity just above the GUT scale. Thus, the MPM solves the DTS problem – but trades it for $SU(5)$ becoming non-perturbative much below the Planck scale M_{pl} .

9.1.2 The double missing partner mechanism

This trade-off can be avoided in the DMPM, where the number of Higgs fields in **5**, $\overline{\mathbf{5}}$, **50**, and $\overline{\mathbf{50}}$ representations gets doubled [179]. The fields H_5 and \bar{H}_5 couple to the matter fields \mathcal{F}_i and \mathcal{T}_i , whereas H'_5 and \bar{H}'_5 do not. The superpotential for the DMPM is given by

$$\begin{aligned} \mathcal{W}_{\text{DMPM}} = & \bar{H}_5 H_{75} Z_{50} + \bar{Z}_{50} H_{75} H'_5 + \bar{H}'_5 H_{75} Z'_{50} + \bar{Z}'_{50} H_{75} H_5 \\ & + M_{50} Z_{50} \bar{Z}_{50} + M'_{50} Z'_{50} \bar{Z}'_{50} + \mu' H'_5 \bar{H}'_5. \end{aligned} \quad (9.15)$$

The mass matrices of the doublet and triplet components of the Higgs fields H_5 , H'_5 , Z_{50} , Z'_{50} and their corresponding conjugated fields after H_{75} gets a vev V are given by

$$m_D = \begin{pmatrix} 0 & 0 \\ 0 & \mu' \end{pmatrix}, \quad m_T = \begin{pmatrix} 0 & 0 & 0 & V \\ 0 & \mu' & V & 0 \\ V & 0 & M_{50} & 0 \\ 0 & V & 0 & M'_{50} \end{pmatrix}. \quad (9.16)$$

While the Higgs doublets coupling to matter remain massless, the second pair of Higgs doublets contained in H'_5 and \bar{H}'_5 has mass μ' . The improvement of the DMPM compared to the MPM can be seen from the effective triplet mass

$$M_T^{\text{dim}=5} = (m_T^{-1})_{11}^{-1} = -\frac{V^4}{\mu' M_{50} M'_{50}}. \quad (9.17)$$

³In the text when we quote numbers for $M_T^{\text{dim}=5}$, $M_T^{\text{dim}=6}$, and $M_{\bar{T}}^{\text{dim}=6}$ we will always refer to their absolute values.

The same effective triplet mass of $M_T^{\text{dim}=5} \approx 10^{17}$ GeV can now be obtained while keeping high masses $M_{50} \approx M'_{50} \approx 10^{18}$ GeV, provided the heavier doublet pair has a (relatively) small mass $\mu' \approx 10^{11}$ GeV. With the large representations of $SU(5)$ having large masses, the perturbativity of the model can be preserved up to (almost) the Planck scale.

Dimension six proton decay is suppressed by

$$(M_T^{\text{dim}=6})^2 = \left(m_T^{-1} m_T^{\dagger-1}\right)_{11}^{-1} = \frac{|V|^8}{|V|^6 + |M_{50}|^2 (|V|^4 + |M'_{50} \mu'|^2 + |V \mu'|^2)} \approx (10^{14} \text{ GeV})^2, \quad (9.18)$$

$$(M_T^{\text{dim}=6})^2 = \left(m_T^{\dagger-1} m_T^{-1}\right)_{11}^{-1} = \frac{|V|^8}{|V|^6 + |M'_{50}|^2 (|V|^4 + |M_{50} \mu'|^2 + |V \mu'|^2)} \approx (10^{14} \text{ GeV})^2, \quad (9.19)$$

in agreement with the bounds on proton decay.

9.2 Combining predictive flavour GUT models and DMPM

We saw that the DMPM can solve the DTS problem while preserving perturbativity. In order to construct SUSY flavour GUT models with viable GUT scale predictions for the quark - lepton Yukawa coupling ratios, we want to combine the DMPM with the novel CG factors of 4.4, which require the GUT breaking Higgs field to be in the adjoint representation of $SU(5)$, **24**. Thus we will want to replace the Higgs field H_{75} with the effective combination $\frac{H_{24}^2}{\Lambda}$ [181].

On the other hand, we must require renormalisability, since otherwise the predictability for unique $SU(5)$ index contractions yielding specific CG factors would be lost. Analogously to the previous chapters, we now introduce a shaping symmetry and heavy messenger fields, to construct a renormalisable DMPM with an adjoint and forbid dangerous Planck scale suppressed operators.

9.2.1 Planck scale suppressed operators

In the last chapters we carefully constructed the messenger sectors of the SUSY flavour GUT models and thoroughly checked that that the shaping symmetries forbid dangerous Planck scale suppressed effective operators.

The superpotentials (9.4) and (9.15) include mass terms for the **50** messengers. Thus, there are no symmetries to forbid non-renormalisable Planck scale suppressed operators such as

$$\frac{1}{M_{\text{pl}}} H_5 H_{75}^2 \bar{H}_5 \quad (9.20)$$

for the MPM, and

$$\frac{1}{M_{\text{pl}}} H_5 H_{75}^2 \bar{H}'_5 \quad \text{and} \quad \frac{1}{M_{\text{pl}}} H'_5 H_{75}^2 \bar{H}_5 \quad (9.21)$$

for the DMPM. These Planck scale suppressed effective operators do not involve the **50** messengers and therefore spoil the solution to the DTS problem by generating dangerously large contributions to the masses of the doublets contained in the **5s**.

Thus, in order to forbid these effective operators, a shaping symmetry has to be employed. The MPM and DMPM can then be restored by adding a singlet field S , which obtains a non vanishing vev $\langle S \rangle \neq 0$ that yields mass terms to the **50s** by couplings of the form

$$SZ_{50}\bar{Z}_{50} \quad \text{and} \quad SZ'_{50}\bar{Z}'_{50}, \quad (9.22)$$

as shown in the diagram in figure 9.1. A non-trivial charge of S under a shaping symmetry

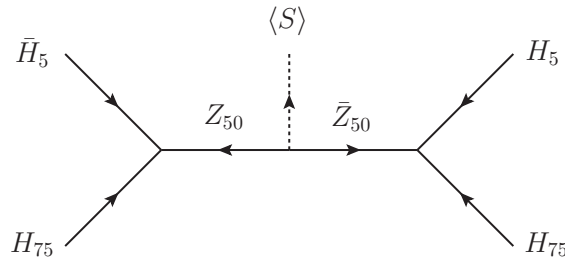


Figure 9.1: MPM supergraph where the mass term for the **50** messengers is given by the vev $\langle S \rangle$. Note that S is generating the mass term and is not acting as an external field.

then forbids the dangerous Planck suppressed effective operators (9.20) and (9.21).

This strategy of generating masses for messenger fields through an additional singlet field will be generalised in 9.2.2 and 9.4, to avoid similarly Planck scale suppressed operators spoiling the DMPM solution or the predictions for the Yukawa coupling ratios.

9.2.2 The double missing partner mechanism with an adjoint

In order to replace H_{75} by an adjoint GUT breaking Higgs field H_{24} , while keeping the model renormalisable, the effective combination $\frac{H_{24}^2}{\Lambda}$ is generated by integrating out heavy messenger fields in the **45** and $\overline{\mathbf{45}}$ representations of $SU(5)$ [183].

In the MPM, we have to introduce a set of messenger fields X_{45} , \bar{X}_{45} , Y_{45} , and \bar{Y}_{45} . For the DMPM, we also need to add a second set X'_{45} , \bar{X}'_{45} , Y'_{45} , and \bar{Y}'_{45} . In figure 9.2 we show the supergraphs generating the non-diagonal entries of the triplet mass matrix in the DMPM with an adjoint H_{24} . In analogy with the discussion in 9.2.1, we forbid direct mass terms for the messenger pairs $Z_{50}\bar{Z}_{50}$ and $Z'_{50}\bar{Z}'_{50}$ in order to avoid dangerous Planck scale suppressed operators that would generate universal mass contributions for both, Higgs doublets and triplets. Similarly, the messenger pairs $X_{45}\bar{X}_{45}$, $Y_{45}\bar{Y}_{45}$, and their corresponding primed versions also obtain masses from the vev of a singlet field S , which

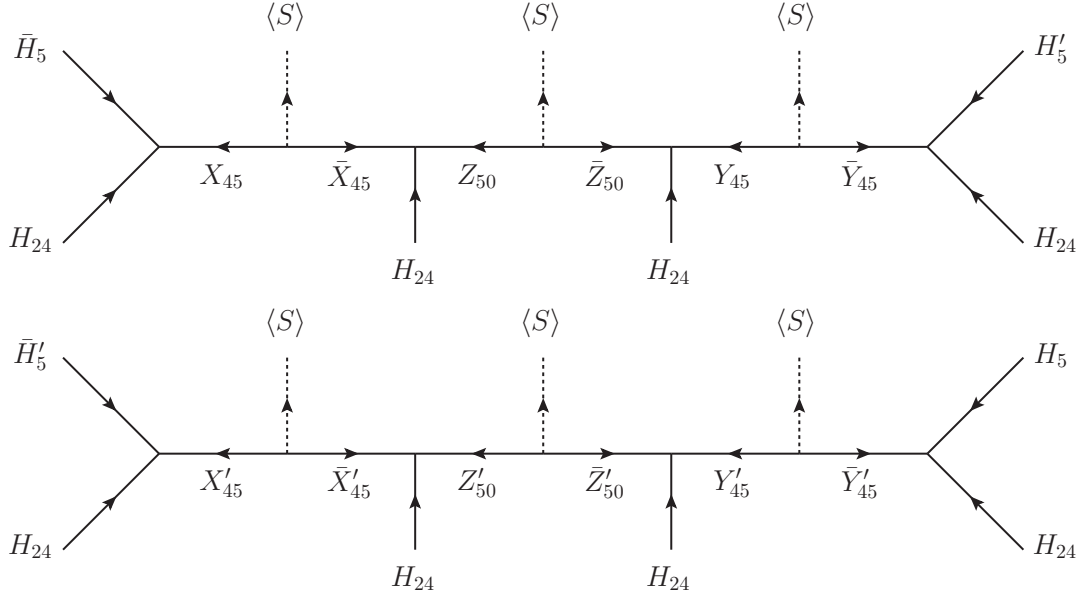


Figure 9.2: Supergraphs generating the non-diagonal entries of the triplet mass matrix.

is charged under the shaping symmetry, since otherwise the symmetry would allow direct mass terms

$$SX_{45}\bar{Y}_{45} \quad \text{and} \quad SX'_{45}\bar{Y}'_{45} \quad (9.23)$$

or non-renormalisable operators

$$\frac{1}{M_{\text{pl}}}S^2X_{45}\bar{Y}_{45} \quad \text{and} \quad \frac{1}{M_{\text{pl}}}S^2X'_{45}\bar{Y}'_{45}, \quad (9.24)$$

which could replace the important **50** messengers in the supergraphs 9.2 and generate universal mass terms for doublets and triplets. We will specify the shaping symmetries of two example models in 9.4.

It is an interesting questions to ask whether some of these heavy **45**s could be the same, such that the number of fields in the spectrum would be reduced while the structure of figure 9.2 would be preserved. But if either $X_{45} \equiv Y_{45}$ or $X'_{45} \equiv Y'_{45}$, it can be seen that the $Z_{50}\bar{Z}_{50}$ mass insertions could be removed, such that the splitting of doublets and triplets would be spoiled and large non-diagonal entries in m_D would be generated. Also, if either $X_{45} \equiv X'_{45}$, $Y_{45} \equiv Y'_{45}$, or $Z_{50} \equiv Z'_{50}$, supergraphs with H_5 and \bar{H}_5 as external fields would be allowed, thereby reducing the DMPM to the MPM and reintroducing the issue of perturbativity. Finally, an identification of $X_{45} \equiv Y'_{45}$ would allow diagrams bypassing the **50** messengers, generating unwanted mass term for both doublet and triplet components of H_5 and \bar{H}_5 , and thus yielding a too large μ -term.

With this messenger superfield content, we carefully checked that no dangerous Planck

suppressed operators spoil the DMPM. The renormalisable superpotential is given by

$$\begin{aligned} \mathcal{W}_{\text{DMPM24}} = & \bar{H}_5 H_{24} X_{45} + \bar{X}_{45} H_{24} Z_{50} + \bar{Z}_{50} H_{24} Y_{45} + \bar{Y}_{45} H_{24} H'_5 \\ & + \bar{H}'_5 H_{24} X'_{45} + \bar{X}'_{45} H_{24} Z'_{50} + \bar{Z}'_{50} H_{24} Y'_{45} + \bar{Y}'_{45} H_{24} H_5 \\ & + S X_{45} \bar{X}_{45} + S Y_{45} \bar{Y}_{45} + S Z_{50} \bar{Z}_{50} + S X'_{45} \bar{X}'_{45} + S Y'_{45} \bar{Y}'_{45} + S Z'_{50} \bar{Z}'_{50} \\ & + \mu' H'_5 \bar{H}'_5 . \end{aligned} \quad (9.25)$$

After H_{24} and S obtain their vevs and integrating out the **45** messenger fields, the mass matrices for the Higgs doublets and triplets are given by

$$m_D = \begin{pmatrix} 0 & 0 \\ 0 & \mu' \end{pmatrix}, \quad m_T = \begin{pmatrix} 0 & 0 & 0 & -\frac{V^2}{\langle S \rangle} \\ 0 & \mu' & -\frac{V^2}{\langle S \rangle} & 0 \\ -\frac{V^2}{\langle S \rangle} & 0 & \langle S \rangle & 0 \\ 0 & -\frac{V^2}{\langle S \rangle} & 0 & \langle S \rangle \end{pmatrix}, \quad (9.26)$$

where $\langle H_{24} \rangle$ is given by (4.13)

$$\langle H_{24} \rangle = V \text{diag} \left(1, 1, 1, -\frac{3}{2}, -\frac{3}{2} \right). \quad (9.27)$$

Note the similarity between the mass matrices of (9.16) and (9.26). Integrating out the heavy **50** fields in a next step, the mass matrices become

$$m_D = \begin{pmatrix} 0 & 0 \\ 0 & \mu' \end{pmatrix}, \quad m_T = \begin{pmatrix} 0 & -\frac{V^4}{\langle S \rangle^3} \\ -\frac{V^4}{\langle S \rangle^3} & \mu' \end{pmatrix}. \quad (9.28)$$

Thus, the doublets in the pair $H_5 \bar{H}_5$ remain massless, while the doublet pair in $H'_5 \bar{H}'_5$ is heavy. Using only H_5 and \bar{H}_5 for the Yukawa couplings of the MSSM matter superfields as in (9.7), the effective triplet component mass relevant for dimension 5 proton decay is given by

$$M_T^{\text{dim}=5} = (m_T^{-1})_{11}^{-1} = -\frac{V^8}{\langle S \rangle^6 \mu'}. \quad (9.29)$$

The effective masses suppressing dimension six proton decay mediated by colour triplets are given by

$$(M_T^{\text{dim}=6})^2 = (M_T^{\text{dim}=6})^2 \approx \frac{|V|^8}{|\langle S \rangle|^6}, \quad (9.30)$$

where we used the fact that $|\langle S \rangle| \gg |V|$ and $|\langle S \rangle^3 \mu'| \ll |V|^4$. With $\langle S \rangle \approx 10^{18}$ GeV it follows from requiring $M_T^{\text{dim}=6} \gtrsim 10^{12}$ GeV in (9.30) that the GUT scale is higher than $V \gtrsim 10^{16}$ GeV. Then in order to obtain an effective triplet mass $M_T^{\text{dim}=5} \approx 10^{17}$ GeV for dimension five proton decay, one finds from (9.29) that $\mu' \approx 10^7$ GeV is needed.

Therefore, with a high enough GUT scale, the effective triplet masses can be large enough to sufficiently suppress proton decay, while the large $SU(5)$ representations used in the DMPM can be heavy enough to keep the theory perturbative up to the Planck scale.

Let us note two remarks: When H_{24} is uncharged under additional symmetries, having μ' several orders of magnitude smaller than V requires μ' to be generated from vevs of fields charged under the shaping symmetry, to forbid the term

$$H_{24}H'_5\bar{H}'_5, \quad (9.31)$$

which would give rise to a much too small effective triplet mass.

Finally note that the effective triplet mass entering dimension five proton decay can be conveniently expressed in terms of the mass eigenstates \tilde{M}_1 and \tilde{M}_2 of the triplet components and μ' of the doublets

$$M_T^{\text{dim}=5} = -\frac{\tilde{M}_1\tilde{M}_2}{\mu'}. \quad (9.32)$$

The effective triplet mass of dimension six proton decay is then excellently approximated by

$$M_{\bar{T}}^{\text{dim}=6} = M_T^{\text{dim}=6} \approx \sqrt{M_T^{\text{dim}=5}\mu'}. \quad (9.33)$$

9.2.3 Introducing a second adjoint

The DMPM with an adjoint GUT breaking Higgs instead of a **75** already solves the DTS problem while providing the necessary building block for the desirable CG factors for flavour model building, if the GUT scale is high enough. Yet, it still suffers from two problems:

Gauge coupling unification As mentioned in 5.5, demanding gauge coupling unification in the minimal renormalisable $SU(5)$ requires the mass of the colour triplets to be about 10^{15} GeV, which violates the bounds on proton decay. Non-renormalisable operators in the GUT breaking superpotential can split the **24** component masses, allowing a higher effective triplet mass [146], at the price of giving up the predictive quark-lepton Yukawa coupling ratios.

Shaping symmetry charge of the adjoint The renormalisable superpotential (5.83) requires H_{24} to be uncharged under shaping symmetries in order for it to obtain a vev. However, such a shaping symmetry charge is vital in the type of flavour models considered here, to avoid unwanted admixtures of additional CG factors involving less insertions of H_{24} . See for example the SUSY flavour GUT models in the previous chapters and tables D.1 and D.3.

Both problems can be solved at once by introducing a second adjoint superfield:

- An additional heavy **24** can be used to UV complete a non-renormalisable superpotential, thereby realising a renormalisable theory which shifts the upper bound for the effective triplet mass to higher values (5.90), by splitting the masses of the **24** components.

- It turns out that the introduction of an additional **24** is not just an UV-completion of the non-renormalisable superpotential of [146]. When both adjoints have approximately the same mass and therefore the second **24** is not integrated out, the additional colour octet and electroweak triplet in the spectrum lead to more freedom for the GUT scale and effective triplet masses.
- Finally, with a second **24**, the adjoint fields can acquire non-vanishing vevs even when charged under shaping symmetries.

There are four possibilities for renormalisable superpotentials of two adjoints with non-vanishing vevs and masses. Classified based on their symmetry, they are:

- $\mathcal{W} = M_{24} \text{Tr } H_{24}^2 + M'_{24} \text{Tr } H_{24}'^2 + \kappa' \text{Tr } H_{24} H_{24}'^2 + \lambda \text{Tr } H_{24}^3$,
 \mathbb{Z}_2 symmetry where H_{24} is uncharged and H_{24}' charged.
- $\mathcal{W} = \tilde{M}_{24} \text{Tr } H_{24} H_{24}' + \lambda \text{Tr } H_{24}^3 + \lambda' \text{Tr } H_{24}'^3$,
 \mathbb{Z}_3 symmetry, where H_{24} has charge 2 and H_{24}' charge 1.
- $\mathcal{W} = \tilde{M}_{24} \text{Tr } H_{24} H_{24}' + \lambda \text{Tr } H_{24}^3 + \kappa' \text{Tr } H_{24} H_{24}'^2$,
 \mathbb{Z}_4^R symmetry where H_{24} has a charge of 2 (with $R(\theta) = 1$) and H_{24}' is uncharged.
- The trivial case with both fields only charged under $SU(5)$ and all (non-linear) terms allowed. We will not consider this case any further.

Let us remark that since the superpotentials (a), (b), and (d) do not feature an R -symmetry and superpotential (c) spontaneously breaks the R -symmetry simultaneously with the GUT gauge group, all four superpotentials are not in conflict with the No-Go theorem that the MSSM with an additional unbroken R -symmetry can not be obtained from the spontaneous breaking of a four-dimensional SUSY GUT [186].

9.2.4 The case of more Higgs fields coupling to matter

Consider the SUSY flavour GUT models of the previous chapters, where an additional Higgs field \bar{H}_{45} transforming as $\overline{\mathbf{45}}$ under $SU(5)$ was introduced in order to construct the CG factor $-\frac{1}{2}$. In 9.1 we have so far only considered the case where a single pair of Higgs fields H_5, \bar{H}_5 couples to the matter superfields. Let us now discuss the case where more than one Higgs triplet is coupling to matter.

With additional Higgs fields (9.7) generalises to

$$\mathcal{W} = \kappa_{ija} \mathcal{T}_i \mathcal{T}_j H_a + \lambda_{ijb} \mathcal{T}_i \mathcal{F}_j \bar{H}_b + m_{H_{ab}} H_a \bar{H}_b, \quad (9.34)$$

where a and b denote different Higgs fields, κ and λ are Yukawa couplings, and m_H is the Higgs mass matrix. When the heavy triplets are integrated out, the proton decay channels

$$\frac{\kappa_{ija} \lambda_{klb}}{(M_T^{\text{dim}=5})_{ba}} (Q_i \cdot Q_j) (Q_k \cdot L_l) \quad \text{and} \quad \frac{\kappa_{ija} \lambda_{klb}}{(M_T^{\text{dim}=5})_{ba}} U_i^c E_j^c U_k^c D_l^c \quad (9.35)$$

are suppressed by the effective triplet mass

$$(M_T^{\dim=5})_{ba}^{-1} \equiv U_{ai}^* \left(m_T^{\text{diag}}\right)_{ij}^{-1} V_{bj} = U_{ai}^* \left(m_T^{\text{diag}}\right)_{ij}^{-1} V_{jb}^T = (m_T^{-1})_{ba}, \quad (9.36)$$

with m_T being the mass matrix of the coloured triplets in H_a, \bar{H}_b . Similarly, the Kähler potential in general reads

$$K_T = T_a T_a^* + \bar{T}_a \bar{T}_a^*. \quad (9.37)$$

When the heavy Higgs triplets are integrated out, baryon number violating operators emerge in the Kähler potential

$$\frac{|\kappa_{ija}|^2}{(M_{\bar{T}}^{\dim=6})_{aa}^2} (Q_i \cdot Q_j) U_i^{c*} E_j^{c*} \quad \text{and} \quad \frac{|\lambda_{ija}|^2}{(M_T^{\dim=6})_{aa}^2} (Q_i \cdot L_j) U_i^{c*} D_j^{c*}, \quad (9.38)$$

where no sum over i, j , and a is implied. The dimension six effective triplet masses are then in general given by

$$(M_T^{\dim=6})_{aa}^{-2} \equiv V_{ai} \left(m_T^{\text{diag}}\right)_{ij}^{-1} U_{jb}^\dagger U_{bm} \left(m_T^{\text{diag}}\right)_{ml}^{-1} V_{la}^\dagger = \left(m_T^{-1} m_T^{\dagger-1}\right)_{aa} \quad (9.39)$$

and

$$(M_{\bar{T}}^{\dim=6})_{aa}^{-2} \equiv \left(m_T^{\dagger-1} m_T^{-1}\right)_{aa}. \quad (9.40)$$

Thus, in models featuring several Higgs fields coupling to specific matter fields, as e.g. to construct predictions for quark-lepton Yukawa coupling ratios from certain CG factors, the individual effective triplet masses for each proton decay channel can be easily calculated.

9.3 Grand unification and the effective triplet mass

In addition to the MSSM superfields, the DMPM introduces one extra pair of $SU(2)_L$ doublets, $D^{(5)}$ and $\bar{D}^{(5)}$, and two additional pairs of $SU(3)_C$ triplets, $T_i^{(5)}$ and $\bar{T}_i^{(5)}$, $i = 1, 2$. Since we introduce a second adjoint, there are furthermore two $SU(3)_C$ octets $O_i^{(24)}$, two $SU(2)_L$ triplet $T_i^{(24)}$, and two singlets $S_i^{(24)}$ of the SM gauge group, when $SU(5)$ gets broken. Finally there is one leptoquark superfield pair $L^{(24)}$ in the spectrum, whereas the other pair yields massive X and Y vector bosons via the BEH mechanism.

All this new superfields enter the RGEs for the gauge couplings at their respective mass scales and therefore their impact on gauge coupling unification has to be studied. Such an analysis has been performed by the author's collaborator Vinzenz Maurer. Thus, in this thesis only some results – which are important to the author's work presented afterwards – are briefly reviewed in this section. Details can be found in our paper [4] and Vinzenz Maurer's PhD thesis [158].

We assume that the heaviest incomplete $SU(5)$ multiplets to enter the RGEs are the X and Y vector bosons, such that the GUT scale corresponds to their heavy mass $M_{\text{GUT}} =$

$M_X = M_Y$. This is a common situation in $SU(5)$ GUTs and it allows to make the effective triplet mass heavy, although cases of other heaviest $SU(5)$ components are possible.

With the definition of the geometric mean

$$M_{T^{(5)}}^2 \equiv M_{T_1^{(5)}} M_{T_2^{(5)}} \quad (9.41)$$

of the masses of the colour triplets and analogously

$$M_{T^{(24)}}^2 \equiv M_{T_1^{(24)}} M_{T_2^{(24)}} , \quad (9.42)$$

$$M_{O^{(24)}}^2 \equiv M_{O_1^{(24)}} M_{O_2^{(24)}} \quad (9.43)$$

for the masses of the components of H_{24} and H'_{24} , one can solve the RGEs for gauge coupling unification and express the results for the effective triplet mass (9.32)

$$M_T^{\text{dim}=5} = \frac{M_{T^{(5)}}^2}{M_{D^{(5)}}} , \quad (9.44)$$

the GUT scale $SU(5)$ gauge coupling α_u , and M_{GUT} at the one-loop level by

$$\pi\alpha_u^{-1} = -\frac{43\pi}{24\alpha_1} + \frac{15\pi}{8\alpha_2} + \frac{11\pi}{12\alpha_3} - \frac{197}{20} \log M_Z + \frac{3}{5} \log M_{DT} \quad (9.45)$$

$$- \frac{3}{4} \log M_{L^{(24)}} + \frac{15}{4} \log M_{T^{(24)}} + \frac{11}{4} \log M_{O^{(24)}} + \frac{7}{2} \log M_{\text{SUSY}} ,$$

$$\log M_T^{\text{dim}=5} = -\frac{5\pi}{6\alpha_1} + \frac{5\pi}{2\alpha_2} - \frac{5\pi}{3\alpha_3} + \frac{1}{6} \log M_Z \quad (9.46)$$

$$+ 5 \log M_{T^{(24)}} - 5 \log M_{O^{(24)}} + \frac{5}{6} \log M_{\text{SUSY}} ,$$

$$\log M_{\text{GUT}} = \frac{5\pi}{12\alpha_1} - \frac{\pi}{4\alpha_2} - \frac{\pi}{6\alpha_3} + \frac{11}{6} \log M_Z \quad (9.47)$$

$$+ \frac{1}{2} \log M_{L^{(24)}} - \frac{1}{2} \log M_{T^{(24)}} - \frac{1}{2} \log M_{O^{(24)}} - \frac{1}{3} \log M_{\text{SUSY}} ,$$

where “ $\log m$ ” should be understood as

$$\log m \equiv \log \left(\frac{m}{\text{GeV}} \right) \quad (9.48)$$

and we have introduced the mass

$$M_{DT}^3 \equiv M_{D^{(5)}}^2 M_{T^{(5)}} . \quad (9.49)$$

Then one finds numerically

$$M_T^{\text{dim}=5} = 2.5_{-0.8}^{+0.6} \cdot 10^{17} \text{ GeV} \left(\frac{M_{\text{SUSY}}}{1 \text{ TeV}} \right)^{\frac{5}{6}} \left(\frac{M_{T^{(24)}}}{M_{O^{(24)}}} \right)^5 , \quad (9.50)$$

$$M_{\text{GUT}} = 1.37_{-0.05}^{+0.05} \cdot 10^{16} \text{ GeV} \left(\frac{M_{\text{SUSY}}}{1 \text{ TeV}} \right)^{-\frac{1}{3}} \left(\frac{M_{L^{(24)}}}{10^{16} \text{ GeV}} \right)^{\frac{1}{2}} \left(\frac{M_{T^{(24)}} M_{O^{(24)}}}{(10^{16} \text{ GeV})^2} \right)^{-\frac{1}{2}} , \quad (9.51)$$

where the resulting uncertainty is dominated by the experimental error on α_s . The change of the relative uncertainty for the different superpotentials (a)-(c) is negligible and hence in the remainder of this section the error is not explicitly shown anymore.

In analogy to $\tan \beta$ of the MSSM, we introduce $\tan \beta_V = \frac{V_1}{V_2}$ for the two GUT breaking superfields H_{24} and H'_{24} with

$$\begin{aligned}\langle H_{24} \rangle &= V_1 e^{i\phi_1} \text{diag}(1, 1, 1, -3/2, -3/2), \\ \langle H'_{24} \rangle &= V_2 e^{i\phi_2} \text{diag}(1, 1, 1, -3/2, -3/2),\end{aligned}\quad (9.52)$$

where $V_1, V_2 > 0$.

Then one finds for the geometric means of the masses of the colour triplets, octets, and the mass of the remaining leptoquark superfield in H_{24} and H'_{24}

$$M_{T(24)}^2 = \frac{35}{4} M^2, \quad M_{O(24)}^2 = \frac{15}{4} M^2, \quad \text{and} \quad M_{L(24)}^2 = \frac{1}{\sin^2(2\beta_V)} M^2, \quad (9.53)$$

for superpotential (b) and

$$M_{T(24)}^2 = \frac{5}{4} M^2, \quad M_{O(24)}^2 = \frac{5}{4} M^2, \quad \text{and} \quad M_{L(24)}^2 = \frac{1}{4 \sin^2(2\beta_V)} M^2, \quad (9.54)$$

for superpotential (c), where $M \equiv |\tilde{M}_{24}|$, i.e. in both cases all mass eigenvalues turn out to be phase independent. The effective triplet mass is then obtained from (9.50)

$$M_T^{\text{dim}=5, 1\text{-loop}} = 2.5 \cdot 10^{17} \text{ GeV} \left(\frac{M_{\text{SUSY}}}{1 \text{ TeV}} \right)^{\frac{5}{6}} \times \begin{cases} \left(\frac{7}{3} \right)^{\frac{5}{2}} \approx 8.3 & \text{(b)} \\ 1 & \text{(c)} \end{cases}, \quad (9.55)$$

and the GUT scale from (9.51)

$$M_{\text{GUT}}^{1\text{-loop}} = \frac{1.37 \cdot 10^{16} \text{ GeV}}{\sqrt{|\sin 2\beta_V|}} \left(\frac{M_{\text{SUSY}}}{1 \text{ TeV}} \right)^{-\frac{1}{3}} \left(\frac{M}{10^{15} \text{ GeV}} \right)^{-\frac{1}{2}} \times \begin{cases} \sqrt{\frac{8}{\sqrt{21}}} \approx 1.32 & \text{(b)} \\ 2 & \text{(c)} \end{cases}. \quad (9.56)$$

Thus, assuming the same parameters, the effective triplet mass in superpotential (b) is ten times higher than in (c).

The effective triplet mass $M_T^{\text{dim}=5}$ receives significant two-loop contributions (cf. e.g. [145]). See our paper [4] and [158] for a numerical two-loop analysis. Its results are given by

$$M_T^{\text{dim}=5, 2\text{-loop}} = \left(\frac{M_{\text{SUSY}}}{1 \text{ TeV}} \right)^{0.74} \cdot \begin{cases} 5.2 \cdot 10^{16} \text{ GeV} \left(\frac{M}{10^{15} \text{ GeV}} \right)^{-0.15} & \text{(b)} \\ 6.8 \cdot 10^{15} \text{ GeV} \left(\frac{M}{10^{15} \text{ GeV}} \right)^{-0.18} & \text{(c)} \end{cases}, \quad (9.57)$$

and

$$M_{\text{GUT}}^{2\text{-loop}} = |\sin 2\beta_V|^{-0.48} \left(\frac{M_{\text{SUSY}}}{1 \text{ TeV}} \right)^{-0.4} \cdot \begin{cases} 2.89 \cdot 10^{16} \text{ GeV} \left(\frac{M}{10^{15} \text{ GeV}} \right)^{-0.61} & \text{(b)} \\ 4.78 \cdot 10^{16} \text{ GeV} \left(\frac{M}{10^{15} \text{ GeV}} \right)^{-0.63} & \text{(c)} \end{cases}, \quad (9.58)$$

where $M_{D^{(5)}} = 1000$ TeV has been fixed and the dependence on other parameters is very small. Thus, a heavy effective triplet mass $M_T^{\text{dim}=5} \gtrsim 10^{17}$ GeV requires $M_{\text{SUSY}} \gtrsim 2.3$ TeV and 35 TeV for superpotential (b) and (c), respectively.

Note that gauge coupling unification depends only weakly on $M_{D^{(5)}}$. The effective triplet mass for dimension six proton decay can be approximated by (9.33) from the square root of the product of $M_{D^{(5)}}$ and $M_T^{\text{dim}=5, 1\text{-loop}}$ or $M_T^{\text{dim}=5, 2\text{-loop}}$ respectively.

Finally we turn to superpotential (a), which is more complicated since it contains two mass parameters M_{24} and M'_{24} . Thus we introduce a second angle β_M and mean mass $M > 0$ such that $M_{24} = Me^{i\alpha_1} \sin \beta_M$ and $M'_{24} = Me^{i\alpha_2} \cos \beta_M$. Then the geometric mean masses of the $SU(3)_C$ octet, $SU(2)_L$ triplet, and of the additional heavy leptoquark superfields are

$$M_{T^{(24)}}^2 = 5 M^2 \cos \beta_M \sqrt{(2 \cos \beta_M - 3 \sin \beta_M \tan^2 \beta_V)^2 + \dots \sin^2 \bar{\phi}}, \quad (9.59a)$$

$$M_{O^{(24)}}^2 = 5 M^2 \cos \beta_M \sqrt{(3 \cos \beta_M - 2 \sin \beta_M \tan^2 \beta_V)^2 + \dots \sin^2 \bar{\phi}}, \quad (9.59b)$$

$$M_{L^{(24)}}^2 = \frac{1}{4} M^2 \frac{\cos^2 \beta_M}{\sin^4 \beta_V}, \quad (9.59c)$$

where not only the geometric mean masses, but also the mass eigenvalues themselves, only depend on the phase combination

$$\bar{\phi} \equiv (\alpha_1 - \alpha_2)/2 + \phi_1 - \phi_2, \quad (9.60)$$

and are invariant under $\bar{\phi} \rightarrow \bar{\phi} + \pi$. Due to (9.50), the effective triplet mass is heaviest when the ratio $\frac{M_{T^{(24)}}}{M_{O^{(24)}}}$ is not bounded from above, and hence when $\bar{\phi}$ is 0, π , or 2π . In figure 9.3 the resulting plots for $M_T^{\text{dim}=5}$ and M_{GUT} are shown with $M_{\text{SUSY}} = 1$ TeV, $M = 10^{15}$ GeV, $M_{D^{(5)}} = 1000$ TeV, and $\bar{\phi} = 0$, including a comparison between one- and two-loop results. $M_T^{\text{dim}=6}$ and $M_{\bar{T}}^{\text{dim}=6}$ are again approximately given by $\sqrt{M_T^{\text{dim}=5} M_{D^{(5)}}$.

9.4 SUSY Flavour GUT models with DMPM

After the interlude of the last section, we return to the author's contribution to [4] and present two example models, combining the DMPM (featuring two adjoint superfields) and predictive GUT scale quark-lepton Yukawa coupling ratios due to CG factors. Both models are UV complete and we give the shaping symmetries and messenger superfields, which guarantee that only the desired effective GUT operators are generated when the heavy degrees of freedom are integrated out.

Note that we construct only the Yukawa matrices of the quarks and charged leptons explicitly. Adding one of the ubiquitous mechanisms to generate neutrino masses and lepton mixing angles would be straightforward. Since they are however not directly relevant for the discussion of proton decay, doublet-triplet splitting, and the CG factors between Y_d and Y_e , we do not consider neutrinos in this chapter.

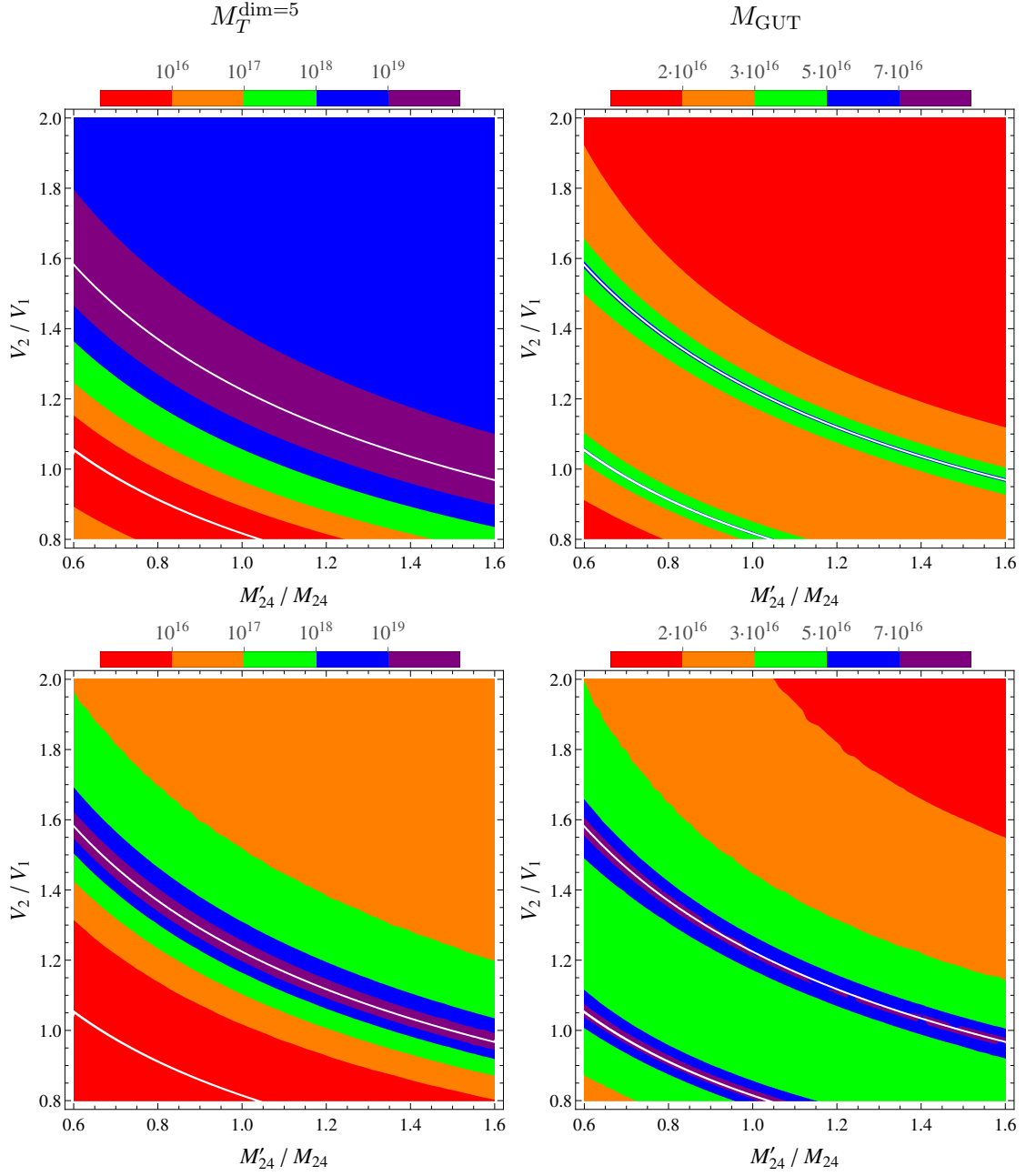


Figure 9.3: The effective colour triplet mass $M_T^{\text{dim}=5}$ (left) and GUT scale M_{GUT} (right) in GeV at one-loop (upper) and two-loop (lower) order as resulting from superpotential (a) for $M_{\text{SUSY}} = 1$ TeV, $M = 10^{15}$ GeV, $M_{D^{(5)}} = 1000$ TeV, and $\bar{\phi} = 0$. Note the different colour coding between left and right. For illustration, the white strips denote areas with light $M_{T^{(24)}}$ or $M_{O^{(24)}} (< 10^{13}$ GeV). Such relatively low values for these components can arise either from cancellation between terms, or from a generic suppression due to small parameters, cf. (9.59). For more details see [4, 158].

We also remark, that our two models are not yet predictive for the quark mixing parameters, but the experimentally observed values can be fitted by both of the models. They thus should be viewed as proof of existence, showing that a successful solution to DTS and experimentally viable predictions for GUT scale Yukawa coupling ratios can indeed be combined. The strategies discussed here, however, provide the tools for the construction of more ambitious SUSY flavour GUT models, which should include the observed neutrino masses and finally also predict the quark and lepton mixing angles and CP phases.

Thus there are two types of predictions our example models make: As discussed in 4.4, in general one can directly constrain GUT models from their GUT scale double ratio (4.43)

$$\left| \frac{y_\mu y_d}{y_s y_e} \right|, \quad (9.61)$$

which as mentioned previously is not affected by RG evolution or SUSY threshold corrections. As for the SUSY flavour GUT models of the previous chapters, we will again use the CG factors $\frac{y_\tau}{y_b} = -\frac{3}{2}$, $\frac{y_\mu}{y_s} = 6$, and $\frac{y_e}{y_d} = -\frac{1}{2}$ in agreement with (4.43), whereas the ubiquitous GJ relations are challenged with more than two sigma deviation from the experimental value.

Secondly, the predictions for the Yukawa coupling ratios at the GUT scale imply – via SUSY threshold corrections – constraints on the SUSY breaking parameters, which may be tested at future collider searches if SUSY is discovered. See e.g. [187] for a discussion and an explicit example of such constraints. We will discuss this link between GUT predictions and SUSY spectrum in general in chapter 10.

Our two examples will feature different Yukawa matrix structures. In the first model we construct diagonal down-type quark and charged lepton Yukawa matrices Y_d and Y_e , with all quark mixing originating from the up-type quark Yukawa matrix Y_u . Then, in the second model we realise the attractive feature of θ_C originating from Y_d .

9.4.1 A model with diagonal Y_d and Y_e Yukawa matrices

We now turn to our first model featuring diagonal down-type quark and charged lepton Yukawa matrices Y_d and Y_e in the flavour basis. An approach to flavour (GUT) model building with diagonal Y_e (and Y_d) has been discussed in [188]. In this case all the mixing in the quark sector has to come exclusively from the up-type quark Yukawa matrix Y_u . Explicitly, our model has the following structure for the Yukawa matrices

$$Y_d = \begin{pmatrix} y_d & 0 & 0 \\ 0 & y_s & 0 \\ 0 & 0 & y_b \end{pmatrix}, \quad Y_e = \begin{pmatrix} -\frac{1}{2}y_d & 0 & 0 \\ 0 & 6y_s & 0 \\ 0 & 0 & -\frac{3}{2}y_b \end{pmatrix}, \quad Y_u = \begin{pmatrix} y_{11} & y_{12} & y_{13} \\ y_{12} & y_{22} & y_{23} \\ y_{13} & y_{23} & y_{33} \end{pmatrix}. \quad (9.62)$$

We introduce flavon superfields θ_1 , θ_2 , θ_3 , and θ_4 that obtain a vev and generate the hierarchical structure of the Yukawa matrices. After the flavons and the GUT breaking H_{24} and H'_{24} obtain their vevs, the Yukawa matrices (9.62) originate from the effective

superpotentials

$$\begin{aligned} \mathcal{W}_u &= \frac{1}{\Lambda^4} H_5 \mathcal{T}_1 \mathcal{T}_1 \theta_1^2 \theta_2^2 + \frac{1}{\Lambda^3} H_5 \mathcal{T}_1 \mathcal{T}_2 \theta_1^2 \theta_2 + \frac{1}{\Lambda^2} H_5 \mathcal{T}_1 \mathcal{T}_3 \theta_1 \theta_2 + \frac{1}{\Lambda^2} H_5 \mathcal{T}_2 \mathcal{T}_2 \theta_1^2 \\ &\quad + \frac{1}{\Lambda} H_5 \mathcal{T}_2 \mathcal{T}_3 \theta_1 + H_5 \mathcal{T}_3 \mathcal{T}_3 , \end{aligned} \quad (9.63)$$

$$\begin{aligned} \mathcal{W}_d &= \frac{1}{\langle S' \rangle} (H'_{24} \mathcal{F}_3)_{\bar{5}} (\bar{H}_5 \mathcal{T}_3)_5 + \frac{\theta_3}{\langle S' \rangle^2} [H'_{24} \mathcal{T}_2]_{10} [\bar{H}_5 \mathcal{F}_2]_{\bar{10}} \\ &\quad + \frac{\theta_4}{\langle S' \rangle^2 \langle S \rangle} [H'_{24} \mathcal{F}_1]_{\bar{45}} [\mathcal{T}_1 H_{24} \bar{H}_5]_{45} , \end{aligned} \quad (9.64)$$

where like for the SUSY flavour GUT models in the previous chapters, we do not show order one coefficients, and denote the different messenger masses generating \mathcal{W}_u by a generic Λ . However, keep in mind that this is just for the sake of simplicity and different entries in the Yukawa matrix should be understood as independent parameters. The ratios of flavon vevs and messenger masses is small of about $10^{-2} - 10^{-1}$. A list of all superfields, including their charges under the shaping symmetry, is presented in tables D.5 and D.6 in appendix D.

In order to construct the desired CG factors and to guarantee the unique contraction of $SU(5)$ indices as shown in (9.64), the effective superpotential has to be UV completed by messenger fields Z_i, \bar{Z}_i , and the adjoint H'_{24} must be charged under shaping symmetries. We therefore implement superpotential (a) for the adjoint superfields. Since in this case the second adjoint H_{24} is left uncharged, direct mass terms for the messenger fields $M_i Z_i \bar{Z}_i$ would always be accompanied by terms of the form

$$\langle H_{24} \rangle Z_i \bar{Z}_i , \quad (9.65)$$

which would inevitably spoil the desired CG factors between Y_d and Y_e^T [93]. To avoid this problem and still generate the desired operators, the masses of the messenger fields that give rise to \mathcal{W}_d originate from vevs of the $SU(5)$ singlet superfields S and S' , which are charged under the shaping symmetry (but with different charges than H'_{24}). The full messenger sector, which yields the effective superpotentials \mathcal{W}_d and \mathcal{W}_u when it is integrated out, can be read off from the supergraphs presented in figures D.13 and D.14 in appendix D. We would like to make two remarks: First, note that the vev of S also gives masses to the heavy messengers of the DMPM (see 9.2.2). Secondly the CG factor $-\frac{1}{2}$ for the 1-1 element of Y_e emerges from the heavy messenger \bar{X}_{45} of the DMPM, as shown in figure 9.4. Therefore there is no requirement to introduce another Higgs field \bar{H}_{45} transforming as **45**, as we had to in the SUSY flavour GUT models of the previous chapters. Let us discuss the effective triplet masses for the proton decay channels involving the triplet of \bar{X}_{45} . The full mass matrix for all triplets of the DMPM before any messengers are integrated out is

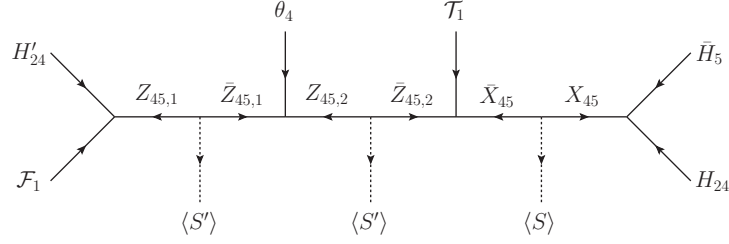


Figure 9.4: Supergraph leading to $y_e = -\frac{1}{2}y_d$ when the heavy messenger fields are integrated out.

given by

$$m_T = \begin{matrix} & \bar{H}_5 & \bar{H}'_5 & \bar{X}_{45} & \bar{Y}_{45} & \bar{Z}_{50} & \bar{X}'_{45} & \bar{Y}'_{45} & \bar{Z}'_{50} \\ \begin{matrix} H_5 \\ H'_5 \\ X_{45} \\ Y_{45} \\ Z_{50} \\ X'_{45} \\ Y'_{45} \\ Z'_{50} \end{matrix} & \begin{pmatrix} 0 & 0 & 0 & 0 & 0 & 0 & V_1 & 0 \\ 0 & \mu' & 0 & V_1 & 0 & 0 & 0 & 0 \\ V_1 & 0 & \langle S \rangle & 0 & 0 & 0 & 0 & 0 \\ 0 & 0 & 0 & \langle S \rangle & V_1 & 0 & 0 & 0 \\ 0 & 0 & V_1 & 0 & \langle S \rangle & 0 & 0 & 0 \\ 0 & V_1 & 0 & 0 & 0 & \langle S \rangle & 0 & 0 \\ 0 & 0 & 0 & 0 & 0 & 0 & \langle S \rangle & V_1 \\ 0 & 0 & 0 & 0 & 0 & V_1 & 0 & \langle S \rangle \end{pmatrix} \end{matrix}, \quad (9.66)$$

where V_1 is defined in (9.52) and we have annotated the rows and columns for a better overview. The proton decay mediated by the triplet pair in H_5 and \bar{X}_{45} is then suppressed by the effective triplet mass (9.36)

$$(M_T^{\text{dim}=5})_{31} = (m_T^{-1})_{31}^{-1} = -\frac{V_1^7}{\langle S \rangle^5 \mu'}, \quad (9.67)$$

which is about two orders of magnitude larger than the effective triplet mass associated with proton decay mediated by the triplets in H_5 and \bar{H}_5 (9.29)

$$(M_T^{\text{dim}=5})_{11} = -\frac{V_1^8}{\langle S \rangle^6 \mu'}. \quad (9.68)$$

Also the dimension six proton decay mediated by the triplets in \bar{X}_{45} (9.40)

$$(M_T^{\text{dim}=6})_{33}^2 \approx \frac{|V_1|^6}{|\langle S \rangle|^4}, \quad (9.69)$$

is approximately four orders of magnitude larger than (9.30)

$$(M_T^{\text{dim}=6})_{11}^2 \approx \frac{|V_1|^8}{|\langle S \rangle|^6}. \quad (9.70)$$

It is thus sufficient to limit our discussion to the effective triplet masses of proton decay mediated by the triplets in H_5 and \bar{H}_5 .

Finally note that the additional colour triplets of all DMPM messengers, H'_5 , and \bar{H}'_5 can couple to the matter superfields only via effective operators, which can contribute to proton decay but are suppressed compared to the leading operators by one or more powers of $\frac{H_{24}}{M_{\text{pl}}}$ and $\frac{H'_{24}}{M_{\text{pl}}}$. Their contribution can thus safely be neglected.

Let us now comment on the phenomenology of Y_d and Y_u . The hierarchical structure of Y_d is enforced due to the use of higher order effective operators in \mathcal{W}_d . The eigenvalues of Y_u and the mixing angles are given in leading order in a small angle approximations as

$$y_u \approx y_{11} - \frac{y_{12}^2}{y_{22}}, \quad y_c \approx y_{22}, \quad y_t \approx y_{33}, \quad \theta_C \approx \frac{y_{12}}{y_{22}}, \quad \theta_{23} \approx \frac{y_{23}}{y_{33}}, \quad \theta_{13} \approx \frac{y_{13}}{y_{33}}. \quad (9.71)$$

Phenomenology requires that all parameters y_{ij} of Y_u are independent, which needs to be carefully considered in the construction of the messenger sector. When we present the messenger sector in appendix D we also discuss that a similar choice of messenger fields, which generates the same structure (9.62) for the Yukawa matrices and thus would seem as an equally viable choice, in fact predicts invalid dependencies between the quark mixing angles.

We argued in 9.2.2 that for the case of an uncharged H_{24} , as it appears in the selected superpotential (a) for our model, the mass term for the additional Higgs fields $H'_5 \bar{H}'_5$ must come from the vev of some singlet field. In our model an effective μ' term is generated from a higher-dimensional operator and with an even higher suppression, there is also a μ -term for the Higgs fields coupling to matter

$$\mathcal{W}_5^{\text{eff}} = \mu H_5 \bar{H}_5 + \mu' H'_5 \bar{H}'_5, \quad (9.72)$$

where

$$\mu' \equiv \frac{\langle \theta_3 \rangle^4}{M_{\text{pl}}^3} \quad \text{and} \quad \mu \equiv \frac{\langle \theta_3 \rangle \langle \theta_4 \rangle^4}{M_{\text{pl}}^4}. \quad (9.73)$$

Alternatively, we checked that an UV-complete generation of these μ and μ' operators via messenger fields would be possible. However, the necessary messenger fields are not included in the model since it turns out that the desired masses are already generated by Planck scale suppressed effective operators.

Integrating out the heavy **45** and **50** messengers and after $SU(5)$ gets spontaneously broken, the effective triplet mass for dimension five proton decay is given by (9.29)

$$M_T^{\text{dim}=5} = \mu - \frac{V_1^8}{\langle S \rangle^6 \mu'} \approx -\frac{V_1^8 M_{\text{pl}}^3}{\langle S \rangle^6 \langle \theta_3 \rangle^4}, \quad (9.74)$$

and the effective triplet masses suppressing dimension six proton decay by (9.30)

$$M_T^{\text{dim}=6} = M_{\bar{T}}^{\text{dim}=6} \approx \frac{V_1^4}{\langle S \rangle^3}. \quad (9.75)$$

Let us give an explicit example for the scales involved in the model: Because of perturbativity the mass of the **50** messengers has to be almost at the Planck scale. We therefore assume

$$\langle S \rangle \sim 10^{-1} M_{\text{pl}}. \quad (9.76)$$

Using the known values of the Yukawa couplings, we can estimate the values of the relevant masses of our model. At the GUT scale with $\tan\beta = 30$ the Yukawa couplings are approximately given by [91]

$$y_d \approx 1.6 \cdot 10^{-4}, \quad y_s \approx 3 \cdot 10^{-3}, \quad \text{and} \quad y_b \approx 0.18, \quad (9.77)$$

which in our example model are (up to order one couplings) given by the operators

$$y_d \sim \frac{\langle H_{24} \rangle \langle H'_{24} \rangle \langle \theta_4 \rangle}{\langle S' \rangle^2 \langle S \rangle}, \quad y_s \sim \frac{\langle H'_{24} \rangle \langle \theta_3 \rangle}{\langle S' \rangle^2}, \quad \text{and} \quad y_b \sim \frac{\langle H'_{24} \rangle}{\langle S' \rangle}. \quad (9.78)$$

Then we find from (9.52), (9.74) – (9.78) for the effective triplet masses, the μ -term, and the mass of the additional heavy Higgs doublet the following values

$$\begin{aligned} M_T^{\text{dim}=5} &\approx 1.4 \cdot 10^{19} \text{ GeV}, \quad \mu \approx 225 \text{ GeV}, \\ M_T^{\text{dim}=6} &\approx 1.4 \cdot 10^{12} \text{ GeV}, \quad \mu' \approx 130 \text{ TeV}, \end{aligned} \quad (9.79)$$

where we assumed a SUSY scale $M_{\text{SUSY}} = 1 \text{ TeV}$, $\frac{M'_{24}}{M_{24}} = 1$, and $\frac{V_2}{V_1} = 1.2$.⁴ With these parameters, the GUT scale is given by

$$M_{\text{GUT}} \approx 6.4 \cdot 10^{16} \text{ GeV}. \quad (9.80)$$

Although these numbers are only estimates, which neglect order one couplings, they illustrate the model's key features: the DTS problem is solved by the DMPM with large effective triplet masses suppressing the proton decay rate and the fermion mass ratios are realistic. The small μ -term emerges from a Planck scale suppressed operator. We remark that the DMPM does not suffer from any dangerous Planck scale suppressed operators, due to the charge assignment of the singlet field S .

9.4.2 A model with θ_C from Y_d

Motivated by our SUSY flavour GUT models [2, 3] presented in the previous chapters to explain $\theta_{13}^{\text{PMNS}} \approx \theta_C \sin \theta_{23}^{\text{PMNS}}$ via charged lepton corrections [1] and a right-angled quark unitarity triangle [157], we present a second example model, which realises the attractive feature of θ_C emerging dominantly from the down-type quark mixing $\theta_C \approx \theta_{12}^d$. The Yukawa matrices are given by the following structure

$$Y_d = \begin{pmatrix} 0 & y_{d_{12}} & 0 \\ y_{d_{21}} & y_s & 0 \\ 0 & 0 & y_b \end{pmatrix}, \quad Y_e = \begin{pmatrix} 0 & 6y_{d_{21}} & 0 \\ -\frac{1}{2}y_{d_{12}} & 6y_s & 0 \\ 0 & 0 & -\frac{3}{2}y_b \end{pmatrix}, \quad Y_u = \begin{pmatrix} y_{11} & y_{12} & 0 \\ y_{12} & y_{22} & y_{23} \\ 0 & y_{23} & y_{33} \end{pmatrix}. \quad (9.81)$$

Our strategy requires to couple \mathcal{F}_1 and \mathcal{F}_2 to \mathcal{T}_2 , but both fields need to be distinguished from each other by shaping symmetry since \mathcal{F}_2 needs to couple to \mathcal{T}_1 while \mathcal{F}_1 must not

⁴Vevs V_1 and V_2 with $\cot\beta_V = 1.2$ and $V_1 = 3.4 \cdot 10^{16} \text{ GeV}$ are obtained in superpotential (a) with the real parameters $\lambda \sim 0.19$, $\kappa' \sim 0.04$, and $M'_{24} = M_{24} \sim 7 \cdot 10^{14} \text{ GeV}$, see [4, 158].

couple to \mathcal{T}_1 . This suggests to employ at least a \mathbb{Z}_3 shaping symmetry and we therefore use superpotential (b) from section 9.2.3, where H_{24} and H'_{24} are charged.

The effective superpotentials that yield the desired Yukawa matrices after integrating out heavy messenger fields and breaking of the GUT gauge group are

$$\mathcal{W}_u = \frac{1}{\Lambda^2} H_5 \mathcal{T}_1 \mathcal{T}_1 \theta_5^2 + \frac{1}{\Lambda^2} H_5 \mathcal{T}_1 \mathcal{T}_2 \theta_2^2 + \frac{1}{\Lambda^2} H_5 \mathcal{T}_2 \mathcal{T}_2 \theta_1^2 + \frac{1}{\Lambda} H_5 \mathcal{T}_2 \mathcal{T}_3 \theta_1 + H_5 \mathcal{T}_3 \mathcal{T}_3, \quad (9.82)$$

$$\begin{aligned} \mathcal{W}_d = & \frac{1}{\langle S' \rangle} (H'_{24} \mathcal{F}_3)_{\bar{5}} (\bar{H}_5 \mathcal{T}_3)_5 + \frac{\theta_3}{\langle S' \rangle^2} (H_{24} \mathcal{T}_2)_{10} (\bar{H}_5 \mathcal{F}_1)_{\bar{10}} + \frac{\theta_4}{\langle S' \rangle^2} (H'_{24} \mathcal{T}_2)_{10} (\bar{H}_5 \mathcal{F}_2)_{\bar{10}} \\ & + \frac{1}{\langle S \rangle^2} (H_{24} \mathcal{F}_2)_{\bar{45}} (\mathcal{T}_1 H_{24} \bar{H}_5)_{45}, \end{aligned} \quad (9.83)$$

where again we use a common placeholder Λ to denote a generic messenger mass and the messenger fields responsible for \mathcal{W}_d obtain their masses from vevs of singlet fields. Note that in comparison to Y_u of the previous example model (9.62), the vanishing $Y_{u_{13}}$ element requires to introduce an additional flavon field θ_5 .

The supergraphs that generate these effective operators are shown in figures D.15 and D.16 in appendix D. A complete list of all superfields including their charges and representations is given in tables D.7 and D.8. Note that again we do not introduce a new Higgs field \bar{H}_{45} that couples to matter superfields, but the CG factor $-\frac{1}{2}$ emerges from the DMPM messenger \bar{X}_{45} , see figure 9.5. Analogously to the discussion below figure 9.4, it is

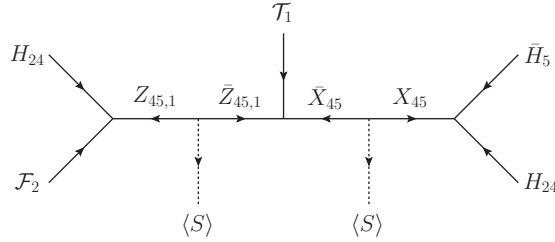


Figure 9.5: Supergraph yielding the CG factor $-\frac{1}{2}$ when the heavy messenger fields are integrated out.

sufficient to limit our discussion to the effective triplet masses of proton decay mediated by the triplet pair in H_5 and \bar{H}_5 , since the effective triplet mass of the \bar{X}_{45} decay channel is orders of magnitude higher. Other effective operators coupling matter superfields to other triplets of the DMPM are again sufficiently suppressed by powers of $\frac{\tilde{M}_{24}}{M_{\text{pl}}}$.

In a small angle approximation the mixing angles and Yukawa couplings are given by

$$\begin{aligned} y_d \approx \frac{y_{d_{12}} y_{d_{21}}}{y_s}, \quad \theta_C \approx \theta_{12}^d \approx \frac{y_{d_{12}}}{y_s}, \\ y_u \approx y_{11} - \frac{y_{12}^2}{y_{22}}, \quad y_c \approx y_{22}, \quad y_t \approx y_{33}, \quad \theta_{23} \approx \frac{y_{23}}{y_{33}}, \quad \theta_{13} \approx \frac{y_{12}}{y_{22}} \theta_{23}, \end{aligned} \quad (9.84)$$

and in leading order the strange and bottom quark Yukawa couplings are given by the parameters y_s and y_b of Y_d in (9.81). Thus the Yukawa matrices can fit the experimental values without tension.

Let us now discuss the DMPM details of the model. As in 9.4.1, the mass terms of the Higgs fields $H_5 \bar{H}_5$ and $H'_5 \bar{H}'_5$ are generated from Planck suppressed effective operators (9.72) with

$$\mu \equiv \frac{\langle \theta_3 \rangle^4}{M_{\text{pl}}^3} \quad \text{and} \quad \mu' \equiv \frac{\langle \theta_4 \rangle^4}{M_{\text{pl}}^3} . \quad (9.85)$$

Although μ and μ' appear at the same order, a modest hierarchy $\langle \theta_3 \rangle < \langle \theta_4 \rangle$ sufficiently splits their masses. We will see below that indeed such a slight hierarchy is realised in our model.

The effective triplet masses (9.29) and (9.30) are given by

$$M_T^{\text{dim}=5} = \mu - \frac{V_1^8}{\langle S \rangle^6 \mu'} \approx - \frac{V_1^8 M_{\text{pl}}^3}{\langle S \rangle^6 \langle \theta_4 \rangle^4} , \quad (9.86)$$

$$M_T^{\text{dim}=6} = M_T^{\text{dim}=6} \approx \frac{V_1^4}{\langle S \rangle^3} . \quad (9.87)$$

As for the first example model we can estimate the values of the relevant masses in an explicit example from the known Yukawa couplings [91]. In a small angle approximation the down-type Yukawa couplings are given by

$$y_d \sim \frac{\langle H_{24} \rangle^2 \langle H_{24} \rangle \langle \theta_3 \rangle}{\langle S \rangle^2 \langle S' \rangle^2} \frac{1}{y_s} \approx 1.6 \cdot 10^{-4} \quad \text{with} \quad y_s \sim \frac{\langle H'_{24} \rangle \langle \theta_4 \rangle}{\langle S' \rangle^2} \approx 3 \cdot 10^{-3} \quad (9.88)$$

and

$$y_b \sim \frac{\langle H'_{24} \rangle}{\langle S' \rangle} \approx 0.18 , \quad (9.89)$$

where the numerical values are valid for $\tan \beta = 30$ and again order one coefficients have been neglected. Again, because of perturbativity we assume $\langle S \rangle = 10^{-1} M_{\text{pl}}$. Then the numerical values of the effective triplet masses, μ , and μ' can be estimated

$$M_T^{\text{dim}=5} \approx 1.4 \cdot 10^{18} \text{ GeV} , \quad M_T^{\text{dim}=6} \approx 10^{12} \text{ GeV} , \quad \mu \approx 7 \text{ TeV} , \quad \mu' \approx 800 \text{ TeV} , \quad (9.90)$$

where we assumed $\tan \beta_V = \frac{1}{2}$.⁵ Note the solutions for $\langle \theta_3 \rangle$ and $\langle \theta_4 \rangle$, which are

$$\langle \theta_3 \rangle \approx 2 \cdot 10^{15} \text{ GeV} \quad \text{and} \quad \langle \theta_4 \rangle \approx 6 \cdot 10^{15} \text{ GeV} , \quad (9.91)$$

whose slight splitting explains the huge hierarchy between μ and μ' , as mentioned above. We also find

$$M_{\text{SUSY}} \approx 26 \text{ TeV} \quad \text{and} \quad M_{\text{GUT}} \approx 3.4 \cdot 10^{17} \text{ GeV} . \quad (9.92)$$

Also in our second model we thus successfully suppress proton decay via large effective triplet masses, where the DTS is achieved via the DMPM with two adjoints. The Yukawa sector of the model features viable fermion masses and mixing angles. A small μ -term for the Higgs doublets emerges from Planck suppressed effective operators.

⁵In superpotential (b) this $\tan \beta_V$ can be obtained with $V_1 = 3.2 \cdot 10^{16} \text{ GeV}$ from real parameters $\lambda \sim 10^{-4}$, $\lambda' \sim 1.3 \cdot 10^{-5}$, and $M \sim 2.4 \cdot 10^{12} \text{ GeV}$, see [4, 158].

9.5 Proton Decay

We now turn to a discussion of proton decay and start by discussing the dimension five operators (5.85)

$$\mathcal{W}_T = (Y_{ql}Q \cdot L - Y_{ud}U^c D^c) \bar{T}^{(5)} + (Y_{ue}U^c E^c - Y_{qq}Q \cdot Q) T^{(5)}, \quad (9.93)$$

which are usually considered to be the greatest danger for the validity of any SUSY GUT model. To suppress proton decay sufficiently, the colour triplets have to be very heavy or their couplings to the matter fields should be very strongly suppressed.

Minimal $SU(5)$ models lead to wrong predictions for the quark-lepton mass ratios. In many models it is thus assumed that non-renormalisable operators resolve this problem, at least for the first two generations, as for example [146, 189]. In such settings the model loses predictability and usually it is impossible to calculate the strength of the coupling between matter fields and Higgs triplets.⁶

In our method viable GUT scale quark-lepton mass ratios are predicted by new CG factors due to specific effective operators, which are uniquely obtained by integrating out a distinct set of messenger fields charged under a shaping symmetry. With the same technique also the GUT scale Yukawa couplings to Higgs triplets are predicted from group-theoretical CG factors. These CG factors for the triplet Yukawa couplings have been calculated by the author's collaborateur Vinzenz Maurer from dimension five and dimension six operators containing one or two adjoints [4, 158]. The CG factors used in our models are listed in figure 9.6.

Then the Yukawa matrices of our first model 9.4.1 are given by

$$Y_d = \text{diag}(y_d, y_s, y_b), \quad Y_e = \text{diag}\left(-\frac{1}{2}y_d, 6y_s, -\frac{3}{2}y_b\right), \quad (9.94)$$

$$Y_{ql} = \text{diag}\left(y_d, y_s, -\frac{3}{2}y_b\right), \quad Y_{ud} = \text{diag}\left(\frac{2}{3}y_d, -4y_s, y_b\right), \quad (9.95)$$

$$Y_{qq} = \frac{1}{2}Y_u, \quad Y_{ue} = Y_u, \quad (9.96)$$

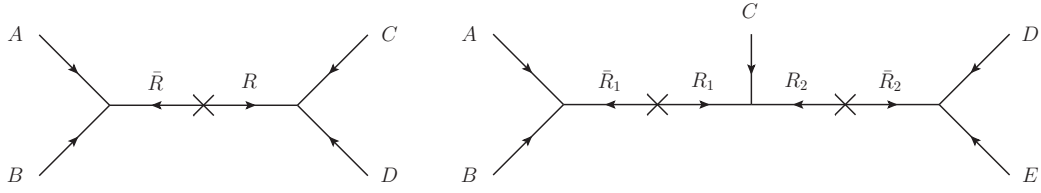
where the structure of Y_u can be read off from (9.62). For the second model 9.4.2 we find

$$Y_d = \begin{pmatrix} 0 & y_{d,12} & 0 \\ y_{d,21} & y_s & 0 \\ 0 & 0 & y_b \end{pmatrix}, \quad Y_e^T = \begin{pmatrix} 0 & -\frac{1}{2}y_{d,12} & 0 \\ 6y_{d,21} & 6y_s & 0 \\ 0 & 0 & -\frac{3}{2}y_b \end{pmatrix}, \quad (9.97)$$

$$Y_{ql} = \begin{pmatrix} 0 & y_{d,12} & 0 \\ y_{d,21} & y_s & 0 \\ 0 & 0 & -\frac{3}{2}y_b \end{pmatrix}, \quad Y_{ud} = \begin{pmatrix} 0 & \frac{2}{3}y_{d,12} & 0 \\ -4y_{d,21} & -4y_s & 0 \\ 0 & 0 & y_b \end{pmatrix}, \quad (9.98)$$

$$Y_{qq} = \frac{1}{2}Y_u, \quad Y_{ue} = Y_u, \quad (9.99)$$

⁶GUT textures for proton decay, without fully constructed models, have been considered, for example, in [190].



Dimension five operators										
AB	CD	R	$(Y_d)_{ij}$	$(Y_e)_{ji}$	$(Y_{ql})_{ij}$	$(Y_{ud})_{ij}$				
$H_{24} \mathcal{T}_i$	$\mathcal{F}_j \bar{H}_5$	$\mathbf{10}$	1	:	6	:	1	:	-4	
$H_{24} \mathcal{F}_j$	$\mathcal{T}_i \bar{H}_5$	$\bar{\mathbf{5}}$	1	:	$-\frac{3}{2}$:	$-\frac{3}{2}$:	1	
Dimension six operators										
AB	C	DE	$R_1 R_2$	$(Y_d)_{ij}$	$(Y_e)_{ji}$	$(Y_{ql})_{ij}$	$(Y_{ud})_{ij}$			
$H_{24} \bar{H}_5$	\mathcal{T}_i	$H_{24} \mathcal{F}_j$	$\mathbf{45} \mathbf{45}$	1	:	$-\frac{1}{2}$:	1	:	$\frac{2}{3}$

Figure 9.6: Supergraphs generating Yukawa couplings upon integrating out messengers fields in representation R_i, \bar{R}_i , used in our models. See [4, 158] for an exhaustive list and discussion.

where the structure of Y_u can be read off from eq. (9.81).

When the heavy Higgs triplets are integrated out the baryon number violating effective operators (5.86) emerge

$$\mathcal{W}_{\mathcal{B}} = \frac{Y_{qq_{ij}} Y_{ql_{kl}}}{M_T^{\dim=5}} (Q_i \cdot Q_j) (Q_k \cdot L_l) + \frac{Y_{ud_{ij}} Y_{ue_{kl}}}{M_T^{\dim=5}} U_i^c D_j^c U_k^c E_l^c, \quad (9.100)$$

which are denoted $LLLL$ and $RRRR$ operators, respectively. Note that due to the total anti-symmetry of the $SU(3)_C$ indices the dimension five operators need to be non-diagonal in flavour space [139]. In order to predict the proton decay rate, the RGE evolution to the SUSY scale has to be calculated, where these operators need to be “dressed” by MSSM sparticles to dimension six operators, as shown e.g. in figure 5.5. These sparticles are then integrated out to form dimension six operators, which finally are evolved to the energy scale of the proton, see e.g. [82] and references therein. Such an extensive study, which i.e. would ultimately require to explicitly construct predictions for sparticle masses and mixings, goes beyond the scope of this thesis.

Let us now turn to a qualitative discussion of dimension five proton decay in the considered class of models. Firstly, note that due to the predicted flavour structure of our models and especially for the model 9.4.1 which features diagonal Y_{ql} and Y_{ud} in flavour space, one can expect that decay channels which require a flavour transition in these matrices are suppressed. Thus, combining the DMPM with our setup of CG factors, messenger fields, and shaping symmetries is more predictive than conventional GUT models, since it

allows to determine the specific flavour structure of all Yukawa matrices relevant for proton decay. Note that due to the shaping symmetry, both of our models guarantee the absence of Yukawa matrix entries from other DMPM messengers' triplet components, which would lead to a lower $M_T^{\text{dim}=5}$. This is, of course, model dependent and has to be checked for any specific model.

Also, by introducing a second adjoint into the DMPM, we have seen that the effective triplet mass $M_T^{\text{dim}=5}$ can become conveniently heavy, while keeping the GUT breaking superpotential renormalisable and thus maintaining predictability for CG factors. With a SUSY scale of one TeV superpotential (b) yields an effective triplet mass of roughly $5 \cdot 10^{16}$ GeV, which raises higher with increasing M_{SUSY} . And as can be seen in figure 9.3, for superpotential (a) there is a broad region of parameter space where the effective triplet mass can be easily above 10^{18} GeV.

Finally, let us comment on the SUSY dressing of the $LLLL$ and $RRRR$ operators. Because gluino and neutralino dressings are flavour diagonal⁷, the dominant diagrams are due to chargino exchange [140, 142], where wino and Higgsino dressings are related to the $LLLL$ and $RRRR$ operators, respectively, as illustrated for the example diagrams in figure 5.5. Then, the Wilson coefficient for the effective dimension six operator due to wino exchange contains the gauge coupling g^2 , whereas the Wilson coefficient for Higgsino exchange contains additional Yukawa couplings. Thus, the contribution of the $RRRR$ operator is enhanced by $\tan^2 \beta$ (for large values of $\tan \beta$) [191], thereby posing a challenge for many GUT models relying on $\tan \beta \approx 50$. Compared to such models, our setup with $\frac{y_\tau}{y_b} = -\frac{3}{2}$ requires only moderate $\tan \beta \approx 30$ and thus the $RRRR$ operator is relatively suppressed by a factor of roughly three.

Therefore, in total we expect the proton decay rate to be sufficiently small, but possibly in the reach of the next generation of proton decay experiments, due to the very large effective triplet mass in the DMPM and predictive Yukawa coupling matrix structures.

Let us now turn to a discussion of dimension six proton decay operators, which appear also in non-SUSY GUTs. First, we discuss the dimension six proton decay mediated by colour triplets, which originates from the Kähler potential (9.37)

$$K_T = T_a T_a^* + \bar{T}_a \bar{T}_a^* . \quad (9.101)$$

When the colour triplets are integrated out of the superpotential (9.93), they also have to be integrated out of the Kähler potential, yielding dimension six baryon number violating Kähler operators

$$K_{\mathcal{B}} = -\frac{Y_{qqij} Y_{uemn}^*}{(M_T^{\text{dim}=6})^2} Q_i Q_j U_m^{c*} E_n^{c*} - \frac{Y_{qlij} Y_{udmn}^*}{(M_T^{\text{dim}=6})^2} Q_i L_j U_m^{c*} D_n^{c*} + h.c. . \quad (9.102)$$

Again, these operators have to be evolved from the GUT scale to the energy scale of the proton mass. Proton decay is suppressed by high enough effective triplet masses $M_T^{\text{dim}=6}$

⁷Note that for degenerate squark masses of the first two generations, as is typical in many SUSY scenarios, the diagrams with gluino dressing approximately cancel each other due to a Fierz identity [139].

and $M_{\bar{T}}^{\text{dim}=6}$. Since in terms of superfield components the dimension six operators are effective four fermion operators, there is no need for a sparticle dressing. Therefore, the resulting proton decay rates are independent of the details of the SUSY spectrum.

We close this chapter by commenting on dimension six proton decay due to heavy X and Y gauge boson exchange, which due to the higher unification scale in SUSY GUTs are considered to be less dangerous [145]. The gauge sector of our $SU(5)$ model is exactly the same as in minimal $SU(5)$, therefore the proton life time can be estimated by (4.30)

$$\Gamma_p \approx \alpha_u^2 \frac{m_p^5}{M_{\text{GUT}}^4}, \quad (9.103)$$

neglecting effects due to RGE evolution and order one coefficients due to nuclear matrix elements. Since the GUT scale can be easily above 10^{16} GeV and $\sqrt{\alpha_u} \approx \frac{1}{5}$, the proton decay rate from dimension six operators is sufficiently small, but possibly in the reach of the next generation of proton decay experiments.

PART V

Supersymmetric threshold corrections

CHAPTER 10

Predicting the Sparticle Spectrum from GUTs via SUSY threshold corrections with SusyTC

In the final chapter of this thesis, we close the last edge of the triangle in figure 1.2 and discuss supersymmetric one-loop threshold corrections. In part III of this thesis we discussed how GUTs can feature predictions for quark-lepton Yukawa coupling ratios and for relations between quark and lepton mixing angles. Whether a flavour GUT model can successfully explain the observations in the flavour sector, depends on the RGE evolution of the Yukawa matrices from the GUT scale to lower energies. In supersymmetric theories, when the MSSM is matched to the SM, $\tan\beta$ -enhanced supersymmetric threshold corrections [131, 132] are essential in the investigation of quark-lepton relations and thus link a given GUT flavour model to the sparticle spectrum.

Two predictive flavour GUT models were presented in chapters 7 and 8. Here we present our software tool `SusyTC`, which was introduced as extension to the Mathematica package `REAP` [163] in [5], where we calculated the one-loop SUSY threshold corrections for the full down-type quark, up-type quark, and charged lepton Yukawa coupling matrices in the electroweak unbroken phase.

10.1 The REAP extension `SusyTC`

In our SUSY flavour GUT models in part III, we constructed the GUT scale predictions $y_e = -\frac{1}{2}y_d$, $y_\mu = 6y_s$, and $y_\tau = -\frac{3}{2}y_b$.¹ Other promising quark-lepton mass ratios at the GUT scale have been discussed in [83, 92, 93], e.g. $y_\mu = \frac{9}{2}y_s$, see the discussion in 4.4. Moreover, many GUT models feature $b - \tau$ or $b - \tau - t$ unification (for early work see e.g. [138, 141, 192]), or the Georgi-Jarlskog relations (4.28) [87] as predictions.

¹Although Y_d and Y_e are non-diagonal in (7.10) and (8.11), these GUT scale relations are approximately satisfied after the Yukawa matrices are diagonalised. This can also be seen from a small angle approximation (6.26).

As mentioned in 5.4 and above, in supersymmetric GUT models the SUSY threshold corrections can have an important influence on the Yukawa coupling ratios. When the MSSM is matched to the SM, integrating out the sparticles at loop-level leads to the emergence of effective operators, which can contribute sizeably to the Yukawa couplings, depending on the values of the sparticle masses, $\tan\beta$, and the soft-breaking trilinear couplings. Thereby, via the SUSY threshold corrections, a given set of GUT predictions for the ratios $\frac{y_\tau}{y_b}$, $\frac{y_\mu}{y_s}$, and $\frac{y_e}{y_d}$ imposes important constraints on the SUSY spectrum.

With the discovery of the Higgs boson at the LHC [193] and the possible discovery of sparticles in the near future, the question whether a set of SUSY soft-breaking parameters can be in agreement with both, specific SUSY threshold corrections as required for realising the flavour structure of a GUT model, and constraints from the Higgs boson mass and results on the sparticle spectrum, gains importance. To accurately study this question, we introduced the new software tool **SusyTC** as a major extension to **REAP** [163].

REAP, which is designed to run Yukawa matrices and neutrino parameters in (SUSY) seesaw scenarios with a proper treatment of the right-handed neutrino thresholds, is a convenient tool for top-down analyses of flavour (GUT) models, with the advantage of an user-friendly Wolfram Mathematica front-end. However, the SUSY soft-breaking sector is not included. In the analysis of our SUSY flavour GUT models in part III, we therefore had to incorporate the effect of SUSY threshold corrections as mere model parameters at an user-defined ‘‘SUSY’’ scale in a simplified treatment assuming, e.g., degenerate first and second generation sparticle masses, without specialising any details on the SUSY sector. Although this procedure is quite SUSY model-independent, it only allows to study the constraints on the SUSY sector indirectly (i.e. via the introduced additional parameters and with simplifying assumptions), and it is unclear whether an explicit SUSY scenario with these assumptions and requirements can be realised. Let us remark here that the latest version of **REAP** has implemented such a treatment of SUSY threshold corrections as additional model parameters.

In this chapter however, we want to make full use of the SUSY threshold corrections to gain information on the SUSY flavour structure from GUTs. We have thus extended and generalised various formulae in the literature which are needed for a precision analysis of SUSY flavour GUT models and implemented them in our software tool **SusyTC**. It includes the full (i.e. CP violating) MSSM sector, a computation of the sparticle masses, and a careful calculation of the one-loop SUSY threshold corrections for the full Yukawa coupling matrices in the electroweak-unbroken phase. The matching of the MSSM to the SM, including $\overline{\text{DR}}$ to $\overline{\text{MS}}$ conversion, is then automatically performed at the SUSY scale. For a further processing of its results by external software, e.g. for performing a two-loop Higgs mass calculation, **SusyTC** also calculates the one-loop corrected $\overline{\text{DR}}$ value of μ , the one-loop corrected pole mass of the charged (or the CP-odd) Higgs boson and provides output in SLHA conventions as *Les Houches* file [123, 194].

We have developed **SusyTC** specifically to perform top-down analyses of SUSY flavour GUT models. This is a major difference to other well-known SUSY spectrum generators (e.g. [195–198], see e.g. [199] for a comparison), which run experimental constraints from

low energies to high energies, apply GUT scale boundary conditions, run back to low energies and repeat this procedure iteratively. SusyTC instead starts directly from GUT scale input, which can be defined as general (complex) Yukawa, trilinear, and soft-breaking mass matrices, as well as non-universal gaugino masses and $m_{h_u}^2$ and $m_{h_d}^2$. The RGEs for these parameters are solved to obtain their values at low energies, thereby enabling an investigation whether the GUT scale Yukawa matrix structures of a given SUSY flavour GUT model are in agreement with experimental data.

10.2 SUSY threshold corrections & numerical procedure

We now present the numerical procedure and the formulae for the SUSY threshold corrections. Note that in this chapter we follow the notation of REAP [163] (see also [105]) and use an RL convention for the Yukawa matrices. These differ from the SLHA conventions [123] used in the previous chapters. They can easily be translated by

$$\begin{array}{c} \text{REAP \& SusyTC} \\ \text{SLHA} \end{array} \left| \begin{array}{ccccccccc} Y_u & Y_d & Y_e & T_u & T_d & T_e & m_u^2 & m_d^2 & m_e^2 \\ Y_u^T & Y_d^T & Y_e^T & T_u^T & T_d^T & T_e^T & (m_u^2)^T & (m_d^2)^T & (m_e^2)^T \end{array} \right.$$

Thus the MSSM superpotential extended by a type-I seesaw mechanism is given by

$$\begin{aligned} \mathcal{W}_{\text{MSSM}} = & Y_{e_{ij}} E_i^c H_d \cdot L_j + Y_{\nu_{ij}} N_i^c H_u \cdot L_j \\ & + Y_{d_{ij}} D_i^c H_d \cdot Q_j - Y_{u_{ij}} U_i^c H_u \cdot Q_j + \frac{1}{2} M_{n_{ij}} N_i^c N_j^c + \mu H_u \cdot H_d, \end{aligned} \quad (10.1)$$

and the soft-breaking Lagrange density by

$$\begin{aligned} -\mathcal{L}_{\text{soft}} = & \frac{1}{2} M_a \lambda^a \lambda^a + c.c. \\ & + T_{e_{ij}} \tilde{e}_{R_i}^* h_d \cdot \tilde{L}_j + T_{\nu_{ij}} \tilde{\nu}_{R_i}^* h_u \cdot \tilde{L}_j + T_{d_{ij}} \tilde{d}_{R_i}^* h_d \cdot \tilde{Q}_j - T_{u_{ij}} \tilde{u}_{R_i}^* h_u \cdot \tilde{Q}_j + c.c. \\ & + \tilde{Q}_i^\dagger m_{\tilde{Q}_{ij}}^2 \tilde{Q}_j + \tilde{L}_i^\dagger m_{\tilde{L}_{ij}}^2 \tilde{L}_j + \tilde{u}_{R_i}^* m_{\tilde{u}_{ij}}^2 \tilde{u}_{R_j} + \tilde{d}_{R_i}^* m_{\tilde{d}_{ij}}^2 \tilde{d}_{R_j} + \tilde{e}_{R_i}^* m_{\tilde{e}_{ij}}^2 \tilde{e}_{R_j} + \tilde{\nu}_{R_i}^* m_{\tilde{\nu}_{ij}}^2 \tilde{\nu}_{R_j} \\ & + m_{h_u}^2 |h_u|^2 + m_{h_d}^2 |h_d|^2 + (m_3^2 h_u \cdot h_d + c.c.). \end{aligned} \quad (10.2)$$

Since REAP includes the RGEs in the type-I seesaw extension of the MSSM (with the $\overline{\text{DR}}$ two-loop β -functions for the MSSM Yukawa matrices and the neutrino mass operator given in [105]), we have calculated the $\overline{\text{DR}}$ two-loop β -functions of the gaugino mass parameters M_a , the trilinear couplings T_f , the sfermion squared mass matrices m_f^2 , and of the soft-breaking Higgs mass parameters $m_{h_u}^2$ and $m_{h_d}^2$ in the presence of Y_ν , M_n , and m_ν^2 , using the general formulae of [136]. We list these β -functions in appendix E.

SusyTC calculates the SUSY scale

$$Q = \sqrt{m_{\tilde{t}_1} m_{\tilde{t}_2}}, \quad (10.3)$$

where the stop masses are defined by the up-type squark mass eigenstates \tilde{u}_i with the largest mixing to \tilde{t}_1 and \tilde{t}_2 .² The Yukawa matrices and soft-breaking parameters are then evolved from the GUT scale to the SUSY scale and **REAP** automatically integrates out the right-handed neutrinos at their respective mass scales in doing so. Note that we assume the mass of the right-handed neutrinos to be much larger than the SUSY scale Q . **REAP** also features the possibility to add one-loop right-handed neutrino thresholds for the SM parameters, following [200].

At the SUSY scale Q , **SusyTC** then calculates the tree-level sparticle masses, mixings and the SUSY threshold corrections. These can be subdivided into two classes: Firstly there are $\tan\beta$ -enhanced threshold corrections, which arise for Y_d and Y_e since at the one-loop level down-type quarks and charged leptons couple to h_u via exchange of sparticles, as shown in figure 10.1. These are the most relevant contributions to the corrections of the quark-lepton Yukawa coupling ratios. The corresponding threshold effects to Y_u , arising from effective couplings to h_d , are $\tan\beta$ -suppressed. The second class of threshold corrections emerges from the supersymmetric loops shown in figure 10.2. While some of them are strongly suppressed, others are proportional to the soft SUSY-breaking trilinear couplings and can become important in some cases. A third class of threshold corrections, due to wave-function renormalisation of the external fields, will be implemented into a future version of **SusyTC**. Given the precision of our numerical analysis in 10.4, their additional contribution can be neglected at present.

Considering heavy sparticles and large $Q \gtrsim \text{TeV}$, **SusyTC** calculates the SUSY threshold corrections in the electroweak unbroken phase. There are in total twelve types of loop diagrams, which are shown in figures 10.1 and 10.2 for Y_d . In the basis of diagonal squark masses the SUSY threshold corrections for Y_d are (in terms of $\overline{\text{DR}}$ quantities) given by

$$\begin{aligned} \tilde{Y}_{d_{ij}}^{\text{SM}} &= \tilde{Y}_{d_{ij}}^{\text{MSSM}} \cos\beta \left(1 + \frac{1}{16\pi^2} \tan\beta (\eta_{ij}^G + \eta_{ij}^W + \eta_{ij}^B + \eta_{ij}^T) + \frac{1}{16\pi^2} (\epsilon_{ij}^W + \epsilon_{ij}^B + \epsilon_{ij}^T) \right) \\ &+ \tilde{T}_{d_{ij}}^{\text{MSSM}} \cos\beta \frac{1}{16\pi^2} (\zeta_{ij}^G + \zeta_{ij}^B), \end{aligned} \quad (10.4)$$

where

$$\begin{aligned} \eta_{ij}^G &= -\frac{8}{3} g_3^2 \frac{\mu^*}{M_3} H_2 \left(\frac{m_{\tilde{d}_i}^2}{M_3^2}, \frac{m_{\tilde{Q}_j}^2}{M_3^2} \right), \\ \eta_{ij}^W &= \frac{3}{2} g_2^2 \frac{M_2^*}{\mu} H_2 \left(\frac{M_2^2}{\mu^2}, \frac{m_{\tilde{Q}_j}^2}{\mu^2} \right), \\ \eta_{ij}^B &= \frac{3}{5} g_1^2 \left(\frac{1}{9} \frac{\mu^*}{M_1} H_2 \left(\frac{m_{\tilde{d}_i}^2}{M_1^2}, \frac{m_{\tilde{Q}_j}^2}{M_1^2} \right) + \frac{1}{3} \frac{M_1^*}{\mu} H_2 \left(\frac{m_{\tilde{d}_i}^2}{\mu^2}, \frac{M_1^2}{\mu^2} \right) + \frac{1}{6} \frac{M_1^*}{\mu} H_2 \left(\frac{M_1^2}{\mu^2}, \frac{m_{\tilde{Q}_j}^2}{\mu^2} \right) \right), \end{aligned}$$

²**SusyTC** can also be set to use the convention $Q = \sqrt{m_{\tilde{u}_1} m_{\tilde{u}_6}}$ or an user-defined fixed value for the SUSY scale, as described in appendix G.

$$\eta_{ij}^T = -\frac{1}{\mu \tilde{Y}_{d_{ij}}} \sum_{n,m} \tilde{Y}_{d_{im}} \tilde{T}_{u_{mn}}^\dagger \tilde{Y}_{u_{nj}} H_2 \left(\frac{m_{\tilde{u}_n}^2}{\mu^2}, \frac{m_{\tilde{Q}_m}^2}{\mu^2} \right), \quad (10.5)$$

correspond to the $\tan \beta$ -enhanced loops of Figure 10.1, and

$$\begin{aligned} \epsilon_{ij}^W &= 12g_2^2 C_{00} \left(\frac{\mu^2}{Q^2}, \frac{M_2^2}{\mu^2}, \frac{m_{\tilde{Q}_j}^2}{\mu^2} \right), \\ \epsilon_{ij}^B &= \frac{3}{5}g_1^2 \left(\frac{4}{3}C_{00} \left(\frac{\mu^2}{Q^2}, \frac{M_1^2}{\mu^2}, \frac{m_{\tilde{d}_i}^2}{\mu^2} \right) + \frac{2}{3}C_{00} \left(\frac{\mu^2}{Q^2}, \frac{M_1^2}{\mu^2}, \frac{m_{\tilde{Q}_j}^2}{\mu^2} \right) \right), \\ \epsilon_{ij}^T &= \frac{1}{\tilde{Y}_{d_{ij}}} \sum_{n,m} \tilde{Y}_{d_{im}} \tilde{Y}_{u_{mn}}^\dagger \tilde{Y}_{u_{nj}} H_2 \left(\frac{m_{\tilde{u}_n}^2}{\mu^2}, \frac{m_{\tilde{Q}_m}^2}{\mu^2} \right), \\ \zeta_{ij}^G &= \frac{8}{3}g_2^2 \frac{1}{M_3} H_2 \left(\frac{m_{\tilde{d}_i}^2}{M_3^2}, \frac{m_{\tilde{Q}_j}^2}{M_3^2} \right), \\ \zeta_{ij}^B &= -\frac{3}{5}g_1^2 \frac{1}{9} \frac{1}{M_1} H_2 \left(\frac{m_{\tilde{d}_i}^2}{M_1^2}, \frac{m_{\tilde{Q}_j}^2}{M_1^2} \right), \end{aligned} \quad (10.6)$$

correspond to the loops in Figure 10.2, respectively, where the contributions ζ_{ij}^G and ζ_{ij}^B can become important in cases of small $\tan \beta$ and large trilinear couplings. The loop functions H_2 and C_{00} are defined as

$$H_2(x, y) \equiv \frac{x \log(x)}{(1-x)(x-y)} + \frac{y \log(y)}{(1-y)(y-x)}, \quad (10.7)$$

$$C_{00}(q, x, y) \equiv \frac{1}{4} \left(\frac{3}{2} - \log(q) + \frac{x^2 \log(x)}{(1-x)(x-y)} + \frac{y^2 \log(y)}{(1-y)(y-x)} \right). \quad (10.8)$$

\tilde{Y} , \tilde{T} are the Yukawa and trilinear coupling matrices rotated into the basis where the squark mass matrices are diagonal, using the transformations

$$\begin{aligned} m_{\tilde{Q}}^2 &= \tilde{W}_{\tilde{Q}} m_{\tilde{Q}}^2 \text{diag} \tilde{W}_{\tilde{Q}}^\dagger, \\ m_{\tilde{u}}^2 &= \tilde{W}_{\tilde{u}} m_{\tilde{u}}^2 \text{diag} \tilde{W}_{\tilde{u}}^\dagger, \\ Y_u &= \tilde{W}_{\tilde{u}} \tilde{Y}_u \tilde{W}_{\tilde{Q}}^\dagger, \\ T_u &= \tilde{W}_{\tilde{u}} \tilde{T}_u \tilde{W}_{\tilde{Q}}^\dagger, \end{aligned} \quad (10.9)$$

and analogously for down-type (s)quarks and charged (s)leptons.

The SUSY threshold corrections to Y_e are given by

$$\begin{aligned} \tilde{Y}_{e_{ij}}^{\text{SM}} &= \tilde{Y}_{e_{ij}}^{\text{MSSM}} \cos \beta \left(1 + \frac{1}{16\pi^2} \tan \beta (\tau_{ij}^W + \tau_{ij}^B) + \frac{1}{16\pi^2} (\delta_{ij}^W + \delta_{ij}^B) \right) \\ &+ \tilde{T}_{e_{ij}}^{\text{MSSM}} \cos \beta \frac{1}{16\pi^2} \xi_{ij}^B, \end{aligned} \quad (10.10)$$

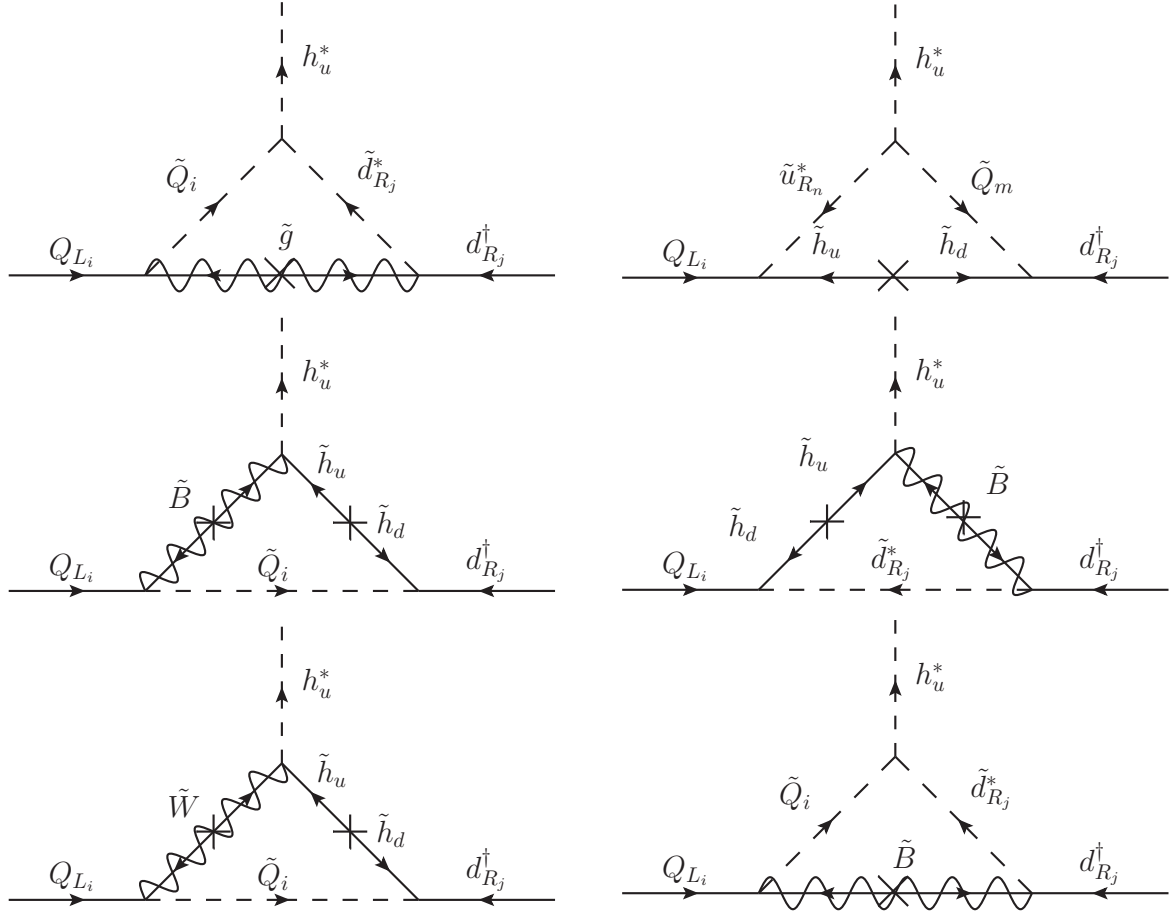


Figure 10.1: $\tan \beta$ - enhanced SUSY threshold corrections to Y_d .

with the $\tan \beta$ -enhanced contributions

$$\begin{aligned} \tau_{ij}^W &= \frac{3}{2} g_2^2 \frac{M_2^*}{\mu} H_2 \left(\frac{M_2^2}{\mu^2}, \frac{m_{\tilde{L}_j}^2}{\mu^2} \right), \\ \tau_{ij}^B &= \frac{3}{5} g_1^2 \left(-\frac{\mu^*}{M_1} H_2 \left(\frac{m_{\tilde{e}_i}^2}{M_1^2}, \frac{m_{\tilde{L}_j}^2}{M_1^2} \right) + \frac{M_1^*}{\mu} H_2 \left(\frac{m_{\tilde{e}_i}^2}{\mu^2}, \frac{M_1^2}{\mu^2} \right) - \frac{1}{2} \frac{M_1^*}{\mu} H_2 \left(\frac{M_1^2}{\mu^2}, \frac{m_{\tilde{L}_j}^2}{\mu^2} \right) \right), \end{aligned} \quad (10.11)$$

and

$$\begin{aligned} \delta_{ij}^W &= 12 g_2^2 C_{00} \left(\frac{\mu^2}{Q^2}, \frac{M_2^2}{\mu^2}, \frac{m_{\tilde{L}_j}^2}{\mu^2} \right), \\ \delta_{ij}^B &= \frac{3}{5} g_1^2 \left(-2 C_{00} \left(\frac{\mu^2}{Q^2}, \frac{M_1^2}{\mu^2}, \frac{m_{\tilde{L}_j}^2}{\mu^2} \right) + 4 C_{00} \left(\frac{\mu^2}{Q^2}, \frac{M_1^2}{\mu^2}, \frac{m_{\tilde{e}_i}^2}{\mu^2} \right) \right), \end{aligned}$$

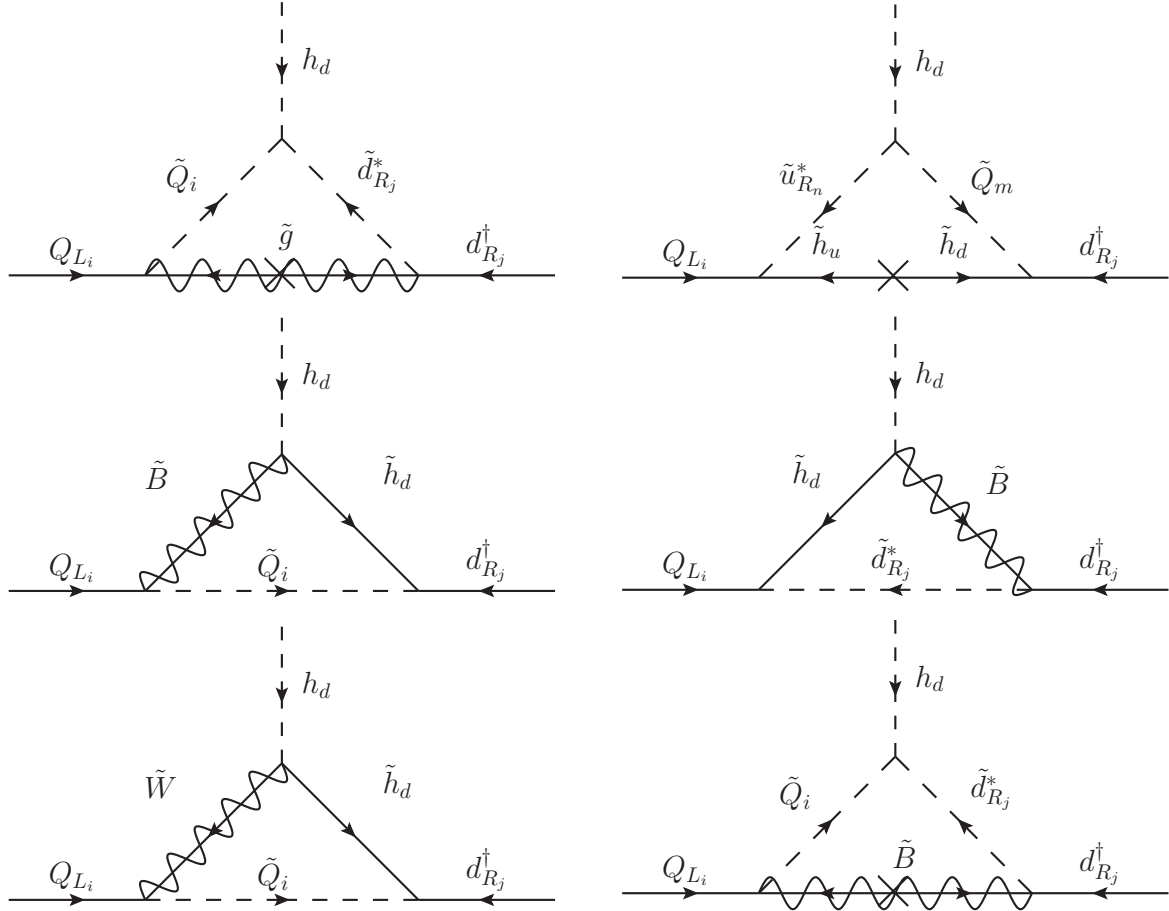


Figure 10.2: None $\tan\beta$ - enhanced SUSY threshold corrections to Y_d .

$$\xi_{ij}^B = \frac{3}{5} g_1^2 \frac{1}{M_1} H_2 \left(\frac{m_{\tilde{e}_i}^2}{M_1^2}, \frac{m_{\tilde{L}_j}^2}{M_1^2} \right). \quad (10.12)$$

The diagrams for the Y_e SUSY threshold corrections are analogous to the ones in figures 10.1 and 10.2, with the exception that the loop diagrams shown in the top rows do not exist.

Turning to Y_u , the types of diagrams which were $\tan\beta$ -enhanced for Y_d and Y_e are now $\tan\beta$ -suppressed. However, there also exist SUSY threshold corrections which are independent of $\tan\beta$ and enhanced by large trilinear couplings. These SUSY threshold corrections to Y_u could have important effects. For example the SUSY threshold corrections to the top Yukawa coupling y_t can be of significance in analyses of the Higgs mass and vacuum stability. The expression for the Y_u SUSY threshold corrections can be readily obtained from the SUSY threshold corrections to Y_d (10.4)–(10.6) by the replacement

$$\begin{aligned} d &\rightarrow u, \\ \cos\beta &\rightarrow \sin\beta, \end{aligned} \quad (10.13)$$

with the exception of the bino-loops, whose contribution become

$$\begin{aligned}
\eta_{ij}^B &= \frac{3}{5} g_1^2 \left(-\frac{2}{9} \frac{\mu^*}{M_1} H_2 \left(\frac{m_{d_i}^2}{M_1^2}, \frac{m_{Q_j}^2}{M_1^2} \right) + \frac{2}{3} \frac{M_1^*}{\mu} H_2 \left(\frac{m_{u_i}^2}{\mu^2}, \frac{M_1^2}{\mu^2} \right) - \frac{1}{6} \frac{M_1^*}{\mu} H_2 \left(\frac{M_1^2}{\mu^2}, \frac{m_{Q_j}^2}{\mu^2} \right) \right), \\
\epsilon_{ij}^B &= \frac{3}{5} g_1^2 \left(\frac{8}{3} C_{00} \left(\frac{\mu^2}{Q^2}, \frac{M_1^2}{\mu^2}, \frac{m_{u_i}^2}{\mu^2} \right) - \frac{2}{3} C_{00} \left(\frac{\mu^2}{Q^2}, \frac{M_1^2}{\mu^2}, \frac{m_{Q_j}^2}{\mu^2} \right) \right), \\
\zeta_{ij}^B &= \frac{3}{5} g_1^2 \frac{2}{9} \frac{1}{M_1} H_2 \left(\frac{m_{u_i}^2}{M_1^2}, \frac{m_{Q_j}^2}{M_1^2} \right), \tag{10.14}
\end{aligned}$$

due to the different $U(1)_Y$ hypercharges of the (s)particles in the loop. The loop diagrams are identical to the ones of Figure 10.1 and 10.2, with u exchanged by d .

After the SUSY threshold corrections are calculated in the $\overline{\text{DR}}$ scheme, REAP converts the Yukawa and gauge couplings to the $\overline{\text{MS}}$ scheme following [194].

Finally SusyTC calculates the values of $|\mu|$ and m_3 from $m_{h_u}^2$, $m_{h_d}^2$, $\tan \beta$, and M_Z by requiring the existence of spontaneously broken EW vacuum, analogously to the discussion in 5.4. This is equivalent to vanishing tadpole coefficients, and we employ the one-loop tadpole equations of h_u and h_d to obtain the one-loop corrected $\overline{\text{DR}}$ expressions of (5.69)

$$\mu = e^{i\phi_\mu} \sqrt{\frac{1}{2} (\tan(2\beta) (\bar{m}_{h_u}^2 \tan \beta - \bar{m}_{h_d}^2 \cot \beta) - M_Z^2 - \text{Re}(\Pi_{ZZ}^T(M_Z^2)))}, \tag{10.15}$$

with $\bar{m}_{h_u}^2 \equiv m_{h_u}^2 - t_u$ and $\bar{m}_{h_d}^2 \equiv m_{h_d}^2 - t_d$. In the real (CP conserving) MSSM the phase ϕ_μ is restricted to 0 and π . The expressions for the one-loop tadpoles t_u , t_d , and the transverse Z-boson self energy Π_{ZZ}^T are based on [201], but extended to include inter-generational mixing, and presented in appendix F. Because μ enters the one-loop formulae for the threshold corrections, treating t_u , t_d , and Π_{ZZ}^T as functions of tree-level parameters is sufficiently accurate. The one-loop expression of the SUSY soft-breaking mass m_3 is calculated as

$$m_3 = \sqrt{\frac{1}{2} (\tan(2\beta) (\bar{m}_{h_u}^2 - \bar{m}_{h_d}^2) - (M_Z^2 + \text{Re}(\Pi_{ZZ}^T(M_Z^2))) \sin(2\beta))}. \tag{10.16}$$

If desired, SusyTC allows to outsource a two-loop Higgs mass calculation to external software, e.g. FeynHiggs [127–129], by calculating the one-loop corrected pole mass m_{H^+} (m_A) as input for the complex (real) MSSM

$$\begin{aligned}
m_{H^+}^2 &= \frac{1}{\cos(2\beta)} \left(\bar{m}_{h_u}^2 - \bar{m}_{h_d}^2 - M_Z^2 - \text{Re}(\Pi_{ZZ}^T(M_Z^2)) + \hat{M}_W^2 \right. \\
&\quad \left. - \text{Re}(\Pi_{H^+H^-}(m_{H^+})) + t_d \sin^2 \beta + t_u \cos^2 \beta \right), \tag{10.17} \\
m_A^2 &= \frac{1}{\cos(2\beta)} \left(\bar{m}_{h_u}^2 - \bar{m}_{h_d}^2 - M_Z^2 - \text{Re}(\Pi_{ZZ}^T(M_Z^2)) \right)
\end{aligned}$$

$$\text{Re}(\Pi_{AA}(m_A) + t_d \sin^2 \beta + t_u \cos^2 \beta) , \quad (10.18)$$

where \hat{M}_W is the $\overline{\text{DR}}$ W-boson mass given as

$$\hat{M}_W^2(Q) = M_W^2 + \text{Re}(\Pi_{WW}^T(M_W^2)) = g_2^2 \frac{\hat{v}(Q)}{2} , \quad (10.19)$$

with M_Z and M_W pole masses and the $\overline{\text{DR}}$ vacuum expectation value $\hat{v}(Q)$ given by

$$\hat{v}^2(Q) = 4 \frac{M_Z^2 + \text{Re}(\Pi_{ZZ}^T(M_Z^2))}{\frac{3}{5}g_1^2(Q) + g_2^2(Q)} . \quad (10.20)$$

As in the previous formulae, the self energies $\Pi_{H^+H^-}$ and Π_{AA} are based on [201], but are extended to include inter-generational mixing and understood as functions of tree-level parameters. They are given in appendix F.

10.3 A brief introduction to SusyTC

In this section we provide a ‘‘Getting Started’’ calculation for SusyTC. A full documentation of all features is included in appendix G. Since SusyTC is an extension to REAP, an up-to-date version of REAP-MPT [163] (available at <http://reapmpt.hepforge.org>) needs to be installed on your system. SusyTC consists out of the REAP model file `RGEMSSMsoftbroken.m`, which is based on the model file `RGEMSSM.m` of REAP 1.11.2 and additionally contains, among other things, the RGEs of the MSSM soft-breaking parameters and the matching to the SM, and the file `SusyTC.m`, which includes the formulae for the sparticle spectrum and SUSY threshold correction calculations. Both files can be downloaded from <http://particlesandcosmology.unibas.ch/pages/SusyTC.htm> and have to be copied into the local REAP directory.

To begin a calculation with SusyTC, one first needs to import `RGEMSSMsoftbroken.m`:

```
Needs["REAP'RGEMSSMsoftbroken'"];
```

The model `MSSMsoftbroken` is then defined by `RGEAdd`, including additional options such as `RGEtanβ`:

```
RGEAdd["MSSMsoftbroken",RGEtanβ → 30];
```

In `MSSMsoftbroken` all REAP options of the model MSSM are available. The options additionally available in SusyTC are given in appendix G. The input is given by `RGESetInitial`. Let us illustrate some features of SusyTC: To test for example the GUT scale prediction for the Yukawa coupling ratio $\frac{y_\mu}{y_s} = 6$, considering a given example parameter point in the Constrained MSSM, one can type:

```

RGESetInitial[2·1016,
  RGEYd → DiagonalMatrix[{1.2·10-3, 2.2·10-3, 0.16}],
  RGEYe → DiagonalMatrix[{1.2·10-3, 6.2·2·10-3, 0.16}],
  RGE $m_{12}$  → 2000, RGE $A_0$  → 1000, RGE $m_0$  → 2500];

```

Of course, any general matrices can be used as input for the Yukawa, trilinear, and soft-breaking matrices, as given by the specific SUSY flavour GUT model under consideration. Also, non-universal gaugino masses, $m_{\tilde{h}_u}^2$, and $m_{\tilde{h}_d}^2$ can be specified. The RGEs are then solved from the GUT scale to the Z-boson mass scale by

```

RGESolve[91, 2·1016];

```

The ratio of the μ and strange quark Yukawa couplings at the Z-boson mass scale can now be obtained with `RGEGetSolution`, `CKMParameters`, and `MNSParameters`:

```

Yu = RGEGetSolution[91, RGEYu];
Yd = RGEGetSolution[91, RGEYd];
Ye = RGEGetSolution[91, RGEYe];
M $\nu$  = RGEGetSolution[91, RGE $m_{\nu}$ ];
MNSParameters[M $\nu$ , Ye][[3, 2]]/CKMParameters[Yu, Yd][[3, 2]]

```

Repeating this calculation with all $SU(5)$ CG factors listed in table 2 of [83] and (4.45), one obtains the results shown in figure 10.3.

As described in appendix G, `SusyTC` can also read and write *Les Houches* files [123,194] as input and output.

10.4 The Sparticle Spectrum predicted from CG factors

In this section we apply `SusyTC` to investigate the constraints on the sparticle spectrum which arise from a set of GUT scale predictions for the quark-lepton Yukawa coupling ratios when assuming Constrained MSSM boundary conditions for the GUT scale SUSY soft-breaking parameters.

10.4.1 General discussion

Before performing the numerical analysis for a specific example, let us first outline the connection between the SUSY spectrum and GUT scale Yukawa coupling predictions in a mostly model-independent discussion, with the only assumption of universal SUSY soft-breaking parameters. This assumption might be relaxed in realistic models, however it can be highly motivated in certain SUSY flavour GUT models. The unification of MSSM superfields into joint GUT or flavour symmetry representations for example predicts universal

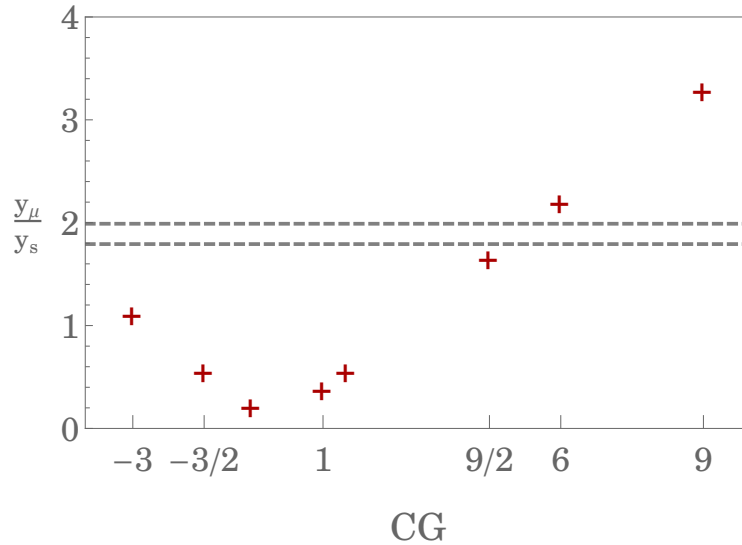


Figure 10.3: Example results for $\frac{y_\mu}{y_s}$ at the electroweak scale, considering the $SU(5)$ CG factors from (4.45), i.e. the GUT scale predictions $\frac{y_\mu}{y_s} = \text{CG}$, for a given example Constrained MSSM parameter point with $\tan\beta = 30$, $m_{1/2} = 2000$ GeV, $A_0 = 1000$ GeV, and $m_0 = 2500$ GeV. The area between the dashed gray lines corresponds to the experimental one sigma range [91].

soft-breaking mass matrices for all superfields in the respective multiplets.³ The absence of deviation from SM predictions for flavour physics observables is a phenomenological hint towards approximately flavour-universal soft-breaking parameters. Finally let us remark that specific SUSY breaking mechanisms can indeed predict universal soft-breaking parameters.

Then, the origin for predictions and constraints on the SUSY spectrum arises from the fact that to our knowledge there exists no viable combination of GUT scale quark-lepton Yukawa coupling ratios which fit the experimental data without the need for a certain amount of SUSY threshold corrections. In order to obtain the required size of these corrections, the ratios of trilinear couplings, gaugino masses, μ , and sfermion masses are constrained by the loop functions of 10.2.⁴ In particular the SUSY spectrum has to lie close to a common SUSY scale, in contrast to e.g. *Split SUSY* scenarios [202], where these loop functions would get too suppressed. For CMSSM boundary conditions one obtains constraints for the ratios between m_0 , $m_{1/2}$, and A_0 . Furthermore, since $\tan\beta$ -enhanced SUSY threshold corrections are most relevant, $\tan\beta$ must not be too small. So far, only

³For example, in $SU(5)$ only two soft-breaking mass matrices, one for \mathcal{F} and one for \mathcal{T} remain, and in $SO(10)$, where all MSSM superfields are embedded into one $\mathbf{16}$, there is only one soft-breaking mass matrix.

⁴Note that this argument is also valid when only one of the first two generation quark-lepton ratios is predicted together with the third family, since the SUSY threshold corrections in CMSSM-like scenarios are approximately equal for the first two generations.

constraints for relative relations between SUSY parameters were discussed. The overall scale is finally constrained by the measured Higgs mass, which is sensitive to the sparticle spectrum due to significant loop corrections.

10.4.2 Numerical analysis with SusyTC

Let us now perform a numerical analysis using our new software **SusyTC**. We consider GUT scale Yukawa coupling ratios $\frac{y_e}{y_d} = -\frac{1}{2}$, $\frac{y_\mu}{y_s} = 6$, and $\frac{y_\tau}{y_b} = -\frac{3}{2}$, which have been used in the construction of the SUSY flavour $SU(5)$ models of [2–4] presented in the previous chapters of this thesis, and also e.g. in [203]. A subset of these relation, $y_\mu = 6y_s$, and $y_\tau = -\frac{3}{2}y_b$, has been used in [204]. Note that these relations can either emerge as direct result of CG factors in $SU(5)$ GUTs or as approximate relation after diagonalisation of the GUT scale Yukawa matrices Y_d and Y_e . Specifically, our GUT scale Yukawa matrices are given by

$$Y_d = \begin{pmatrix} y_d & 0 & 0 \\ 0 & y_s & 0 \\ 0 & 0 & y_b \end{pmatrix}, \quad Y_e = \begin{pmatrix} -\frac{1}{2}y_d & 0 & 0 \\ 0 & 6y_s & 0 \\ 0 & 0 & -\frac{3}{2}y_b \end{pmatrix},$$

$$Y_u = \begin{pmatrix} y_u & 0 & 0 \\ 0 & y_c & 0 \\ 0 & 0 & y_t \end{pmatrix} U_{\text{CKM}}(\theta_{12}, \theta_{13}, \theta_{23}, \delta). \quad (10.21)$$

As discussed above, we assume CMSSM boundary conditions and restrict our analysis to the parameters m_0 , $m_{1/2}$, and A_0 . The parameter μ is determined from requiring the breaking of Electroweak symmetry as in (10.15) and we set $\text{sgn}(\mu) = +1$. This choice of real μ is not in conflict with the framework of the complex MSSM, since in specific models of the GUT Higgs potential, as for example the ones discussed in chapter 9, μ can be realised as an effective parameter of the superpotential with a fixed phase, including the case that μ is real. The last CMSSM parameter $\tan\beta$ is not explicitly included in our analysis, however we have scanned over different values of $\tan\beta$ and found that the best fit can be obtained for values of $\tan\beta \approx 30$. For our main analysis we have therefore set $\tan\beta = 30$.

REAP requires a neutrino sector, we have thus added a CSD like (3.43) neutrino Yukawa matrix Y_ν and right-handed neutrino mass matrix. The entries of Y_ν have been set to very small values below $\mathcal{O}(10^{-3})$, such that their effects on the RG evolution can be safely neglected, and the masses of the right-handed neutrinos to values about 10^{14} GeV, many orders of magnitude higher than the expected SUSY scale. Such a neutrino sector is similar to the ones studied in the models of part III and also [203].

Using one-loop RGEs, **REAP 1.11.2**, and **SusyTC** we determine the SUSY soft-breaking parameters and μ at the calculated SUSY scale, as well as the pole mass m_{H^+} . Parameter points which lead to tachyonic sfermion masses at any renormalisation scale or which do not allow for Electroweak symmetry breaking are discarded. We then pass our results to **FeynHiggs 2.11.2** [127–129] in order to calculate the two-loop corrected Higgs pole masses in the complex MSSM. Finally the MSSM is matched to the SM and we compare our results

at the electroweak scale with the measured Higgs boson mass of $m_H = 125.7 \pm 0.4$ GeV [14] and the quark and charged lepton Yukawa couplings and quark mixing parameters taken from [91]. Note that we set the uncertainty of the charged lepton Yukawa couplings to one percent to account for the estimated theoretical uncertainty, which in our analysis exceeds the experimental one. Similarly, we estimate a theoretical uncertainty of the Higgs mass calculation of ± 3 GeV, as is commonly assumed.⁵

10.4.3 Results

Of our thirteen parameters, it turned out that by adjusting the seven parameters of Y_u , we could always fit the up-type quark Yukawa couplings, the CKM mixing angles, and the CP phase to agree with at least 10^{-3} relative precision with experimental data.

Thus, the remaining six parameters y_d , y_s , y_b , m_0 , $m_{1/2}$, and A_0 are used to fit the mass of the SM-like Higgs boson and the Yukawa couplings of down-type quarks and charged leptons. We found a benchmark point with a $\chi^2 = 3.9$:

GUT scale input parameters			
y_d	y_s	y_b	
$1.30 \cdot 10^{-4}$	$2.29 \cdot 10^{-3}$	0.162	
m_0	A_0	$m_{1/2}$	
1607.09	-4373.61	786.95	

low energy results			
y_e	y_μ	y_τ	
$2.79 \cdot 10^{-6}$	$5.92 \cdot 10^{-4}$	$1.00 \cdot 10^{-2}$	
y_d	y_s	y_b	m_{h^0}
$1.60 \cdot 10^{-5}$	$2.82 \cdot 10^{-4}$	$1.64 \cdot 10^{-2}$	125.0 GeV

Let us discuss our results in detail. First note that by looking at the low energy scale Yukawa coupling ratios

$$\frac{y_e}{y_d} = 0.17, \quad \frac{y_\mu}{y_s} = 2.10, \quad \text{and} \quad \frac{y_\tau}{y_b} = 0.61, \quad (10.22)$$

the importance of SUSY threshold corrections in evaluating the GUT scale predictions for Yukawa coupling ratios becomes evident. Note that the ratios yield an double ratio (4.43)

$$\left| \frac{y_\mu y_d}{y_s y_e} \right| = 12.4, \quad (10.23)$$

⁵Recently, indications that the theoretical uncertainty in the “large stop mixing” region of parameter space, which will turn out to be most relevant to our analysis, may be larger, have been discussed [205], however there is no full agreement on this aspect. The improvement of the Higgs mass computation is an active field of research and future studies will benefit from more precise calculations.

within the reported one sigma range. The effect of SUSY threshold corrections can also clearly be seen in figure 10.4 as offset at the SUSY scale. Note that the SUSY threshold

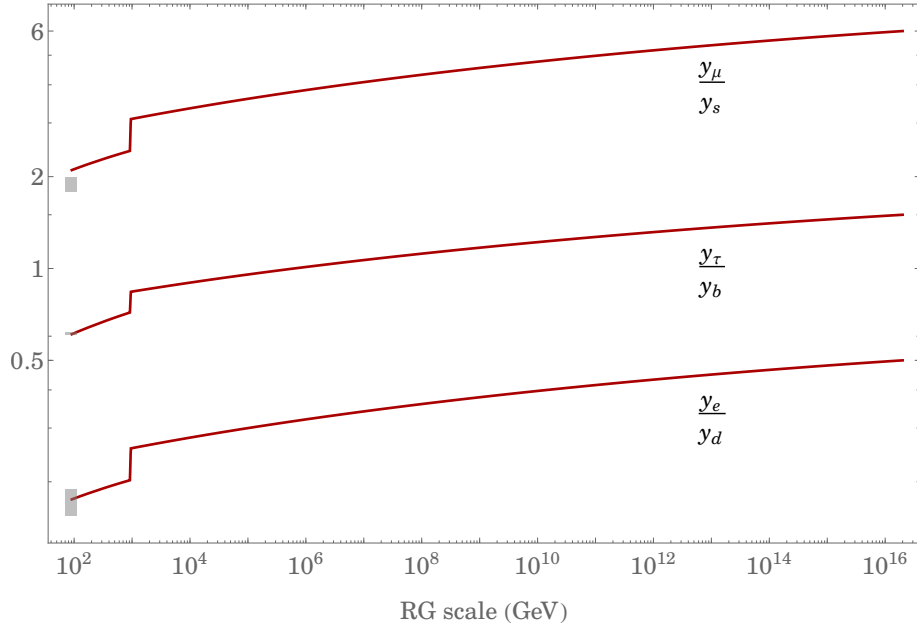


Figure 10.4: RG evolution of the Yukawa coupling ratios of the first, second, and third family from the GUT scale to the electroweak scale. The GUT scale parameters correspond to our benchmark point. The effects of the threshold corrections are clearly visible at the SUSY scale $Q = 940$ GeV. The light grey areas indicate the experimental Yukawa coupling ratios at M_Z , taken from [91].

correction necessary to correct the third generation GUT scale prediction $y_\tau = -\frac{3}{2}$ is the smallest. In fact one can express the ratio of the Yukawa coupling ratios above and below the SUSY scale in terms of the parametrisation (7.26), which was employed in chapters 7 and 8 to approximate the effect of SUSY threshold corrections without specific knowledge of the SUSY parameters. We find

$$\mathbb{1} + \text{diag}(\eta_{Q_{12}}, \eta_{Q_{12}}, \eta_{Q_3}) \approx \text{diag}(1.27, 1.27, 1.17) , \quad (10.24)$$

i.e. our assumption of equal SUSY threshold corrections for the first and second generations was justified. This of course is not a surprise, since we assume CMSSM GUT scale boundary conditions and therefore, as we will see in a moment, the squarks of the first and second generations are approximately degenerate in mass. Such a mass degeneracy was stated in 7.4 as condition for (7.26) to be valid.

Because `SusyTC` calculates the SUSY threshold corrections for the full Yukawa matrices, additionally to the quark-lepton mass ratios, as shown in figure 10.5 one can also determine a considerable effect of the SUSY threshold corrections on the CKM angles, which in general

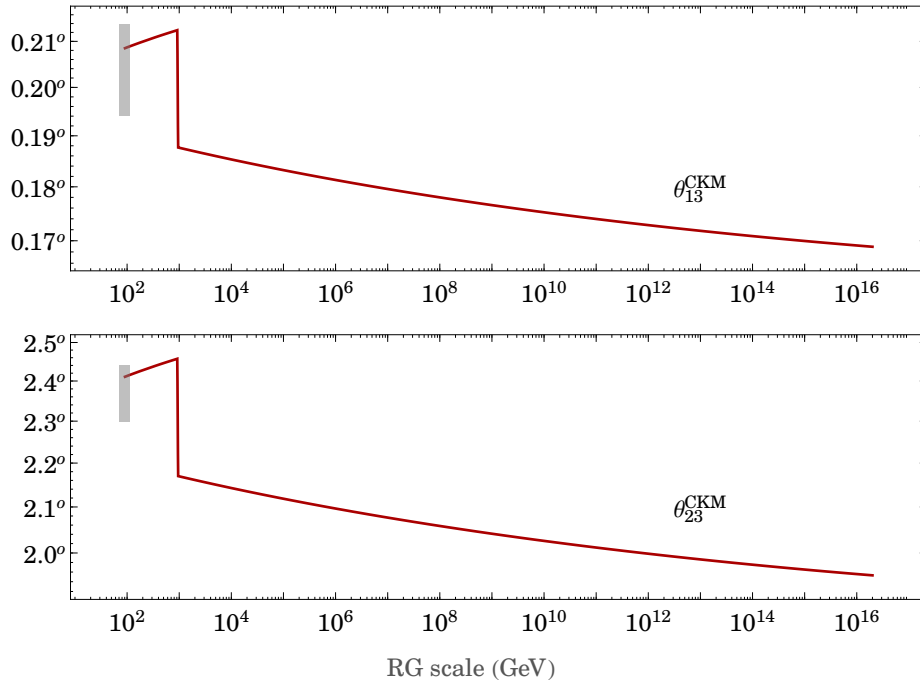


Figure 10.5: RG evolution of the CKM mixing angles θ_{13}^{CKM} and θ_{23}^{CKM} from the GUT scale to electroweak scale. The GUT scale parameters correspond to our benchmark point. The effects of the threshold corrections are clearly visible at the SUSY scale $Q = 940$ GeV. The light grey areas indicate the experimental values at M_Z .

are important in the light of the very precise experimental values of the CKM parameters.

Let us now turn to a discussion of the SUSY spectrum. Our benchmark point yields a SUSY scale of $Q = 940$ GeV. We find that the lightest SUSY particle (LSP) is a bino-like neutralino with a mass of about 346 GeV. The next-to-lightest SUSY particle (NLSP) is a stop of about 577 GeV. Note that these values were obtained as direct results of fitting our GUT scale model to the observed Higgs boson mass and fermion masses and mixing parameters. In particular, no bounds or cuts on the sparticle masses were applied as well as no restrictions from the neutralino relic density.⁶ By requiring spontaneous electroweak symmetry breaking SusyTC calculates $\mu = 2013$ GeV. We show the resulting SUSY spectrum in figure 10.6. The two lightest up-type squark mass eigenstates \tilde{u}_1 and \tilde{u}_2 are stop-like, whereas the stops and scharmions yield the mass eigenstates $\tilde{u}_3 - \tilde{u}_6$ with almost degenerate mass eigenvalues. Similarly, the masses of the first and second generations of down-type squarks and charged sleptons are approximately degenerate.

An important concern in SUSY models with large trilinear couplings is vacuum stabil-

⁶To use the neutralino relic density as constraint, further assumptions on the cosmological evolution would be required. For example, the neutralino relic density may be diluted if additional entropy gets produced at late times (cf. e.g. [206]).

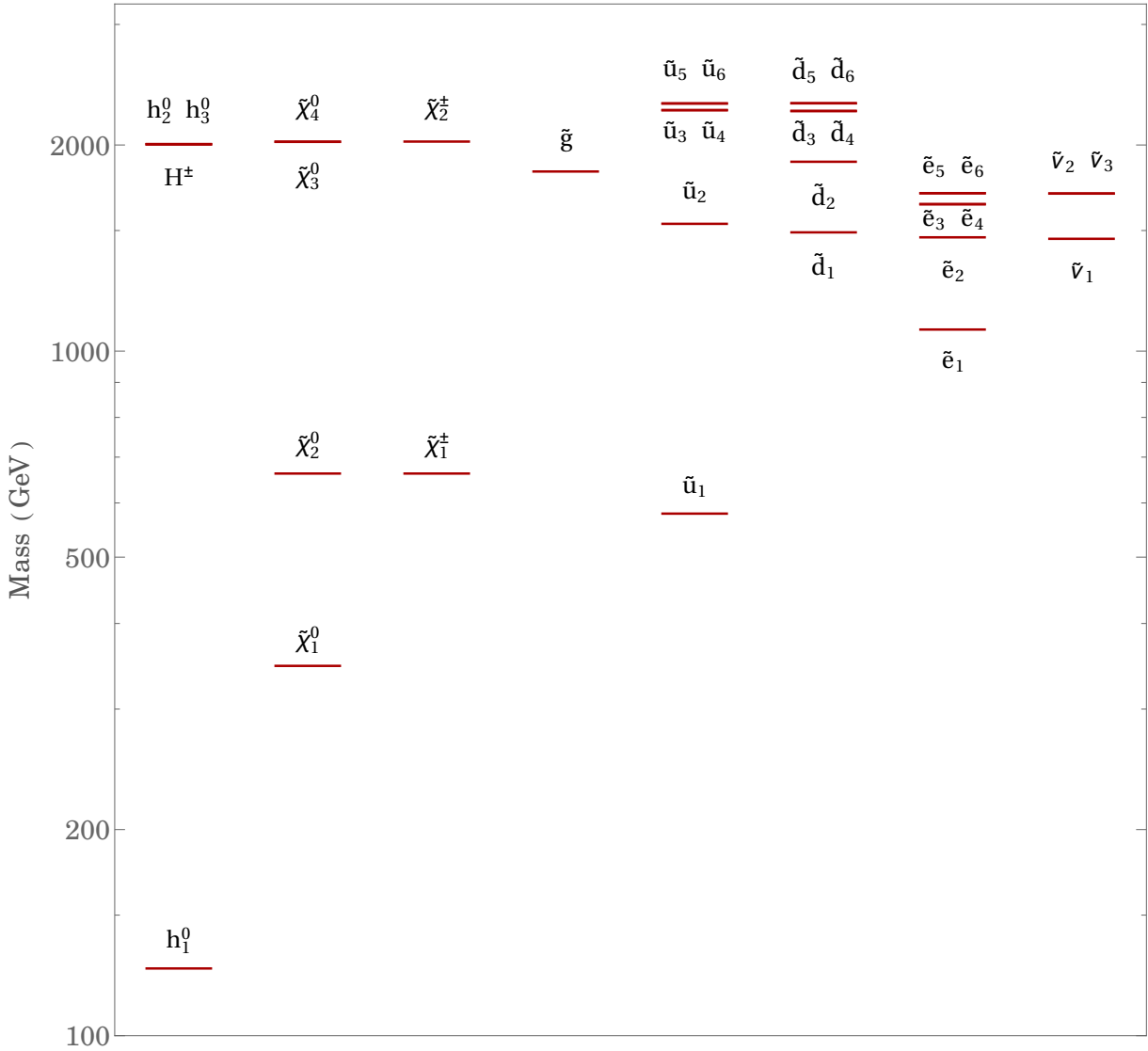


Figure 10.6: SUSY spectrum with $SU(5)$ GUT scale boundary conditions $\frac{y_c}{y_d} = -\frac{1}{2}$, $\frac{y_\mu}{y_s} = 6$, and $\frac{y_\tau}{y_b} = -\frac{3}{2}$, corresponding to our benchmark point from section 5.

ity. Using the constraints from [134] we find that our benchmark point’s scalar potential possesses charge and colour breaking (CCB) vacua, as well as one “unbounded from below” (UFB) field direction in parameter space. This however not necessarily poses a threat to our model, since the lifetime of the vacuum can still be orders of magnitude larger than the age of the universe. The decay probability of a false vacuum can be estimated per unit time and unit volume as [207]

$$\frac{\Gamma}{V} \approx e^{-S_E} , \quad (10.25)$$

where S_E is the Euclidean action of the *bounce solution*, which describes an $O(4)$ -symmetric

field configuration which, starting at the false vacuum for Euclidean time $\tau \rightarrow -\infty$, “bounces” off the true vacuum at $\tau = 0$, and returns into the false vacuum at $\tau \rightarrow \infty$. Requiring that the probability of a vacuum decay to happen in our past lightcone is sufficiently small translates into a lower bound

$$S_E > 400 . \quad (10.26)$$

S_E can be approximated by considering a straight path $\vec{\phi} = \phi \vec{v}$ connecting false and true vacuum in field space [208].⁷ We thus study a single scalar field ϕ with potential $U(\phi)$, which has a false vacuum at $\phi = \phi_f$. The bounce solution is then obtained from minimising

$$S_E = 2\pi^2 \int_0^\infty dr r^3 \left(\frac{z}{2} \partial_i \phi \partial^i \phi + U(\phi) \right) , \quad (10.27)$$

with the boundary conditions $\phi(\tau \rightarrow \infty) \equiv \phi_f$, $\phi'(0) \equiv 0$, and $z = 1$ if ϕ is canonically normalised. The equation of motion is

$$\phi''(r) + \frac{3}{r} \phi'(r) = U'(\phi) , \quad (10.28)$$

which corresponds to a classical field ϕ moving in a potential $-U(\phi)$ and subject to some friction force [207]. Following the program of [209], S_E can be determined by rephrasing the directions of “improved CCB” constraints in field space of [134] into the general form

$$U(\phi) = M_2^2 \phi^2 - M_3 \phi^3 + \lambda \phi^4 . \quad (10.29)$$

Then S_E can be approximated by [210]

$$S_E = \frac{z^2 M_2^2}{M_3^2} \hat{S}_E(\kappa) , \quad (10.30)$$

$$\kappa \equiv \lambda \frac{M_2^2}{M_3^2} . \quad (10.31)$$

Note that \hat{S}_E depends only on a single parameter and can be approximated by the expression [210]

$$\hat{S}_E(\kappa) \approx \begin{cases} -0.7 + \frac{2\pi^2}{12(1-4\kappa)^3} + \frac{16.5}{(1-4\kappa)^2} + \frac{28}{1-4\kappa} & \kappa \geq 0 \\ 45.4 \left(1 + \left(\frac{3 \cdot 45.4}{2\pi^2} \right)^{1.1} |\kappa|^{1.1} \right)^{-\frac{1}{1.1}} & \kappa \leq 0 \end{cases} . \quad (10.32)$$

Tunneling is possible for any value $\kappa < \frac{1}{4}$ and values of $\kappa < 0$ correspond to “unbounded from below” directions. The “improved CCB” directions involve one trilinear term T_f and are in generally D -flat. Only for the case of the top squarks the scalar potential can suffer

⁷Note that this method yields an upper bound for S_E . A complete minimisation of S_E over all non-trivial paths is very elaborate and beyond the scope of this thesis. Since our smallest value of $S_E \approx 1090$ satisfies (10.26) by far, the simplified method can be used to estimate a generally small enough decay probability.

from CCB vacua with non-vanishing D -terms. For all trilinear couplings $T_{u_{ij}}$, $T_{d_{ij}}$, and $T_{e_{ij}}$ we numerically minimised (10.30) for the corresponding ‘‘improved CCB’’ field direction and checked that $S_E > 400$ is satisfied.

Another strong constraint on the MSSM parameter space comes from the UFB-3 direction [134]

$$U_{\text{UFB-3}} = \begin{cases} m_{h_u}^2 |h_u|^2 + \frac{|\mu|}{y_{d_j}} \left(\hat{m}_{\tilde{Q}_{jj}}^2 + \hat{m}_{\tilde{d}_{jj}}^2 \right) |h_u| + \frac{1}{8} (g'^2 + g_2^2) \left(|h_u|^2 + \frac{|\mu|}{y_{d_j}} |h_u| \right)^2 & |h_u| < H_c \\ \left(m_{h_u}^2 + \hat{m}_{\tilde{L}_{ii}}^2 \right) |h_u|^2 + \frac{|\mu|}{y_{d_j}} \left(\hat{m}_{\tilde{Q}_{jj}}^2 + \hat{m}_{\tilde{d}_{jj}}^2 + \hat{m}_{\tilde{L}_{ii}}^2 \right) |h_u| - \frac{2\hat{m}_{\tilde{L}_{ii}}}{g'^2 + g_2^2} & |h_u| > H_c \end{cases}, \quad (10.33)$$

where

$$H_c \equiv \sqrt{\frac{\mu^2}{4y_{d_j}^2} + \frac{2\hat{m}_{\tilde{L}_{ii}}}{g'^2 + g_2^2}} - \frac{|\mu|}{2y_{d_j}}, \quad (10.34)$$

and \hat{m}^2 are the soft-breaking matrices in the Super-CKM/Super-PMNS basis, as defined in appendix B. A second potentially dangerous UFB-3 direction is given by (10.33) with the replacement $Q_j, d_j \rightarrow L_j, e_j$. Both directions depend only on $|h_u|$, thus we use (10.28) to calculate S_E . We find that the lifetime of the electroweak vacuum is many orders of magnitude larger than the age of the universe, which shows that our model’s benchmark point is phenomenologically viable.

We now discuss confidence intervals for our model’s sparticle masses and parameters, which we obtain as in part III as Bayesian hpd intervals from a Markov Chain Monte Carlo analysis, using a Metropolis algorithm. Looking at fit results for several fixed values of $|A_0|$, we find that in order to avoid potentially dangerous vacuum decay rates, the MCMC analysis must include a prior for $|A_0|$. A detailed, individual computation of each parameter point’s vacuum lifetime, although more desirable than a prior, would consume too much computation time. In our analysis we restrict $|A_0| < 7.5$ TeV, although we remark that our predicted confidence intervals could be somewhat enlarged by a more sophisticated inclusion of the lifetime constraints. In figure 10.7 on page 151 we show our results for the one sigma hpd intervals of the sparticle masses. We find that for all parameter points the LSP and NLSP are a bino-like neutralino and a stop, respectively. As a result of the fit and without applying any constraints, the masses of all sparticles are above current bounds from LHC or dark matter searches. The lower band of our predicted sparticle spectrum is within reach of a future LHC high-luminosity upgrade, and the full range is possibly testable at future $\mathcal{O}(100)$ TeV proton-proton colliders like the FCC-hh or the SppC (see e.g. [211]). For the SUSY scale we find an hpd interval of $Q_{\text{hpd}} = [841, 3092]$ GeV. Correlation between LSP, NLSP, and gluino masses are shown in figure 10.8 as two-dimensional hpd regions. Finally we show the one sigma hpd intervals for the CMSSM soft-breaking parameters in figure 10.9. The correlations between the CMSSM parameters and the resulting mass of the SM-like Higgs boson is shown in figure 10.10.

10.4.4 Remarks

We close this chapter with some remarks and comments on our analysis.

Other GUT scale predictions For our analysis we investigated the GUT scale Yukawa coupling ratios that have been constructed in the various models of this thesis, i.e. $\frac{y_\tau}{y_b} = -\frac{3}{2}$, $\frac{y_\mu}{y_s} = 6$, and $\frac{y_e}{y_d} = -\frac{1}{2}$. Certainly, other GUT scale relations like Georgi-Jarlskog or the other CG factors of (4.45) can be constructed, too. We have published `SusyTC` to provide the SUSY GUT model building community with an useful tool for model analyses and it will be interesting to compare predictions and constrains on the SUSY spectra from other promising GUT scale Yukawa predictions in the future. Also note that some GUT models do not predict any quark-lepton Yukawa coupling ratios, hence they lack a link to the SUSY threshold corrections and do not yield constraints on the SUSY spectrum.

Universal soft-breaking terms As discussed in 10.4.1, universal SUSY soft-breaking parameters are well motivated in SUSY flavour GUT models. However, it will be interesting to study constraints on the non-universality of the soft-breaking parameters in future analyses. In this context the results obtained with `SusyTC` can be obtained as SLHA output files and the obtained SUSY spectrum can conveniently be forwarded to software tools specialised on flavour observables.

Gauge coupling unification A discussion on gauge coupling unification depends strongly on the GUT Higgs potential and was therefore omitted in this chapter (see e.g. 9.3). Note however that GUT threshold effects can be implemented into `REAP` and one can study the effects on gauge coupling unification within a complete GUT model. For our analysis, we have simply fixed the GUT scale at the common $2 \cdot 10^{16}$ GeV, which is of similar size as e.g. the GUT scale of the model in 9.4.1. Let us however point at the interesting possibility, that the GUT scale is shifted to much higher values. In this case, the RGEs for the Yukawa couplings have to be solved for a larger range and thus the predictions for the SUSY spectrum will change. Eventually, a higher GUT scale can possibly even favour other quark-lepton Yukawa coupling ratios than a model with lower GUT scale.

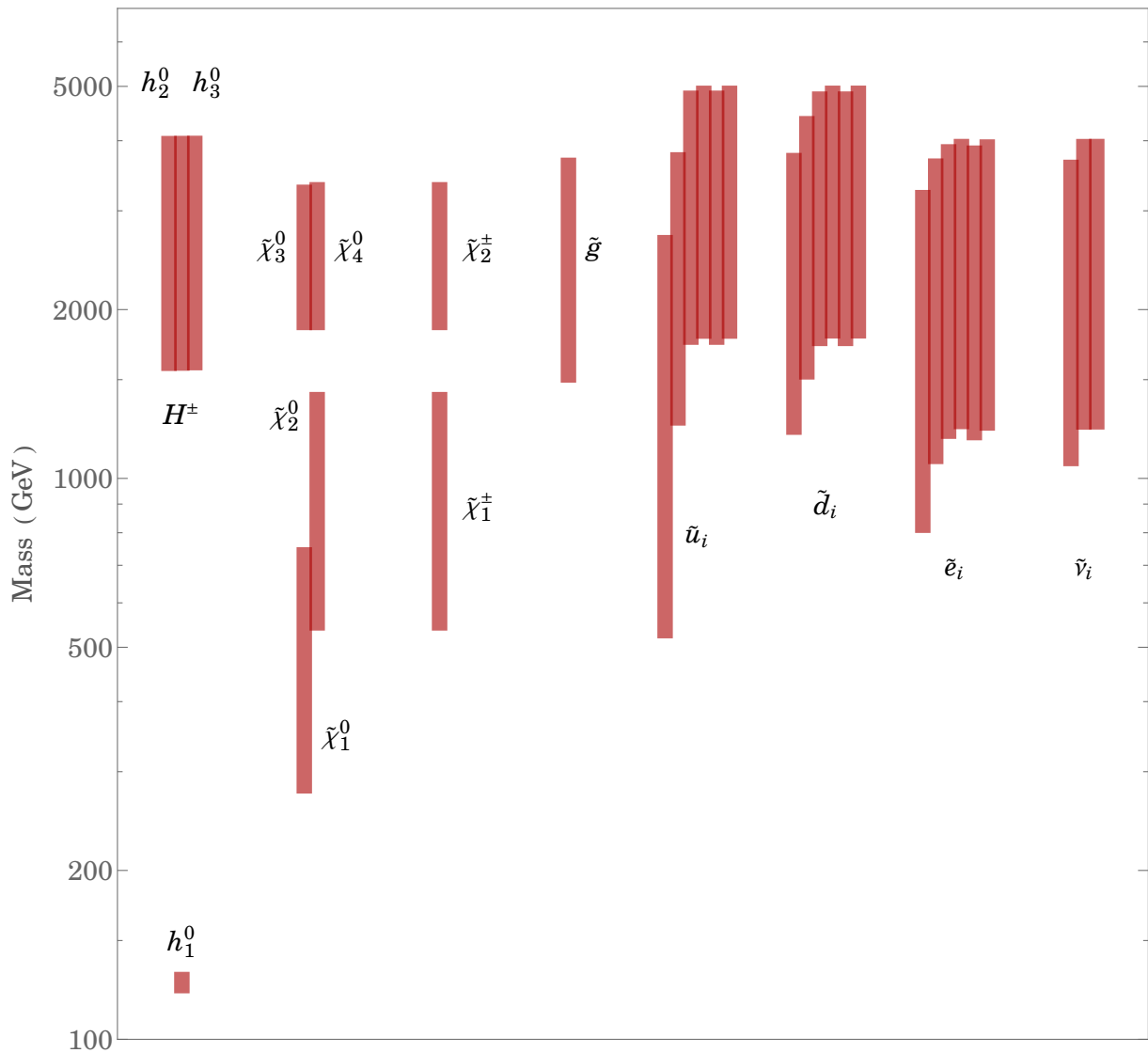


Figure 10.7: One sigma hpd intervals for the sparticle spectrum and Higgs boson masses with $SU(5)$ GUT scale boundary conditions $\frac{y_e}{y_d} = -\frac{1}{2}$, $\frac{y_\mu}{y_s} = 6$, and $\frac{y_\tau}{y_b} = -\frac{3}{2}$, corresponding to our benchmark point. The LSP is always $\tilde{\chi}_1^0$ and the NLSP is always a stop.

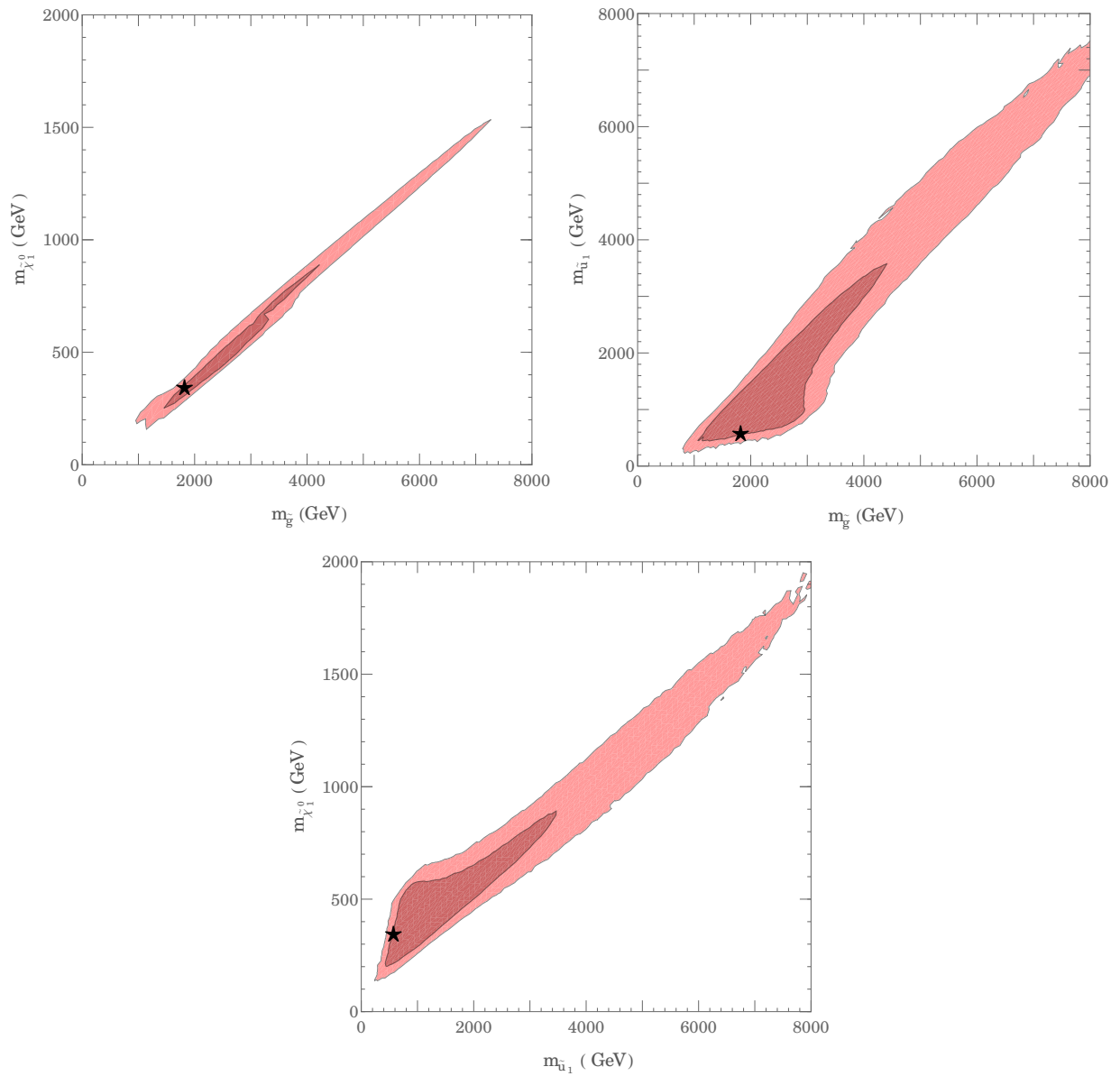


Figure 10.8: Two-dimensional one sigma (dark) and two sigma (bright) hpd regions for the masses of the LSP, NLSP, and gluino. The black star marks the benchmark point.

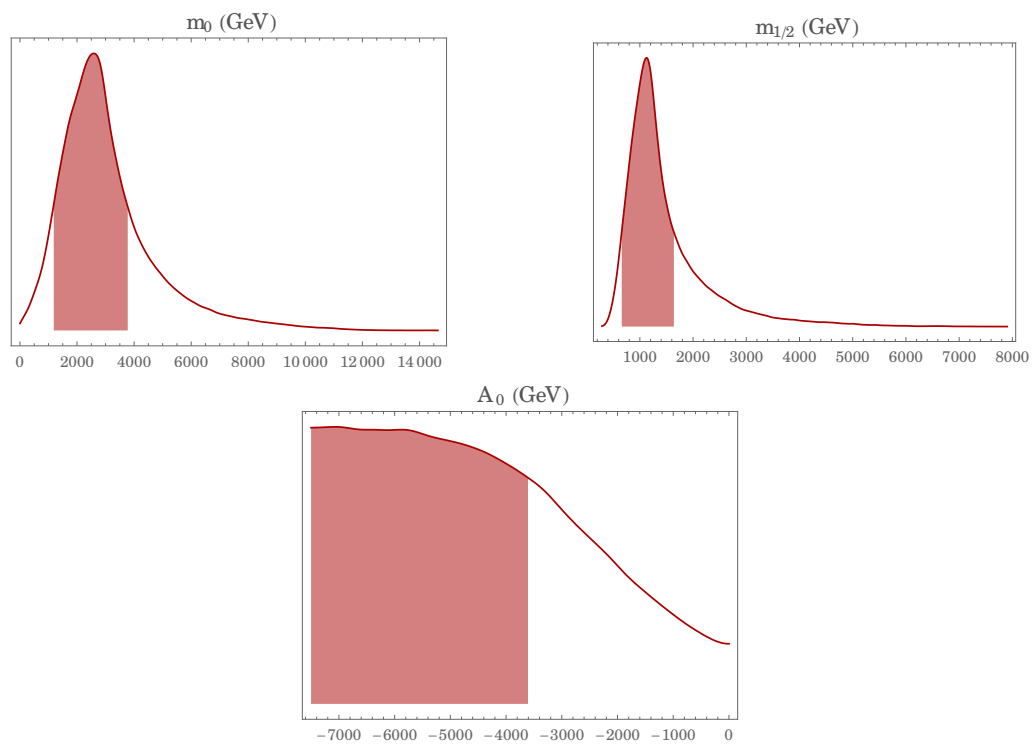


Figure 10.9: One sigma hpd intervals for the Constrained MSSM soft-breaking parameters.

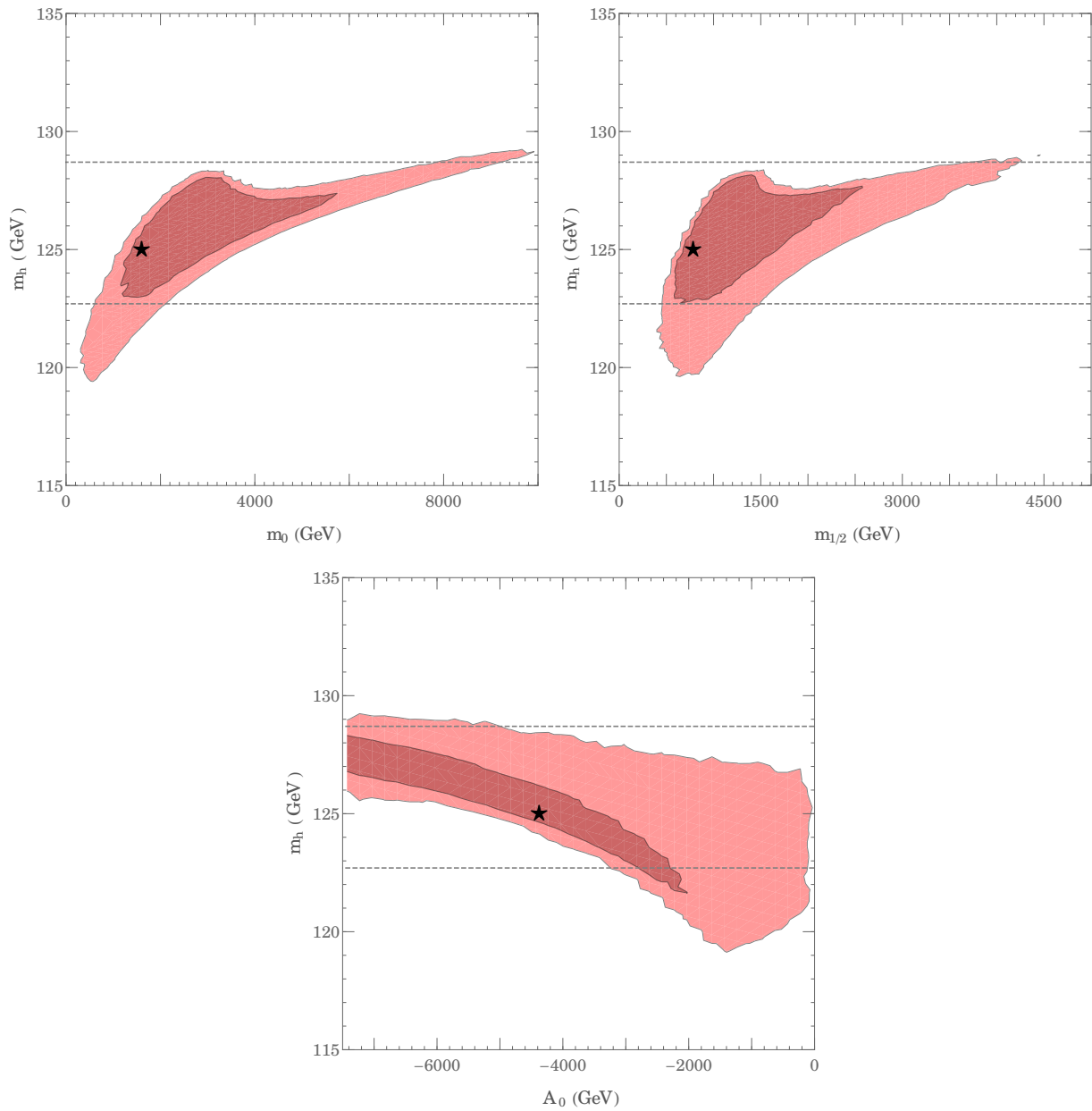


Figure 10.10: Two-dimensional one sigma (dark) and two sigma (bright) hpd regions for the CMSSM soft-breaking parameters and the SM-like Higgs mass. The black star marks the benchmark point. The dashed lines correspond to the region 125.7 ± 3 GeV.

PART VI

Summary

CHAPTER 11

Summary and Conclusions

In this thesis we derived and discussed multiple predictions, in particular for the flavour and SUSY flavour structure, arising from a certain class of supersymmetric Grand Unified Theories. Combining SUSY, GUTs, and discrete flavour symmetries into predictive SUSY flavour GUT models, we investigated the interplay between these three beyond the Standard Model concepts.

When a flavour symmetry gets spontaneously broken, the observed hierarchies and structures in the flavour sector of a model are explained via flavon fields, which obtain vevs pointing into specific directions in flavour space. Relations between quark and lepton observables can be explained by GUTs, which can feature predictions for ratios between quark and lepton Yukawa couplings. In SUSY flavour GUT models, these predictions are affected by SUSY threshold corrections, thereby linking a particular flavour GUT model to the SUSY spectrum. Finally, SUSY GUTs can predict too rapid proton decay, establishing constraints on the GUT breaking Higgs sector and the model's symmetries.

We motivated SUSY flavour GUT models, outlined the problems discussed in this thesis, and introduced the necessary theoretical framework in parts I and II.

In part III we focused on the construction of SUSY flavour GUT models. In particular, we discussed in chapter 6 four simple conditions to construct the interesting phenomenological relation $\theta_{13}^{\text{PMNS}} \approx \theta_C \sin \theta_{23}^{\text{PMNS}}$ in $SU(5)$ GUTs and Pati-Salam models. The basic principle is the generation of the down-type quark and charged lepton Yukawa matrix elements from the same joint GUT operators, which implies that the resulting matrix elements are equal up to group theoretical Clebsch-Gordan factors. This can impose $\theta_C \approx \theta_{12}^e$ and thus the Cabibbo angle emerges in the charged lepton corrections to $\theta_{13}^{\text{PMNS}}$. In detail, the four conditions are

Condition 1: The mixing angles θ_{13}^ν and θ_{13}^e should be vanishing.

Condition 2: The Cabibbo angle should be given by $\theta_C \approx \theta_{12}^d$, as for example in models with $\theta_{12}^u \ll \theta_{12}^d$.

Condition 3: The GUT scale ratios between the relevant elements of Y_e and Y_d have to be predicted, e.g. from CG factors when the entries of Y_d and Y_e are generated from single joint GUT operators.

Condition 4: The ratio of the two CG factors in $\theta_C \approx \left| \frac{c_1}{c_2} \right| \theta_{12}^e$ must be one, i.e. c_1 and c_2 have to be equal. In $SU(5)$ GUTs an approximate equality between the 1-2 and 2-1 elements of Y_d has to be required in addition, e.g. by a symmetry in the 1-2 submatrix or via the GST relation and a vanishing 1-1 element.

In a model-independent way, we estimated the possible corrections due to e.g. RG evolution, next-to-leading order terms in the small angle expansion, and the experimental uncertainty of $\theta_{23}^{\text{PMNS}}$ and found it to be less than about $\mathcal{O}(10\%)$. Within an explicit flavour GUT model, the uncertainty can decrease to about $\pm 0.25^\circ$, since the estimate can be replaced by explicit calculations. Specific flavour GUT models can thus possibly be differentiated in careful analyses.

Furthermore, we discussed the connection between different neutrino mixing patterns and the Dirac CP phase via the lepton mixing sum rule. With $\theta_{13}^\nu \ll \theta_C$ being the only restriction on the neutrino sector, a future measurement of δ^{PMNS} may be viewed as “reconstructing” the value of θ_{12}^ν , provided that a hierarchic charged lepton Yukawa matrix $\theta_{13}^e, \theta_{23}^e \ll \theta_C$ is given.

In chapter 7 we then proposed a first SUSY flavour GUT model, based on $SU(5)$ and an A_4 flavour symmetry, where $\theta_{13}^{\text{PMNS}} \approx \theta_C \sin \theta_{23}^{\text{PMNS}}$ is realised, following the conditions discussed in chapter 6. In order to construct a predictive GUT model, in addition to the matter and flavon superpotential, we carefully built the full renormalisable messenger sector, which guarantees that only specific GUT contractions emerge in the effective superpotentials when the heavy messenger superfields are integrated out. In this way condition 3 is ensured: the GUT scale Yukawa matrix elements are generated from single joint operators, yielding predictive quark-lepton relations via group-theoretical CG factors. We made use of a novel set of CG-factors, namely $c_{12} = c_{22} = 6$ and $c_{21} = -\frac{1}{2}$, which are in excellent agreement with the current experimental data for $\frac{m_s}{m_d}$ and satisfy condition 4. Our model is invariant under generalised CP symmetry, which is broken spontaneously by the vevs of flavon fields. In the neutrino sector we constructed tri-bimaximal mixing, which predicts close-to-maximal CP violation $\delta^{\text{PMNS}} \approx 270^\circ$ via the lepton mixing sum rule. In the quark sector our model features a right-angled unitarity triangle.

We performed a detailed fit of the model’s 14 parameters to 18 measured observables, taking into account the RG evolution from the GUT scale to lower energies and approximate formulae for SUSY threshold corrections, and found a good best-fit point with a $\chi^2/\text{d.o.f.}$ of 2.0. Bayesian one sigma highest posterior density intervals were obtained from a Markov Chain Monte Carlo analysis. Including the unmeasured neutrino CP phases, our model makes six predictions. We discussed our results in the light of newly available data and outlined how future more precise measurements of the lepton mixing parameters, δ^{CKM} , $\frac{m_s}{m_d}$, and of neutrino-less double beta decay can be used to test our predictions.

Part III is completed with chapter 8, where a strong inverse neutrino mass hierarchy was constructed in a second SUSY flavour GUT model with $SU(5)$ and A_4 . The strong inverse hierarchy was constructed without fine-tuning, based on an off-diagonal mass matrix of the right-handed neutrinos and a novel vacuum alignment for the flavons constituting the neutrino Yukawa matrix, which features θ'_{23} as free parameter and therefore can explain $\theta_{23}^{\text{PMNS}} \neq 45^\circ$ without the need for charged lepton corrections. Due to the specific phases of the flavon vevs, our model predicts $\delta^{\text{PMNS}} = \varphi^{\text{PMNS}} = 180^\circ$.

Constructing the model similar to the one in chapter 7, we again realised the specific relation $\theta_{13}^{\text{PMNS}} \approx \theta_C \sin \theta_{23}^{\text{PMNS}}$ from charged lepton mixing corrections, linked to quark mixing by GUT relations. Comparing to chapter 7, we found an even better best-fit with $\chi^2/\text{d.o.f.} = 1.1$ in an analogous phenomenological analysis. We discussed the model's predictions and found a new non-compliance with the most recent global fit value of $\theta_{23}^{\text{PMNS}}$, which lies in the second octant for inverse neutrino mass ordering, as opposed to the 2013 data. However, we also pointed out that precise measurements of $\theta_{23}^{\text{PMNS}}$ are still work in progress and future experiments will be able to settle this question.

We finally pointed out the differences between the predictions of both models of chapters 7 and 8 and discussed how they can be discriminated with the data of running and future experiments. For the inverse hierarchy model we found the effective mass parameter of neutrino-less double beta decay to be in reach of the nEXO and AMoRE experiments. A future 50 – 70 km baseline reactor measurement of $\theta_{12}^{\text{PMNS}}$ with high precision would allow to distinguish both models. Interestingly, although both models differ mainly in the neutrino sector from each other, they feature different predictions of δ^{CKM} and could be distinguished by a precise measurement of the quark mixing CP phase.

Both models of chapters 7 and 8 can be viewed as proof of principle, demonstrating the successful construction of predictive flavour GUT models with $\theta_{13}^{\text{PMNS}} \approx \theta_C \sin \theta_{23}^{\text{PMNS}}$ and realistic quark-lepton mass ratios. In particular, the sets of shaping symmetries and messenger superfields presented in appendix D are not expected to be one-of-a-kind implementations of our models' features. We thus understand our constructed realisations as classes of models, defined by the strategy of predictive GUT scale Yukawa coupling matrices, built via shaping symmetries, *UV-completion* due to messenger superfields, and specific group-theoretical CG factors.

In part IV of this thesis, we discussed how the double missing partner mechanism solution to the doublet-triplet splitting problem in SUSY $SU(5)$ GUTs can be combined with the strategy to construct predictive flavour models via specific CG factors for the GUT scale quark-lepton Yukawa coupling ratios.

We have argued that towards this goal a second $SU(5)$ breaking Higgs superfield in the adjoint representation is very useful:

- An additional **24** can be used to split the triplet and octet components of **24** in a renormalisable superpotential, thereby shifting the upper bound (obtained from the requirement of gauge coupling unification) of the effective triplet mass mediating dimension

five proton decay to higher values, i.e. above the lower bound from non-observation of proton decay.

- The introduction of a second adjoint is not only an UV-completion, but generally leads to more freedom for the GUT scale and the effective triplet mass.
- A second adjoint field allows the **24**s to be charged under shaping symmetries, which is necessary for predictive GUT flavour models.

Then the GUT scale and effective triplet masses can be easily made high enough to avoid problems with proton decay.

We discussed the shaping symmetry and messenger sector of the DMPM with an adjoint, which guarantee the absence of dangerous Planck scale suppressed operators and generalised the notion of effective triplet masses to the case of more than one pair of Higgs fields H, \bar{H} coupling to matter.

Two explicit flavour models with different predictions for the GUT scale Yukawa matrices were constructed, including shaping symmetry and messenger sector, and we presented a discussion on the careful choice of messenger superfields with respect to phenomenology. We found that both models feature effective triplet masses above current bounds from proton decay. We included all possible effective Planck scale suppressed operators consistent with our symmetries and found the welcomed emergence of small μ -terms for the light Higgs doublets, while no dangerous operator existed that could have spoiled our results. Both models stay perturbative until close to the Planck scale.

Finally we discussed proton decay and outlined that flavour GUT models also determine the Yukawa matrix structures for the Higgs triplet couplings, and thus enable a more predictive analysis of different proton decay channels than conventional GUT models.

In the final part V, we studied SUSY threshold corrections and discussed their importance for the investigation of GUT scale quark-lepton Yukawa coupling ratios, thereby linking a given flavour GUT model to the SUSY parameters. Thus, via SUSY threshold corrections, GUT models can predict properties of the sparticle spectrum from the pattern of quark-lepton mass ratios at the GUT scale.

We extended and generalised various formulae in the literature needed for a precision analysis of SUSY flavour GUT models, e.g. we calculated the two-loop RGEs of the MSSM soft-breaking parameters in the seesaw type-I extension and generalised the one-loop calculation of μ and of the pole masses m_A and m_{H^+} to include inter-generational mixing in the self energies. We then carefully calculated the one-loop SUSY threshold corrections for the full down-type quark, up-type quark, and charged lepton Yukawa coupling matrices in the electroweak unbroken phase.

We implemented these formulae into a new software tool **SusyTC**, a major extension to the Mathematica package **REAP**. **SusyTC** also calculates the $\overline{\text{DR}}$ sparticle spectrum and the SUSY scale Q , and can provide output in SLHA “Les Houches” files which are the necessary input for external software, e.g. for performing a two-loop Higgs mass calculation.

With `SusyTC` we introduced a convenient tool for top-down analyses of SUSY flavour GUT models, accepting general matrices as input for the GUT scale trilinear and soft-breaking mass matrices, analogously to the input of general GUT scale Yukawa matrices in `REAP`, and non-universal gaugino masses. Together with `REAP`, the RG evolution to low energies is performed, including an automatic calculation of the SUSY scale, automatic matching of the MSSM to the SM, and $\overline{\text{DR}}$ to $\overline{\text{MS}}$ conversion.

We applied `SusyTC` to study the predictions of the GUT scale Yukawa coupling relations $\frac{y_e}{y_d} = -\frac{1}{2}$, $\frac{y_\mu}{y_s} = 6$, and $\frac{y_\tau}{y_b} = -\frac{3}{2}$, which were used in the construction of the SUSY flavour GUT models in parts III and IV for the Constrained MSSM parameters and the sparticle masses. We found a benchmark point with $\chi^2 = 3.9$ where the LSP is a bino-like neutralino with a mass of about 346 GeV and the NLSP a stop with a mass of 577 GeV. We performed a Markov Chain Monte Carlo analysis to obtain Bayesian highest posterior density intervals for the sparticle masses. Remarkably, without having applied any constraints from LHC SUSY searches or dark matter searches, we found that the considered GUT scenario predicts a sparticle spectrum above past LHC sensitivities, but partly within reach of a future LHC high-luminosity upgrade. $\mathcal{O}(100)$ TeV proton-proton colliders like the FCC-hh or the SppC will be able to test our findings in the future.

In summary, we demonstrated the successful construction of SUSY flavour GUT models with realistic quark-lepton mass ratios and mixing angle relations by presenting and analysing two explicit models with normal and inverse neutrino mass ordering, respectively. In order to predict the flavour structure, we emphasised the importance of a careful construction of additional shaping symmetries and messenger sectors. We then presented a strategy to combine such predictive SUSY flavour GUT models with the double missing partner mechanism solution to the doublet-triplet splitting problem by introducing a second GUT breaking Higgs field in the adjoint representation, constructed two example models, and found their proton decay rate sufficiently suppressed due to heavy effective triplet masses. Finally we investigated SUSY threshold corrections and found predictions for the sparticle spectrum arising from given flavour GUT models, by introducing a new software tool `SusyTC`, which enables convenient top-down analyses of SUSY flavour GUT models. In conclusion, we performed a detailed investigation of predictions for the flavour and SUSY flavour structure arising from different aspects in certain SUSY flavour GUT models and provided an useful software tool for analyses of future models.

Appendices

APPENDIX A

Brief review on group theory

In this appendix a brief review on group theory is presented, where we restrict the discussion to the topics relevant in this thesis. In Particle Physics two types of symmetry groups are important: Lie groups and small discrete groups. Of special relevance in this thesis are the Lie groups $SU(N)$ and the discrete symmetry group A_4 , which will be discussed in this appendix based on [80, 212] for $SU(N)$ and [49, 213, 214] for A_4 . We also briefly review generalised CP transformations in A_4 flavour models, based on [166].

A.1 The special unitary group $SU(N)$

The special unitary group $SU(N)$ is the group of unitary $N \times N$ matrices U with $\det U = 1$. A $N \times N$ unitary matrix has $2N + 2\frac{N(N-1)}{2} = N^2$ degrees of freedom. It follows from including the additional constraint $\det U = 1$ that $SU(N)$ has dimension $N^2 - 1$. Therefore every element of the group connected to $\mathbb{1}_N$ can be written as

$$U(\theta) = e^{i\theta_a T^a} = \mathbb{1} + i\theta_a T^a + \mathcal{O}(\theta^2), \quad (\text{A.1})$$

where T^a are $N^2 - 1$ hermitian, traceless¹ $N \times N$ matrices, called the generators of $SU(N)$. The generators are normalised as

$$\text{Tr } T^a T^b = \frac{1}{2} \delta^{ab}. \quad (\text{A.2})$$

They furnish the Lie algebra $\mathfrak{su}(N)$ and satisfy the commutator relation

$$[T^a, T^b] = i f^{ab}_c T^c, \quad (\text{A.3})$$

where f^{ab}_c are called *structure constants* of $\mathfrak{su}(N)$. It can be shown that they are totally anti-symmetric.

A representation \mathbf{R} of a group is a set of matrices M associated with group elements such that the group multiplication is satisfied. More generally, one can find a set of matrices

¹Using $\det e^A = e^{\text{Tr } A}$.

$T_{\mathbf{R}}^a$ specific to the representation \mathbf{R} , which satisfy the same commutation rule Eq. (A.3) as the generators of $\mathfrak{su}(N)$ and span a basis of the matrices of \mathbf{R} . Representations of $SU(N)$ are named after the rank of the representation matrices.

If a representation \mathbf{R} has a basis where all $T_{\mathbf{R}}^a$ can be brought into block-diagonal form, \mathbf{R} is called *reducible*. A reducible representation can be decomposed into the direct sum of *irreducible* representation. For every irreducible representation \mathbf{r} the matrices $T_{\mathbf{r}}^a$ are normalised as

$$\mathrm{Tr} T_{\mathbf{r}}^a T_{\mathbf{r}}^b = l(r) \delta^{ab}, \quad (\text{A.4})$$

where the constants $l(r)$ are named *Dynkin index*. Another important constant of $SU(N)$ irreducible representations are the *quadratic Casimir invariants* C_2 defined by

$$\sum_a (T_{\mathbf{r}}^a T_{\mathbf{r}}^a)_{ij} = C_2 \delta_{ij}. \quad (\text{A.5})$$

The simplest irreducible representation is the singlet representation $\mathbf{1}$ where $M(g) = \mathbf{1}$ for all elements g and $T_{\mathbf{R}}^a = 0$. In order for the Lagrange density to be invariant under an $SU(N)$ symmetry, it has to transform under the singlet representation.

The structure constants themselves span a representation of real $(N^2 - 1) \times (N^2 - 1)$ matrices, known as *adjoint* representation with $(T_{N^2-1}^a)_{ij} = -if^a_{ij}$.

Of course, the matrices U also form a representation themselves. This irreducible representation is called the *fundamental representation* \mathbf{N} and its representation matrices are spanned by $T_{\mathbf{N}}^a = T^a$. A field transforming under the fundamental representation of $SU(N)$ is an N -dimensional vector

$$\psi_i \rightarrow U_i^j \psi_j. \quad (\text{A.6})$$

For every representation \mathbf{R} exists a conjugate representation $\bar{\mathbf{R}}$, whose representation matrices are given by the complex conjugates M^* . The conjugate representation to the fundamental representation is called *anti-fundamental*. Its representation matrices are spanned by $T_{\bar{\mathbf{N}}}^a = -T^a$. With the convention $\psi^i \equiv \psi_i^*$ for the position of the indices, a field transforming in the anti-fundamental representation is an N -dimensional row vector

$$\psi^i \rightarrow \psi_j U^j_i. \quad (\text{A.7})$$

Fields transforming under higher dimensional representations are defined as tensors, whose transformation properties are given by the direct product of the transformations of the corresponding vectors

$$\psi_{j_1 j_2 \dots j_m}^{i_1 i_2 \dots i_n} \rightarrow U^{i_1}_{i'_1} U^{i_2}_{i'_2} \dots U^{i_n}_{i'_n} U_{j_1}^{j'_1} U_{j_2}^{j'_2} \dots U_{j_m}^{j'_m} \psi_{j'_1 j'_2 \dots j'_m}^{i'_1 i'_2 \dots i'_n}. \quad (\text{A.8})$$

There are two invariant tensors, which can be used to raise and lower indices: The Kronecker delta δ_i^j and the totally anti-symmetric Levi-Civita tensor² $\epsilon_{i_1 i_2 \dots i_N}$. Products of $SU(N)$ tensors are then obtained by the various possibilities to contract $SU(N)$ indices.

²Note that in $SU(2)$ ϵ_{ij} can be used to flip the anti-fundamental $\bar{\mathbf{2}}$ into the fundamental $\mathbf{2}$.

A.2 The discrete group A_4

The symmetry group A_4 is the group of even permutations of four elements, i.e. the symmetry group of a solid tetrahedron, and thus has order $\frac{4!}{2} = 12$. The twelve elements of A_4 are

- The identity ().
- Three *double transpositions*, which are the interchanges of two unrelated pairs $(i_1, i_2) \circ (i_3, i_4)$, and have order two.
- Eight 3-cycles $(i_1, i_2, i_3) = (i_1, i_3) \circ (i_1, i_2)$ of order three.

Therefore, the generators of A_4 are one double transposition S and one 3-cycle T , see table A.1.

Generator	Cycle	order n
S	$(1, 2) \circ (3, 4)$	2
T	$(1, 2, 3) = (1, 3) \circ (1, 2)$	3

Table A.1: The generators of A_4 .

A_4 has four conjugacy classes $N_i C^{n_i}$, where N_i is the number of elements in the conjugacy class, n_i denotes the order of the elements in the conjugacy class, and g_i is one element of the conjugacy class. Besides the trivial $1C^1(\mathbf{1})$, they are $3C^2(S) = \{S, TST^2, T^2ST\}$, $4C^3(T) = \{T, STS, ST, TS\}$, and $4C^3(T^2) = \{T^2, ST^2S, ST^2, T^2S\}$. Since the number of conjugacy classes equals the number of irreducible representations, there are four irreducible representations in A_4 . Furthermore, it follows from the group theory theorem that the order of a finite group equals the sum of the squares of the dimensions of its irreducible representations, that A_4 has three singlets $\mathbf{1}$, $\mathbf{1}'$, and $\mathbf{1}''$, and one triplet $\mathbf{3}$. Then the character table of A_4 is given by table A.2. From the character table one can find the multiplication rules

$$\mathbf{r} \times \mathbf{s} = \sum_t d(\mathbf{r}, \mathbf{s}, \mathbf{t}) \mathbf{t}, \quad (\text{A.9})$$

	$1C^1(\mathbf{1})$	$3C^2(S)$	$4C^3(T)$	$4C^3(T^2)$
$\chi_i(\mathbf{1})$	1	1	1	1
$\chi_i(\mathbf{1}')$	1	1	w	w^2
$\chi_i(\mathbf{1}'')$	1	1	w^2	w
$\chi_i(\mathbf{3})$	3	-1	0	0

Table A.2: Character table of A_4 , where $\omega \equiv e^{\frac{2\pi i}{3}}$. The character table is unique up to an exchange of $\mathbf{1}'$ and $\mathbf{1}''$.

with

$$d(\mathbf{r}, \mathbf{s}, \mathbf{t}) = \frac{1}{12} \sum_i n_i \chi_i(\mathbf{r}) \chi_i(\mathbf{s}) \chi_i^*(\mathbf{t}). \quad (\text{A.10})$$

One obtains for A_4

$$\begin{aligned} \mathbf{1}' \times \mathbf{1}' &= \mathbf{1}'' , \\ \mathbf{1}'' \times \mathbf{1}'' &= \mathbf{1}' , \\ \mathbf{1}' \times \mathbf{1}'' &= \mathbf{1} , \\ \mathbf{1}' \times \mathbf{3} &= \mathbf{3} , \\ \mathbf{1}'' \times \mathbf{3} &= \mathbf{3} , \\ \mathbf{3} \times \mathbf{3} &= \mathbf{1} + \mathbf{1}' + \mathbf{1}'' + \mathbf{3}_s + \mathbf{3}_a , \end{aligned} \quad (\text{A.11})$$

where $\mathbf{3}_s$ and $\mathbf{3}_a$ denote a symmetric and antisymmetric product, respectively.

In this thesis we use the A_4 basis of Ma and Rajasekaran [76], with the generating elements S and T as shown in table A.3. In this basis, the $\mathbf{1}$ in $\mathbf{3} \times \mathbf{3}$ is given by the

	S	T
$\mathbf{1}$	1	1
$\mathbf{1}'$	1	w
$\mathbf{1}''$	1	w^2
$\mathbf{3}$	$\begin{pmatrix} 1 & 0 & 0 \\ 0 & -1 & 0 \\ 0 & 0 & -1 \end{pmatrix}$	$\begin{pmatrix} 0 & 1 & 0 \\ 0 & 0 & 1 \\ 1 & 0 & 0 \end{pmatrix}$

Table A.3: The generating elements of S and T for the irreducible representations of A_4 in the *Ma-Rajasekaran* basis.

$SO(3)$ -type inner product

$$\mathbf{3} \times \mathbf{3} = \mathbf{1} : \begin{pmatrix} \alpha_1 \\ \alpha_2 \\ \alpha_3 \end{pmatrix} \times \begin{pmatrix} \beta_1 \\ \beta_2 \\ \beta_3 \end{pmatrix} = \alpha_1 \beta_1 + \alpha_2 \beta_2 + \alpha_3 \beta_3 . \quad (\text{A.12})$$

The other singlets in $\mathbf{3} \times \mathbf{3}$ are given by

$$\mathbf{3} \times \mathbf{3} = \mathbf{1}' : \begin{pmatrix} \alpha_1 \\ \alpha_2 \\ \alpha_3 \end{pmatrix} \times \begin{pmatrix} \beta_1 \\ \beta_2 \\ \beta_3 \end{pmatrix} = \alpha_1 \beta_1 + \omega^2 \alpha_2 \beta_2 + \omega \alpha_3 \beta_3 , \quad (\text{A.13})$$

$$\mathbf{3} \times \mathbf{3} = \mathbf{1}'' : \begin{pmatrix} \alpha_1 \\ \alpha_2 \\ \alpha_3 \end{pmatrix} \times \begin{pmatrix} \beta_1 \\ \beta_2 \\ \beta_3 \end{pmatrix} = \alpha_1 \beta_1 + \omega \alpha_2 \beta_2 + \omega^2 \alpha_3 \beta_3 , \quad (\text{A.14})$$

where $\omega \equiv e^{\frac{2\pi i}{3}}$. For the two triplets in $\mathbf{3} \times \mathbf{3}$ we denote the symmetric product by “ \star ” and the antisymmetric by “ \times ”

$$\mathbf{3} \star \mathbf{3} = \mathbf{3}_s : \begin{pmatrix} \alpha_1 \\ \alpha_2 \\ \alpha_3 \end{pmatrix} \star \begin{pmatrix} \beta_1 \\ \beta_2 \\ \beta_3 \end{pmatrix} = \frac{1}{2} \begin{pmatrix} \alpha_2\beta_3 + \alpha_3\beta_2 \\ \alpha_3\beta_1 + \alpha_1\beta_3 \\ \alpha_1\beta_2 + \alpha_2\beta_1 \end{pmatrix}, \quad (\text{A.15})$$

$$\mathbf{3} \times \mathbf{3} = \mathbf{3}_a : \begin{pmatrix} \alpha_1 \\ \alpha_2 \\ \alpha_3 \end{pmatrix} \times \begin{pmatrix} \beta_1 \\ \beta_2 \\ \beta_3 \end{pmatrix} = \frac{1}{2} \begin{pmatrix} \alpha_2\beta_3 - \alpha_3\beta_2 \\ \alpha_3\beta_1 - \alpha_1\beta_3 \\ \alpha_1\beta_2 - \alpha_2\beta_1 \end{pmatrix}. \quad (\text{A.16})$$

The remaining products are given by

$$\mathbf{1}' \times \mathbf{3} = \mathbf{3} : \alpha \times \begin{pmatrix} \beta_1 \\ \beta_2 \\ \beta_3 \end{pmatrix} = \alpha \begin{pmatrix} \beta_1 \\ \omega\beta_2 \\ \omega^2\beta_2 \end{pmatrix}, \quad (\text{A.17})$$

$$\mathbf{1}'' \times \mathbf{3} = \mathbf{3} : \alpha \times \begin{pmatrix} \beta_1 \\ \beta_2 \\ \beta_3 \end{pmatrix} = \alpha \begin{pmatrix} \beta_1 \\ \omega^2\beta_2 \\ \omega\beta_2 \end{pmatrix}, \quad (\text{A.18})$$

$$\mathbf{1}' \times \mathbf{1}'' = \mathbf{1} : \alpha\beta, \quad (\text{A.19})$$

$$\mathbf{1}' \times \mathbf{1}' = \mathbf{1}'' : \alpha\beta, \quad (\text{A.20})$$

$$\mathbf{1}'' \times \mathbf{1}'' = \mathbf{1}' : \alpha\beta. \quad (\text{A.21})$$

A.3 Generalised CP transformations

The so called *canonical* CP violation acts on a scalar field ϕ as

$$CP : \phi \rightarrow e^{i\varphi} \phi^*. \quad (\text{A.22})$$

If the field transforms as a (not necessarily irreducible) representation ρ of a flavour symmetry group G

$$\phi \rightarrow \rho(g)\phi \quad g \in G, \quad (\text{A.23})$$

a *generalised* CP transformation [215] is defined by [166]

$$CP' : \phi \rightarrow U\phi^*, \quad (\text{A.24})$$

where U is an unitary matrix acting on flavour space, which has to satisfy a consistency equation

$$U^{-1}\rho(g')U = \rho(g)^*, \quad (\text{A.25})$$

since flavour group and generalised CP transformations have to commute.³ Thus, generalised CP is an automorphism of the flavour group. If CP' is an additional symmetry, U

³Note that the trivial solution $U = \mathbb{1}$ exists for fields transforming in real representations of G .

must not be constructed from the generators of G , hence CP' is an outer automorphism. Their action on the character table correspond to an exchange of rows and columns.

For the flavour symmetry group A_4 , the only possibility for a generalised CP transformation is the outer automorphism

$$u : T \rightarrow T^2, \quad (\text{A.26})$$

since automorphism map elements to elements of the same order. We can check that u also exchanges the irreducible representations $\mathbf{1}'$ and $\mathbf{1}''$

$$\rho_{\mathbf{1}'}(u(T)) = \rho_{\mathbf{1}'}(T^2) = U \rho_{\mathbf{1}'}(T)^* U^{-1} = \rho_{\mathbf{1}'}(T)^* = \rho_{\mathbf{1}''}(T), \quad (\text{A.27})$$

since for one-dimensional representations the unitary matrix U can be represented as phase. We can choose U to be real and therefore for the irreducible representations $\mathbf{1}$, $\mathbf{1}'$, and $\mathbf{1}''$ we find

$$\phi_{\mathbf{1}} \xrightarrow{CP'} \phi_{\mathbf{1}}^*, \quad \phi_{\mathbf{1}'} \xrightarrow{CP'} \phi_{\mathbf{1}'}^*, \quad \text{and} \quad \phi_{\mathbf{1}''} \xrightarrow{CP'} \phi_{\mathbf{1}''}^*. \quad (\text{A.28})$$

For the triplet representation one can solve for U

$$\rho_{\mathbf{3}}(u(T)) = \rho_{\mathbf{3}}(T^2) = \begin{pmatrix} 0 & 0 & 1 \\ 1 & 0 & 0 \\ 0 & 1 & 0 \end{pmatrix} = U \rho_{\mathbf{3}}(T)^* U^{-1} = U \begin{pmatrix} 0 & 1 & 0 \\ 0 & 0 & 1 \\ 1 & 0 & 0 \end{pmatrix} U^{-1} \quad (\text{A.29})$$

and generalised CP is given by

$$\phi_{\mathbf{3}} \xrightarrow{CP'} \begin{pmatrix} 1 & 0 & 0 \\ 0 & 0 & 1 \\ 0 & 1 & 0 \end{pmatrix} \phi_{\mathbf{3}}^*. \quad (\text{A.30})$$

Let us briefly illustrate why generalised CP is important by considering a real field χ transforming as $\mathbf{3}$ under A_4 and a singlet ζ transforming as $\mathbf{1}''$. The canonical CP transformations would be

$$CP : \quad \chi \rightarrow \chi, \quad \zeta \rightarrow \zeta^*. \quad (\text{A.31})$$

Let us investigate the A_4 product

$$(\chi\chi)_{\mathbf{1}'} \zeta = (\chi_1^2 + \omega^2 \chi_2^2 + \omega \chi_3^2) \zeta. \quad (\text{A.32})$$

Under canonical CP this transforms into

$$(\chi\chi)_{\mathbf{1}'} \zeta \xrightarrow{CP'} (\chi\chi)_{\mathbf{1}'} \zeta^*, \quad (\text{A.33})$$

and the transformed product is no longer invariant under A_4 , since ζ^* transforms as $\mathbf{1}'$ and $\mathbf{1}' \times \mathbf{1}' = \mathbf{1}''$. Thus canonical CP is not a viable CP transformation, because there are fields transforming in complex representations in the product.

On the other hand, under generalised CP we have

$$CP' : \begin{pmatrix} \chi_1 \\ \chi_2 \\ \chi_3 \end{pmatrix} \rightarrow \begin{pmatrix} \chi_1 \\ \chi_3 \\ \chi_2 \end{pmatrix}, \quad \zeta \rightarrow \zeta^*. \quad (\text{A.34})$$

Then (A.32) transforms into

$$(\chi\chi)_{1'} \zeta \xrightarrow{CP'} (\chi_1^2 + \omega^2 \chi_3^2 + \omega \chi_2^2) \zeta^*, \quad (\text{A.35})$$

which, since $(\chi_1^2 + \omega^2 \chi_3^2 + \omega \chi_2^2)$ transforms as $\mathbf{1}''$, is invariant under A_4 .

Therefore, in theories with discrete flavour symmetries and fields in complex representations, the absence of a canonical CP transformation does in general not necessarily correspond to CP violation, but rather the physical CP symmetry can correspond to a generalised CP transformation of the flavour group. A categorisation of discrete groups into explicitly CP violating groups and groups with generalised CP can be found for example in [216].

APPENDIX B

Sparticle Mass and Mixing Matrices

Here we show our conventions for the sparticle mass and mixing matrices. We employ SLHA 2 conventions [123] in the Super-CKM (SCKM) and Super-PMNS (SPMNS) basis. These bases are obtained from rotating the sfermion fields correspondingly to their fermion partners, when those are rotated into the mass basis (2.23)

$$y_f \equiv Y_f^{\text{diag}} = \left(U_L^{(f)} \right)^T Y_f \left(U_R^{(f)} \right)^* . \quad (\text{B.1})$$

Then the soft-breaking matrices in the Super-CKM/Super-PMNS basis are obtained from our flavour basis (5.65) by

$$\begin{aligned} \hat{T}_f &\equiv \left(U_R^{(f)} \right)^\dagger T_f^T \left(U_L^{(f)} \right) , \\ \hat{m}_{\tilde{Q}}^2 &\equiv \left(U_L^{(d)} \right)^\dagger m_{\tilde{Q}}^2 \left(U_L^{(d)} \right) , \\ \hat{m}_{\tilde{L}}^2 &\equiv \left(U_L^{(e)} \right)^\dagger m_{\tilde{L}}^2 \left(U_L^{(d)} \right) , \\ \hat{m}_{\tilde{u}}^2 &\equiv \left(U_R^{(u)} \right)^\dagger \left(m_{\tilde{u}}^2 \right)^T \left(U_R^{(u)} \right) , \\ \hat{m}_{\tilde{d}}^2 &\equiv \left(U_R^{(d)} \right)^\dagger \left(m_{\tilde{d}}^2 \right)^T \left(U_R^{(d)} \right) , \\ \hat{m}_{\tilde{e}}^2 &\equiv \left(U_R^{(e)} \right)^\dagger \left(m_{\tilde{e}}^2 \right)^T \left(U_R^{(e)} \right) . \end{aligned} \quad (\text{B.2})$$

The sparticle mass matrices are then defined by

$$\mathcal{L} = -\Phi_f^\dagger M_f^2 \Phi_f , \quad (\text{B.3})$$

with $\Phi_f = (\tilde{f}_{L1}, \tilde{f}_{L2}, \tilde{f}_{L3}, \tilde{f}_{R1}, \tilde{f}_{R2}, \tilde{f}_{R3})^T$ and the sparticle mass matrices by

$$\begin{aligned}
M_{\tilde{u}}^2 &= \begin{pmatrix} V_{\text{CKM}} \hat{m}_{\tilde{Q}}^2 V_{\text{CKM}}^\dagger + \frac{v^2}{2} y_u^2 \sin^2 \beta + D_{u,L} & \frac{v}{\sqrt{2}} \hat{T}_u^\dagger \sin \beta - \mu \frac{v}{\sqrt{2}} y_u \cos \beta \\ \frac{v}{\sqrt{2}} \hat{T}_u \sin \beta - \mu^* \frac{v}{\sqrt{2}} y_u \cos \beta & \hat{m}_{\tilde{u}}^2 + \frac{v^2}{2} y_u^2 \sin^2 \beta + D_{u,R} \end{pmatrix}, \\
M_{\tilde{d}}^2 &= \begin{pmatrix} \hat{m}_{\tilde{Q}}^2 + \frac{v^2}{2} y_d^2 \cos^2 \beta + D_{d,L} & \frac{v}{\sqrt{2}} \hat{T}_d^\dagger \cos \beta - \mu \frac{v}{\sqrt{2}} y_d \sin \beta \\ \frac{v}{\sqrt{2}} \hat{T}_d \cos \beta - \mu^* \frac{v}{\sqrt{2}} y_d \sin \beta & \hat{m}_{\tilde{d}}^2 + \frac{v^2}{2} y_d^2 \cos^2 \beta + D_{d,R} \end{pmatrix}, \\
M_{\tilde{e}}^2 &= \begin{pmatrix} \hat{m}_{\tilde{L}}^2 + \frac{v^2}{2} y_e^2 \cos^2 \beta + D_{e,L} & \frac{v}{\sqrt{2}} \hat{T}_e^\dagger \cos \beta - \mu \frac{v}{\sqrt{2}} y_e \sin \beta \\ \frac{v}{\sqrt{2}} \hat{T}_e \cos \beta - \mu^* \frac{v}{\sqrt{2}} y_e \sin \beta & \hat{m}_{\tilde{e}}^2 + \frac{v^2}{2} y_e^2 \cos^2 \beta + D_{e,R} \end{pmatrix}, \\
M_{\tilde{\nu}}^2 &= V_{\text{PMNS}}^\dagger \hat{m}_{\tilde{L}}^2 V_{\text{PMNS}} + D_{\nu,L}.
\end{aligned} \tag{B.4}$$

The D -terms are

$$\begin{aligned}
D_{f,L} &= \hat{M}_Z^2 (I_3 - Q_e \sin^2 \theta_W) \cos(2\beta) \mathbf{1}_3, \\
D_{f,R} &= \hat{M}_Z^2 Q_e \cos(2\beta) \sin^2 \theta_W \mathbf{1}_3,
\end{aligned} \tag{B.5}$$

where I_3 denotes the $SU(2)_L$ isospin and Q_e the electric charge of the flavour f , and θ_W denotes the weak mixing angle. Note that our convention for μ differs by a sign from the convention in [201].

We define the sfermion mixing matrices by¹

$$\hat{M}_{\tilde{f}}^2 = W_{\tilde{f}} \hat{M}_{\tilde{f}}^{\text{diag}} W_{\tilde{f}}^\dagger. \tag{B.6}$$

The neutralino mixing matrix is defined by

$$M_{\psi^0} = N^T M_{\psi^0}^{\text{diag}} N, \tag{B.7}$$

with

$$M_{\psi^0} = \begin{pmatrix} M_1 & 0 & -M_Z \cos \beta \sin \theta_W & M_Z \sin \beta \sin \theta_W \\ 0 & M_2 & M_Z \cos \beta \cos \theta_W & -M_Z \sin \beta \cos \theta_W \\ -M_Z \cos \beta \sin \theta_W & M_Z \cos \beta \cos \theta_W & 0 & -\mu \\ M_Z \sin \beta \sin \theta_W & -M_Z \sin \beta \cos \theta_W & -\mu & 0 \end{pmatrix}. \tag{B.8}$$

The chargino mixing matrix is defined by

$$M_{\psi^\pm} = U^T M_{\psi^\pm}^{\text{diag}} V, \tag{B.9}$$

with

$$M_{\psi^\pm} = \begin{pmatrix} M_2 & \sqrt{2} M_W \sin \beta \\ \sqrt{2} M_W \cos \beta & \mu \end{pmatrix}. \tag{B.10}$$

¹The SLHA 2 convention sfermion mixing matrices $R_{\tilde{f}}$ can be obtained via $R_{\tilde{f}} = W_{\tilde{f}}^\dagger$.

APPENDIX C

Markov Chain Monte Carlo techniques

In this appendix we briefly review Markov Chain Monte Carlo methods, based on [14,217].

The *Monte Carlo* technique uses large numbers of (pseudo) random numbers to calculate approximations for integrals, e.g. the expectation value of a complicated probability density distribution (pdf). A *Markov Chain* (MC) is a sequence of random variables¹ X_t , where the prediction for the next random variable X_{t+1} depends only on the current variable X_t , and not on any earlier states. Under the conditions that the MC is

irreducible : The MC does not possess independent cycles. In other words, every state can be reached from every other state (not necessarily in one step, though).

aperiodic : The lengths of all possible cycles starting at any state and returning to it have greatest common divisor one.

positive recurrent : Any state of the MC is revisited in finite time.

it has a stationary distribution π , where the probability of being in a particular state is independent of the initial condition. For a large number of time steps the MC approaches π as limit.

A *Markov Chain Monte Carlo* method samples a complicated (posterior) pdf $p(\theta)$ by generating a Markov Chain whose stationary distribution is given by p . A simple MCMC method is the Metropolis algorithm [218].

1. Start with any initial point θ_0 with $p(\theta_0) > 0$.
2. With the current value θ_0 , draw a new candidate point θ' from a *proposal density function* $q(\theta'|\theta_0)$. q can be any symmetric pdf, i.e. $q(\theta_1|\theta_2) = q(\theta_2|\theta_1)$. We will use an uncorrelated multivariate normal distribution with mean θ_0 .
3. Form the *acceptance probability* $\alpha = \min\left(1, \frac{p(\theta')}{p(\theta_0)}\right)$.

¹We restrict the discussion here to one-dimensional random variables. A generalisation to more dimensions is straightforward.

4. Generate a random number u uniformly distributed in $[0, 1]$.
5. If $u \leq \alpha$, accept the new value and set $\theta_0 = \theta'$. Otherwise, θ' is rejected and the old point θ_0 stays.
6. Repeat from step 2.

When fitting a model to data points with mean \bar{y}_i and standard deviation σ_i , the posterior pdf we are interested in is the likelihood function

$$\mathcal{L}(\theta) = e^{-\frac{\chi^2(\theta)}{2}} \quad (\text{C.1})$$

with

$$\chi^2(\theta) = \sum_i \frac{(y_i(\theta) - \bar{y}_i)^2}{\sigma_i^2}. \quad (\text{C.2})$$

Starting from θ_0 , the Metropolis algorithm will draw new candidates θ' . While all parameter points with higher likelihood are accepted, a few parameters with worse χ^2 are also accepted and allow the chain to browse a wider region of parameters space and e.g. escape local minima. Eventually the MC converges to its equilibrium, which constitutes the desired result. The first time steps until equilibrium is reached are denoted as “burn-in phase” and removed from the analysis. The efficiency of the Metropolis algorithm can be tuned by the *step width* Δ of the proposal density function, which in our case are the standard deviations of the multivariate normal distribution. For too small Δ , the stay count for each step is very small and parameter space is explored very badly. For too large Δ , the stay counts are high and the MCMC has to be run longer to build up statistics. Optimal performance is achieved with an acceptance rate r_{acc} of about 40%, decreasing towards 20% for large numbers of parameters. This is illustrated for three choices of Δ in figure C.1. The optimal choice for the proposal pdf is similar to the target pdf and its step-width is close to the target pdf standard deviation.

Whether the Metropolis algorithm has converged can be inspected by looking at the trace plots. A numerical criteria for convergence we use in this thesis is the *potential scale reduction factor* (psrf) \hat{R} suggested by Gelman and Rubin [219]

1. Instead of a single, very long MCMC, calculate m chains of length n .
2. Calculate the *within-chain variance* $W \equiv \frac{1}{m} \sum_{j=1}^m s_j^2$, where s_j is the variance of the $i = 1 \dots n$ values θ_j^i in the j th chain: $s_j^2 \equiv \frac{1}{n-1} \sum_{i=1}^n (\theta_j^i - \bar{\theta}_j)^2$ and $\bar{\theta}_j$ is the mean of all θ_j^i .
3. Calculate the *between-chain variance* $B \equiv \frac{n}{m-1} \sum_{j=1}^m (\bar{\theta}_j - \bar{\bar{\theta}})^2$, where $\bar{\bar{\theta}}$ is the mean of the $j = 1 \dots m$ values of $\bar{\theta}_j$.
4. Calculate $\hat{R} = \sqrt{\frac{n-1}{n} + \frac{1}{n} \frac{B}{W}}$.

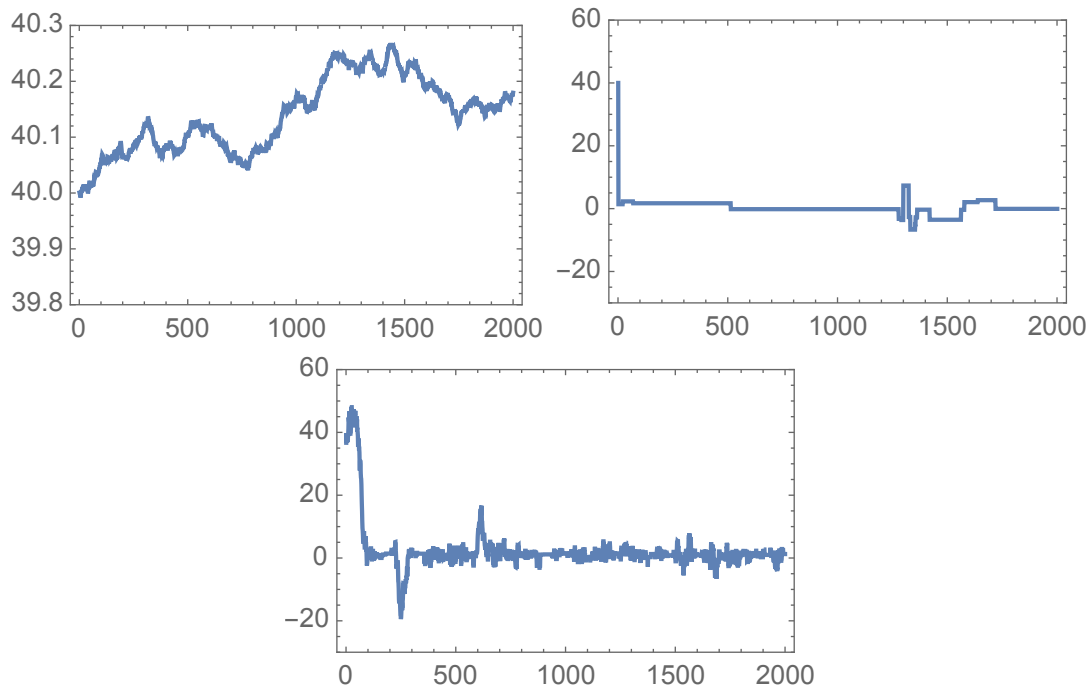


Figure C.1: Trace plots for Metropolis MCMC analyses. For too small Δ with small stay counts and $r_{\text{acc}} = 1$ (left). With too high Δ and *bad mixing* with $r_{\text{acc}} = 0.1\%$ (right). And with optimal Δ and *good mixing* with $r_{\text{acc}} = 40\%$ (center). The burn-in-phase makes up about 400 steps.

The psrf thus compares within-chain and between-chain variance. For $\hat{R} > 1.1$ the MCMC should be run longer to improve convergence. The MCMC is assumed to have converged for $\hat{R} \approx 1$. For higher-dimensional θ the psrf have to be calculated for each parameter individually.

Let us now briefly discuss Bayesian confidence intervals. We obtain a posterior pdf from the MCMC analysis and are interested in the marginalised posterior probability density for particular parameters.² The confidence interval is then given by the region where the posterior pdf is highest. A z sigma *highest posterior density* (hpd) interval is the interval $[\theta_L, \theta_H]$, such that

$$\int_{\theta_L}^{\theta_H} p(\theta) d\theta = \text{erf}\left(\frac{z}{\sqrt{2}}\right) \quad \text{and} \quad p(\theta \in \text{hpd}) > p(\theta \notin \text{hpd}) . \quad (\text{C.3})$$

As shown in figure C.2 the definition of the hpd “confidence interval” agrees with the Frequentist’s confidence interval (CI) if the posterior pdf is a normal distribution. For non-symmetric posterior pdfs or pdfs with several peaks, the hpd intervals allow for a generalisation of the common CIs.

In order to investigate correlations between parameters, (C.3) can be generalised for two

²Here we use the word parameter to describe the fit parameters as well as variables of the fit results.

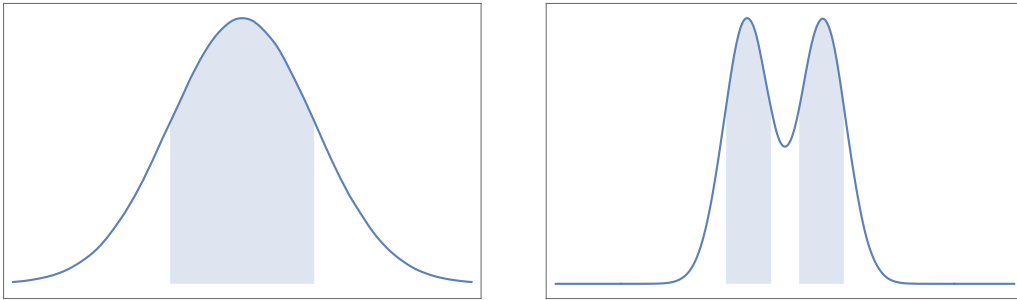


Figure C.2: One sigma hpd intervals for a normal distribution (left) and for an example posterior pdf with two peaks.

or more parameters. An example for a two-dimensional hpd region is shown in figure C.3.

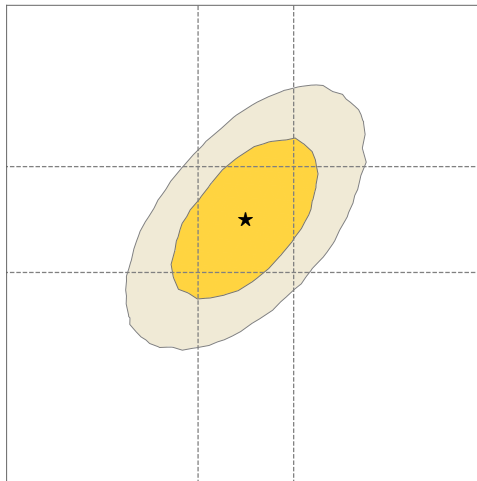


Figure C.3: Example for a two-dimensional hpd region for one sigma (gold) and three sigma (grey). The one sigma hpd intervals for the individual parameters are shown as dashed lines. The star marks the mean value of the MCMC analysis.

APPENDIX D

Appendices to the flavour GUT models

In this appendix we give detailed lists of the messenger fields, shaping symmetries, and supergraphs, which yield the effective superpotentials of the flavour models of parts III and IV.

D.1 Appendix to chapter 7

The quantum numbers of the matter, Higgs, flavon, and driving superfields under $SU(5)$, A_4 , and the shaping symmetry, are presented in table D.1. In table D.2 the quantum numbers of the messenger fields Φ_i are explicitly shown. For each field Φ_i there is a corresponding field $\bar{\Phi}_i$ with “opposite” quantum numbers, i.e. quantum numbers such that a mass term $\Lambda_i \Phi_i \bar{\Phi}_i$ is allowed in the superpotential. Since the quantum numbers of $\bar{\Phi}_i$ can be trivially reconstructed from the corresponding Φ_i , we do not show them explicitly for the sake of brevity.

As discussed in 7.1, in order not to generate undesired effective operators, the messenger sector has to be selected carefully and the choice of the messenger fields is not unique. In the following figures D.1–D.6 we present the supergraphs that give rise to the effective superpotential operators of 7.2 and 7.3, when the heavy messenger fields are integrated out. Each supergraph topology in figures D.1–D.5 corresponds to several operators, which are shown in the table below each graph. In each of the supergraphs, the external fields, which can be either matter, Higgs, flavon, or driving superfields, are labelled by φ_i , whereas the messenger fields are labelled by γ_i and $\bar{\gamma}_i$, respectively. Note that many of the messenger fields occur in more than one operator.

Finally let us comment on the consistency of the different orders of magnitude for the numerical values of the ϵ -parameters defined in (7.10) and (7.12) and given in table 7.2. They arise as effective couplings after the heavy messenger fields are intergrated out and the vevs of the flavon and GUT Higgs superfields are inserted in the corresponding non-renormalisable operators. As can be checked from figures D.1–D.6, the different orders of magnitude of the parameters, which are needed to fit the data, can originate from an appropriate choice for the masses of the individual messenger fields, which appear in the

	$SU(5)$	A_4	$\mathbb{Z}_2^{(a)}$	$\mathbb{Z}_2^{(b)}$	$\mathbb{Z}_6^{(a)}$	$\mathbb{Z}_6^{(b)}$	$\mathbb{Z}_6^{(c)}$	$\mathbb{Z}_6^{(d)}$	$\mathbb{Z}_6^{(e)}$	$U(1)_a$	$U(1)_b$	$U(1)_R$
Matter superfields												
\mathcal{F}	$\bar{\mathbf{5}}$	$\mathbf{3}$.	.	.	4	4	.	.	.	2	1
\mathcal{T}_1	$\mathbf{10}$	1	1
\mathcal{T}_2	$\mathbf{10}$.	.	.	1	.	4	.	.	.	1	1
\mathcal{T}_3	$\mathbf{10}$.	1	.	.	.	2	.	.	.	1	1
N_1^c	2	2	1	.	.	.	1
N_2^c	2	2	1	1	.	.	1
Higgs superfields												
H_5	$\mathbf{5}$	2	.	.	.	-2	.
\bar{H}_5	$\bar{\mathbf{5}}$.	.	1	.	2	.	.	.	-1	.	.
H_{45}	$\mathbf{45}$	4	5	.	.	1	.	2
\bar{H}_{45}	$\bar{\mathbf{45}}$	2	1	.	.	-1	.	.
H_{24}	$\mathbf{24}$	1	-3	.
Flavon superfields												
ϕ_2	.	$\mathbf{3}$	1
ϕ_3	.	$\mathbf{3}$	1	1
ϕ_{ab}	.	$\mathbf{3}$.	1	5	.	4
ϕ_{N_1}	.	$\mathbf{3}$	4	5
ϕ_{N_2}	.	$\mathbf{3}$	4	5	5	.	.	.
χ	.	$\mathbf{1}'$	1	1	.	.	5
ξ_{12}	1
ξ_{23}	.	.	1	.	5	.	4
ξ_M	1
Driving superfields												
S	2
D_{ab}^α	2	.	4	2
D_{ab}^β	.	.	.	1	3	2
D_{ab}^γ	4	.	2	2
D_{N_1}	3	.	.	.	2
D'_{N_2}	.	$\mathbf{1}'$	4	2	2	.	.	2
D''_{N_2}	.	$\mathbf{1}''$	4	2	2	.	.	2
A_2	.	$\mathbf{3}$	4	2
A_3	.	$\mathbf{3}$	2
$O_{2;3}$.	.	1	1	.	.	5	2
$O_{N_1;N_2}$	4	2	1	.	.	2

Table D.1: The matter, Higgs, flavon, and driving superfields of the model in chapter 7. A dot means that the field is an invariant singlet under the respective symmetry. Note that the $U(1)$ symmetries will get explicitly broken to \mathbb{Z}_n symmetries by the Higgs sector.

	SU(5)	A_4	$\mathbb{Z}_2^{(a)}$	$\mathbb{Z}_2^{(b)}$	$\mathbb{Z}_6^{(a)}$	$\mathbb{Z}_6^{(b)}$	$\mathbb{Z}_6^{(c)}$	$\mathbb{Z}_6^{(d)}$	$\mathbb{Z}_6^{(e)}$	$U(1)_a$	$U(1)_b$	$U(1)_R$
Φ_1	$\bar{\mathbf{5}}$	4	2	5	.	.	2	1
Φ_2	$\bar{\mathbf{5}}$	4	2	5	5	.	2	1
Φ_3	$\bar{\mathbf{5}}$.	1	.	1	2	2
Φ_4	.	$\mathbf{3}$.	.	2	.	4	2
Φ_5	.	$\mathbf{3}$	4	2	.	.	.	2
Φ_6	$\overline{\mathbf{45}}$	4	5	.	.	1	-1	1
Φ_7	$\mathbf{5}$	2	1	.	.	.	-2	1
Φ_8	$\mathbf{5}$	$\mathbf{3}$.	.	1	4	2	.	.	1	.	2
Φ_9	$\overline{\mathbf{10}}$.	.	.	5	.	2	.	.	-1	2	1
Φ_{10}	$\bar{\mathbf{5}}$.	1	1	.	4	4	.	.	1	-1	1
Φ_{11}	$\mathbf{5}$.	1	1	.	2	2	.	.	.	-2	1
Φ_{12}	$\overline{\mathbf{10}}$	$\mathbf{3}$.	1	.	.	4	.	.	.	-1	1
Φ_{13}	.	$\mathbf{1}'$.	.	2	.	4	2
Φ_{14}	.	$\mathbf{1}''$.	.	2	.	4	2
Φ_{15}	4	2
Φ_{16}	3
Φ_{17}	4	2
Φ_{18}	3
Φ_{19}	.	$\mathbf{1}'$	2	2
Φ_{20}	.	.	1	1	.	.	3
Φ_{21}	.	$\mathbf{3}$	1	.	3
Φ_{22}	4	4	2	2	.	.	2
Φ_{23}	4	2	2	.	.	2
Φ_{24}	4	4	2	.	.	.	2
Φ_{25}	4	2	.	.	.	2
Φ_{26}	4	2
Φ_{27}	2	2
Φ_{28}	$\mathbf{10}$	4	.	.	.	1	.
Φ_{29}	2	4	4	.	.	2
Φ_{30}	.	$\mathbf{3}$	2	4	.	.	.	2
Φ_{31}	5
Φ_{32}	$\mathbf{5}$	$\mathbf{3}$.	1	.	4	5	.	.	1	.	2
Φ_{33}	$\overline{\mathbf{10}}$	$\mathbf{1}''$.	1	.	.	5	.	.	-1	2	1
Φ_{34}	$\overline{\mathbf{10}}$	$\mathbf{1}''$.	1	.	.	5	.	.	.	-1	1

Table D.2: The messenger fields of the SUSY flavour GUT model in chapter 7. To each Φ_i there exists an $\bar{\Phi}_i$ with “opposite” quantum numbers. A dot means that the field is an invariant singlet under the respective symmetry. Note that the $U(1)$ symmetries will get explicitly broken to \mathbb{Z}_n symmetries by the Higgs sector.

corresponding effective operators. For example, consider the parameters $\tilde{\epsilon}_2$, $\tilde{\epsilon}_3$, and $\hat{\epsilon}_\chi$. Up

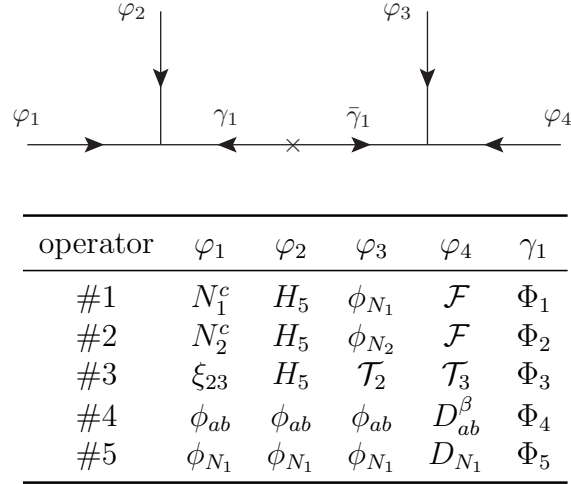


Figure D.1: List of order 4 operators in the effective superpotential.

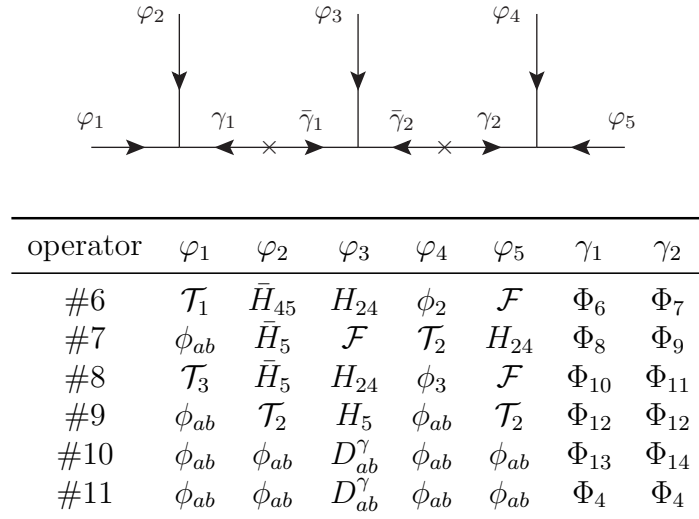


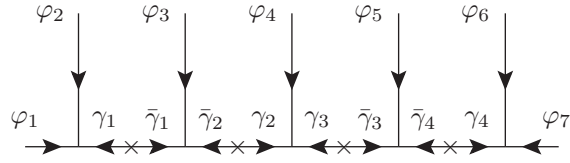
Figure D.2: List of order 5 operators in the effective superpotential.

to messenger couplings which may be assumed to be $\mathcal{O}(1)$, they are given by

$$\tilde{\epsilon}_2 = \frac{\langle H_{24} \rangle \langle \phi_2 \rangle}{\Lambda_6 \Lambda_7}, \quad \tilde{\epsilon}_3 = \frac{\langle H_{24} \rangle \langle \phi_3 \rangle}{\Lambda_{10} \Lambda_{11}}, \quad \hat{\epsilon}_\chi = \frac{\langle H_{24} \rangle \langle \phi_2 \rangle \langle \chi \rangle}{\Lambda_{32} \Lambda_{33} \Lambda_{34}}. \quad (\text{D.1})$$

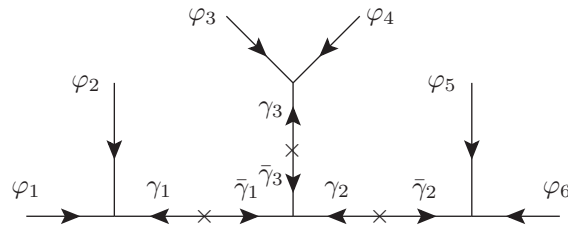
These messenger mass scales are specific to these parameters and therefore the hierarchy

$$|\tilde{\epsilon}_2| \ll |\hat{\epsilon}_\chi| \ll |\tilde{\epsilon}_3| \quad (\text{D.2})$$



operator	φ_1	φ_2	φ_3	φ_4	φ_5	φ_6	φ_7	γ_1	γ_2	γ_3	γ_4
#12	ξ_{12}	ξ_{12}	ξ_{12}	S	ξ_{12}	ξ_{12}	ξ_{12}	Φ_{15}	Φ_{16}	Φ_{16}	Φ_{15}
#13	ξ_M	ξ_M	ξ_M	S	ξ_M	ξ_M	ξ_M	Φ_{17}	Φ_{18}	Φ_{18}	Φ_{17}
#14	χ	χ	χ	S	χ	χ	χ	Φ_{19}	Φ_{20}	Φ_{20}	Φ_{19}
#15	ϕ_{ab}	ϕ_{ab}	ξ_{23}	S	ξ_{23}	ϕ_{ab}	ϕ_{ab}	Φ_4	Φ_{21}	Φ_{21}	Φ_4

Figure D.3: List of order 7 operators in the effective superpotential from supergraphs with linear topology.



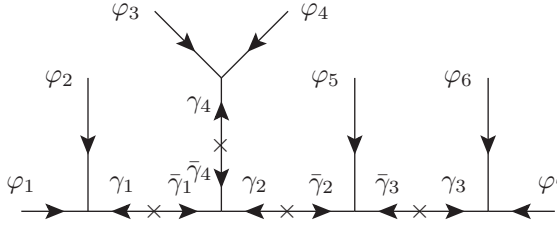
operator	φ_1	φ_2	φ_3	φ_4	φ_5	φ_6	γ_1	γ_2	γ_3
#16	ξ_M	ξ_M	ϕ_{N_2}	ϕ_{N_2}	N_2^c	N_2^c	Φ_{17}	Φ_{22}	Φ_{23}
#17	ξ_M	ξ_M	ϕ_{N_1}	ϕ_{N_1}	N_1^c	N_1^c	Φ_{17}	Φ_{24}	Φ_{25}

Figure D.4: List of order 6 operators in the effective superpotential from supergraphs with non-linear topology.

can arise from a hierarchy of

$$\Lambda_{10}\Lambda_{11} \ll \frac{\Lambda_{32}\Lambda_{33}\Lambda_{34}}{\langle\chi\rangle} \ll \Lambda_6\Lambda_7. \tag{D.3}$$

Similar arguments hold for the other parameters in chapter 7.



operator	φ_1	φ_2	φ_3	φ_4	φ_5	φ_6	φ_7	γ_1	γ_2	γ_3	γ_4
#18	ϕ_2	ϕ_2	ϕ_2	ϕ_2	\mathcal{T}_1	\mathcal{T}_1	H_5	Φ_{26}	Φ_{27}	Φ_{28}	Φ_{26}
#19	ϕ_{N_2}	ϕ_{N_2}	ϕ_{N_2}	ϕ_{N_2}	S	ϕ_{N_2}	ϕ_{N_2}	Φ_{23}	Φ_{29}	Φ_{23}	Φ_{23}
#20	ϕ_{N_1}	ϕ_{N_1}	ϕ_{N_1}	ϕ_{N_1}	S	ϕ_{N_1}	ϕ_{N_1}	Φ_{25}	Φ_{30}	Φ_5	Φ_5
#21	S	ξ_{12}	ξ_{12}	ξ_{12}	ξ_{12}	ξ_{12}	ξ_{12}	Φ_{31}	Φ_{16}	Φ_{15}	Φ_{15}
#22	ϕ_2	ϕ_2	ϕ_2	ϕ_2	S	ϕ_2	ϕ_2	Φ_{26}	Φ_{27}	Φ_{26}	Φ_{26}

Figure D.5: List of order 7 operators in the effective superpotential from supergraphs with non-linear topology.

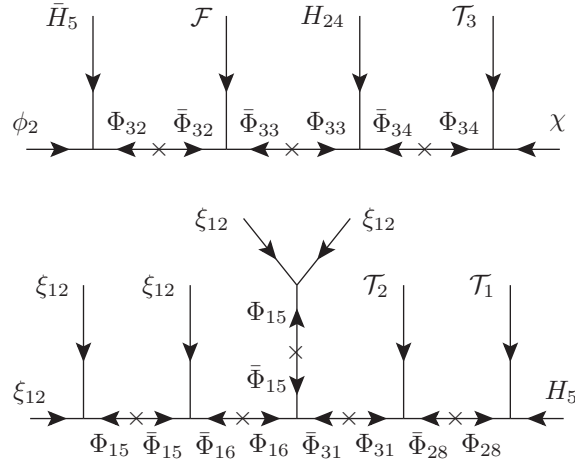


Figure D.6: Additional effective operators of order 6: $[\mathcal{T}_3 H_{24}]_{10}$ $[\mathcal{F} \bar{H}_5]_{\overline{10}}$ $\chi \phi_2$ (top) and of order 8: $\mathcal{T}_1 \mathcal{T}_2 \xi_{12}^5 H_5$ (bottom).

D.2 Appendix to chapter 8

First we show the quantum numbers of the matter, Higgs, flavon, and driving superfields of our second SUSY flavour GUT model under $SU(5)$, A_4 , and the shaping symmetry in table D.3. In table D.4, half of the messenger superfields and their charges under the model's

symmetry are listed. Again, to each messenger superfield Φ_i a “partner” $\bar{\Phi}_i$ exists, such that they form a mass term $\Lambda_i \Phi_i \bar{\Phi}_i$ in the renormalisable superpotential. The charges of $\bar{\Phi}_i$ are not given in the table, since they can be trivially determined from the charges of the corresponding field Φ_i .

Let us stress again the importance of the messenger sector to obtain a predictive SUSY flavour GUT model. Without a renormalisable superpotential that UV completes the effective superpotentials in chapter 8, the model’s symmetries could e.g. allow for effective operators which yield undesired large Yukawa matrix elements where a vanishing entry is desired. In addition, due to many possibilities to contract $SU(5)$ indices, linear combinations of effective terms with different CG factors would appear and the model would lose its ability to predict viable GUT scale quark-lepton mass ratios. We have therefore carefully constructed the renormalisable messenger superpotential, which gives rise to the superpotentials of chapter 8 when the heavy messenger superfields are integrated out. It is presented in the form of supergraphs shown in the figures D.7–D.12. As in the appendix to chapter 7, for each supergraph topology we list all operators in tables below each graph, denoting external fields as φ_i and messenger fields as γ_i and $\bar{\gamma}_i$.

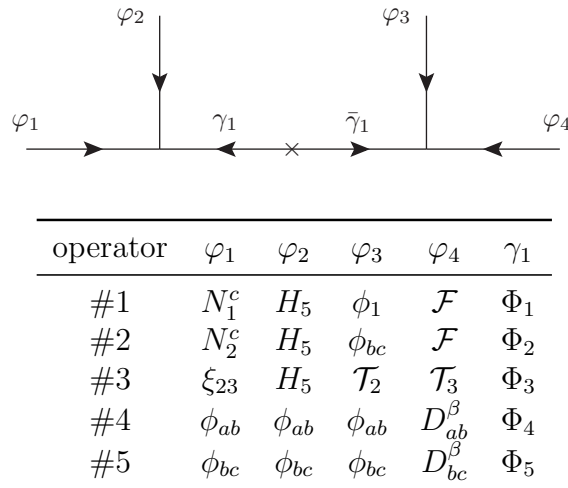
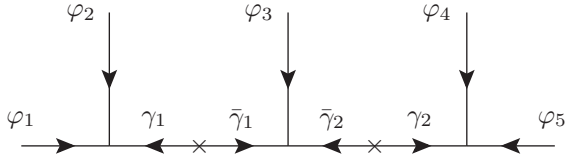


Figure D.7: List of order 4 operators in the effective superpotential.



operator	φ_1	φ_2	φ_3	φ_4	φ_5	γ_1	γ_2
#6	\mathcal{T}_1	\bar{H}_{45}	H_{24}	ϕ_2	\mathcal{F}	Φ_6	Φ_7
#7	\mathcal{T}_2	H_{24}	\mathcal{F}	ϕ_{ab}	\bar{H}_5	Φ_8	Φ_9
#8	\mathcal{T}_3	\bar{H}_5	H_{24}	ϕ_3	\mathcal{F}	Φ_{10}	Φ_{11}
#9	\mathcal{T}_2	ϕ_{ab}	H_5	ϕ_{ab}	\mathcal{T}_2	Φ_{12}	Φ_{12}
#10	ϕ_{ab}	ϕ_{ab}	D_{ab}^γ	ϕ_{ab}	ϕ_{ab}	Φ_4	Φ_4
#11	ϕ_{ab}	ϕ_{ab}	D_{ab}^γ	ϕ_{ab}	ϕ_{ab}	Φ_{13}	Φ_{14}
#12	ϕ_{bc}	ϕ_{bc}	D_{bc}^γ	ϕ_{bc}	ϕ_{bc}	Φ_5	Φ_5
#13	ϕ_{bc}	ϕ_{bc}	D_{bc}^γ	ϕ_{bc}	ϕ_{bc}	Φ_{15}	Φ_{15}

Figure D.8: List of order 5 operators in the effective superpotential and corresponding messenger fields.

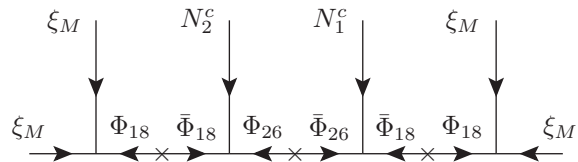


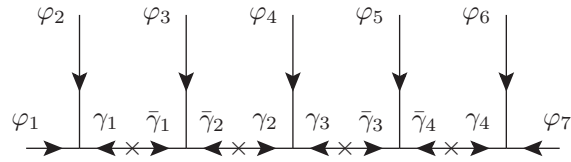
Figure D.9: The only effective operator of order 6 (#14): $N_1 N_2 \xi_M^4$.

	SU(5)	A_4	$\mathbb{Z}_2^{(a)}$	$\mathbb{Z}_2^{(b)}$	$\mathbb{Z}_6^{(a)}$	$\mathbb{Z}_6^{(b)}$	$\mathbb{Z}_6^{(c)}$	$\mathbb{Z}_6^{(d)}$	$U(1)_a$	$U(1)_b$	$U(1)_R$
Matter superfields											
\mathcal{F}	$\bar{\mathbf{5}}$	$\mathbf{3}$.	.	2	.	.	1	2	.	1
\mathcal{T}_1	$\mathbf{10}$.	1	.	.	.	1	.	1	.	1
\mathcal{T}_2	$\mathbf{10}$	1	.	.	1	.	1
\mathcal{T}_3	$\mathbf{10}$.	.	1	1	.	1
N_1^c	4	.	.	2	.	.	1
N_2^c	4	.	.	4	.	.	1
Higgs superfields											
H_5	$\mathbf{5}$	-2	.	.
\bar{H}_5	$\bar{\mathbf{5}}$	-1	.
H_{45}	$\mathbf{45}$.	1	.	.	.	2	.	.	1	2
\bar{H}_{45}	$\bar{\mathbf{45}}$.	1	.	.	.	4	.	.	-1	.
H_{24}	$\mathbf{24}$.	.	.	4	.	.	5	-3	1	.
Flavon superfields											
ϕ_1	.	$\mathbf{3}$	3	.	.	.
ϕ_2	.	$\mathbf{3}$	1
ϕ_3	.	$\mathbf{3}$.	1
ϕ_{ab}	.	$\mathbf{3}$.	.	.	5
ϕ_{bc}	.	$\mathbf{3}$	1	.	.	.
ξ_{12}	.	.	1	.	.	1	1
ξ_{23}	.	.	.	1	.	5
ξ_M	1
Driving superfields											
S	2
D_{ab}^α	2	2
D_{ab}^β	3	2
D_{ab}^γ	4	2
D_{bc}^β	3	.	.	2
D_{bc}^γ	2	.	.	2
$O_{1;2}, O'_{1;2}$.	$\mathbf{1}, \mathbf{1}'$	5	3	.	.	2
$O_{1;3}, O'_{1;3}$.	$\mathbf{1}, \mathbf{1}'$.	1	.	.	.	3	.	.	2
$O_{2;3}, O'_{2;3}$.	$\mathbf{1}, \mathbf{1}'$.	1	.	.	5	.	.	.	2

Table D.3: The matter, Higgs, flavon, and driving superfields of the SUSY flavour GUT model in chapter 8. A dot indicates that the field is an invariant singlet under the corresponding symmetry. Note that the $U(1)$ symmetries will get explicitly broken to \mathbb{Z}_n symmetries by the Higgs sector.

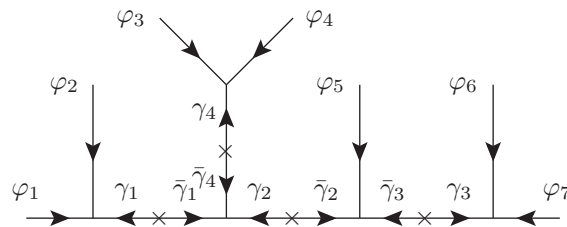
	SU(5)	A_4	$Z_2^{(a)}$	$Z_2^{(b)}$	$Z_6^{(a)}$	$Z_6^{(b)}$	$Z_6^{(c)}$	$Z_6^{(d)}$	$U(1)_a$	$U(1)_b$	$U(1)_R$
Φ_1	$\bar{\mathbf{5}}$.	.	.	2	.	.	4	2	.	1
Φ_2	$\bar{\mathbf{5}}$.	.	.	2	.	.	2	2	.	1
Φ_3	$\bar{\mathbf{5}}$.	.	1	.	1	.	.	2	.	2
Φ_4	.	$\mathbf{3}$.	.	.	2	2
Φ_5	.	$\mathbf{3}$	4	.	.	2
Φ_6	$\overline{\mathbf{45}}$	1	.	-1	1	1
Φ_7	$\mathbf{5}$.	.	.	4	.	5	5	-2	.	1
Φ_8	$\overline{\mathbf{10}}$.	.	.	2	5	.	1	2	-1	1
Φ_9	$\mathbf{5}$	$\mathbf{3}$.	.	.	1	.	.	.	1	2
Φ_{10}	$\bar{\mathbf{5}}$.	.	1	-1	1	1
Φ_{11}	$\mathbf{5}$.	.	1	4	.	.	5	-2	.	1
Φ_{12}	$\overline{\mathbf{10}}$	$\mathbf{3}$	-1	.	1
Φ_{13}	.	$\mathbf{1}'$.	.	.	2	2
Φ_{14}	.	$\mathbf{1}''$.	.	.	2	2
Φ_{15}	4	.	.	2
Φ_{16}	4	4	.	.	.	2
Φ_{17}	.	.	1	.	.	3	3
Φ_{18}	4	2
Φ_{19}	3
Φ_{20}	.	$\mathbf{3}$.	1	.	3
Φ_{21}	4	.	.	.	2
Φ_{22}	2	.	.	.	2
Φ_{23}	$\mathbf{10}$.	1	.	.	.	5	.	1	.	1
Φ_{24}	.	$\mathbf{3}$	2	.	.	2
Φ_{25}	.	.	1	.	.	5	5
Φ_{26}	2	.	.	1

Table D.4: The messenger superfields used to generate the effective operators of the model in chapter 8. To each Φ_i there exists an $\bar{\Phi}_i$ with “opposite” quantum numbers. A dot means that the field is an invariant singlet under the respective symmetry. Note that the $U(1)$ symmetries will get explicitly broken to \mathbb{Z}_n symmetries by the Higgs sector.



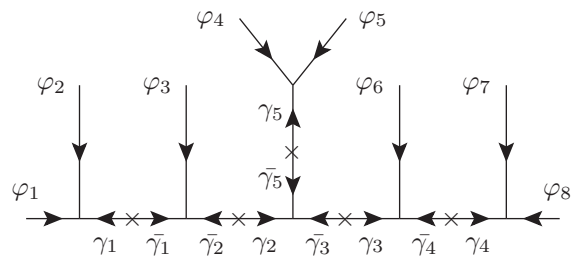
operator	φ_1	φ_2	φ_3	φ_4	φ_5	φ_6	φ_7	γ_1	γ_2	γ_3	γ_4
#15	ξ_{12}	ξ_{12}	ξ_{12}	S	ξ_{12}	ξ_{12}	ξ_{12}	Φ_{16}	Φ_{17}	Φ_{17}	Φ_{16}
#16	ξ_M	ξ_M	ξ_M	S	ξ_M	ξ_M	ξ_M	Φ_{18}	Φ_{19}	Φ_{19}	Φ_{18}
#17	ϕ_{ab}	ϕ_{ab}	ξ_{23}	S	ξ_{23}	ϕ_{ab}	ϕ_{ab}	Φ_4	Φ_{20}	Φ_{20}	Φ_4

Figure D.10: List of order 7 operators in the effective superpotential from supergraphs with linear topology.



operator	φ_1	φ_2	φ_3	φ_4	φ_5	φ_6	φ_7	γ_1	γ_2	γ_3	γ_4
#18	ϕ_2	ϕ_2	ϕ_2	ϕ_2	\mathcal{T}_1	\mathcal{T}_1	H_5	Φ_{21}	Φ_{22}	Φ_{23}	Φ_{21}
#19	ϕ_{bc}	ϕ_{bc}	ϕ_{bc}	ϕ_{bc}	S	ϕ_{bc}	ϕ_{bc}	Φ_{15}	Φ_{24}	Φ_5	Φ_5
#20	S	ξ_{12}	ξ_{12}	ξ_{12}	ξ_{12}	ξ_{12}	ξ_{12}	Φ_{25}	Φ_{17}	Φ_{16}	Φ_{16}
#21	ϕ_2	ϕ_2	ϕ_2	ϕ_2	S	ϕ_2	ϕ_2	Φ_{21}	Φ_{22}	Φ_{21}	Φ_{21}

Figure D.11: List of order 7 operators in the effective superpotential from supergraphs with non-linear topology.



operator	φ_1	φ_2	φ_3	φ_4	φ_5	φ_6	φ_7	φ_8	γ_1	γ_2	γ_3	γ_4	γ_5
#22	ξ_{12}	ξ_{12}	ξ_{12}	ξ_{12}	ξ_{12}	\mathcal{T}_2	\mathcal{T}_1	H_5	Φ_{16}	Φ_{17}	Φ_{25}	Φ_{23}	Φ_{16}
#23	ξ_M	ξ_M	N_1^c	ϕ_{bc}	ϕ_{bc}	N_1^c	ξ_M	ξ_M	Φ_{18}	Φ_{26}	$\bar{\Phi}_{26}$	Φ_{18}	Φ_{15}

Figure D.12: List of order 8 operators in the effective superpotential from supergraphs with non-linear topology.

D.3 Appendix to the first model of chapter 9

In figures D.13 and D.14 we show the supergraphs yielding the effective superpotentials \mathcal{W}_d and \mathcal{W}_u when the heavy messengers are integrated out.

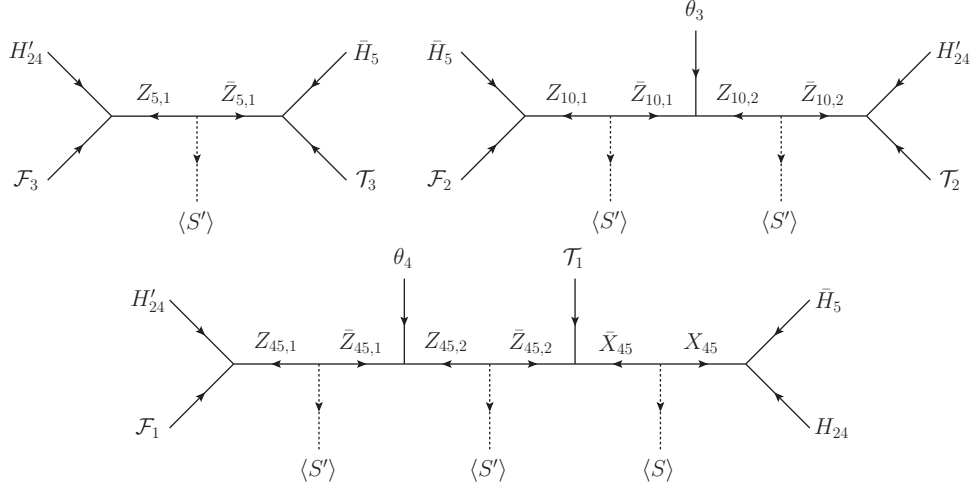


Figure D.13: Supergraphs leading to the effective superpotential \mathcal{W}_d of our model in 9.4.1 when the heavy messenger fields get integrated out.

All superfields of the model 9.4.1 are presented in the tables D.5 and D.6, including their charges under the discrete shaping symmetry. As shown in figures D.13 and D.14 the messenger pairs $Z_{5,1}\bar{Z}_{5,1}$, $Z_{10,1}\bar{Z}_{10,1}$, $Z_{10,2}\bar{Z}_{10,2}$, $Z_{45,1}\bar{Z}_{45,1}$, and $Z_{45,2}\bar{Z}_{45,2}$ get their masses through the vevs of S and S' . The other messengers in the lower part of table D.6 have direct mass terms, so we do not show the charges of their corresponding conjugated partners \bar{Z}_i , which can be trivially obtained from the charges of Z_i .

Let us now discuss the messenger fields appearing in figure D.14 closer. There are three supergraphs generating the superpotential term y_{12} . The renormalisable superpotential corresponding to figure D.14 is

$$\begin{aligned}
\mathcal{W} \supset & \gamma_1 H_5 \mathcal{T}_1 Z_{10,4} + \gamma_2 H_5 \mathcal{T}_2 Z_{10,3} + \gamma_3 \mathcal{T}_3 \theta_1 \bar{Z}_{10,3} + \gamma_\theta \theta_1^2 Z_1 \\
& + \lambda_1 \theta_2 Z_2 \bar{Z}_1 + \lambda_{10} \theta_2 Z_{10,3} \bar{Z}_{10,4} \\
& + \eta_1 \mathcal{T}_1 \bar{Z}_{10,3} \bar{Z}_2 + \eta_2 \mathcal{T}_2 \bar{Z}_{10,4} \bar{Z}_2 + \eta'_2 \mathcal{T}_2 \bar{Z}_{10,3} \bar{Z}_1 \\
& + M_1 Z_1 \bar{Z}_1 + M_2 Z_2 \bar{Z}_2 + M_{10,3} Z_{10,3} \bar{Z}_{10,3} + M_{10,4} Z_{10,4} \bar{Z}_{10,4} , \tag{D.4}
\end{aligned}$$

where we explicitly denote the coupling constants at the ends of a diagram with γ_x , coupling constants in the middle of the diagrams with λ_x if they involve θ_j , η_i if they involve \mathcal{T}_i , and messenger masses with M_x .

After Z_x and \bar{Z}_x are integrated out and the flavons θ_i obtain vevs, the elements (9.62)

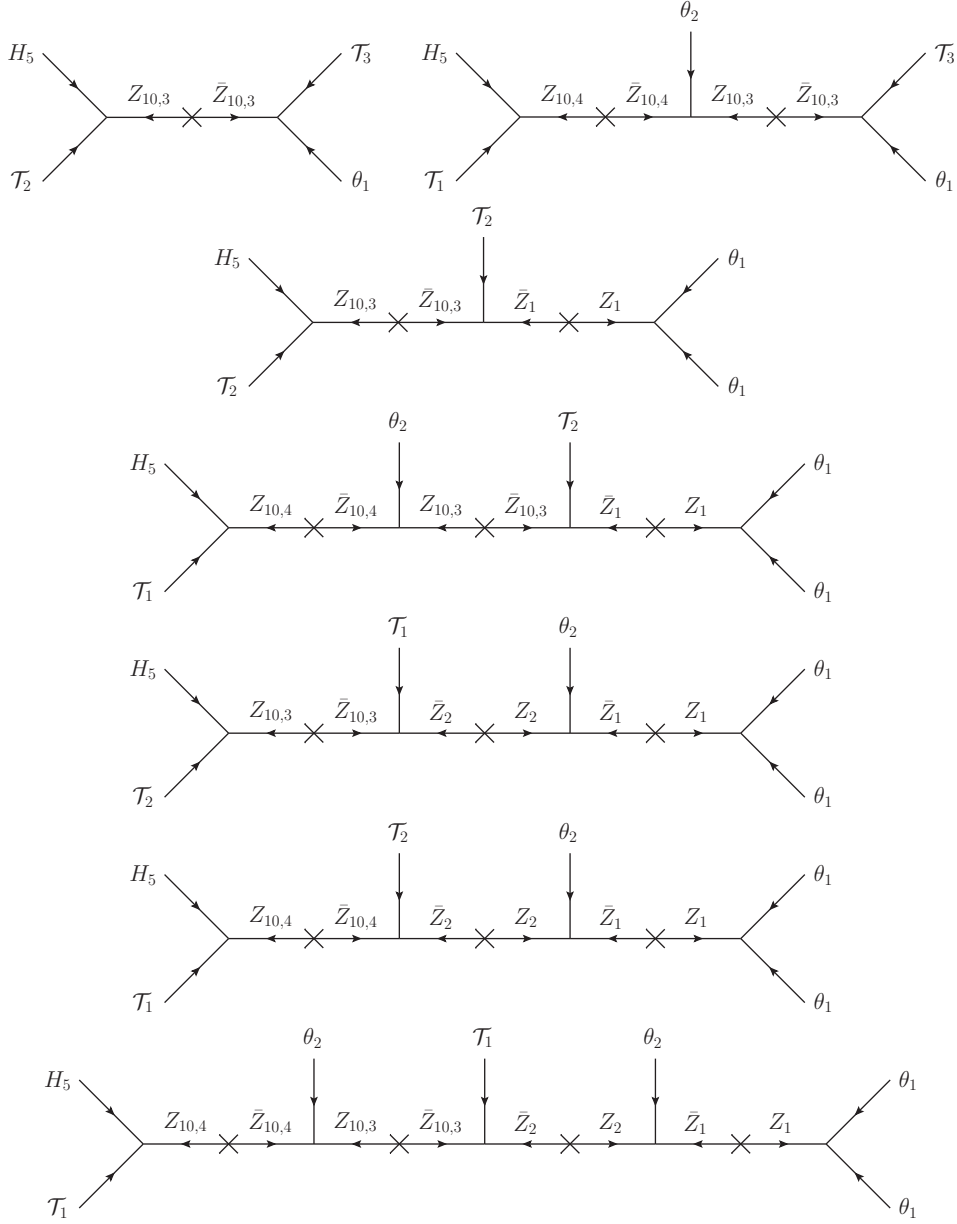


Figure D.14: Supergraphs leading to the effective superpotential \mathcal{W}_u of our model in 9.4.1 when the heavy messenger fields get integrated out. Note that there are three supergraphs contributing to the superpotential term generating y_{12} .

of Y_u are given by

$$y_{11} = \gamma_1 \lambda_{10} \eta_1 \lambda_1 \gamma_\theta \frac{\langle \theta_1 \rangle^2 \langle \theta_2 \rangle^2}{M_1 M_2 M_{10,3} M_{10,4}},$$

$$y_{12} = \gamma_2 \eta_1 \lambda_1 \gamma_\theta \frac{\langle \theta_1 \rangle^2 \langle \theta_2 \rangle}{M_1 M_2 M_{10,3}} + \gamma_1 \eta_2 \lambda_1 \gamma_\theta \frac{\langle \theta_1 \rangle^2 \langle \theta_2 \rangle}{M_1 M_2 M_{10,4}} + \gamma_1 \lambda_{10} \eta'_2 \gamma_\theta \frac{\langle \theta_1 \rangle^2 \langle \theta_2 \rangle}{M_1 M_{10,3} M_{10,4}},$$

$$\begin{aligned}
y_{22} &= \gamma_2 \eta'_2 \gamma_\theta \frac{\langle \theta_1 \rangle^2}{M_1 M_{10,3}} , \\
y_{13} &= \gamma_1 \lambda_{10} \gamma_3 \frac{\langle \theta_1 \rangle \langle \theta_2 \rangle}{M_{10,3} M_{10,4}} , \\
y_{23} &= \gamma_2 \gamma_3 \frac{\langle \theta_1 \rangle}{M_{10,3}} ,
\end{aligned} \tag{D.5}$$

and y_{33} is a renormalisable Yukawa coupling coefficient.

One might feel motivated to remove the messenger pair Z_2, \bar{Z}_2 from the spectrum, thereby eliminating two supergraphs and thus the first two terms contributing to y_{12} .¹ In this case however, without $Z_2 \bar{Z}_2$, evaluating y_{12} would yield

$$\begin{aligned}
y_{12} &= \gamma_1 \lambda_{10} \eta'_2 \gamma_\theta \frac{\langle \theta_1 \rangle^2 \langle \theta_2 \rangle}{M_1 M_{10,3} M_{10,4}} = y_{13} \frac{\langle \theta_1 \rangle}{M_1} \frac{\eta'_2 \gamma_\theta}{\gamma_3} \\
&= y_{13} y_{22} \frac{M_{10,3}}{\langle \theta_1 \rangle} \frac{1}{\gamma_2 \gamma_3} = \frac{y_{13} y_{22}}{y_{23}} .
\end{aligned} \tag{D.6}$$

From a small angle expansion of Y_u one finds for the mixing angles

$$\theta_{12}^u = \frac{y_{12}}{y_{22}} , \quad \theta_{13}^u = \frac{y_{13}}{y_{33}} , \quad \text{and} \quad \theta_{23}^u = \frac{y_{23}}{y_{33}} , \tag{D.7}$$

which are identical to the GUT scale CKM mixing angles since our model features diagonal Y_d . Therefore (D.6) would imply the phenomenologically bad GUT scale relation

$$\theta_C = \frac{\theta_{13}^{\text{CKM}}}{\theta_{23}^{\text{CKM}}} . \tag{D.8}$$

To fit Y_u to the observed data an additional degree of freedom is needed. In our model this is realised through $Z_2 \bar{Z}_2$ enabling additional diagrams contributing to y_{12} .

This illustrates that besides guaranteeing a certain Yukawa matrix structure and unique CG factors, the messenger sector also has to be carefully chosen with respect to its couplings, to avoid non-phenomenological predictions for observables.

¹A different pair of fields Z'_2, \bar{Z}'_2 would need to be introduced anyway (using different charge assignment than Z_2, \bar{Z}_2) in order to generate y_{11} . The charges can be assigned such that no extra contributions to y_{12} appear.

	$SU(5)$	\mathbb{Z}_2	\mathbb{Z}_4	\mathbb{Z}_4	\mathbb{Z}_4	\mathbb{Z}_7	\mathbb{Z}_7	\mathbb{Z}_9	\mathbb{Z}_2
Matter and light Higgs superfields									
H_5	5
\bar{H}_5	$\bar{5}$.	2	.	.	.	1	2	.
\mathcal{T}_1	10	.	.	3	.	6	.	.	1
\mathcal{T}_2	10	6	.	.	1
\mathcal{T}_3	10	1
\mathcal{F}_1	$\bar{5}$	1	1	1	2	1	1	2	1
\mathcal{F}_2	$\bar{5}$	1	.	.	2	1	.	2	1
\mathcal{F}_3	$\bar{5}$	1	2	.	1	.	6	7	1
Superfields with vevs around the GUT scale									
H_{24}	24
H'_{24}	24	1
S	1	.	3	.	.	.	2	.	.
S'	1	.	.	.	1
θ_1	1	1	.	.	.
θ_2	1	.	.	1
θ_3	1	.	2	.	.	.	6	5	.
θ_4	1	5	.
DMPM superfields									
H'_5	5	.	3	.	.	.	5	7	.
\bar{H}'_5	$\bar{5}$.	1	.	.	.	6	.	.
X_{45}	45	.	2	.	.	.	6	7	.
\bar{X}_{45}	$\bar{45}$.	3	.	.	.	6	2	.
Y_{45}	45	3	7	.
\bar{Y}_{45}	$\bar{45}$.	1	.	.	.	2	2	.
Z_{50}	50	.	1	.	.	.	1	7	.
\bar{Z}_{50}	$\bar{50}$	4	2	.
X'_{45}	45	.	3	.	.	.	1	.	.
\bar{X}'_{45}	$\bar{45}$.	2	.	.	.	4	.	.
Y'_{45}	45	.	1	.	.	.	5	.	.
\bar{Y}'_{45}	$\bar{45}$
Z'_{50}	50	.	2	.	.	.	3	.	.
\bar{Z}'_{50}	$\bar{50}$.	3	.	.	.	2	.	.

Table D.5: $SU(5)$ representations and charges under the discrete shaping symmetry for the model of 9.4.1. A dot denotes charge zero.

	$SU(5)$	\mathbb{Z}_2	\mathbb{Z}_4	\mathbb{Z}_4	\mathbb{Z}_4	\mathbb{Z}_7	\mathbb{Z}_7	\mathbb{Z}_9	\mathbb{Z}_2
$Z_{5,1}$	5	.	2	.	3	.	1	2	1
$\bar{Z}_{5,1}$	$\bar{\mathbf{5}}$.	2	.	.	.	6	7	1
$Z_{10,1}$	10	1	.	.	3	6	.	.	1
$\bar{Z}_{10,1}$	$\bar{\mathbf{10}}$	1	.	.	.	1	.	.	1
$Z_{10,2}$	10	1	2	.	2	6	6	5	1
$\bar{Z}_{10,2}$	$\bar{\mathbf{10}}$	1	2	.	1	1	1	4	1
$Z_{45,1}$	45	.	3	3	2	6	6	7	1
$\bar{Z}_{45,1}$	$\bar{\mathbf{45}}$.	1	1	1	1	1	2	1
$Z_{45,2}$	45	.	3	3	3	6	6	2	1
$\bar{Z}_{45,2}$	$\bar{\mathbf{45}}$.	1	1	.	1	1	7	1
$Z_{10,3}$	10	1	.	.	1
$Z_{10,4}$	10	.	.	1	.	1	.	.	1
Z_1	1	5	.	.	.
Z_2	1	.	.	3	.	5	.	.	.

Table D.6: $SU(5)$ representations and charges under the discrete shaping symmetry of the flavon and flavour messenger fields of the model in 9.4.1. Note that the messenger pairs $Z_{5,1}\bar{Z}_{5,1}$, $Z_{10,1}\bar{Z}_{10,1}$, $Z_{10,2}\bar{Z}_{10,2}$, $Z_{45,1}\bar{Z}_{45,1}$, and $Z_{45,2}\bar{Z}_{45,2}$ have no direct mass term, but get their masses through the vevs of S and S' . The other messengers in the lower part of the table have direct mass terms, so we omit their corresponding conjugated partner \bar{Z}_i . A dot denotes charge zero.

D.4 Appendix to the second model of chapter 9

Let us first show the supergraphs which generate the effective superpotentials (9.82) and (9.83) in figures D.15 and D.16.

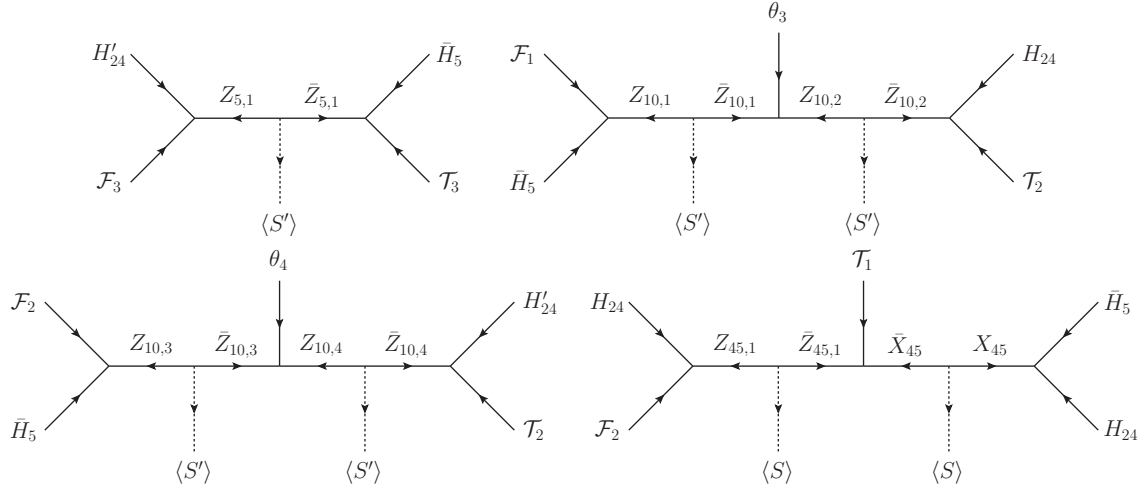


Figure D.15: Supergraphs leading to the effective superpotential \mathcal{W}_d when the heavy messenger fields get integrated out in the model 9.4.2.

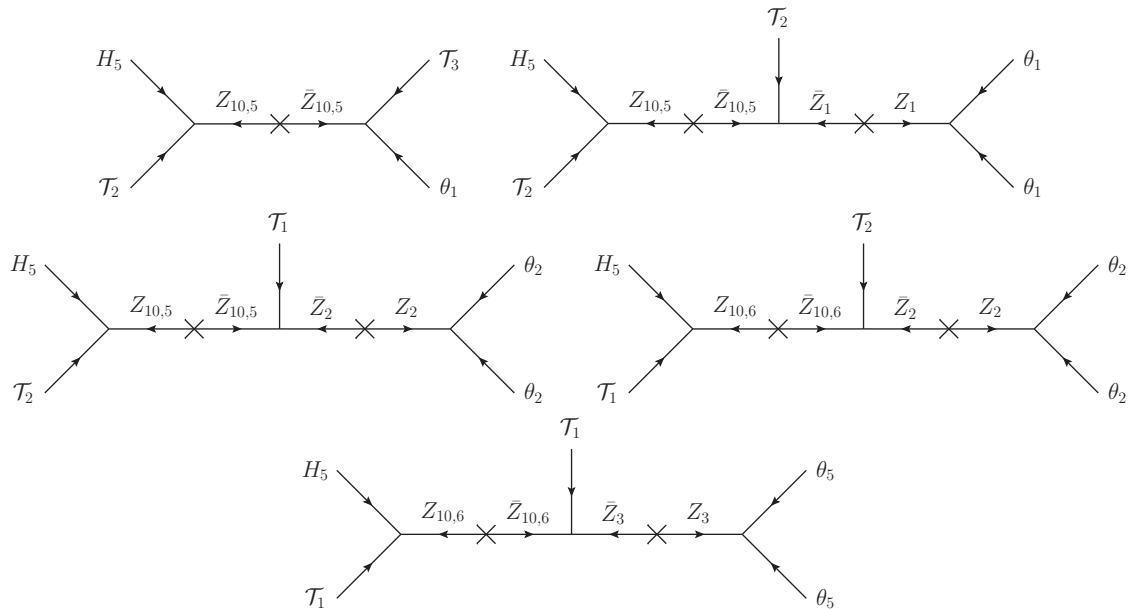


Figure D.16: Supergraphs leading to the effective superpotential \mathcal{W}_u when the heavy messenger fields get integrated out in the model 9.4.2.

All superfields of the model and their charges under the model's symmetries are shown in tables D.7 and D.8. As for the model 9.4.1, some messengers get their masses through vevs of S and S' instead of direct mass terms, as can be seen in figures D.15 and D.16. The messenger fields in the lower part of table D.7 have direct mass terms, so their corresponding conjugated fields are not shown in the table.

	$SU(5)$	\mathbb{Z}_2	\mathbb{Z}_3	\mathbb{Z}_4	\mathbb{Z}_5	\mathbb{Z}_6	\mathbb{Z}_7	\mathbb{Z}_7	\mathbb{Z}_2
Z_5	5	.	2	1	1	4	6	6	1
\bar{Z}_5	$\bar{5}$.	1	.	4	2	1	1	1
$Z_{10,1}$	10	.	1	.	1	.	3	2	1
$\bar{Z}_{10,1}$	$\bar{10}$.	2	1	4	.	4	5	1
$Z_{10,2}$	10	.	.	1	.	4	1	.	1
$\bar{Z}_{10,2}$	$\bar{10}$	2	6	.	1
$Z_{10,3}$	10	.	2	.	1	2	6	5	1
$\bar{Z}_{10,3}$	$\bar{10}$.	1	1	4	4	1	2	1
$Z_{10,4}$	10	.	.	1	.	2	1	.	1
$\bar{Z}_{10,4}$	$\bar{10}$	4	6	.	1
$Z_{45,1}$	45	.	1	.	2	2	5	4	1
$\bar{Z}_{45,1}$	$\bar{45}$	1	.	.	1	4	2	3	1
$Z_{10,5}$	10	6	.	1
$Z_{10,6}$	10	1	2	1
Z_1	1	2	.	.
Z_2	1	5	.
Z_3	1	5	3	.

Table D.7: $SU(5)$ representations and charges under the discrete shaping symmetry of the flavon and flavour messenger fields of the model 9.4.2. Note that the messengers $Z_{5,1}\bar{Z}_{5,1}$, $Z_{10,1}\bar{Z}_{10,1}$, $Z_{10,2}\bar{Z}_{10,2}$, $Z_{10,3}\bar{Z}_{10,3}$, $Z_{10,4}\bar{Z}_{10,4}$, and $Z_{45,1}\bar{Z}_{45,1}$ have no direct mass term, but get their masses through vevs of S and S' , as shown in figures D.15 and D.16. The other messenger fields in the lower part of the table have direct mass terms, so their corresponding barred fields are not shown in the table. A dot denotes charge zero.

	$SU(5)$	\mathbb{Z}_2	\mathbb{Z}_3	\mathbb{Z}_4	\mathbb{Z}_5	\mathbb{Z}_6	\mathbb{Z}_7	\mathbb{Z}_7	\mathbb{Z}_2
Matter and light Higgs superfields									
H_5	5
\bar{H}_5	$\bar{5}$.	2	.	1	4	6	6	.
\mathcal{T}_1	10	6	5	1
\mathcal{T}_2	10	1	.	1
\mathcal{T}_3	10	1
\mathcal{F}_1	$\bar{5}$.	.	.	3	2	5	6	1
\mathcal{F}_2	$\bar{5}$.	2	.	3	.	2	3	1
\mathcal{F}_3	$\bar{5}$.	1	3	4	.	1	1	1
Superfields with vevs around the GUT scale									
H_{24}	24	4	.	.	.
H'_{24}	24	2	.	.	.
S	1	1	2	.	2
S'	1	.	.	3
θ_1	1	6	.	.
θ_2	1	1	.
θ_3	1	.	1	2	1	2	2	2	.
θ_4	1	.	2	2	1	.	5	5	.
θ_5	1	3	1	2	.
DMPM Superfields									
H'_5	5	1	1	.	.	4	1	1	.
\bar{H}'_5	$\bar{5}$	1	.	.	1	2	.	.	.
X_{45}	45	.	1	.	4	4	1	1	.
\bar{X}_{45}	$\bar{45}$	1	.	.	4	2	6	6	.
Y_{45}	45	.	2	.	3	2	1	1	.
\bar{Y}_{45}	$\bar{45}$	1	2	.	.	4	6	6	.
Z_{50}	50	1	.	.	1	.	1	1	.
\bar{Z}_{50}	$\bar{50}$.	1	.	2	.	6	6	.
X'_{45}	45	1	.	.	4
\bar{X}'_{45}	$\bar{45}$.	1	.	4
Y'_{45}	45	1	1	.	3	4	.	.	.
\bar{Y}'_{45}	$\bar{45}$	2	.	.	.
Z'_{50}	50	.	2	.	1	2	.	.	.
\bar{Z}'_{50}	$\bar{50}$	1	2	.	2	4	.	.	.

Table D.8: $SU(5)$ representations and charges under discrete shaping symmetries for the model of 9.4.2. A dot denotes charge zero.

APPENDIX E

The β -functions in the seesaw type-I extension of the MSSM

In this appendix we list the β -functions of the SUSY soft-breaking parameters in the MSSM extended by the additional terms in the seesaw type-I extension (obtained using the general formulae of [136]), which are implemented into `REAP` and `SusyTC`. Thus they are given here in our conventions (10.1) and (10.2) for \mathcal{W} and $\mathcal{L}_{\text{soft}}$, respectively.

E.1 One-Loop β -functions

$$16\pi^2\beta_{M_1} = \frac{66}{5}g_1^2M_1, \quad (\text{E.1})$$

$$16\pi^2\beta_{M_2} = 2g_2^2M_2, \quad (\text{E.2})$$

$$16\pi^2\beta_{M_3} = -6g_3^2M_3, \quad (\text{E.3})$$

$$\begin{aligned} 16\pi^2\beta_{T_u} &= Y_u \left(2Y_d^\dagger T_d + 4Y_u^\dagger T_u \right) + T_u \left(Y_d^\dagger Y_d + 5Y_u^\dagger Y_u \right) \\ &\quad + Y_u \left(6\text{Tr}(Y_u^\dagger T_u) + 2\text{Tr}(Y_\nu^\dagger T_\nu) + \frac{26}{15}g_1^2M_1 + 6g_2^2M_2 + \frac{32}{3}g_3^2M_3 \right) \\ &\quad + T_u \left(3\text{Tr}(Y_u^\dagger Y_u) + \text{Tr}(Y_\nu^\dagger Y_\nu) - \frac{13}{15}g_1^2 - 3g_2^2 - \frac{16}{3}g_3^2 \right), \end{aligned} \quad (\text{E.4})$$

$$\begin{aligned} 16\pi^2\beta_{T_d} &= Y_d \left(4Y_d^\dagger T_d + 2Y_u^\dagger T_u \right) + T_d \left(5Y_d^\dagger Y_d + Y_u^\dagger Y_u \right) \\ &\quad + Y_d \left(6\text{Tr}(Y_d^\dagger T_d) + 2\text{Tr}(Y_e^\dagger T_e) + \frac{14}{15}g_1^2M_1 + 6g_2^2M_2 + \frac{32}{3}g_3^2M_3 \right) \\ &\quad + T_d \left(3\text{Tr}(Y_d^\dagger Y_d) + \text{Tr}(Y_e^\dagger Y_e) - \frac{7}{15}g_1^2 - 3g_2^2 - \frac{16}{3}g_3^2 \right), \end{aligned} \quad (\text{E.5})$$

$$\begin{aligned}
16\pi^2\beta_{T_e} &= Y_e (4Y_e^\dagger T_e + 2Y_\nu^\dagger T_\nu) + T_e (5Y_e^\dagger Y_e + Y_\nu^\dagger Y_\nu) \\
&\quad + Y_e \left(6\text{Tr}(Y_d^\dagger T_d) + 2\text{Tr}(Y_e^\dagger T_e) + \frac{18}{5}g_1^2 M_1 + 6g_2^2 M_2 \right) \\
&\quad + T_e \left(3\text{Tr}(Y_d^\dagger Y_d) + \text{Tr}(Y_e^\dagger Y_e) - \frac{9}{5}g_1^2 - 3g_2^2 \right) , \tag{E.6}
\end{aligned}$$

$$\begin{aligned}
16\pi^2\beta_{T_\nu} &= Y_\nu (4Y_\nu^\dagger T_\nu + 2Y_e^\dagger T_e) + T_\nu (5Y_\nu^\dagger Y_\nu + Y_e^\dagger Y_e) \\
&\quad + Y_\nu \left(6\text{Tr}(Y_u^\dagger T_u) + 2\text{Tr}(Y_\nu^\dagger T_\nu) + \frac{6}{5}g_1^2 M_1 + 6g_2^2 M_2 \right) \\
&\quad + T_\nu \left(3\text{Tr}(Y_u^\dagger Y_u) + \text{Tr}(Y_\nu^\dagger Y_\nu) - \frac{3}{5}g_1^2 - 3g_2^2 \right) , \tag{E.7}
\end{aligned}$$

$$\begin{aligned}
16\pi^2\beta_{m_L^2} &= 2Y_e^\dagger m_e^2 Y_e + 2Y_\nu^\dagger m_\nu^2 Y_\nu \\
&\quad + m_L^2 (Y_e^\dagger Y_e + Y_\nu^\dagger Y_\nu) + (Y_e^\dagger Y_e + Y_\nu^\dagger Y_\nu) m_L^2 \\
&\quad + 2m_{h_u}^2 Y_\nu^\dagger Y_\nu + 2m_{h_d}^2 Y_e^\dagger Y_e + 2T_e^\dagger T_e + 2T_\nu^\dagger T_\nu \\
&\quad - \frac{6}{5}g_1^2 |M_1|^2 \mathbf{1}_3 - 6g_2^2 |M_2|^2 \mathbf{1}_3 - \frac{3}{5}g_1^2 S \mathbf{1}_3 , \tag{E.8}
\end{aligned}$$

$$\begin{aligned}
16\pi^2\beta_{m_Q^2} &= 2Y_u^\dagger m_u^2 Y_u + 2Y_d^\dagger m_d^2 Y_d \\
&\quad + m_Q^2 (Y_u^\dagger Y_u + Y_d^\dagger Y_d) + (Y_u^\dagger Y_u + Y_d^\dagger Y_d) m_Q^2 \\
&\quad + 2m_{h_u}^2 Y_u^\dagger Y_u + 2m_{h_d}^2 Y_d^\dagger Y_d + 2T_u^\dagger T_u + 2T_d^\dagger T_d \\
&\quad - \frac{2}{15}g_1^2 |M_1|^2 \mathbf{1}_3 - 6g_2^2 |M_2|^2 \mathbf{1}_3 - \frac{32}{3}g_3^2 |M_3|^2 \mathbf{1}_3 + \frac{1}{5}g_1^2 S \mathbf{1}_3 , \tag{E.9}
\end{aligned}$$

$$\begin{aligned}
16\pi^2\beta_{m_u^2} &= 4Y_u m_Q^2 Y_u^\dagger + 2Y_u Y_u^\dagger m_u^2 + 2m_u^2 Y_u Y_u^\dagger \\
&\quad + 4m_{h_u}^2 Y_u Y_u^\dagger + 4T_u T_u^\dagger \\
&\quad - \frac{32}{15}g_1^2 |M_1|^2 \mathbf{1}_3 - \frac{32}{3}g_3^2 |M_3|^2 \mathbf{1}_3 - \frac{4}{5}g_1^2 S \mathbf{1}_3 , \tag{E.10}
\end{aligned}$$

$$\begin{aligned}
16\pi^2\beta_{m_d^2} &= 4Y_d m_Q^2 Y_d^\dagger + 2Y_d Y_d^\dagger m_d^2 + 2m_d^2 Y_d Y_d^\dagger \\
&\quad + 4m_{h_d}^2 Y_d Y_d^\dagger + 4T_d T_d^\dagger \\
&\quad - \frac{8}{15}g_1^2 |M_1|^2 \mathbf{1}_3 - \frac{32}{3}g_3^2 |M_3|^2 \mathbf{1}_3 + \frac{2}{5}g_1^2 S \mathbf{1}_3 , \tag{E.11}
\end{aligned}$$

$$\begin{aligned}
16\pi^2\beta_{m_{\tilde{e}}^2} &= 4Y_e m_{\tilde{L}}^2 Y_e^\dagger + 2Y_e Y_e^\dagger m_{\tilde{e}}^2 + 2m_{\tilde{e}}^2 Y_e Y_e^\dagger \\
&\quad + 4m_{h_d}^2 Y_e Y_e^\dagger + 4T_e T_e^\dagger \\
&\quad - \frac{24}{5}g_1^2 |M_1|^2 \mathbf{1}_3 + \frac{6}{5}g_1^2 S \mathbf{1}_3 ,
\end{aligned} \tag{E.12}$$

$$\begin{aligned}
16\pi^2\beta_{m_{\tilde{\nu}}^2} &= 4Y_\nu m_{\tilde{L}}^2 Y_\nu^\dagger + 2Y_\nu Y_\nu^\dagger m_{\tilde{\nu}}^2 + 2m_{\tilde{\nu}}^2 Y_\nu Y_\nu^\dagger \\
&\quad + 4m_{h_u}^2 Y_\nu Y_\nu^\dagger + 4T_\nu T_\nu^\dagger ,
\end{aligned} \tag{E.13}$$

$$\begin{aligned}
16\pi^2\beta_{m_{h_d}^2} &= 6\text{Tr}(Y_d m_{\tilde{Q}}^2 Y_d^\dagger + Y_d^\dagger m_{\tilde{d}}^2 Y_d) \\
&\quad + 2\text{Tr}(Y_e m_{\tilde{L}}^2 Y_e^\dagger + Y_e^\dagger m_{\tilde{e}}^2 Y_e) \\
&\quad + 6m_{h_d}^2 \text{Tr}(Y_d^\dagger Y_d) + 2m_{h_d}^2 \text{Tr}(Y_e^\dagger Y_e) \\
&\quad + 6\text{Tr}(T_d^\dagger T_d) + 2\text{Tr}(T_e^\dagger T_e) \\
&\quad - \frac{6}{5}g_1^2 |M_1|^2 - 6g_2^2 |M_2|^2 - \frac{3}{5}g_1^2 S ,
\end{aligned} \tag{E.14}$$

$$\begin{aligned}
16\pi^2\beta_{m_{h_u}^2} &= 6\text{Tr}(Y_u m_{\tilde{Q}}^2 Y_u^\dagger + Y_u^\dagger m_{\tilde{u}}^2 Y_u) \\
&\quad + 2\text{Tr}(Y_\nu m_{\tilde{L}}^2 Y_\nu^\dagger + Y_\nu^\dagger m_{\tilde{\nu}}^2 Y_\nu) \\
&\quad + 6m_{h_u}^2 \text{Tr}(Y_u^\dagger Y_u) + 2m_{h_u}^2 \text{Tr}(Y_\nu^\dagger Y_\nu) \\
&\quad + 6\text{Tr}(T_u^\dagger T_u) + 2\text{Tr}(T_\nu^\dagger T_\nu) \\
&\quad - \frac{6}{5}g_1^2 |M_1|^2 - 6g_2^2 |M_2|^2 + \frac{3}{5}g_1^2 S ,
\end{aligned} \tag{E.15}$$

with

$$S = m_{h_u}^2 - m_{h_d}^2 + \text{Tr} \left(m_{\tilde{Q}}^2 - m_{\tilde{L}}^2 + m_{\tilde{d}}^2 + m_{\tilde{e}}^2 - 2m_{\tilde{u}}^2 \right) . \tag{E.16}$$

E.2 Two-Loop β -functions

$$\begin{aligned}
(16\pi^2)^2\beta_{M_1}^{(2)} &= \frac{12}{5}g_1^2 \text{Tr}(T_\nu Y_\nu^\dagger) + \frac{28}{5}g_1^2 \text{Tr}(T_d Y_d^\dagger) + \frac{36}{5}g_1^2 \text{Tr}(T_e Y_e^\dagger) + \frac{52}{5}g_1^2 \text{Tr}(T_u Y_u^\dagger) \\
&\quad - \frac{12}{5}g_1^2 M_1 \text{Tr}(Y_\nu Y_\nu^\dagger) - \frac{28}{5}g_1^2 M_1 \text{Tr}(Y_d Y_d^\dagger) \\
&\quad - \frac{36}{5}g_1^2 M_1 \text{Tr}(Y_e Y_e^\dagger) - \frac{52}{5}g_1^2 M_1 \text{Tr}(Y_u Y_u^\dagger) \\
&\quad + \frac{176}{5}g_1^2 g_3^2 M_1 + \frac{176}{5}g_1^2 g_3^2 M_3 + \frac{54}{5}g_1^2 g_2^2 M_1 + \frac{54}{5}g_1^2 g_2^2 M_2 + \frac{796}{25}g_1^4 M_1 ,
\end{aligned} \tag{E.17}$$

$$\begin{aligned}
(16\pi^2)^2 \beta_{M_2}^{(2)} = & 4g_2^2 \text{Tr}(T_\nu Y_\nu^\dagger) + 4g_2^2 \text{Tr}(T_e Y_e^\dagger) + 12g_2^2 \text{Tr}(T_d Y_d^\dagger) + 12g_2^2 \text{Tr}(T_u Y_u^\dagger) \\
& - 4g_2^2 M_2 \text{Tr}(Y_\nu Y_\nu^\dagger) - 4g_2^2 M_2 \text{Tr}(Y_e Y_e^\dagger) \\
& - 12g_2^2 M_2 \text{Tr}(Y_u Y_u^\dagger) - 12g_2^2 M_2 \text{Tr}(Y_d Y_d^\dagger) \\
& + \frac{18}{5} g_1^2 g_2^2 M_1 + \frac{18}{5} g_1^2 g_3^2 M_2 + 48g_2^2 g_3^2 M_2 + 48g_2^2 g_3^2 M_3 + 100g_2^4 M_2, \quad (\text{E.18})
\end{aligned}$$

$$\begin{aligned}
(16\pi^2)^2 \beta_{M_3}^{(2)} = & 8g_3^2 \text{Tr}(T_d Y_d^\dagger) + 8g_3^2 \text{Tr}(T_u Y_u^\dagger) - 8g_3^2 M_3 \text{Tr}(Y_d Y_d^\dagger) - 8g_3^2 M_3 \text{Tr}(Y_u Y_u^\dagger) \\
& + \frac{22}{5} g_1^2 g_3^2 M_1 + \frac{22}{5} g_1^2 g_3^2 M_3 + 18g_2^2 g_3^2 M_2 + 18g_2^2 g_3^2 M_3 + 56g_3^4 M_3, \quad (\text{E.19})
\end{aligned}$$

$$\begin{aligned}
(16\pi^2)^2 \beta_{T_u}^{(2)} = & -2T_u \left(Y_d^\dagger Y_d Y_d^\dagger Y_d + 2Y_d^\dagger Y_d Y_u^\dagger Y_u + 3Y_u^\dagger Y_u Y_u^\dagger Y_u \right) \\
& -2Y_u \left(2Y_d^\dagger T_d Y_d^\dagger Y_d + 2Y_d^\dagger T_d Y_u^\dagger Y_u + 2Y_d^\dagger Y_d Y_d^\dagger T_d \right. \\
& \left. + Y_d^\dagger Y_d Y_u^\dagger T_u + 4Y_u^\dagger T_u Y_u^\dagger Y_u + 3Y_u^\dagger Y_u Y_u^\dagger T_u \right) \\
& -T_u \left(Y_d^\dagger Y_d \text{Tr}(Y_e Y_e^\dagger + 3Y_d Y_d^\dagger) + 5Y_u^\dagger Y_u \text{Tr}(Y_\nu Y_\nu^\dagger + 3Y_u Y_u^\dagger) \right) \\
& -2Y_u \left(Y_d^\dagger T_d \text{Tr}(Y_e Y_e^\dagger + 3Y_d Y_d^\dagger) + Y_d^\dagger Y_d \text{Tr}(T_e Y_e^\dagger + 3T_d Y_d^\dagger) \right. \\
& \left. + 2Y_u^\dagger T_u \text{Tr}(Y_\nu Y_\nu^\dagger + 3Y_u Y_u^\dagger) + 3Y_u^\dagger Y_u \text{Tr}(T_\nu Y_\nu^\dagger + 3T_u Y_u^\dagger) \right) \\
& -T_u \left(\text{Tr}(3Y_\nu Y_\nu^\dagger Y_\nu Y_\nu^\dagger + Y_\nu Y_e^\dagger Y_e Y_\nu^\dagger) + 3\text{Tr}(Y_u Y_d^\dagger Y_d Y_u^\dagger + 3Y_u Y_u^\dagger Y_u Y_u^\dagger) \right) \\
& -2Y_u \left(\text{Tr}(6T_\nu Y_\nu^\dagger Y_\nu Y_\nu^\dagger + T_\nu Y_e^\dagger Y_e Y_\nu^\dagger + Y_\nu Y_e^\dagger T_e Y_\nu^\dagger) \right. \\
& \left. + 3\text{Tr}(Y_u Y_d^\dagger T_d Y_u^\dagger + T_u Y_d^\dagger Y_d Y_u^\dagger + 6T_u Y_u^\dagger Y_u Y_u^\dagger) \right) \\
& + \frac{2}{5} g_1^2 \left(T_u Y_d^\dagger Y_d + 2Y_u Y_d^\dagger T_d + 3Y_u Y_u^\dagger T_u - 2M_1 (Y_u Y_d^\dagger Y_d + Y_u Y_u^\dagger Y_u) \right) \\
& + 6g_2^2 \left(Y_u Y_u^\dagger T_u + 2T_u Y_u^\dagger Y_u - 2M_2 Y_u Y_u^\dagger Y_u \right) \\
& + \left(16g_3^2 + \frac{4}{5} g_1^2 \right) \left(2Y_u \text{Tr}(Y_u^\dagger T_u) + T_u \text{Tr}(Y_u^\dagger Y_u) \right) \\
& + \frac{136}{45} g_1^2 g_3^2 T_u + \frac{15}{2} g_2^4 T_u - \frac{16}{9} g_3^4 T_u + \frac{2743}{450} g_1^4 T_u + g_1^2 g_2^2 T_u + 8g_2^2 g_3^2 T_u \\
& - Y_u \text{Tr}(Y_u^\dagger Y_u) \left(32g_3^2 M_3 + \frac{8}{5} g_1^2 M_1 \right) - \frac{272}{45} g_1^2 g_3^2 Y_u (M_1 + M_3) \\
& - 2g_1^2 g_2^2 Y_u (M_1 + M_2) - 16g_2^2 g_3^2 Y_u (M_2 + M_3) \\
& - 30g_2^4 M_2 Y_u - \frac{5486}{225} g_1^4 M_1 Y_u + \frac{64}{9} g_3^4 M_3 Y_u, \quad (\text{E.20})
\end{aligned}$$

$$\begin{aligned}
(16\pi^2)^2 \beta_{T_d}^{(2)} = & -2T_d \left(3Y_d^\dagger Y_d Y_d^\dagger Y_d + 2Y_u^\dagger Y_u Y_d^\dagger Y_d + Y_u^\dagger Y_u Y_u^\dagger Y_u \right) \\
& -2Y_d \left(4Y_d^\dagger T_d Y_d^\dagger Y_d + 3Y_d^\dagger Y_d Y_d^\dagger T_d + 2Y_u^\dagger T_u Y_d^\dagger Y_d \right. \\
& + 2Y_u^\dagger T_u Y_u^\dagger Y_u + Y_u^\dagger Y_u Y_d^\dagger T_d + 2Y_u^\dagger Y_u Y_u^\dagger T_u \left. \right) \\
& -T_d \left(5Y_d^\dagger Y_d \text{Tr}(Y_e Y_e^\dagger + 3Y_d Y_d^\dagger) + Y_u^\dagger Y_u \text{Tr}(Y_\nu Y_\nu^\dagger + 3Y_u Y_u^\dagger) \right) \\
& -2Y_d \left(2Y_d^\dagger T_d \text{Tr}(Y_e Y_e^\dagger + 3Y_d Y_d^\dagger) + 3Y_d^\dagger Y_d \text{Tr}(T_e Y_e^\dagger + 3T_d Y_d^\dagger) \right. \\
& + Y_u^\dagger T_u \text{Tr}(Y_\nu Y_\nu^\dagger + 3Y_u Y_u^\dagger) + Y_u^\dagger Y_u \text{Tr}(T_\nu Y_\nu^\dagger + 3T_u Y_u^\dagger) \left. \right) \\
& -T_d \left(\text{Tr}(Y_e Y_\nu^\dagger Y_\nu Y_e^\dagger + 3Y_e Y_e^\dagger Y_e Y_e^\dagger) + 3\text{Tr}(Y_u Y_d^\dagger Y_d Y_u^\dagger + 3Y_d Y_d^\dagger Y_d Y_d^\dagger) \right) \\
& -2Y_d \left(\text{Tr}(Y_e Y_\nu^\dagger T_\nu Y_e^\dagger + T_e Y_\nu^\dagger Y_\nu Y_e^\dagger + 6T_e Y_e^\dagger Y_e Y_e^\dagger) \right. \\
& + 3\text{Tr}(T_d Y_u^\dagger Y_u Y_d^\dagger + T_u Y_d^\dagger Y_d Y_u^\dagger + 6T_d Y_d^\dagger Y_d Y_d^\dagger) \left. \right) \\
& + \frac{2}{5} g_1^2 \left(2T_d Y_u^\dagger Y_u + 3T_d Y_d^\dagger Y_d + 3Y_d Y_d^\dagger T_d + 4Y_d Y_u^\dagger T_u - 4M_1(Y_d Y_d^\dagger Y_d + Y_d Y_u^\dagger Y_u) \right) \\
& + 6g_2^2 \left(Y_d Y_d^\dagger T_d + 2T_d Y_d^\dagger Y_d - 2M_2 Y_d Y_d^\dagger Y_d \right) \\
& + \left(16g_3^2 - \frac{2}{5} g_1^2 \right) \left(2Y_d \text{Tr}(Y_d^\dagger T_d) + T_d \text{Tr}(Y_d^\dagger Y_d) \right) \\
& + \frac{6}{5} g_1^2 \left(2Y_d \text{Tr}(Y_e^\dagger T_e) + T_d \text{Tr}(Y_e^\dagger Y_e) \right) \\
& + \frac{8}{9} g_1^2 g_3^2 T_d + \frac{15}{2} g_2^4 T_d - \frac{16}{9} g_3^4 T_d + \frac{287}{90} g_1^4 T_d + g_1^2 g_2^2 T_d + 8g_2^2 g_3^2 T_d \\
& - Y_d \text{Tr}(Y_d^\dagger Y_d) \left(32g_3^2 M_3 - \frac{4}{5} g_1^2 M_1 \right) - \frac{12}{5} g_1^2 M_1 Y_d \text{Tr}(Y_e^\dagger Y_e) \\
& - \frac{16}{9} g_1^2 g_3^2 Y_d (M_1 + M_3) - 2g_1^2 g_2^2 Y_d (M_1 + M_2) - 16g_2^2 g_3^2 Y_d (M_2 + M_3) \\
& - 30g_2^4 M_2 Y_d - \frac{574}{45} g_1^4 M_1 Y_d + \frac{64}{9} g_3^4 M_3 Y_d, \tag{E.21}
\end{aligned}$$

$$\begin{aligned}
(16\pi^2)^2 \beta_{T_e}^{(2)} = & -2T_e \left(3Y_e^\dagger Y_e Y_e^\dagger Y_e + 2Y_\nu^\dagger Y_\nu Y_e^\dagger Y_e + Y_\nu^\dagger Y_\nu Y_\nu^\dagger Y_\nu \right) \\
& -2Y_e \left(4Y_e^\dagger T_e Y_e^\dagger Y_e + 3Y_e^\dagger Y_e Y_e^\dagger T_e + 2Y_\nu^\dagger T_\nu Y_e^\dagger Y_e \right. \\
& + 2Y_\nu^\dagger T_\nu Y_\nu^\dagger Y_\nu + Y_\nu^\dagger Y_\nu Y_e^\dagger T_e + 2Y_\nu^\dagger Y_\nu Y_\nu^\dagger T_\nu \left. \right) \\
& -T_e \left(5Y_e^\dagger Y_e \text{Tr}(Y_e Y_e^\dagger + 3Y_d Y_d^\dagger) + Y_\nu^\dagger Y_\nu \text{Tr}(Y_\nu Y_\nu^\dagger + 3Y_u Y_u^\dagger) \right) \\
& -2Y_e \left(2Y_e^\dagger T_e \text{Tr}(Y_e Y_e^\dagger + 3Y_d Y_d^\dagger) + 3Y_e^\dagger Y_e \text{Tr}(T_e Y_e^\dagger + 3T_d Y_d^\dagger) \right)
\end{aligned}$$

$$\begin{aligned}
& + Y_\nu^\dagger T_\nu \text{Tr}(Y_\nu Y_\nu^\dagger + 3Y_u Y_u^\dagger) + Y_\nu^\dagger Y_\nu \text{Tr}(T_\nu Y_\nu^\dagger + 3T_u Y_u^\dagger) \\
& - T_e \left(\text{Tr}(Y_e Y_\nu^\dagger Y_\nu Y_e^\dagger + 3Y_e Y_e^\dagger Y_e Y_e^\dagger) + 3\text{Tr}(Y_d Y_u^\dagger Y_u Y_d^\dagger + 3Y_d Y_d^\dagger Y_d Y_d^\dagger) \right) \\
& - 2Y_e \left(\text{Tr}(Y_e Y_\nu^\dagger T_\nu Y_e^\dagger + T_e Y_\nu^\dagger Y_\nu Y_e^\dagger + 6T_e Y_e^\dagger Y_e Y_e^\dagger) \right. \\
& \left. + 3\text{Tr}(T_d Y_u^\dagger Y_u Y_d^\dagger + T_u Y_d^\dagger Y_d Y_u^\dagger + 6T_d Y_d^\dagger Y_d Y_d^\dagger) \right) \\
& + \frac{6}{5} g_1^2 (Y_e Y_e^\dagger T_e - T_e Y_e^\dagger Y_e) \\
& + 6g_2^2 (Y_e Y_e^\dagger T_e + 2T_e Y_e^\dagger Y_e - 2M_2 Y_e Y_e^\dagger Y_e) \\
& + \left(16g_3^2 - \frac{2}{5} g_1^2 \right) \left(2Y_e \text{Tr}(Y_d^\dagger T_d) + T_e \text{Tr}(Y_d^\dagger Y_d) \right) \\
& + \frac{6}{5} g_1^2 (2Y_e \text{Tr}(Y_e^\dagger T_e) + T_e \text{Tr}(Y_e^\dagger Y_e)) \\
& + \frac{15}{2} g_2^4 T_e + \frac{27}{2} g_1^4 T_e + \frac{9}{5} g_1^2 g_2^2 T_e \\
& - Y_e \text{Tr}(Y_d^\dagger Y_d) \left(32g_3^2 M_3 - \frac{4}{5} g_1^2 M_1 \right) - \frac{12}{5} g_1^2 M_1 Y_e \text{Tr}(Y_e^\dagger Y_e) \\
& - \frac{18}{5} g_1^2 g_2^2 Y_d (M_1 + M_2) - 30g_2^4 M_2 Y_e - 54g_1^4 M_1 Y_e, \tag{E.22}
\end{aligned}$$

$$\begin{aligned}
(16\pi^2)^2 \beta_{T_\nu}^{(2)} = & - 2T_\nu \left(Y_e^\dagger Y_e Y_e^\dagger Y_e + 2Y_e^\dagger Y_e Y_\nu^\dagger Y_\nu + 3Y_\nu^\dagger Y_\nu Y_\nu^\dagger Y_\nu \right) \\
& - 2Y_\nu \left(2Y_e^\dagger T_e Y_e^\dagger Y_e + 2Y_e^\dagger T_e Y_\nu^\dagger Y_\nu + 2Y_e^\dagger Y_e Y_e^\dagger T_e \right. \\
& \left. + Y_e^\dagger Y_e Y_\nu^\dagger T_\nu + 4Y_\nu^\dagger T_\nu Y_\nu^\dagger Y_\nu + 3Y_\nu^\dagger Y_\nu Y_\nu^\dagger T_\nu \right) \\
& - T_\nu \left(Y_e^\dagger Y_e \text{Tr}(Y_e Y_e^\dagger + 3Y_d Y_d^\dagger) + 5Y_\nu^\dagger Y_\nu \text{Tr}(Y_\nu Y_\nu^\dagger + 3Y_u Y_u^\dagger) \right) \\
& - 2Y_\nu \left(Y_e^\dagger T_e \text{Tr}(Y_e Y_e^\dagger + 3Y_d Y_d^\dagger) + Y_e^\dagger Y_e \text{Tr}(T_e Y_e^\dagger + 3T_d Y_d^\dagger) \right. \\
& \left. + 2Y_\nu^\dagger T_\nu \text{Tr}(Y_\nu Y_\nu^\dagger + 3Y_u Y_u^\dagger) + 3Y_\nu^\dagger Y_\nu \text{Tr}(T_\nu Y_\nu^\dagger + 3T_u Y_u^\dagger) \right) \\
& - T_\nu \left(\text{Tr}(3Y_\nu Y_\nu^\dagger Y_\nu Y_\nu^\dagger + Y_\nu Y_e^\dagger Y_e Y_\nu^\dagger) + 3\text{Tr}(Y_u Y_d^\dagger Y_d Y_u^\dagger + 3Y_u Y_u^\dagger Y_u Y_u^\dagger) \right) \\
& - 2Y_\nu \left(\text{Tr}(T_\nu Y_e^\dagger Y_e Y_\nu^\dagger + Y_\nu Y_e^\dagger T_e Y_\nu^\dagger + 6T_\nu Y_\nu^\dagger Y_\nu Y_\nu^\dagger) \right. \\
& \left. + 3\text{Tr}(T_d Y_u^\dagger Y_u Y_d^\dagger + T_u Y_d^\dagger Y_d Y_u^\dagger + 6T_u Y_u^\dagger Y_u Y_u^\dagger) \right) \\
& + \frac{6}{5} g_1^2 \left(2T_\nu Y_\nu^\dagger Y_\nu + 2Y_\nu Y_e^\dagger T_e + Y_\nu Y_\nu^\dagger T_\nu + T_\nu Y_e^\dagger Y_e - 2M_1 (Y_\nu Y_\nu^\dagger Y_\nu + Y_\nu Y_e^\dagger Y_e) \right) \\
& + 6g_2^2 (Y_\nu Y_\nu^\dagger T_\nu + 2T_\nu Y_\nu^\dagger Y_\nu - 2M_2 Y_\nu Y_\nu^\dagger Y_\nu) \\
& + \left(16g_3^2 + \frac{4}{5} g_1^2 \right) (2Y_\nu \text{Tr}(Y_u^\dagger T_u) + T_\nu \text{Tr}(Y_u^\dagger Y_u))
\end{aligned}$$

$$\begin{aligned}
& + \frac{15}{2}g_2^4 T_\nu + \frac{207}{50}g_1^4 T_\nu + \frac{9}{5}g_1^2 g_2^2 T_\nu \\
& - Y_\nu \text{Tr}(Y_u^\dagger Y_u) \left(32g_3^2 M_3 + \frac{8}{5}g_1^2 M_1 \right) \\
& - \frac{18}{5}g_1^2 g_2^2 Y_\nu (M_1 + M_2) - 30g_2^4 M_2 Y_\nu - \frac{414}{25}g_1^4 M_1 Y_\nu, \tag{E.23}
\end{aligned}$$

$$\begin{aligned}
(16\pi^2)^2 \beta_{m_L^2}^{(2)} = & -4T_e^\dagger \left(T_e Y_e^\dagger Y_e + Y_e Y_e^\dagger T_e \right) - 4T_\nu^\dagger \left(T_\nu Y_\nu^\dagger Y_\nu + Y_\nu Y_\nu^\dagger T_\nu \right) \\
& - 2Y_e^\dagger \left(2m_e^2 Y_e Y_e^\dagger Y_e + 2T_e T_e^\dagger Y_e + 2Y_e T_e^\dagger T_e \right. \\
& \left. + 2Y_e Y_e^\dagger m_e^2 Y_e + Y_e Y_e^\dagger Y_e m_L^2 + 2Y_e m_L^2 Y_e^\dagger Y_e \right) \\
& - 2Y_\nu^\dagger \left(2m_\nu^2 Y_\nu Y_\nu^\dagger Y_\nu + 2T_\nu T_\nu^\dagger Y_\nu + 2Y_\nu T_\nu^\dagger T_\nu \right. \\
& \left. + 2Y_\nu Y_\nu^\dagger m_\nu^2 Y_\nu + Y_\nu Y_\nu^\dagger Y_\nu m_L^2 + 2Y_\nu m_L^2 Y_\nu^\dagger Y_\nu \right) \\
& - 2(4m_{h_d}^2 + m_L^2) Y_e^\dagger Y_e Y_e^\dagger Y_e - 2(4m_{h_u}^2 + m_L^2) Y_\nu^\dagger Y_\nu Y_\nu^\dagger Y_\nu \\
& - 2T_e^\dagger \left(T_e \text{Tr}(Y_e Y_e^\dagger + 3Y_d Y_d^\dagger) + Y_e \text{Tr}(T_e Y_e^\dagger + 3T_d Y_d^\dagger) \right) \\
& - 2T_\nu^\dagger \left(T_\nu \text{Tr}(Y_\nu Y_\nu^\dagger + 3Y_u Y_u^\dagger) + Y_\nu \text{Tr}(T_\nu Y_\nu^\dagger + 3T_u Y_u^\dagger) \right) \\
& - Y_e^\dagger \left(2m_e^2 Y_e \text{Tr}(Y_e Y_e^\dagger + 3Y_d Y_d^\dagger) + 2T_e \text{Tr}(Y_e T_e^\dagger + 3Y_d T_d^\dagger) \right. \\
& \left. + 2Y_e \text{Tr}(T_e T_e^\dagger + 3T_d T_d^\dagger) + Y_e m_L^2 \text{Tr}(Y_e Y_e^\dagger + 3Y_d Y_d^\dagger) \right) \\
& - Y_\nu^\dagger \left(2m_\nu^2 Y_\nu \text{Tr}(Y_\nu Y_\nu^\dagger + 3Y_u Y_u^\dagger) + 2T_\nu \text{Tr}(Y_\nu T_\nu^\dagger + 3Y_u T_u^\dagger) \right. \\
& \left. + 2Y_\nu \text{Tr}(T_\nu T_\nu^\dagger + 3T_u T_u^\dagger) + Y_\nu m_L^2 \text{Tr}(Y_\nu Y_\nu^\dagger + 3Y_u Y_u^\dagger) \right) \\
& - (4m_{h_d}^2 + m_L^2) Y_e^\dagger Y_e \text{Tr}(Y_e Y_e^\dagger + 3Y_d Y_d^\dagger) \\
& - (4m_{h_u}^2 + m_L^2) Y_\nu^\dagger Y_\nu \text{Tr}(Y_\nu Y_\nu^\dagger + 3Y_u Y_u^\dagger) \\
& - 2Y_e^\dagger Y_e \text{Tr} \left(Y_e m_L^2 Y_e^\dagger + Y_e^\dagger m_e^2 Y_e + 3Y_d m_Q^2 Y_d^\dagger + 3Y_d^\dagger m_d^2 Y_d \right) \\
& - 2Y_\nu^\dagger Y_\nu \text{Tr} \left(Y_\nu m_L^2 Y_\nu^\dagger + Y_\nu^\dagger m_\nu^2 Y_\nu + 3Y_u m_Q^2 Y_u^\dagger + 3Y_u^\dagger m_u^2 Y_u \right) \\
& + \frac{6}{5}g_1^2 \left(2m_{h_d}^2 Y_e^\dagger Y_e + m_L^2 Y_e^\dagger Y_e + Y_e^\dagger Y_e m_L^2 + 2Y_e^\dagger m_e^2 Y_e + 2T_e^\dagger T_e \right) \\
& - \frac{12}{5}g_1^2 \left(M_1^* Y_e^\dagger T_e - 2|M_1|^2 Y_e^\dagger Y_e + M_1 T_e^\dagger Y_e \right) \\
& + \frac{621}{25}g_1^4 |M_1|^2 \mathbf{1}_3 + \frac{18}{5}g_1^2 g_2^2 (|M_1|^2 + |M_2|^2) \mathbf{1}_3 \\
& + \frac{18}{5}g_1^2 g_2^2 \text{Re}(M_1 M_2^*) \mathbf{1}_3 + 33g_2^4 |M_2|^2 \mathbf{1}_3
\end{aligned}$$

$$+ \frac{3}{5}g_1^2\sigma_1 \mathbf{1}_3 + 3g_2^2\sigma_2 \mathbf{1}_3 - \frac{6}{5}g_1^2S' \mathbf{1}_3, \quad (\text{E.24})$$

$$\begin{aligned}
(16\pi^2)^2\beta_{m_{\tilde{Q}}^2}^{(2)} = & -4T_d^\dagger \left(T_d Y_d^\dagger Y_d + Y_d Y_d^\dagger T_d \right) - 4T_u^\dagger \left(T_u Y_u^\dagger Y_u + Y_u Y_u^\dagger T_u \right) \\
& - 2Y_d^\dagger \left(2m_{\tilde{d}}^2 Y_d Y_d^\dagger Y_d + 2T_d T_d^\dagger Y_d + 2Y_d T_d^\dagger T_d \right. \\
& \left. + 2Y_d Y_d^\dagger m_{\tilde{d}}^2 Y_d + Y_d Y_d^\dagger Y_d m_{\tilde{Q}}^2 + 2Y_d m_{\tilde{Q}}^2 Y_d^\dagger Y_d \right) \\
& - 2Y_u^\dagger \left(2m_{\tilde{u}}^2 Y_u Y_u^\dagger Y_u + 2T_u T_u^\dagger Y_u + 2Y_u T_u^\dagger T_u \right. \\
& \left. + 2Y_u Y_u^\dagger m_{\tilde{u}}^2 Y_u + Y_u Y_u^\dagger Y_u m_{\tilde{Q}}^2 + 2Y_u m_{\tilde{Q}}^2 Y_u^\dagger Y_u \right) \\
& - 2 \left(4m_{h_d}^2 + m_{\tilde{Q}}^2 \right) Y_d^\dagger Y_d Y_d^\dagger Y_d - 2 \left(4m_{h_u}^2 + m_{\tilde{Q}}^2 \right) Y_u^\dagger Y_u Y_u^\dagger Y_u \\
& - 2T_d^\dagger \left(T_d \text{Tr}(Y_e Y_e^\dagger + 3Y_d Y_d^\dagger) + Y_d \text{Tr}(T_e Y_e^\dagger + 3T_d Y_d^\dagger) \right) \\
& - 2T_u^\dagger \left(T_u \text{Tr}(Y_\nu Y_\nu^\dagger + 3Y_u Y_u^\dagger) + Y_u \text{Tr}(T_\nu Y_\nu^\dagger + 3T_u Y_u^\dagger) \right) \\
& - Y_d^\dagger \left(2m_{\tilde{d}}^2 Y_d \text{Tr}(Y_e Y_e^\dagger + 3Y_d Y_d^\dagger) + 2T_d \text{Tr}(Y_e T_e^\dagger + 3Y_d T_d^\dagger) \right. \\
& \left. + 2Y_d \text{Tr}(T_e T_e^\dagger + 3T_d T_d^\dagger) + Y_d m_{\tilde{Q}}^2 \text{Tr}(Y_e Y_e^\dagger + 3Y_d Y_d^\dagger) \right) \\
& - Y_u^\dagger \left(2m_{\tilde{u}}^2 Y_u \text{Tr}(Y_\nu Y_\nu^\dagger + 3Y_u Y_u^\dagger) + 2T_u \text{Tr}(Y_\nu T_\nu^\dagger + 3Y_u T_u^\dagger) \right. \\
& \left. + 2Y_u \text{Tr}(T_\nu T_\nu^\dagger + 3T_u T_u^\dagger) + Y_u m_{\tilde{Q}}^2 \text{Tr}(Y_\nu Y_\nu^\dagger + 3Y_u Y_u^\dagger) \right) \\
& - \left(4m_{h_d}^2 + m_{\tilde{Q}}^2 \right) Y_d^\dagger Y_d \text{Tr}(Y_e Y_e^\dagger + 3Y_d Y_d^\dagger) \\
& - \left(4m_{h_u}^2 + m_{\tilde{Q}}^2 \right) Y_u^\dagger Y_u \text{Tr}(Y_\nu Y_\nu^\dagger + 3Y_u Y_u^\dagger) \\
& - 2Y_d^\dagger Y_d \text{Tr} \left(Y_e m_{\tilde{L}}^2 Y_e^\dagger + Y_e^\dagger m_{\tilde{e}}^2 Y_e + 3Y_d m_{\tilde{Q}}^2 Y_d^\dagger + 3Y_d^\dagger m_{\tilde{d}}^2 Y_d \right) \\
& - 2Y_u^\dagger Y_u \text{Tr} \left(Y_\nu m_{\tilde{L}}^2 Y_\nu^\dagger + Y_\nu^\dagger m_{\tilde{\nu}}^2 Y_\nu + 3Y_u m_{\tilde{Q}}^2 Y_u^\dagger + 3Y_u^\dagger m_{\tilde{u}}^2 Y_u \right) \\
& + \frac{2}{5}g_1^2 \left(2m_{h_d}^2 Y_d^\dagger Y_d + 4m_{h_u}^2 Y_u^\dagger Y_u + m_{\tilde{Q}}^2 Y_d^\dagger Y_d + Y_d^\dagger Y_d m_{\tilde{Q}}^2 + 2Y_d^\dagger m_{\tilde{d}}^2 Y_d \right. \\
& \left. + 2m_{\tilde{Q}}^2 Y_u^\dagger Y_u + 2Y_u^\dagger Y_u m_{\tilde{Q}}^2 + 4Y_u^\dagger m_{\tilde{u}}^2 Y_u + 2T_d^\dagger T_d + 4T_u^\dagger T_u \right) \\
& - \frac{4}{5}g_1^2 \left(M_1^* Y_d^\dagger T_d + 2M_1^* Y_u^\dagger T_u - 4|M_1|^2 Y_u^\dagger Y_u \right. \\
& \left. + M_1 T_d^\dagger Y_d + 2M_1 T_u^\dagger Y_u - 2|M_1|^2 Y_d^\dagger Y_d \right) \\
& - \frac{128}{3}g_3^4 |M_3|^2 \mathbf{1}_3 + \frac{2}{5}g_1^2 g_2^2 \text{Re}(M_1 M_2^*) \mathbf{1}_3 + \frac{32}{45}g_1^2 g_3^2 \text{Re}(M_1 M_3^*) \mathbf{1}_3 \\
& + \frac{199}{75}g_1^4 |M_1|^2 \mathbf{1}_3 + \frac{2}{5}g_1^2 g_2^2 (|M_1|^2 + |M_2|^2) \mathbf{1}_3
\end{aligned}$$

$$\begin{aligned}
& + 32g_2^2g_3^2(|M_2|^2 + \text{Re}(M_2M_3^*) + |M_3|^2) \mathbf{1}_3 \\
& + \frac{32}{45}g_1^2g_3^2(|M_1|^2 + |M_3|^2) \mathbf{1}_3 + 33g_2^4|M_2|^2 \mathbf{1}_3 \\
& + \frac{1}{15}g_1^2\sigma_1 \mathbf{1}_3 + 3g_2^2\sigma_2 \mathbf{1}_3 + \frac{16}{3}g_3^2\sigma_3 \mathbf{1}_3 + \frac{2}{5}g_1^2S' \mathbf{1}_3, \tag{E.25}
\end{aligned}$$

$$\begin{aligned}
(16\pi^2)^2\beta_{m_u^2}^{(2)} = & -2\left(2m_{h_d}^2 + 2m_{h_u}^2 + m_{\tilde{u}}^2\right) Y_u Y_d^\dagger Y_d Y_u^\dagger - 2\left(4m_{h_u}^2 + m_{\tilde{u}}^2\right) Y_u Y_u^\dagger Y_u Y_u^\dagger \\
& - 4T_u \left(T_d^\dagger Y_d Y_u^\dagger + T_u^\dagger Y_u Y_u^\dagger + Y_d^\dagger Y_d T_u^\dagger + Y_u^\dagger Y_u T_u^\dagger\right) \\
& - 4Y_u \left(T_d^\dagger T_d Y_u^\dagger + T_u^\dagger T_u Y_u^\dagger + Y_d^\dagger T_d T_u^\dagger + Y_u^\dagger T_u T_u^\dagger\right) \\
& - 2Y_u \left(2Y_d^\dagger m_d^2 Y_d Y_u^\dagger + Y_d^\dagger Y_d Y_u^\dagger m_{\tilde{u}}^2 + 2Y_d^\dagger Y_d m_{\tilde{Q}}^2 Y_u^\dagger + 2Y_u^\dagger m_{\tilde{u}}^2 Y_u Y_u^\dagger\right. \\
& \left. + Y_u^\dagger Y_u Y_u^\dagger m_{\tilde{u}}^2 + 2Y_u^\dagger Y_u m_{\tilde{Q}}^2 Y_u^\dagger + 2m_{\tilde{Q}}^2 Y_d^\dagger Y_d Y_u^\dagger + 2m_{\tilde{Q}}^2 Y_u^\dagger Y_u Y_u^\dagger\right) \\
& - 2\left(4m_{h_u}^2 + m_{\tilde{u}}^2\right) Y_u Y_u^\dagger \text{Tr}(Y_\nu Y_\nu^\dagger + 3Y_u Y_u^\dagger) \\
& - 4T_u \left(T_u^\dagger \text{Tr}(Y_\nu Y_\nu^\dagger + 3Y_u Y_u^\dagger) + Y_u^\dagger \text{Tr}(Y_\nu T_\nu^\dagger + 3Y_u T_u^\dagger)\right) \\
& - 4Y_u \left(T_u^\dagger \text{Tr}(T_\nu Y_\nu^\dagger + 3T_u Y_u^\dagger) + Y_u^\dagger \text{Tr}(T_\nu T_\nu^\dagger + 3T_u T_u^\dagger)\right) \\
& - 2Y_u^\dagger \left(Y_u^\dagger m_{\tilde{u}}^2 \text{Tr}(Y_\nu Y_\nu^\dagger + 3Y_u Y_u^\dagger) + 2m_{\tilde{Q}}^2 Y_u^\dagger \text{Tr}(Y_\nu Y_\nu^\dagger + 3Y_u Y_u^\dagger)\right) \\
& + 2Y_u^\dagger \text{Tr}(Y_\nu m_L^2 Y_\nu^\dagger + Y_\nu^\dagger m_\nu^2 Y_\nu + 3Y_u m_{\tilde{Q}}^2 Y_u^\dagger + 3Y_u^\dagger m_{\tilde{u}}^2 Y_u) \\
& + \left(6g_2^2 - \frac{2}{5}g_1^2\right) \left(m_{\tilde{u}}^2 Y_u Y_u^\dagger + Y_u Y_u^\dagger m_{\tilde{u}}^2 + 2m_{h_u}^2 Y_u Y_u^\dagger + 2Y_u m_{\tilde{Q}}^2 Y_u^\dagger + 2T_u T_u^\dagger\right) \\
& - 12g_2^2 \left(M_2^* T_u Y_u^\dagger - 2|M_2|^2 Y_u Y_u^\dagger + M_2 Y_u T_u^\dagger\right) \\
& + \frac{4}{5}g_1^2 \left(M_1^* T_u Y_u^\dagger - 2|M_1|^2 Y_u Y_u^\dagger + M_1 Y_u T_u^\dagger\right) \\
& - \frac{128}{3}g_3^4|M_3|^2 \mathbf{1}_3 + \frac{512}{45}g_1^2g_3^2(|M_1|^2 + \text{Re}(M_1M_3^*) + |M_3|^2) \mathbf{1}_3 \\
& + \frac{3424}{75}g_1^4|M_1|^2 \mathbf{1}_3 + \frac{16}{15}g_1^2\sigma_1 \mathbf{1}_3 + \frac{16}{3}g_3^2\sigma_3 \mathbf{1}_3 - \frac{8}{5}g_1^2S' \mathbf{1}_3, \tag{E.26}
\end{aligned}$$

$$\begin{aligned}
(16\pi^2)^2\beta_{m_d^2}^{(2)} = & -2\left(2m_{h_d}^2 + 2m_{h_u}^2 + m_{\tilde{d}}^2\right) Y_d Y_u^\dagger Y_u Y_d^\dagger - 2\left(4m_{h_d}^2 + m_{\tilde{d}}^2\right) Y_d Y_d^\dagger Y_d Y_d^\dagger \\
& - 4T_d \left(T_d^\dagger Y_d Y_d^\dagger + T_u^\dagger Y_u Y_d^\dagger + Y_d^\dagger Y_d T_d^\dagger + Y_u^\dagger Y_u T_d^\dagger\right) \\
& - 4Y_d \left(T_d^\dagger T_d Y_d^\dagger + T_u^\dagger T_u Y_d^\dagger + Y_d^\dagger T_d T_d^\dagger + Y_u^\dagger T_u T_d^\dagger\right) \\
& - 2Y_d \left(2Y_d^\dagger m_d^2 Y_d Y_d^\dagger + Y_d^\dagger Y_d Y_d^\dagger m_{\tilde{d}}^2 + 2Y_d^\dagger Y_d m_{\tilde{Q}}^2 Y_d^\dagger + 2Y_u^\dagger m_{\tilde{u}}^2 Y_u Y_d^\dagger\right)
\end{aligned}$$

$$\begin{aligned}
& + Y_u^\dagger Y_u Y_d^\dagger m_{\tilde{d}}^2 + 2Y_u^\dagger Y_u m_{\tilde{Q}}^2 Y_d^\dagger + 2m_{\tilde{Q}}^2 Y_d^\dagger Y_d Y_d^\dagger + 2m_{\tilde{Q}}^2 Y_u^\dagger Y_u Y_d^\dagger \\
& - 2 \left(4m_{h_d}^2 + m_{\tilde{d}}^2 \right) Y_d Y_d^\dagger \text{Tr}(Y_e Y_e^\dagger + 3Y_d Y_d^\dagger) \\
& - 4T_d \left(T_d^\dagger \text{Tr}(Y_e Y_e^\dagger + 3Y_d Y_d^\dagger) + Y_d^\dagger \text{Tr}(Y_e T_e^\dagger + 3Y_d T_d^\dagger) \right) \\
& - 4Y_d \left(T_d^\dagger \text{Tr}(T_e Y_e^\dagger + 3T_d Y_d^\dagger) + Y_d^\dagger \text{Tr}(T_e T_e^\dagger + 3T_d T_d^\dagger) \right) \\
& - 2Y_d^\dagger \left(Y_d^\dagger m_{\tilde{d}}^2 \text{Tr}(Y_e Y_e^\dagger + 3Y_d Y_d^\dagger) + 2m_{\tilde{Q}}^2 Y_d^\dagger \text{Tr}(Y_e Y_e^\dagger + 3Y_d Y_d^\dagger) \right) \\
& + 2Y_d^\dagger \text{Tr}(Y_e m_L^2 Y_e^\dagger + Y_e^\dagger m_{\tilde{e}}^2 Y_e + 3Y_d m_{\tilde{Q}}^2 Y_d^\dagger + 3Y_d^\dagger m_{\tilde{d}}^2 Y_d) \\
& + \left(6g_2^2 + \frac{2}{5}g_1^2 \right) \left(m_{\tilde{d}}^2 Y_d Y_d^\dagger + Y_d Y_d^\dagger m_{\tilde{d}}^2 + 2m_{h_d}^2 Y_d Y_d^\dagger + 2Y_d m_{\tilde{Q}}^2 Y_d^\dagger + 2T_d T_d^\dagger \right) \\
& - 12g_2^2 \left(M_2^* T_d Y_d^\dagger - 2|M_2|^2 Y_d Y_d^\dagger + M_2 Y_d T_d^\dagger \right) \\
& - \frac{4}{5}g_1^2 \left(M_1^* T_d Y_d^\dagger - 2|M_1|^2 Y_d Y_d^\dagger + M_1 Y_d T_d^\dagger \right) \\
& - \frac{128}{3}g_3^4 |M_3|^2 \mathbf{1}_3 + \frac{128}{45}g_1^2 g_3^2 \left(|M_1|^2 + \text{Re}(M_1 M_3^*) + |M_3|^2 \right) \mathbf{1}_3 \\
& + \frac{808}{75}g_1^4 |M_1|^2 \mathbf{1}_3 + \frac{4}{15}g_1^2 \sigma_1 \mathbf{1}_3 + \frac{16}{3}g_3^2 \sigma_3 \mathbf{1}_3 + \frac{4}{5}g_1^2 S' \mathbf{1}_3, \tag{E.27}
\end{aligned}$$

$$\begin{aligned}
(16\pi^2)^2 \beta_{m_{\tilde{e}}^2}^{(2)} = & - 2 \left(2m_{h_d}^2 + 2m_{h_u}^2 + m_{\tilde{e}}^2 \right) Y_e Y_\nu^\dagger Y_\nu Y_e^\dagger - 2 \left(4m_{h_d}^2 + m_{\tilde{e}}^2 \right) Y_e Y_e^\dagger Y_e Y_e^\dagger \\
& - 4T_e \left(T_e^\dagger Y_e Y_e^\dagger + T_\nu^\dagger Y_\nu Y_e^\dagger + Y_e^\dagger Y_e T_e^\dagger + Y_\nu^\dagger Y_\nu T_e^\dagger \right) \\
& - 4Y_e \left(T_e^\dagger T_e Y_e^\dagger + T_\nu^\dagger T_\nu Y_e^\dagger + Y_e^\dagger T_e T_e^\dagger + Y_\nu^\dagger T_\nu T_e^\dagger \right) \\
& - 2Y_e \left(2Y_e^\dagger m_{\tilde{e}}^2 Y_e Y_e^\dagger + Y_e^\dagger Y_e Y_e^\dagger m_{\tilde{e}}^2 + 2Y_e^\dagger Y_e m_L^2 Y_e^\dagger + 2Y_\nu^\dagger m_{\tilde{\nu}}^2 Y_\nu Y_e^\dagger \right. \\
& \left. + Y_\nu^\dagger Y_\nu Y_e^\dagger m_{\tilde{e}}^2 + 2Y_\nu^\dagger Y_\nu m_L^2 Y_e^\dagger + 2m_{\tilde{L}}^2 Y_e^\dagger Y_e Y_e^\dagger + 2m_{\tilde{L}}^2 Y_\nu^\dagger Y_\nu Y_e^\dagger \right) \\
& - 2 \left(4m_{h_d}^2 + m_{\tilde{e}}^2 \right) Y_e Y_e^\dagger \text{Tr}(Y_e Y_e^\dagger + 3Y_d Y_d^\dagger) \\
& - 4T_e \left(T_e^\dagger \text{Tr}(Y_e Y_e^\dagger + 3Y_d Y_d^\dagger) + Y_e^\dagger \text{Tr}(Y_e T_e^\dagger + 3Y_d T_d^\dagger) \right) \\
& - 4Y_e \left(T_e^\dagger \text{Tr}(T_e Y_e^\dagger + 3T_d Y_d^\dagger) + Y_e^\dagger \text{Tr}(T_e T_e^\dagger + 3T_d T_d^\dagger) \right) \\
& - 2Y_e^\dagger \left(Y_e^\dagger m_{\tilde{e}}^2 \text{Tr}(Y_e Y_e^\dagger + 3Y_d Y_d^\dagger) + 2m_L^2 Y_e^\dagger \text{Tr}(Y_e Y_e^\dagger + 3Y_d Y_d^\dagger) \right) \\
& + 2Y_e^\dagger \text{Tr}(Y_e m_L^2 Y_e^\dagger + Y_e^\dagger m_{\tilde{e}}^2 Y_e + 3Y_d m_{\tilde{Q}}^2 Y_d^\dagger + 3Y_d^\dagger m_{\tilde{d}}^2 Y_d) \\
& + \left(6g_2^2 - \frac{6}{5}g_1^2 \right) \left(m_{\tilde{e}}^2 Y_e Y_e^\dagger + Y_e Y_e^\dagger m_{\tilde{e}}^2 + 2m_{h_d}^2 Y_e Y_e^\dagger + 2Y_e m_L^2 Y_e^\dagger + 2T_e T_e^\dagger \right) \\
& - 12g_2^2 \left(M_2^* T_e Y_e^\dagger - 2|M_2|^2 Y_e Y_e^\dagger + M_2 Y_e T_e^\dagger \right)
\end{aligned}$$

$$\begin{aligned}
& + \frac{12}{5} g_1^2 \left(M_1^* T_e Y_e^\dagger - 2|M_1|^2 Y_e Y_e^\dagger + M_1 Y_e T_e^\dagger \right) \\
& + \frac{2808}{25} g_1^4 |M_1|^2 \mathbf{1}_3 + \frac{12}{5} g_1^2 \sigma_1 \mathbf{1}_3 + \frac{12}{5} g_1^2 S' \mathbf{1}_3 ,
\end{aligned} \tag{E.28}$$

$$\begin{aligned}
(16\pi^2)^2 \beta_{m_{\tilde{\nu}}^2}^{(2)} = & -2 \left(2m_{h_d}^2 + 2m_{h_u}^2 + m_{\tilde{\nu}}^2 \right) Y_\nu Y_e^\dagger Y_e Y_\nu^\dagger - 2 \left(4m_{h_u}^2 + m_{\tilde{\nu}}^2 \right) Y_\nu Y_\nu^\dagger Y_\nu Y_\nu^\dagger \\
& - 4T_\nu \left(T_e^\dagger Y_e Y_\nu^\dagger + T_\nu^\dagger Y_\nu Y_\nu^\dagger + Y_e^\dagger Y_e T_\nu^\dagger + Y_\nu^\dagger Y_\nu T_\nu^\dagger \right) \\
& - 4Y_\nu \left(T_e^\dagger T_e Y_\nu^\dagger + T_\nu^\dagger T_\nu Y_\nu^\dagger + Y_e^\dagger T_e T_\nu^\dagger + Y_\nu^\dagger T_\nu T_\nu^\dagger \right) \\
& - 2Y_\nu \left(2Y_e^\dagger m_{\tilde{e}}^2 Y_e Y_\nu^\dagger + Y_e^\dagger Y_e Y_\nu^\dagger m_{\tilde{\nu}}^2 + 2Y_e^\dagger Y_e m_{\tilde{L}}^2 Y_\nu^\dagger + 2Y_\nu^\dagger m_{\tilde{\nu}}^2 Y_\nu Y_\nu^\dagger \right. \\
& \left. + Y_\nu^\dagger Y_\nu Y_\nu^\dagger m_{\tilde{\nu}}^2 + 2Y_\nu^\dagger Y_\nu m_{\tilde{L}}^2 Y_\nu^\dagger + 2m_{\tilde{L}}^2 Y_e^\dagger Y_e Y_\nu^\dagger + 2m_{\tilde{L}}^2 Y_\nu^\dagger Y_\nu Y_\nu^\dagger \right) \\
& - 2 \left(4m_{h_u}^2 + m_{\tilde{\nu}}^2 \right) Y_\nu Y_\nu^\dagger \text{Tr}(Y_\nu Y_\nu^\dagger + 3Y_u Y_u^\dagger) \\
& - 4T_\nu \left(T_\nu^\dagger \text{Tr}(Y_\nu Y_\nu^\dagger + 3Y_u Y_u^\dagger) + Y_\nu^\dagger \text{Tr}(Y_\nu T_\nu^\dagger + 3Y_u T_u^\dagger) \right) \\
& - 4Y_\nu \left(T_\nu^\dagger \text{Tr}(T_\nu Y_\nu^\dagger + 3T_u Y_u^\dagger) + Y_\nu^\dagger \text{Tr}(T_\nu T_\nu^\dagger + 3T_u T_u^\dagger) \right) \\
& - 2Y_\nu^\dagger \left(Y_\nu^\dagger m_{\tilde{\nu}}^2 \text{Tr}(Y_\nu Y_\nu^\dagger + 3Y_u Y_u^\dagger) + 2m_{\tilde{L}}^2 Y_\nu^\dagger \text{Tr}(Y_\nu Y_\nu^\dagger + 3Y_u Y_u^\dagger) \right. \\
& \left. + 2Y_\nu^\dagger \text{Tr}(Y_\nu m_{\tilde{L}}^2 Y_\nu^\dagger + Y_\nu^\dagger m_{\tilde{\nu}}^2 Y_\nu + 3Y_u m_{\tilde{Q}}^2 Y_u^\dagger + 3Y_u^\dagger m_{\tilde{u}}^2 Y_u) \right) \\
& + \left(6g_2^2 + \frac{6}{5} g_1^2 \right) \left(m_{\tilde{\nu}}^2 Y_\nu Y_\nu^\dagger + Y_\nu Y_\nu^\dagger m_{\tilde{\nu}}^2 + 2m_{h_u}^2 Y_\nu Y_\nu^\dagger + 2Y_\nu m_{\tilde{L}}^2 Y_\nu^\dagger + 2T_\nu T_\nu^\dagger \right) \\
& - 12g_2^2 \left(M_2^* T_\nu Y_\nu^\dagger - 2|M_2|^2 Y_\nu Y_\nu^\dagger + M_2 Y_\nu T_\nu^\dagger \right) \\
& - \frac{12}{5} g_1^2 \left(M_1^* T_\nu Y_\nu^\dagger - 2|M_1|^2 Y_\nu Y_\nu^\dagger + M_1 Y_\nu T_\nu^\dagger \right) ,
\end{aligned} \tag{E.29}$$

$$\begin{aligned}
(16\pi^2)^2 \beta_{m_{h_d}^2}^{(2)} = & -2 \left(m_{h_d}^2 + m_{h_u}^2 \right) \text{Tr}(Y_e Y_\nu^\dagger Y_\nu Y_e^\dagger + 3Y_d Y_u^\dagger Y_u Y_d^\dagger) \\
& - 12m_{h_d}^2 \text{Tr}(Y_e Y_e^\dagger Y_e Y_e^\dagger + 3Y_d Y_d^\dagger Y_d Y_d^\dagger) \\
& - 12\text{Tr}(T_e^\dagger T_e Y_e^\dagger Y_e + 3T_d^\dagger T_d Y_d^\dagger Y_d + T_e^\dagger Y_e Y_e^\dagger T_e + 3T_d^\dagger Y_d Y_d^\dagger T_d) \\
& - 2\text{Tr}(T_e T_\nu^\dagger Y_\nu Y_e^\dagger + 3T_d T_u^\dagger Y_u Y_d^\dagger + T_e Y_\nu^\dagger Y_\nu T_e^\dagger + 3T_d Y_u^\dagger Y_u T_d^\dagger) \\
& - 2\text{Tr}(Y_e T_\nu^\dagger T_\nu Y_e^\dagger + 3Y_d T_u^\dagger T_u Y_d^\dagger + Y_e Y_\nu^\dagger T_\nu T_e^\dagger + 3Y_d Y_u^\dagger T_u T_d^\dagger) \\
& - 36\text{Tr}(Y_d Y_d^\dagger m_{\tilde{d}}^2 Y_d Y_d^\dagger + Y_d^\dagger Y_d m_{\tilde{Q}}^2 Y_d^\dagger Y_d) \\
& - 12\text{Tr}(Y_e Y_e^\dagger m_{\tilde{e}}^2 Y_e Y_e^\dagger + Y_e^\dagger Y_e m_{\tilde{L}}^2 Y_e^\dagger Y_e) \\
& - 6\text{Tr}(Y_u Y_d^\dagger m_{\tilde{d}}^2 Y_d Y_u^\dagger + Y_d Y_u^\dagger m_{\tilde{u}}^2 Y_u Y_d^\dagger + Y_u^\dagger Y_u m_{\tilde{Q}}^2 Y_d^\dagger Y_d + Y_d^\dagger Y_d m_{\tilde{Q}}^2 Y_u^\dagger Y_u) \\
& - 2\text{Tr}(Y_\nu Y_e^\dagger m_{\tilde{e}}^2 Y_e Y_\nu^\dagger + Y_e Y_\nu^\dagger m_{\tilde{\nu}}^2 Y_\nu Y_e^\dagger + Y_\nu^\dagger Y_\nu m_{\tilde{L}}^2 Y_e^\dagger Y_e + Y_e^\dagger Y_e m_{\tilde{L}}^2 Y_\nu^\dagger Y_\nu)
\end{aligned}$$

$$\begin{aligned}
& + \left(32g_3^2 - \frac{4}{5}g_1^2 \right) \text{Tr}(T_d^\dagger T_d + m_{h_d}^2 Y_d^\dagger Y_d + Y_d m_Q^2 Y_d^\dagger + Y_d^\dagger m_d^2 Y_d) \\
& + \frac{12}{5}g_1^2 \text{Tr}(T_e^\dagger T_e + m_{h_d}^2 Y_e^\dagger Y_e + Y_e m_L^2 Y_e^\dagger + Y_e^\dagger m_e^2 Y_e) \\
& - \frac{12}{5}g_1^2 \text{Tr}(M_1^* Y_e^\dagger T_e + M_1 T_e^\dagger Y_e - 2|M_1|^2 Y_e^\dagger Y_e) \\
& + \frac{4}{5}g_1^2 \text{Tr}(M_1^* Y_d^\dagger T_d + M_1 T_d^\dagger Y_d - 2|M_1|^2 Y_d^\dagger Y_d) \\
& - 32g_3^2 \text{Tr}(M_3^* Y_d^\dagger T_d + M_3 T_d^\dagger Y_d - 2|M_3|^2 Y_d^\dagger Y_d) \\
& + \frac{18}{5}g_1^2 g_2^2 \left(|M_1|^2 + \text{Re}(M_1 M_2^*) + |M_2|^2 \right) \\
& + \frac{621}{25}g_1^4 |M_1|^2 + 33g_2^4 |M_2|^2 + \frac{3}{5}g_1^2 \sigma_1 + 3g_2^2 \sigma_2 - \frac{6}{5}g_1^2 S' , \tag{E.30}
\end{aligned}$$

$$\begin{aligned}
(16\pi^2)^2 \beta_{m_{h_u}^2}^{(2)} & = -2 \left(m_{h_d}^2 + m_{h_u}^2 \right) \text{Tr}(Y_e Y_\nu^\dagger Y_\nu Y_e^\dagger + 3Y_d Y_u^\dagger Y_u Y_d^\dagger) \\
& - 12m_{h_u}^2 \text{Tr}(Y_\nu Y_\nu^\dagger Y_\nu Y_\nu^\dagger + 3Y_u Y_u^\dagger Y_u Y_u^\dagger) \\
& - 12\text{Tr}(T_\nu^\dagger T_\nu Y_\nu^\dagger Y_\nu + 3T_u^\dagger T_u Y_u^\dagger Y_u + T_\nu^\dagger Y_\nu Y_\nu^\dagger T_\nu + 3T_u^\dagger Y_u Y_u^\dagger T_u) \\
& - 2\text{Tr}(T_e T_\nu^\dagger Y_\nu Y_e^\dagger + 3T_d T_u^\dagger Y_u Y_d^\dagger + T_e Y_\nu^\dagger Y_\nu T_e^\dagger + 3T_d Y_u^\dagger Y_u T_d^\dagger) \\
& - 2\text{Tr}(Y_e T_\nu^\dagger T_\nu Y_e^\dagger + 3Y_d T_u^\dagger T_u Y_d^\dagger + Y_e Y_\nu^\dagger T_\nu T_e^\dagger + 3Y_d Y_u^\dagger T_u T_d^\dagger) \\
& - 36\text{Tr}(Y_u Y_u^\dagger m_u^2 Y_u Y_u^\dagger + Y_u^\dagger Y_u m_Q^2 Y_u^\dagger Y_u) \\
& - 12\text{Tr}(Y_\nu Y_\nu^\dagger m_\nu^2 Y_\nu Y_\nu^\dagger + Y_\nu^\dagger Y_\nu m_L^2 Y_\nu^\dagger Y_\nu) \\
& - 6\text{Tr}(Y_u Y_d^\dagger m_d^2 Y_d Y_u^\dagger + Y_d Y_u^\dagger m_u^2 Y_u Y_d^\dagger + Y_u^\dagger Y_u m_Q^2 Y_d^\dagger Y_d + Y_d^\dagger Y_d m_Q^2 Y_u^\dagger Y_u) \\
& - 2\text{Tr}(Y_\nu Y_e^\dagger m_e^2 Y_e Y_\nu^\dagger + Y_e Y_\nu^\dagger m_\nu^2 Y_\nu Y_e^\dagger + Y_\nu^\dagger Y_\nu m_L^2 Y_e^\dagger Y_e + Y_e^\dagger Y_e m_L^2 Y_\nu^\dagger Y_\nu) \\
& + \left(32g_3^2 + \frac{8}{5}g_1^2 \right) \text{Tr}(T_u^\dagger T_u + m_{h_u}^2 Y_u^\dagger Y_u + Y_u m_Q^2 Y_u^\dagger + Y_u^\dagger m_u^2 Y_u) \\
& - \frac{8}{5}g_1^2 \text{Tr}(M_1^* Y_u^\dagger T_u + M_1 T_u^\dagger Y_u - 2|M_1|^2 Y_u^\dagger Y_u) \\
& - 32g_3^2 \text{Tr}(M_3^* Y_u^\dagger T_u + M_3 T_u^\dagger Y_u - 2|M_3|^2 Y_u^\dagger Y_u) \\
& + \frac{18}{5}g_1^2 g_2^2 \left(|M_1|^2 + \text{Re}(M_1 M_2^*) + |M_2|^2 \right) \\
& + \frac{621}{25}g_1^4 |M_1|^2 + 33g_2^4 |M_2|^2 + \frac{3}{5}g_1^2 \sigma_1 + 3g_2^2 \sigma_2 + \frac{6}{5}g_1^2 S' , \tag{E.31}
\end{aligned}$$

with

$$\sigma_1 = \frac{1}{5}g_1^2 \left(3m_{h_u}^2 + 3m_{h_d}^2 + \text{Tr} \left(m_Q^2 + 3m_L^2 + 2m_d^2 + 6m_e^2 + 8m_u^2 \right) \right) , \tag{E.32}$$

$$\sigma_2 = g_2^2 \left(m_{h_u}^2 + m_{h_d}^2 + \text{Tr} \left(3m_Q^2 + m_L^2 \right) \right) , \tag{E.33}$$

$$\sigma_3 = g_3^2 \text{Tr} \left(2m_Q^2 + m_d^2 + m_u^2 \right) , \tag{E.34}$$

and

$$\begin{aligned}
S' = & m_{h_d}^2 \text{Tr} \left(Y_e Y_e^\dagger + 3Y_d Y_d^\dagger \right) - m_{h_u}^2 \text{Tr} \left(Y_\nu Y_\nu^\dagger + 3Y_u Y_u^\dagger \right) \\
& + \text{Tr} \left(m_L^2 Y_e^\dagger Y_e + m_L^2 Y_\nu^\dagger Y_\nu \right) - \text{Tr} \left(m_Q^2 Y_d^\dagger Y_d + m_Q^2 Y_u^\dagger Y_u \right) \\
& - 2\text{Tr} \left(Y_d Y_d^\dagger m_d^2 + Y_e Y_e^\dagger m_e^2 - 2Y_u Y_u^\dagger m_u^2 \right) \\
& + \frac{1}{30} g_1^2 \left(9m_{h_u}^2 - 9m_{h_d}^2 + \text{Tr} \left(m_Q^2 - 9m_L^2 + 4m_d^2 + 36m_e^2 - 32m_u^2 \right) \right) \\
& + \frac{3}{2} g_2^2 \left(m_{h_u}^2 - m_{h_d}^2 + \text{Tr} \left(m_Q^2 - m_L^2 \right) \right) \\
& + \frac{8}{3} g_3^2 \text{Tr} \left(m_Q^2 + m_d^2 - 2m_u^2 \right) . \tag{E.35}
\end{aligned}$$

APPENDIX F

Self-energies and one-loop tadpoles including inter-generational mixing

Here we present formulae used in chapter 10 and `SusyTC` for the self-energies Π_{ZZ}^T , $\Pi_{H^+H^-}$, Π_{AA} , and the one-loop tadpoles t_u , t_d , which are based on [201] but generalised to include inter-generational mixing. In this appendix we employ SLHA 2 conventions [123] in the Super-CKM and Super-PMNS basis, to agree with the convention of [201]. With the R-L REAP conventions (10.1) and (10.2) employed in chapter 10, the SCKM/SPMNS matrices are obtained via

$$\begin{aligned}
 y_f &\equiv Y_f^{\text{diag}} = \left(U_R^{(f)} \right)^\dagger Y_f \left(U_L^{(f)} \right) , \\
 \hat{T}_f &\equiv \left(U_R^{(f)} \right)^\dagger T_f \left(U_L^{(f)} \right) , \\
 \hat{m}_{\tilde{Q}}^2 &\equiv \left(U_L^{(d)} \right)^\dagger m_{\tilde{Q}}^2 \left(U_L^{(d)} \right) , \\
 \hat{m}_{\tilde{L}}^2 &\equiv \left(U_L^{(e)} \right)^\dagger m_{\tilde{L}}^2 \left(U_L^{(d)} \right) , \\
 \hat{m}_{\tilde{u}}^2 &\equiv \left(U_R^{(u)} \right)^\dagger m_{\tilde{u}}^2 \left(U_R^{(u)} \right) , \\
 \hat{m}_{\tilde{d}}^2 &\equiv \left(U_R^{(d)} \right)^\dagger m_{\tilde{d}}^2 \left(U_R^{(d)} \right) , \\
 \hat{m}_{\tilde{e}}^2 &\equiv \left(U_R^{(e)} \right)^\dagger m_{\tilde{e}}^2 \left(U_R^{(e)} \right) .
 \end{aligned} \tag{F.1}$$

Note that all formulae of appendix B, i.e. the definition of sparticle mass and mixing matrices, are in SCKM/SPMNS basis with SLHA 2 conventions and thus valid in this appendix as well. When starting from the flavour basis of chapter 10, one only needs to replace (B.2) by (F.1). Let us remark that the convention in [201] for μ differs by a sign from our convention.

We now present the generalisation of Π_{ZZ}^T , $\Pi_{H^+H^-}$, Π_{AA} , t_u , and t_d of [201] to include inter-generational mixing. For all formulae we have checked that our equations reduce to

the corresponding equations in [201] when

$$\begin{aligned} W_{\tilde{f}_i i} &= W_{\tilde{f}_{i+3} i+3} = \cos \theta_{\tilde{f}_i} \\ W_{\tilde{f}_i i+3} &= -W_{\tilde{f}_{i+3} i} = -\sin \theta_{\tilde{f}_i}, \end{aligned} \quad (\text{F.2})$$

where $i = 1 \dots 3$ and $W_{\tilde{f}}$ is defined in (B.6).

We keep the abbreviations of [201]:

$$s_{\alpha\beta} \equiv \sin(\alpha - \beta), \quad (\text{F.3})$$

$$c_{\alpha\beta} \equiv \cos(\alpha - \beta), \quad (\text{F.4})$$

$$g_{f_L} \equiv I_3 - Q_e \sin^2 \theta_W, \quad (\text{F.5})$$

$$g_{f_R} \equiv Q_e \sin^2 \theta_W, \quad (\text{F.6})$$

$$e \equiv g_2 \sin \theta_W, \quad (\text{F.7})$$

$$N_C \equiv \begin{cases} 3 & \text{for (s)quarks} \\ 1 & \text{for (s)fermions} \end{cases}. \quad (\text{F.8})$$

The conventions for the one-loop scalar functions A_0 , B_{22} , \tilde{B}_{22} , H , G , and F [220] are adopted from appendix B of [201]. Summations \sum_f are over all fermions, whereas summations \sum_{f_u} , \sum_{f_d} are restricted to up-type and down-type fermions, respectively. Summations \sum_Q , $\sum_{\tilde{Q}}$ are over $SU(2)$ (s)quark doublets, and analogously for (s)leptons. In summations over sfermions the indices i , j , s , and t run from 1 to 6 for \tilde{u} , \tilde{d} , and \tilde{e} and from 1 to 3 for $\tilde{\nu}$. In summations of neutralinos (charginos) the indices i , j run from 1 to 4 (2). The summation \sum_{h^0} runs over all neutral Higgs- and Goldstone bosons, the summation \sum_{h^\pm} over the charged ones.

$$\begin{aligned} 16\pi^2 \frac{\cos^2 \theta_W}{g_2^2} \Pi_{ZZ}^T(p^2) &= -s_{\alpha\beta}^2 \left(\tilde{B}_{22}(m_A, m_H) + \tilde{B}_{22}(M_Z, m_h) - M_Z^2 B_0(M_Z, m_h) \right) \\ &\quad - c_{\alpha\beta}^2 \left(\tilde{B}_{22}(M_Z, m_H) + \tilde{B}_{22}(m_A, m_h) - M_Z^2 B_0(M_Z, m_h) \right) \\ &\quad - 2 \cos^4 \theta_W \left(2p^2 + M_W^2 - M_Z^2 \frac{\sin^4 \theta_W}{\cos^2 \theta_W} \right) B_0(M_W, M_W) \\ &\quad - (8 \cos^4 \theta_W + \cos^2(2\theta_W)) \tilde{B}_{22}(M_W, M_W) \\ &\quad - \cos^2(2\theta_W) \tilde{B}_{22}(m_{H^\pm}, m_{H^\pm}) \\ &\quad - \sum_{\tilde{f}} N_C \sum_{s,t} \left| I_3 \sum_i W_{\tilde{f}_{is}}^* W_{\tilde{f}_{it}} - Q_e \sin^2 \theta_W \delta_{st} \right|^2 4B_{22}(m_{\tilde{f}_s}, m_{\tilde{f}_t}) \\ &\quad + \frac{1}{2} \sum_{\tilde{f}} N_C \sum_s \left((1 - 8I_3 Q_e \sin^2 \theta_W) \sum_i W_{\tilde{f}_{is}}^* W_{\tilde{f}_{is}} \right. \\ &\quad \left. + 4Q_e^2 \sin^4 \theta_W \right) A_0(m_{\tilde{f}_s}) \end{aligned}$$

210 F. Self-energies and one-loop tadpoles including inter-generational mixing

$$\begin{aligned}
& + \sum_f N_C \left((g_{f_L}^2 + g_{f_R}^2) H(m_f, m_f) - 4g_{f_L}g_{f_R}m_f^2 B_0(m_f, m_f) \right) \\
& + \frac{\cos^2 \theta_W}{2g_2^2} \sum_{i,j} f_{ijZ}^0 H(m_{\tilde{\chi}_i^0}, m_{\tilde{\chi}_j^0}) + 2g_{ijZ}^0 m_{\tilde{\chi}_i^0} m_{\tilde{\chi}_j^0} B_0(m_{\tilde{\chi}_i^0}, m_{\tilde{\chi}_j^0}) \\
& + \frac{\cos^2 \theta_W}{g_2^2} \sum_{i,j} f_{ijZ}^+ H(m_{\tilde{\chi}_i^+}, m_{\tilde{\chi}_j^+}) + 2g_{ijZ}^+ m_{\tilde{\chi}_i^+} m_{\tilde{\chi}_j^+} B_0(m_{\tilde{\chi}_i^+}, m_{\tilde{\chi}_j^+}) .
\end{aligned} \tag{F.9}$$

The couplings f_Z^0 , f_Z^+ , g_Z^0 , and g_Z^+ are given in Eqs. (A.7) and (D.5) of [201].

$$\begin{aligned}
16\pi^2 \Pi_{H^+H^-}(p^2) = & \sum_Q N_C \left((\cos^2 \beta y_u^2 + \sin^2 \beta y_d^2) G(m_u, m_d) \right. \\
& \left. - 2 \sin(2\beta) y_u y_d m_u m_d B_0(m_u, m_d) \right) \\
& + \sum_L \sin^2 \beta y_e^2 G(0, m_e) \\
& + \sum_{\tilde{Q}} N_C \sum_{i,j} (\lambda_{H+\tilde{Q}})_{ij}^2 B_0(m_{\tilde{u}_i}, m_{\tilde{d}_j}) \\
& + \sum_{\tilde{L}} \sum_{i,j} (\lambda_{H+\tilde{L}})_{ij}^2 B_0(m_{\tilde{\nu}_i}, m_{\tilde{e}_j}) \\
& + \sum_{\tilde{f}} \sum_i (\lambda_{H^+H^-\tilde{f}})_{ii} A_0(m_{\tilde{f}_i}) \\
& + \frac{g_2^2}{4} \left(s_{\alpha\beta}^2 F(m_H, M_W) + c_{\alpha\beta}^2 F(m_h, M_W) + F(m_A, M_W) \right. \\
& \left. + \frac{\cos^2(2\theta_W)}{\cos^2 \theta_W} F(m_{H^+}, M_Z) \right) \\
& + e^2 F(m_{H^+}, 0) + 2g_2^2 A_0(M_W) + g_2^2 \cos^2(2\theta_W) A_0(M_Z) \\
& + \sum_{h^+} \left(\sum_{h^0} (\lambda_{H+h^0h^-})^2 B_0(m_{h^0}, m_{h^+}) + \lambda_{H^+H^-h^0h^+} A_0(m_{h^+}) \right) \\
& + g_2^2 \frac{M_W^2}{4} B_0(M_W, m_A) \\
& + \frac{1}{2} \sum_{h^0} \lambda_{H^+H^-h^0h^0} A_0(m_{h^0}) \\
& + \sum_{j,i} f_{ijH^+} G(m_{\tilde{\chi}_j^+}, m_{\tilde{\chi}_i^0}) - 2m_{\tilde{\chi}_j^+} m_{\tilde{\chi}_i^0} g_{ijH^+} B_0(m_{\tilde{\chi}_j^+}, m_{\tilde{\chi}_i^0}) .
\end{aligned} \tag{F.10}$$

The couplings f_{H^+} and g_{H^+} are given in Eq. (D.70) and Eqs. (D.39-D.42) of [201]. The cou-

plings $\lambda_{H^+H^-h^-}$, $\lambda_{H^+H^-h^+h^-}$, and $\lambda_{H^+H^-h^0h^0}$ are defined in Eqs. (D.63-D.65) and Eq. (D.67) of [201]. The couplings to sfermions in the case of inter-generational mixing are given by

$$\lambda_{H^+\tilde{Q}} = W_{\tilde{u}} \begin{pmatrix} \frac{g_2}{\sqrt{2}} \hat{M}_W \sin(2\beta) \mathbf{1}_3 - (y_u^2 + y_d^2) \cos \beta \frac{v \sin \beta}{\sqrt{2}} & -\hat{T}_d^\dagger \sin \beta - \mu y_d \cos \beta \\ -\hat{T}_u \cos \beta - \mu^* y_u \sin \beta & -y_u y_d \frac{v}{\sqrt{2}} \end{pmatrix} W_{\tilde{d}}, \quad (\text{F.11})$$

$$\lambda_{H^+\tilde{L}} = W_{\tilde{\nu}} \begin{pmatrix} \frac{g_2}{\sqrt{2}} \hat{M}_W \sin(2\beta) \mathbf{1}_3 - y_e^2 \cos \beta \frac{v \sin \beta}{\sqrt{2}} & -\hat{T}_e^\dagger \sin \beta - \mu y_e \cos \beta \end{pmatrix} W_{\tilde{e}}, \quad (\text{F.12})$$

$$\lambda_{H^+H^-\tilde{f}} = -W_{\tilde{f}}^\dagger \begin{pmatrix} -\frac{g_2^2}{2} \cos(2\beta) \left(\frac{\cos(2\theta_W)}{\cos^2 \theta_W} I_3 + \tan^2 \theta_W Q_e \right) \mathbf{1}_3 & 0 \\ 0 & \frac{g_2^2}{2} \cos(2\beta) \tan^2 \theta_W Q_e \mathbf{1}_3 \end{pmatrix} W_{\tilde{f}} + \begin{cases} W_{\tilde{u}}^\dagger \begin{pmatrix} y_d^2 \sin^2 \beta & 0 \\ 0 & y_u^2 \cos^2 \beta \end{pmatrix} W_{\tilde{u}} & \tilde{f} = \tilde{u} \\ W_{\tilde{d}}^\dagger \begin{pmatrix} y_u^2 \cos^2 \beta & 0 \\ 0 & y_d^2 \sin^2 \beta \end{pmatrix} W_{\tilde{d}} & \tilde{f} = \tilde{d} \\ W_{\tilde{e}}^\dagger \begin{pmatrix} 0 & 0 \\ 0 & y_e^2 \sin^2 \beta \end{pmatrix} W_{\tilde{e}} & \tilde{f} = \tilde{e} \end{cases}, \quad (\text{F.13})$$

$$\lambda_{H^+H^-\tilde{\nu}} = -W_{\tilde{\nu}}^\dagger \begin{pmatrix} -\frac{g_2^2}{2} \cos(2\beta) \left(\frac{\cos(2\theta_W)}{\cos^2 \theta_W} I_3 + \tan^2 \theta_W Q_e \right) \mathbf{1}_3 - y_e^2 \sin^2 \beta \end{pmatrix} W_{\tilde{\nu}} \quad (\text{F.14})$$

$$\begin{aligned} 16\pi^2 \Pi_{AA}(p^2) &= \cos^2 \beta \sum_{f_u} N_C y_{f_u}^2 (p^2 B_0(m_{f_u}, m_{f_u}) - 2A_0(m_{f_u})) \\ &+ \sin^2 \beta \sum_{f_d} N_C y_{f_d}^2 (p^2 B_0(m_{f_d}, m_{f_d}) - 2A_0(m_{f_d})) \\ &+ \sum_{\tilde{f}} \sum_i N_C \left((\lambda_{AA\tilde{f}})_{ii} A_0(m_{\tilde{f}_i}) + \sum_j (\lambda_{A\tilde{f}})_{ij}^2 B_0(m_{\tilde{f}_i}, m_{\tilde{f}_j}) \right) \\ &+ \frac{g_2^2}{4} \left(2F(m_{H^+}, M_W) + \frac{s_{\alpha\beta}^2}{\cos^2 \theta_W} F(m_H, M_Z) + \frac{c_{\alpha\beta}^2}{\cos^2 \theta_W} F(m_h, M_Z) \right) \\ &+ \frac{1}{2} \sum_{h_n^0} \left(\sum_{h_m^0} \lambda_{Ah_n^0 h_m^0} B_0(m_{h_n^0}, m_{h_m^0}) + \lambda_{AAh_n^0 h_n^0} A_0(m_{h_n^0}) \right) \\ &+ g_2^2 \left(\frac{M_W^2}{2} B_0(M_W, m_{H_p}) + 2A_0(M_W) + \frac{1}{\cos^2 \theta_W} A_0(M_Z) \right) \\ &+ \sum_{h^+} \lambda_{AAh^+ h^+} A_0(m_{h^+}) \end{aligned}$$

212 F. Self-energies and one-loop tadpoles including inter-generational mixing

$$\begin{aligned}
& + \frac{1}{2} \sum_{i,j} f_{ijA}^0 G(m_{\tilde{\chi}_i^0}, m_{\tilde{\chi}_j^0}) - 2g_{ijA}^0 m_{\tilde{\chi}_i^0} m_{\tilde{\chi}_j^0} B_0(m_{\tilde{\chi}_i^0}, m_{\tilde{\chi}_j^0}) \\
& + \sum_{i,j} f_{ijA}^+ G(m_{\tilde{\chi}_i^+}, m_{\tilde{\chi}_j^+}) - 2g_{ijA}^+ m_{\tilde{\chi}_i^+} m_{\tilde{\chi}_j^+} B_0(m_{\tilde{\chi}_i^+}, m_{\tilde{\chi}_j^+}) .
\end{aligned} \tag{F.15}$$

The couplings f_A^0 , g_A^0 , f_A^+ , and g_A^+ are given in Eq. (D.70) and Eqs. (D.34-D.38) of [201]. The couplings $\lambda_{Ah^0h^0}$, $\lambda_{AAh^0h^0}$, and $\lambda_{AAh^+h^+}$ are defined in Eqs. (D.63-D.65) and Eq. (D.67) of [201]. The couplings to sfermions in the case of inter-generational mixing are given by

$$\lambda_{A\tilde{u}} = W_{\tilde{u}}^\dagger \begin{pmatrix} 0 & -\frac{1}{\sqrt{2}} \left(\hat{T}_u^\dagger \cos \beta + \mu y_u \sin \beta \right) \\ \frac{1}{\sqrt{2}} \left(\hat{T}_u \cos \beta + \mu^* y_u \sin \beta \right) & 0 \end{pmatrix} W_{\tilde{u}} , \tag{F.16}$$

$$\lambda_{A\tilde{e}(\tilde{d})} = W_{\tilde{e}(\tilde{d})}^\dagger \begin{pmatrix} 0 & -\frac{1}{\sqrt{2}} \left(\hat{T}_{e(d)}^\dagger \sin \beta + \mu y_{e(d)} \cos \beta \right) \\ \frac{1}{\sqrt{2}} \left(\hat{T}_{e(d)} \sin \beta + \mu^* y_{e(d)} \cos \beta \right) & 0 \end{pmatrix} W_{\tilde{e}(\tilde{d})} , \tag{F.17}$$

$$\lambda_{A\tilde{\nu}} = 0 , \tag{F.18}$$

$$\begin{aligned}
\lambda_{AA\tilde{f}} &= W_{\tilde{f}}^\dagger \begin{pmatrix} -\frac{g_2^2}{2} \cos(2\beta) \left(\frac{1}{\cos^2 \theta_W} I_3 - \tan^2 \theta_W Q_e \right) \mathbf{1}_3 & 0 \\ 0 & -\frac{g_2^2}{2} \cos(2\beta) \tan^2 \theta_W Q_e \mathbf{1}_3 \end{pmatrix} W_{\tilde{f}} \\
&+ \begin{cases} W_{\tilde{u}}^\dagger \begin{pmatrix} y_u^2 \cos^2 \beta & 0 \\ 0 & y_u^2 \cos^2 \beta \end{pmatrix} W_{\tilde{u}} & \tilde{f} = \tilde{u} \\ W_{\tilde{d}}^\dagger \begin{pmatrix} y_d^2 \sin^2 \beta & 0 \\ 0 & y_d^2 \sin^2 \beta \end{pmatrix} W_{\tilde{d}} & \tilde{f} = \tilde{d} \\ W_{\tilde{e}}^\dagger \begin{pmatrix} y_e^2 \sin^2 \beta & 0 \\ 0 & y_e^2 \sin^2 \beta \end{pmatrix} W_{\tilde{e}} & \tilde{f} = \tilde{e} \end{cases} ,
\end{aligned} \tag{F.19}$$

$$\lambda_{AA\tilde{\nu}} = -\frac{g_2^2}{2} \cos(2\beta) \left(\frac{1}{\cos^2 \theta_W} I_3 - \tan^2 \theta_W Q_e \right) \mathbf{1}_3 \tag{F.20}$$

$$\begin{aligned}
16\pi^2 t_d &= -2 \sum_{f_d} N_C y_{f_d}^2 A_0(m_{f_d}) \\
&+ \sum_{\tilde{f}} N_C \sum_i \frac{g_2^2}{2M_W \cos \beta} (\lambda_{d\tilde{f}})_{ii} A_0(m_{\tilde{f}_i}) \\
&- g_2^2 \frac{\cos(2\beta)}{8 \cos^2 \theta_W} (A_0(m_A) + 2A_0(m_{H^+})) + \frac{g_2^2}{2} A_0(m_{H_p}) \\
&+ \frac{g_2^2}{8 \cos^2 \theta_W} (3 \sin^2 \alpha - \cos^2 \alpha + \sin(2\alpha) \tan \beta) A_0(m_h)
\end{aligned}$$

$$\begin{aligned}
& + \frac{g_2^2}{8 \cos^2 \theta_W} (3 \cos^2 \alpha - \sin^2 \alpha - \sin(2\alpha) \tan \beta) A_0(m_H) \\
& - g_2^2 \sum_i \frac{m_{\tilde{\chi}_i^0}}{M_W \cos \beta} \text{Re} (N_{i3}(N_{i2} - N_{i,1} \tan \theta_W)) A_0(m_{\tilde{\chi}_i^0}) \\
& - \sqrt{2} g_2^2 \sum_i \frac{m_{\tilde{\chi}_i^+}}{M_W \cos \beta} \text{Re} (V_{i1} U_{i2}) A_0(m_{\tilde{\chi}_i^+}) \\
& + \frac{3}{4} g_2^2 \left(2A_0(M_W) + \frac{A_0(M_Z)}{\cos^2 \theta_W} \right) \\
& + g_2^2 \frac{\cos(2\beta)}{8 \cos^2 \theta_W} (2A_0(M_W) + A_0(M_Z)) . \tag{F.21}
\end{aligned}$$

The couplings to sfermion in the case of inter-generational mixing are given by

$$\lambda_{d\tilde{u}} = W_{\tilde{u}}^\dagger \begin{pmatrix} g_2 \frac{M_Z}{\cos \theta_W} g_{uL} \cos \beta \mathbf{1}_3 & -y_u \frac{\mu}{\sqrt{2}} \\ -y_u \frac{\mu^*}{\sqrt{2}} & g_2 \frac{M_Z}{\cos \theta_W} g_{uR} \cos \beta \mathbf{1}_3 \end{pmatrix} W_{\tilde{u}} , \tag{F.22}$$

$$\begin{aligned}
\lambda_{d\tilde{f}} &= W_{\tilde{f}}^\dagger \begin{pmatrix} g_2 \frac{M_Z}{\cos \theta_W} g_{fL} \cos \beta \mathbf{1}_3 & \hat{T}_f^\dagger \frac{1}{\sqrt{2}} \\ \hat{T}_f \frac{1}{\sqrt{2}} & g_2 \frac{M_Z}{\cos \theta_W} g_{fR} \cos \beta \mathbf{1}_3 \end{pmatrix} \\
&+ \begin{cases} W_{\tilde{d}}^\dagger \begin{pmatrix} Y_d^2 v \cos \beta & 0 \\ 0 & Y_d^2 v \cos \beta \end{pmatrix} W_{\tilde{d}} & \tilde{f} = \tilde{d} \\ W_{\tilde{e}}^\dagger \begin{pmatrix} Y_e^2 v \cos \beta & 0 \\ 0 & Y_e^2 v \cos \beta \end{pmatrix} W_{\tilde{e}} & \tilde{f} = \tilde{e} \end{cases} , \tag{F.23}
\end{aligned}$$

$$\lambda_{d\tilde{\nu}} = g_2 \frac{M_Z}{\cos \theta_W} g_{\nu L} \cos \beta \mathbf{1}_3 \tag{F.24}$$

$$\begin{aligned}
16\pi^2 t_u &= -2 \sum_{f_u} N_C y_{f_u}^2 A_0(m_{f_u}) \\
&+ \sum_{\tilde{f}} N_C \sum_i \frac{g_2^2}{2M_W \sin \beta} (\lambda_{u\tilde{f}})_{ii} A_0(m_{\tilde{f}_i}) \\
&+ g_2^2 \frac{\cos(2\beta)}{8 \cos^2 \theta_W} (A_0(m_A) + 2A_0(m_{H^+})) + \frac{g_2^2}{2} A_0(m_{H_p}) \\
&+ \frac{g_2^2}{8 \cos^2 \theta_W} (3 \cos^2 \alpha - \sin^2 \alpha + \sin(2\alpha) \cot \beta) A_0(m_h) \\
&+ \frac{g_2^2}{8 \cos^2 \theta_W} (3 \sin^2 \alpha - \cos^2 \alpha - \sin(2\alpha) \cot \beta) A_0(m_H) \\
&- g_2^2 \sum_i \frac{m_{\tilde{\chi}_i^0}}{M_W \sin \beta} \text{Re} (N_{i4}(N_{i2} - N_{i,1} \tan \theta_W)) A_0(m_{\tilde{\chi}_i^0}) \\
&- \sqrt{2} g_2^2 \sum_i \frac{m_{\tilde{\chi}_i^+}}{M_W \sin \beta} \text{Re} (V_{i2} U_{i1}) A_0(m_{\tilde{\chi}_i^+})
\end{aligned}$$

214 F. Self-energies and one-loop tadpoles including inter-generational mixing

$$\begin{aligned}
& + \frac{3}{4} g_2^2 \left(2A_0(M_W) + \frac{A_0(M_Z)}{\cos^2 \theta_W} \right) \\
& - g_2^2 \frac{\cos(2\beta)}{8 \cos^2 \theta_W} (2A_0(M_W) + A_0(M_Z)) .
\end{aligned} \tag{F.25}$$

The couplings to sfermion in the case of inter-generational mixing are given by

$$\lambda_{u\tilde{u}} = W_{\tilde{u}}^\dagger \left(\begin{array}{cc} -g_2 \frac{M_Z}{\cos \theta_W} g_{u_L} \sin \beta \mathbb{1}_3 + y_u^2 v \sin \beta & \hat{T}_u^\dagger \frac{1}{\sqrt{2}} \\ \hat{T}_u \frac{1}{\sqrt{2}} & -g_2 \frac{M_Z}{\cos \theta_W} g_{u_R} \sin \beta \mathbb{1}_3 + y_u^2 v \sin \beta \end{array} \right) W_{\tilde{u}} , \tag{F.26}$$

$$\lambda_{u\tilde{f}} = W_{\tilde{f}}^\dagger \left(\begin{array}{cc} -g_2 \frac{M_Z}{\cos \theta_W} g_{f_L} \sin \beta \mathbb{1}_3 & -y_{\tilde{f}} \frac{\mu}{\sqrt{2}} \\ -y_{\tilde{f}} \frac{\mu^*}{\sqrt{2}} & -g_2 \frac{M_Z}{\cos \theta_W} g_{f_R} \sin \beta \mathbb{1}_3 \end{array} \right) \quad \tilde{f} = \tilde{e}, \tilde{d} ,$$

$$\lambda_{u\tilde{\nu}} = -g_2 \frac{M_Z}{\cos \theta_W} g_{\nu_L} \sin \beta \mathbb{1}_3 . \tag{F.27}$$

APPENDIX G

SusyTC documentation

Here we present a documentation of the REAP extension `SusyTC`. To get started, please follow first the steps described in 10.3.

We now describe the additional features of `SusyTC`: In addition to the features of the REAP model `RGEMSSM.m` (described in the REAP documentation), `SusyTC` adds the following options to the command `RGEAdd`:

- `STCsign μ` is the general factor $e^{i\phi_\mu}$ in front of μ in (10.15). (default: +1)
- `STCcMSSM` is a switch to change between the CP-violating (complex) MSSM and CP-conserving (real) MSSM. (default: `True`)
- `STCSusyScale` sets the SUSY scale Q (in GeV), where the MSSM is matched to the SM. If set to "Automatic", `SusyTC` determines Q automatically from the sparticle spectrum. (default: "Automatic")
- `STCSusyScaleFromStops` is a switch to choose whether `SusyTC` calculates the SUSY scale Q as geometric mean of the stop masses $Q = \sqrt{m_{\tilde{t}_1} m_{\tilde{t}_2}}$, where the stop masses are defined by the up-type squark mass eigenstates \tilde{u}_i with the largest mixing to \tilde{t}_1 and \tilde{t}_2 , or as geometric mean of the lightest and heaviest up-type squarks $Q = \sqrt{m_{\tilde{u}_1} m_{\tilde{u}_6}}$. Without effect if `STCSusyScale` is not set to "Automatic". (default: `True`)
- `STCSearchSMTransition` is a switch to enable or disable the matching to the SM and the calculation of supersymmetric threshold corrections and sparticle spectrum. (default: `True`)
- `STCCCBConstraints` is a switch to enable or disable a warning message for potentially dangerous charge and colour breaking vacua, if large trilinear couplings violate the constraints of [135] at the SUSY scale Q

$$|T_{ij}|^2 \leq \left(m_{R_{ii}}^2 + m_{L_{jj}}^2 + m_{h_f}^2 + |\mu|^2 \right) \begin{cases} (y_i^2 + y_j^2) & i \neq j \\ 3y_i^2 & i = j \end{cases}, \quad (\text{G.1})$$

where m_L , m_R and m_{h_f} denote the soft-breaking mass parameters of the scalar fields associated with the trilinear coupling T in the basis of diagonal Yukawa matrices. (default: `True`)

- `STCUFBConstraints` is a switch to enable or disable a warning message for possibly dangerous “unbounded from below” directions in the scalar potential, if the constraints of [134] are violated at the SUSY scale Q

$$m_{h_u}^2 + |\mu|^2 + m_{\tilde{L}_i}^2 - \frac{|m_3|^4}{m_{h_d}^2 + |\mu|^2 - m_{\tilde{L}_i}^2} > 0 \quad \text{UFB-2 ,} \quad (\text{G.2})$$

$$m_{h_u}^2 + m_{\tilde{L}_i}^2 > 0 \quad \text{UFB-3 ,} \quad (\text{G.3})$$

evaluated in the basis of (10.9). Note that the UFB-I constraint is automatically satisfied, since `SusyTC` calculates m_3^2 from $m_{h_u}^2$, $m_{h_d}^2$, M_Z , and $\tan \beta$ by requiring the existence of electroweak symmetry breaking. (default: `True`)

- `STCTachyonConstraints` is a switch to enable or disable the rejection of a parameter point with tachyonic running masses of sfermions at any renormalisation scale above the SUSY scale Q . Regardless of this switch, tachyonic sfermion masses at Q are always rejected. (default: `False`)

Thus, a typical call of `RGEAdd` might look like

```
RGEAdd["MSSMsoftbroken",RGETanβ->20,STCcMSSM->False,STCsignμ->-1];
```

In addition to the parameters known from the MSSM REAP model, the following soft-breaking parameters are available as input for `RGESetInitial`:

- `RGETu`, `RGETd`, `RGETe`, and `RGETν` are the soft-breaking trilinear coupling matrices given in GeV. If given, the Constrained MSSM parameter `RGEA0` for the corresponding trilinear coupling is overwritten. (default: Constrained MSSM)
- `RGEM1`, `RGEM2`, and `RGEM3` are the soft-breaking gaugino mass parameters given in GeV. If given, the Constrained MSSM parameter `RGEM12` for the corresponding gaugino is overwritten. (default: Constrained MSSM)
- `RGEEm2Q`, `RGEEm2L`, `RGEEm2u`, `RGEEm2d`, `RGEEm2e`, `RGEEm2ν` are the soft-breaking squared mass matrices m_f^2 for the sfermions given in GeV². If given, the Constrained MSSM parameter `RGEEm0` for the corresponding scalar masses is overwritten. (default: Constrained MSSM)
- `RGEEm2Hd` and `RGEEm2Hu` are the soft-breaking squared masses for h_d and h_u , respectively, given in GeV². If given, the Constrained MSSM parameter `RGEEm0` for the corresponding scalar mass is overwritten. (default: Constrained MSSM)
- `RGEM12` is the Constrained MSSM parameter for gaugino mass parameters in GeV. (default: 750)

- `RGE m 0` is the Constrained MSSM parameter for all soft-breaking masses of scalars in GeV. (default: 1500)
- `RGE A 0` is the Constrained MSSM parameter A_0 for trilinear couplings, e.g. $T_f = A_0 Y_f$, in GeV. (default: -500)

An example for an input at a GUT scale of $2 \cdot 10^{16}$ GeV would be

```
RGESetInitial[2.10^16,RGEM1->863,RGEM2->131,  
RGEM3->-392,RGESuggestion->"GUT"];
```

The solution at a lower energy scale such as $M_Z \approx 91$ GeV can now be obtained by the REAP command `RGESolve`:

```
RGESolve[91.19,2.10^16];
```

Some parameter points might lead to tachyonic sparticle masses. In such instances the evaluation of `SusyTC` is stopped and an error message is returned using the Mathematica command `Throw`. In order to properly catch such error messages, we therefore recommend to use instead

```
Catch[RGESolve[91.19,2.10^16],TachyonicMass];
```

In addition to the parameters known from the MSSM REAP model, the following soft-breaking parameters are available for `RGEGetSolution` at all energy scales between M_{GUT} and the SUSY scale Q :

- `RGET u` , `RGET d` , `RGET e` , and `RGET ν` are used to get the soft-breaking trilinear coupling matrices.
- `RawT ν` is used to get the raw (internal representation) of the soft-breaking trilinear matrix for sneutrinos.
- `RGEM1`, `RGEM2`, and `RGEM3` are used to get the soft-breaking gaugino mass parameters.
- `RGE m 2Q`, `RGE m 2L`, `RGE m 2u`, `RGE m 2d`, `RGE m 2e`, `RGE m 2 ν` are used to get the soft-breaking squared mass matrices $m_{\tilde{f}}^2$ for the sfermions.
- `RGE m 2Hd` and `RGE m 2Hu` are used to get the soft-breaking squared masses for h_d and h_u , respectively.

To obtain the running $\overline{\text{DR}}$ gluino mass at a scale of two TeV for example, one uses

```
RGEGetSolution[2000,RGEM3];
```

With `SusyTC` the $\overline{\text{DR}}$ sparticle spectrum is automatically calculated. The following functions are included in `SusyTC`:

- `STCGetSUSYScale[]` returns the SUSY scale Q in GeV.
- `STCGetSUSYSpectrum[]` returns a list of replacement rules for the SUSY scale Q , the $\overline{\text{DR}}$ tree-level values of μ and m_3 , and the $\overline{\text{DR}}$ sparticle masses in GeV and (tree-level) mixing matrices at the SUSY scale. In detail it contains
 - "Q" the SUSY scale Q .
 - " μ ", " m_3 " the values of μ and m_3 .
 - "M1", "M2", "M3" are the gaugino mass parameters.
 - "Mh", "MH", "MA", "MHp" the (tree-level) masses of the MSSM Higgs bosons.¹
 - "m χ_0 " a list of the four neutralino masses.
 - "m χ_p " a list of the two chargino masses.
 - "msude" a 3×6 array of the six up-type quarks, down-type squarks and charged slepton masses, respectively.
 - "ms ν " a list of the three light sneutrino masses.
 - " θ_W " the weak mixing angle.
 - "tan α " the mixing angle of the CP-even Higgs bosons.
 - "N" the mixing matrix of neutralinos.
 - "U", "V" the mixing matrices for charginos.
 - "Wude" a list of the three sparticle mixing matrices for up-type squarks, down-type squarks and charged sleptons.
 - "W ν " the mixing matrix of the three light sneutrinos.

To obtain for example the SUSY scale and the tree-level masses of the charginos call

```
"Q"/.STCGetSUSYSpectrum[];
"m $\chi_p$ "/.STCGetSUSYSpectrum[];
```

The squark masses and charged slepton masses are contained in a joint list as $\{m_{\tilde{u}}, m_{\tilde{d}}, m_{\tilde{e}}\}$, and analogously for the sfermion mixing matrices. To obtain for example the up-type squark masses, the charged slepton mixing matrix, and the sneutrino masses type

```
("msude"/.STCGetSUSYSpectrum[])[[1]];
("Wude"/.STCGetSUSYSpectrum[])[[3]];
"ms $\nu$ "/.STCGetSUSYSpectrum[];
```

- `STCGetOneLoopValues[]` returns a list of replacement rules containing

¹Note that there is no CP-violation in the MSSM Higgs sector on tree-level.

- " μ ", " m_3 " the one-loop corrected $\overline{\text{DR}}$ μ -parameter and m_3 as in (10.15) and (10.16) at the SUSY scale Q in GeV.
- "vev" the one-loop $\overline{\text{DR}}$ vev \hat{v} as in (10.20) at the SUSY scale Q in GeV.
- "MHp" ("MA") the pole-mass m_{H^+} (m_A) of the charged (CP-odd) Higgs boson for `STCmSSM = True (False)` in GeV.

The value of μ can for example be obtained from

```
"μ"/.STCGetOneLoopValues[];
```

- `STCGetSCKMValues[]` returns a list of replacement rules with the soft-breaking mass squared and trilinear coupling matrices in the SCKM basis, where sparticles are rotated analogously with their corresponding superpartners². Since they are used for the self-energies calculation as described in the previous appendix F, they are returned in SLHA2 convention [123]! In detail, there are
 - "VCKM" the CKM mixing matrix.
 - "VPMNS" the PMNS mixing matrix.
 - `SCKMBasis["m2Q"]`, `SCKMBasis["m2u"]`, `SCKMBasis["m2d"]` the squark soft-breaking mass squared matrices in the Super-CKM basis with SLHA2 conventions in GeV^2 .
 - `SCKMBasis["m2L"]`, `SCKMBasis["m2e"]` the slepton soft-breaking mass squared matrices in the Super-PMNS basis with SLHA2 conventions in GeV^2 .
 - `SCKMBasis["T"]` a list of the three trilinear coupling matrices for up-type squarks, down-type squarks, and charged sleptons in the SCKM basis with SLHA2 conventions in GeV.
 - `SCKMBasis["Y"]` a 3×3 array of the Yukawa coupling singular values for up-type squarks, down-type squarks, and charged sleptons.

To obtain the down-type trilinear coupling matrix and the mass squared matrix of the squark doublet in the SLHA basis for example, type

```
(SCKMBasis["T"/.STCGetSCKMValues[])[[2]];  
SCKMBasis["m2Q"/.STCGetSCKMValues[]];
```

- `STCGetInternalValues[]` returns everything that is internally used for the calculation of the threshold corrections and sparticle spectrum, i.e. the results from `STCGetSCKMValues[]` and `STCGetSUSYSpectrum[]` with the one-loop corrected parameters from `STCGetOneLoopValues[]` replacing tree-level ones if available. We recommend to the user to use those separate functions instead.

As additional feature, `SusyTC` optionally supports input and output as SLHA “Les Houches” files. These files follow SLHA conventions [123, 194]:

²Here we use the term “SCKM” for the Super-CKM and Super-PMNS basis.

- `STCSLHA2Input` [“*Path*”] loads an “Les Houches” input file stored in “*Path*” and executes REAP and SusyTC. If no path is given, the default path is assumed as “*SusyTC.in*” in the Mathematica notebook directory. An important difference to other spectrum calculators is the pure “top-down” approach by SusyTC, i.e. there is no attempt of fitting SM inputs at a low scale or calculating a GUT scale from gauge couplings unification. Instead, all input is given at a user-defined high energy scale, which is then evolved to lower scales. The input should be given in the flavour basis in SLHA 2 convention [123] as in (5.64) and (5.65), and the seesaw parameters in the convention (5.77). The relation between the SusyTC conventions of chapter 10 and the SLHA 2 conventions is given in 10.2. In the following, we list all SLHA 2 input blocks, which are available in SusyTC:
 - Block `MODSEL`: The only available switch is:
 - 5 : (Default = 2) CP violation (STCcmSSM)
 - Block `SusyTCInput`: Switches (1=True, 0=False) are defined for RGEAdd:
 - 1 : (Default = 1) STCSusyScaleFromStops
 - 2 : (Default = 1) STCSearchSMTransition
 - 3 : (Default = 1) STCCCBConstraints
 - 4 : (Default = 1) STCUFBConstraints
 - 5 : (Default = 1) Print a Warning in case of Tachyonic masses
 - 6 : (Default = 1) One or Two Loop RGEs
 - Block `MINPAR`: Constrained MSSM parameters as defined in [123, 194]. Note however, that the input value of $\tan\beta$ is interpreted to be given at the SUSY scale.
 - Block `IMMINPAR`: Reads the $\sin\phi_\mu$ in case of the complex MSSM:
 - 4 : $\sin\phi_\mu$
 - Block `EXTPAR`:
 - 0 : (Default = $2 \cdot 10^{16}$): M_{input} Input scale in GeV
 Note that with SusyTC an automatic calculation of the GUT scale is not possible. The remainder of the block works as usual, e.g. optionally one can overwrite common Constrained MSSM gaugino or Higgs soft-breaking parameters:
 - 1 : $M_1(M_{input})$ bino mass (real part) in GeV
 - 2 : $M_2(M_{input})$ wino mass (real part) in GeV
 - 3 : $M_3(M_{input})$ gluino mass (real part) in GeV
 - 21 : $m_{h_d}^2(M_{input})$ in GeV^2
 - 22 : $m_{h_u}^2(M_{input})$ in GeV^2
 Imaginary components for the gaugino masses can be given in Block `IMEXTPAR`.
 - Block `IMEXTPAR`: as defined in [123].
 - Block `QEXTPAR`: low energy input:
 - 0 : (Default = 91.1876): The low energy scale in GeV to which REAP evolves the SM RGEs.
 - 23 : “SUSY scale” Q , where the MSSM is matched to the SM. If this entry is set, it overwrites the automatically calculated SUSY scale.

-
- Block GAUGE: the $\overline{\text{DR}}$ gauge couplings at the input scale
 - 1 : $g_1(M_{input})$ $U(1)$ gauge coupling
 - 2 : $g_2(M_{input})$ $SU(2)$ gauge coupling
 - 3 : $g_3(M_{input})$ $SU(3)$ gauge coupling
 - Block YU, Block YD, Block YE, Block YN: The real parts of the Yukawa matrices $Y_u, Y_d, Y_e,$ and Y_ν in the flavour basis (5.64) and (5.77). They should be given in the FORTRAN format (1x,I2,1x,I2,3x,1P,E16.8,0P,3x,‘#’,1x,A), where the first two integers correspond to the indices and the double precision number to $Re(Y_{ij})$.
 - Block IMYU, Block IMYD, Block IMYE, Block IMYN: The imaginary parts of the Yukawa matrices $Y_u, Y_d, Y_e,$ and Y_ν in the flavour basis (5.64) and (5.77). They are given in the same format as the real parts.
 - Block MN: The real part of the symmetric Majorana mass matrix M_n of the right-handed neutrinos in the flavour basis (5.77) in GeV. Only the “upper-triangle” entries should be given, the input format is as for the Yukawa matrices.
 - Block IMMN: The imaginary part of the symmetric Majorana mass matrix M_n of the right-handed neutrinos in the flavour basis (5.77) in GeV. Only the “upper-triangle” entries should be given, the input format is as for the Yukawa matrices.

The remaining blocks can be given optionally to overwrite Constrained MSSM input boundary conditions:

- Block TU, Block TD, Block TE, Block TN: The real parts of the trilinear soft-breaking matrices $T_u, T_d, T_e,$ and T_ν in GeV in the flavour basis (5.65). They should be given in the same format as the Yukawa matrices.
 - Block IMTU, Block IMTD, Block IMTE, Block IMTN: The imaginary parts of the trilinear soft-breaking matrices $T_u, T_d, T_e,$ and T_ν in GeV in the flavour basis (5.65). They should be given in the same format as the Yukawa matrices.
 - Block MSQ2, Block MSU2, Block MSD2, Block MSL2, Block MSE2, Block MSN2: The real parts of the soft-breaking mass squared matrices $m_{\tilde{Q}}^2, m_{\tilde{u}}^2, m_{\tilde{d}}^2, m_{\tilde{L}}^2, m_{\tilde{e}}^2,$ and $m_{\tilde{\nu}}^2$ in GeV^2 in the flavour basis (5.65). Only the “upper-triangle” entries should be given, the input format is as for the Yukawa matrices.
 - Block IMMSQ2, Block IMMSU2, Block IMMSD2, Block IMMSEL2, Block IMMSE2, Block IMMSEN2: The imaginary parts of the soft-breaking mass squared matrices $m_{\tilde{Q}}^2, m_{\tilde{u}}^2, m_{\tilde{d}}^2, m_{\tilde{L}}^2, m_{\tilde{e}}^2,$ and $m_{\tilde{\nu}}^2$ in GeV^2 in the flavour basis (5.65). Only the “upper-triangle” entries should be given, the input format is as for the Yukawa matrices.
- STCWriteSLHA2Output [“Path”] writes a “Les Houches” [123,194] output file to “Path”. If no path is given, the output is saved in the Mathematica notebook directory as “SusyTC.out”. The output follows SLHA conventions, with the following exceptions:

- **Block MASS**: The mass spectrum is given as $\overline{\text{DR}}$ masses in GeV at the SUSY scale. The only exception is the pole mass M_{H^+} (M_A) for CP violation turned on (off).
- **Block ALPHA**: the tree-level Higgs mixing angle α_{tree} .
- **Block HMIX**: Instead of M_A we give
101 : m_3

The other blocks follow the SLHA2 output conventions, e.g. $\overline{\text{DR}}$ values at the SUSY scale in the Super-CKM/Super-PMNS basis. To avoid confusion, the blocks **Block DSQMIX**, **Block USQMIX**, **Block SELMIX**, **Block SNUMIX** and the corresponding blocks for the imaginary entries, return the sfermion mixing matrices $R_{\tilde{f}}$ in SLHA 2 convention!

Bibliography

- [1] S. ANTUSCH, C. GROSS, V. MAURER, and C. SLUKA, $\theta_{13}^{PMNS} = \theta_C / \sqrt{2}$ from GUTs, *Nucl. Phys.* **B866**, 255 (2013), arXiv: 1205.1051.
- [2] S. ANTUSCH, C. GROSS, V. MAURER, and C. SLUKA, *A flavour GUT model with $\theta_{13}^{PMNS} \simeq \theta_C / \sqrt{2}$* , *Nucl. Phys.* **B877**, 772 (2013), arXiv: 1305.6612.
- [3] S. ANTUSCH, C. GROSS, V. MAURER, and C. SLUKA, *Inverse neutrino mass hierarchy in a flavour GUT model*, *Nucl. Phys.* **B879**, 19 (2014), arXiv: 1306.3984.
- [4] S. ANTUSCH, I. DE MEDEIROS VARZIELAS, V. MAURER, C. SLUKA, and M. SPINRATH, *Towards predictive flavour models in SUSY SU(5) GUTs with doublet-triplet splitting*, *JHEP* **1409**, 141 (2014), arXiv: 1405.6962.
- [5] S. ANTUSCH and C. SLUKA, *Predicting the Sparticle Spectrum from GUTs via SUSY Threshold Corrections with SusyTC*, (2015), arXiv: 1512.06727.
- [6] S. L. GLASHOW, *Partial Symmetries of Weak Interactions*, *Nucl. Phys.* **22**, 579 (1961).
S. WEINBERG, *A Model of Leptons*, *Phys. Rev. Lett.* **19**, 1264 (1967).
A. SALAM, *Weak and Electromagnetic Interactions*, *Conf. Proc.* **C680519**, 367 (1968), reprinted in A. ALI *et al.* [EDITORS], *Selected papers of Abdus Salam: with commentary*, *World scientific series in 20th century physics* **5**, 244 (1994).
S. L. GLASHOW, J. ILIOPOULOS, and L. MAIANI, *Weak Interactions with Lepton-Hadron Symmetry*, *Phys. Rev.* **D2**, 1285 (1970).
- [7] D. J. GROSS and F. WILCZEK, *Ultraviolet Behavior of Nonabelian Gauge Theories*, *Phys. Rev. Lett.* **30**, 1343 (1973).
S. WEINBERG, *Nonabelian Gauge Theories of the Strong Interactions*, *Phys. Rev. Lett.* **31**, 494 (1973).
H. FRITZSCH, M. GELL-MANN, and H. LEUTWYLER, *Advantages of the Color Octet Gluon Picture*, *Phys. Lett.* **B47**, 365 (1973).
- [8] D. J. GROSS and F. WILCZEK, *Asymptotically Free Gauge Theories. 1*, *Phys. Rev.* **D8**, 3633 (1973).

- D. J. GROSS and F. WILCZEK, *Asymptotically Free Gauge Theories. 2*, *Phys. Rev. D* **9**, 980 (1974).
- H. D. POLITZER, *Reliable Perturbative Results for Strong Interactions?*, *Phys. Rev. Lett.* **30**, 1346 (1973).
- H. D. POLITZER, *Asymptotic Freedom: An Approach to Strong Interactions*, *Phys. Rept.* **14**, 129 (1974).
- [9] G. 'T HOOFT, *Renormalization of Massless Yang-Mills Fields*, *Nucl. Phys.* **B33**, 173 (1971).
- G. 'T HOOFT, *Renormalizable Lagrangians for Massive Yang-Mills Fields*, *Nucl. Phys.* **B35**, 167 (1971).
- [10] F. ENGLERT and R. BROUT, *Broken Symmetry and the Mass of Gauge Vector Mesons*, *Phys. Rev. Lett.* **13**, 321 (1964).
- [11] P. W. HIGGS, *Broken symmetries, massless particles and gauge fields*, *Phys. Lett.* **12**, 132 (1964).
- P. W. HIGGS, *Broken Symmetries and the Masses of Gauge Bosons*, *Phys. Rev. Lett.* **13**, 508 (1964).
- P. W. HIGGS, *Spontaneous Symmetry Breakdown without Massless Bosons*, *Phys. Rev.* **145**, 1156 (1966).
- [12] H. K. DREINER, H. E. HABER, and S. P. MARTIN, *Two-component spinor techniques and Feynman rules for quantum field theory and supersymmetry*, *Physics Reports* **494**, 1 (2010), arXiv: 0812.1594 [hep-ph].
- [13] E. C. G. STUECKELBERG, *Interaction energy in electrodynamics and in the field theory of nuclear forces (Part I)*, *Helv. Phys. Acta* **11**, 225 (1938), [in German], reprinted in J. LACKI, H. RUEGG and G. WANDERS [EDITORS], *E.C.G. Stueckelberg, An Unconventional Figure of Twentieth Century Physics: Selected Scientific Papers with Commentaries*, Birkhäuser Verlag, Basel, 251 (2009).
- E. C. G. STUECKELBERG, *Interaction energy in electrodynamics and in the field theory of nuclear forces (Part II and III)*, *Helv. Phys. Acta* **11**, 299 (1938), [in German], reprinted in J. LACKI, H. RUEGG and G. WANDERS [EDITORS], *E.C.G. Stueckelberg, An Unconventional Figure of Twentieth Century Physics: Selected Scientific Papers with Commentaries*, Birkhäuser Verlag, Basel, 273 (2009).
- [14] K. A. OLIVE et al., *Review of Particle Physics*, *Chin. Phys.* **C38**, 090001 (2014).
- [15] N. CABIBBO, *Unitary Symmetry and Leptonic Decays*, *Phys. Rev. Lett.* **10**, 531 (1963).
- [16] M. KOBAYASHI and T. MASKAWA, *CP Violation in the Renormalizable Theory of Weak Interaction*, *Prog. Theor. Phys.* **49**, 652 (1973).

- [17] S. F. KING, *Constructing the large mixing angle MNS matrix in seesaw models with right-handed neutrino dominance*, *JHEP* **0209**, 011 (2002), arXiv: hep-ph/0204360.
- [18] P. J. MOHR, B. N. TAYLOR, and D. B. NEWELL, *CODATA Recommended Values of the Fundamental Physical Constants: 2010*, *Rev. Mod. Phys.* **84**, 1527 (2012), arXiv: 1203.5425 [atom-ph].
- [19] K. G. WILSON, *Confinement of Quarks*, *Phys. Rev.* **D10**, 2445 (1974).
- [20] S. WEINBERG, *Phenomenological Lagrangians*, *Physica* **A96**, 327 (1979).
- [21] J. GASSER and H. LEUTWYLER, *Chiral Perturbation Theory to One Loop*, *Annals Phys.* **158**, 142 (1984).
- [22] H. LEUTWYLER, *The Ratios of the light quark masses*, *Phys.Lett.* **B378**, 313 (1996), arXiv: hep-ph/9602366.
- [23] N. ISGUR and M. B. WISE, *Weak Decays of Heavy Mesons in the Static Quark Approximation*, *Phys. Lett.* **B232**, 113 (1989).
- [24] S. L. ADLER, *Axial vector vertex in spinor electrodynamics*, *Phys. Rev.* **177**, 2426 (1969).
- [25] J. S. BELL and R. JACKIW, *A PCAC puzzle: $\pi^0 \rightarrow \gamma \gamma$ in the sigma model*, *Nuovo Cim.* **A60**, 47 (1969).
- [26] D. J. GROSS and R. JACKIW, *Effect of anomalies on quasirenormalizable theories*, *Phys. Rev.* **D6**, 477 (1972).
- [27] G. 'T HOOFT, *Naturalness, chiral symmetry, and spontaneous chiral symmetry breaking*, *NATO Sci. Ser. B* **59**, 135 (1980).
- [28] G. 'T HOOFT, *Symmetry Breaking Through Bell-Jackiw Anomalies*, *Phys. Rev. Lett.* **37**, 8 (1976).
G. 'T HOOFT, *Computation of the Quantum Effects Due to a Four-Dimensional Pseudoparticle*, *Phys. Rev.* **D14**, 3432 (1976), [Erratum: *Phys. Rev.* **D18**, 2199 (1978)].
- [29] R. JACKIW and C. REBBI, *Vacuum Periodicity in a Yang-Mills Quantum Theory*, *Phys. Rev. Lett.* **37**, 172 (1976).
- [30] R. D. PECCEI and H. R. QUINN, *CP Conservation in the Presence of Instantons*, *Phys. Rev. Lett.* **38**, 1440 (1977).
- [31] S. WEINBERG, *A New Light Boson?*, *Phys. Rev. Lett.* **40**, 223 (1978).
F. WILCZEK, *Problem of Strong p and t Invariance in the Presence of Instantons*, *Phys. Rev. Lett.* **40**, 279 (1978).

- [32] S. ANTUSCH, M. HOLTHAUSEN, M. A. SCHMIDT, and M. SPINRATH, *Solving the Strong CP Problem with Discrete Symmetries and the Right Unitarity Triangle*, *Nucl. Phys.* **B877**, 752 (2013), arXiv: 1307.0710 [hep-ph].
- [33] A. BOSMA, *21-cm line studies of spiral galaxies. 2. The distribution and kinematics of neutral hydrogen in spiral galaxies of various morphological types.*, *Astron. J.* **86**, 1825 (1981).
- [34] G. F. SMOOT et al., *Structure in the COBE differential microwave radiometer first year maps*, *Astrophys. J.* **396**, L1 (1992).
- C. L. BENNETT et al., *Nine-Year Wilkinson Microwave Anisotropy Probe (WMAP) Observations: Final Maps and Results*, *Astrophys. J. Suppl.* **208**, 20 (2013), arXiv: 1212.5225 [astro-ph.CO].
- [35] P. A. R. ADE et al., *Planck 2015 results. XIII. Cosmological parameters*, (2015), arXiv: 1502.01589 [astro-ph.CO].
- [36] M. MARKEVITCH, A. H. GONZALEZ, D. CLOWE, A. VIKHLININ, L. DAVID, W. FORMAN, C. JONES, S. MURRAY, and W. TUCKER, *Direct constraints on the dark matter self-interaction cross-section from the merging galaxy cluster 1E0657-56*, *Astrophys. J.* **606**, 819 (2004), arXiv: astro-ph/0.09303.
- D. CLOWE, A. GONZALEZ, and M. MARKEVITCH, *Weak lensing mass reconstruction of the interacting cluster 1E0657-558: Direct evidence for the existence of dark matter*, *Astrophys. J.* **604**, 596 (2004), arXiv: astro-ph/0312273.
- [37] C. ALCOCK et al., *The MACHO project lmc variable star inventory. ix. frequency analysis of the first overtone rr lyrae stars and the indication for nonradial pulsations*, *Astrophys. J.* **542**, 257 (2000), arXiv: astro-ph/0005361.
- P. TISSERAND et al., *Limits on the Macho Content of the Galactic Halo from the EROS-2 Survey of the Magellanic Clouds*, *Astron. Astrophys.* **469**, 387 (2007), arXiv: astro-ph/0607207.
- L. WYRZYKOWSKI et al., *The OGLE View of Microlensing towards the Magellanic Clouds. IV. OGLE-III SMC Data and Final Conclusions on MACHOs*, *Mon. Not. Roy. Astron. Soc.* **416**, 2949 (2011), arXiv: 1106.2925 [astro-ph.GA].
- [38] B. W. LEE and S. WEINBERG, *Cosmological Lower Bound on Heavy Neutrino Masses*, *Phys. Rev. Lett.* **39**, 165 (1977).
- P. HUT, *Limits on Masses and Number of Neutral Weakly Interacting Particles*, *Phys. Lett.* **B69**, 85 (1977).
- M. I. VYSOTSKY, A. D. DOLGOV, and Y. B. ZELDOVICH, *Cosmological Restriction on Neutral Lepton Masses*, *JETP Lett.* **26**, 188 (1977), [*Pisma Zh. Eksp. Teor. Fiz.* **26**, 200 (1977)].

- J. E. GUNN, B. W. LEE, I. LERCHE, D. N. SCHRAMM, and G. STEIGMAN, *Some Astrophysical Consequences of the Existence of a Heavy Stable Neutral Lepton*, *Astrophys. J.* **223**, 1015 (1978).
- G. STEIGMAN, C. L. SARAZIN, H. QUINTANA, and J. FAULKNER, *Dynamical interactions and astrophysical effects of stable heavy neutrinos*, *Astron. J.* **83**, 1050 (1978).
- [39] M. S. TURNER, *Windows on the Axion*, *Phys. Rept.* **197**, 67 (1990).
- G. G. RAFFELT, *Astrophysical methods to constrain axions and other novel particle phenomena*, *Phys. Rept.* **198**, 1 (1990).
- [40] J. R. ELLIS, J. S. HAGELIN, D. V. NANOPOULOS, K. A. OLIVE, and M. SREDNICKI, *Supersymmetric Relics from the Big Bang*, *Nucl. Phys.* **B238**, 453 (1984).
- [41] A. G. RIESS et al., *Observational evidence from supernovae for an accelerating universe and a cosmological constant*, *Astron. J.* **116**, 1009 (1998), arXiv: astro-ph/9805201.
- S. PERLMUTTER et al., *Measurements of Omega and Lambda from 42 high redshift supernovae*, *Astrophys. J.* **517**, 565 (1999), arXiv: astro-ph/9812133.
- P. A. R. ADE et al., *Planck 2015 results. XIV. Dark energy and modified gravity*, (2015), arXiv: 1502.01590 [astro-ph.CO].
- [42] B. PONTECORVO, *Mesonium and anti-mesonium*, *Sov. Phys. JETP* **6**, 429 (1957), [Zh. Eksp. Teor. Fiz.33,549(1957)].
- B. PONTECORVO, *Inverse beta processes and nonconservation of lepton charge*, *Sov. Phys. JETP* **7**, 172 (1958), [Zh. Eksp. Teor. Fiz.34,247(1957)].
- B. PONTECORVO, *Neutrino Experiments and the Problem of Conservation of Leptonic Charge*, *Sov. Phys. JETP* **26**, 984 (1968), [Zh. Eksp. Teor. Fiz.53,1717(1967)].
- [43] V. N. GRIBOV and B. PONTECORVO, *Neutrino astronomy and lepton charge*, *Phys. Lett.* **B28**, 493 (1969).
- [44] R. DAVIS, *Solar neutrinos. II: Experimental*, *Phys. Rev. Lett.* **12**, 303 (1964).
- R. DAVIS, JR., D. S. HARMER, and K. C. HOFFMAN, *Search for neutrinos from the sun*, *Phys. Rev. Lett.* **20**, 1205 (1968).
- [45] B. T. CLEVELAND, T. DAILY, R. DAVIS, JR., J. R. DISTEL, K. LANDE, C. K. LEE, P. S. WILDENHAIN, and J. ULLMAN, *Measurement of the solar electron neutrino flux with the Homestake chlorine detector*, *Astrophys. J.* **496**, 505 (1998).
- W. HAMPEL et al., *GALLEX solar neutrino observations: Results for GALLEX IV*, *Phys. Lett.* **B447**, 127 (1999).

- Q. R. AHMAD et al., *Direct evidence for neutrino flavor transformation from neutral current interactions in the Sudbury Neutrino Observatory*, *Phys. Rev. Lett.* **89**, 011301 (2002), arXiv: nucl-ex/0204008.
- S. FUKUDA et al., *Determination of solar neutrino oscillation parameters using 1496 days of Super-Kamiokande I data*, *Phys. Lett.* **B539**, 179 (2002), arXiv: hep-ex/0205075.
- Y. ASHIE et al., *Evidence for an oscillatory signature in atmospheric neutrino oscillation*, *Phys. Rev. Lett.* **93**, 101801 (2004), arXiv: hep-ex/0404034.
- T. ARAKI et al., *Measurement of neutrino oscillation with KamLAND: Evidence of spectral distortion*, *Phys. Rev. Lett.* **94**, 081801 (2005), arXiv: hep-ex/0406035.
- M. ALTMANN et al., *Complete results for five years of GNO solar neutrino observations*, *Phys. Lett.* **B616**, 174 (2005), arXiv: hep-ex/0504037.
- J. N. ABDURASHITOV et al., *Measurement of the solar neutrino capture rate with gallium metal. III: Results for the 2002–2007 data-taking period*, *Phys. Rev.* **C80**, 015807 (2009), arXiv: 0901.2200 [nucl-ex].
- P. ADAMSON et al., *Measurement of the neutrino mass splitting and flavor mixing by MINOS*, *Phys. Rev. Lett.* **106**, 181801 (2011), arXiv: 1103.0340 [hep-ex].
- [46] K. ABE et al. [T2K COLLABORATION], *Indication of Electron Neutrino Appearance from an Accelerator-produced Off-axis Muon Neutrino Beam*, *Phys.Rev.Lett.* **107**, 041801 (2011), arXiv: 1106.2822 [hep-ex].
- Y. ABE et al. [DOUBLE-CHOOZ COLLABORATION], *Indication for the disappearance of reactor electron antineutrinos in the Double Chooz experiment*, *Phys.Rev.Lett.* **108**, 131801 (2012), arXiv: 1112.6353 [hep-ex].
- F. P. AN et al. [DAYA-BAY COLLABORATION], *Observation of electron-antineutrino disappearance at Daya Bay*, *Phys.Rev.Lett.* **108**, 171803 (2012), arXiv: 1203.1669 [hep-ex].
- J. K. AHN et al. [RENO COLLABORATION], *Observation of Reactor Electron Antineutrino Disappearance in the RENO Experiment*, *Phys.Rev.Lett.* **108**, 191802 (2012), arXiv: 1204.0626 [hep-ex].
- [47] A. STRUMIA and F. VISSANI, *Neutrino masses and mixings and...*, (2006), arXiv: hep-ph/0606054.
- [48] J. LESGOURGUES, G. MANGANO, G. MIELE, and S. PASTOR, *Neutrino Cosmology*, Cambridge University Press, New York, 2013.
- [49] S. F. KING and C. LUHN, *Neutrino Mass and Mixing with Discrete Symmetry*, *Rept. Prog. Phys.* **76**, 056201 (2013), arXiv: 1301.1340 [hep-ph].
- [50] V. N. ASEEV et al., *An upper limit on electron antineutrino mass from Troitsk experiment*, *Phys. Rev.* **D84**, 112003 (2011).

- [51] S. WEINBERG, *Baryon and Lepton Nonconserving Processes*, *Phys. Rev. Lett.* **43**, 1566 (1979).
S. WEINBERG, *Varieties of Baryon and Lepton Nonconservation*, *Phys. Rev.* **D22**, 1694 (1980).
- [52] P. MINKOWSKI, $\mu \rightarrow e\gamma$ at a Rate of One Out of 10^9 Muon Decays?, *Phys. Lett.* **B67**, 421 (1977).
M. GELL-MANN, P. RAMOND, and R. SLANSKY, *Complex Spinors and Unified Theories*, *Conf. Proc.* **C790927**, 315 (1979), in P. VAN NIEUWENHUIZEN and D. Z. FREEDMAN [EDITORS], *Supergravity: Proceedings of the Supergravity Workshop at Stony Brook, 27-29 September 1979, New York*, 315 (1979), arXiv: 1306.4669 [hep-th].
T. YANAGIDA, *Horizontal symmetry and masses of neutrinos*, *Conf. Proc.* **C7902131**, 95 (1979), in O. SAWADA and A. SUGAMOTO [EDITORS], *Proceedings: Workshop on the Unified Theories and the Baryon Number in the Universe, Tsukuba, Japan, 13-14 Feb 1979*, 95 (1979).
S. L. GLASHOW, *The Future of Elementary Particle Physics*, *NATO Sci. Ser. B* **61**, 687 (1980), in M. LÉVY et al. [EDITORS], *Quarks and Leptons: Cargèse 1979*, Springer US, 687 (1980).
R. N. MOHAPATRA and G. SENJANOVIC, *Neutrino Mass and Spontaneous Parity Violation*, *Phys. Rev. Lett.* **44**, 912 (1980).
J. SCHECHTER and J. W. F. VALLE, *Neutrino Masses in $SU(2) \times U(1)$ Theories*, *Phys. Rev.* **D22**, 2227 (1980).
- [53] G. B. GELMINI and M. RONCADELLI, *Left-Handed Neutrino Mass Scale and Spontaneously Broken Lepton Number*, *Phys. Lett.* **B99**, 411 (1981).
- [54] R. FOOT, H. LEW, X. G. HE, and G. C. JOSHI, *Seesaw Neutrino Masses Induced by a Triplet of Leptons*, *Z. Phys.* **C44**, 441 (1989).
- [55] R. N. MOHAPATRA and J. W. F. VALLE, *Neutrino Mass and Baryon Number Nonconservation in Superstring Models*, *Phys. Rev.* **D34**, 1642 (1986).
- [56] T. P. CHENG and L.-F. LI, *On Weak Interaction Induced Neutrino Oscillations*, *Phys. Rev.* **D17**, 2375 (1978).
A. ZEE, *A Theory of Lepton Number Violation, Neutrino Majorana Mass, and Oscillation*, *Phys. Lett.* **B93**, 389 (1980), [Erratum: *Phys. Lett.* **B95**, 461 (1980)].
T. P. CHENG and L.-F. LI, *Neutrino Masses, Mixings and Oscillations in $SU(2) \times U(1)$ Models of Electroweak Interactions*, *Phys. Rev.* **D22**, 2860 (1980).
- [57] Y. KATAYAMA, K. MATUMOTO, S. TANAKA, and E. YAMADA, *Possible unified models of elementary particles with two neutrinos*, *Prog. Theor. Phys.* **28**, 675 (1962).

- Z. MAKI, M. NAKAGAWA, and S. SAKATA, *Remarks on the unified model of elementary particles*, *Prog. Theor. Phys.* **28**, 870 (1962).
- M. NAKAGAWA, H. OKONOJI, S. SAKATA, and A. TOYODA, *Possible existence of a neutrino with mass and partial conservation of muon charge*, *Prog. Theor. Phys.* **30**, 727 (1963).
- [58] S. P. MIKHEEV and A. YU. SMIRNOV, *Resonance Amplification of Oscillations in Matter and Spectroscopy of Solar Neutrinos*, *Sov. J. Nucl. Phys.* **42**, 913 (1985), [*Yad. Fiz.*42,1441(1985)].
- S. P. MIKHEEV and A. YU. SMIRNOV, *Resonant amplification of neutrino oscillations in matter and solar neutrino spectroscopy*, *Nuovo Cim.* **C9**, 17 (1986).
- L. WOLFENSTEIN, *Neutrino Oscillations in Matter*, *Phys. Rev.* **D17**, 2369 (1978).
- [59] S. NUSSINOV, *Solar Neutrinos and Neutrino Mixing*, *Phys. Lett.* **B63**, 201 (1976).
- B. KAYSER, *On the Quantum Mechanics of Neutrino Oscillation*, *Phys. Rev.* **D24**, 110 (1981).
- C. GIUNTI, C. W. KIM, and U. W. LEE, *When do neutrinos really oscillate?: Quantum mechanics of neutrino oscillations*, *Phys. Rev.* **D44**, 3635 (1991).
- J. RICH, *The Quantum mechanics of neutrino oscillations*, *Phys. Rev.* **D48**, 4318 (1993).
- W. GRIMUS, P. STOCKINGER, and S. MOHANTY, *The Field theoretical approach to coherence in neutrino oscillations*, *Phys. Rev.* **D59**, 013011 (1999), arXiv: hep-ph/9807442.
- [60] L. STODOLSKY, *The Unnecessary wave packet*, *Phys. Rev.* **D58**, 036006 (1998), arXiv: hep-ph/9802387.
- [61] S. M. BILENKY and S. T. PETCOV, *Massive Neutrinos and Neutrino Oscillations*, *Rev. Mod. Phys.* **59**, 671 (1987), [Erratum: *Rev. Mod. Phys.* 60, 575 (1988)].
- [62] M. C. GONZALEZ-GARCIA, M. MALTONI, and T. SCHWETZ, *Global Analyses of Neutrino Oscillation Experiments*, (2015), arXiv: 1512.06856 [hep-ph].
- [63] V. D. BARGER, S. PAKVASA, T. J. WEILER, and K. WHISNANT, *Bimaximal mixing of three neutrinos*, *Phys. Lett.* **B437**, 107 (1998), arXiv: hep-ph/9806387.
- [64] P. F. HARRISON, D. H. PERKINS, and W. G. SCOTT, *Tri-bimaximal mixing and the neutrino oscillation data*, *Phys. Lett.* **B530**, 167 (2002), arXiv: hep-ph/0202074.
- [65] S. ANTUSCH and S. F. KING, *Charged lepton corrections to neutrino mixing angles and CP phases revisited*, *Phys. Lett.* **B631**, 42 (2005), arXiv: hep-ph/0508044.
- [66] S. F. KING, *Predicting neutrino parameters from $SO(3)$ family symmetry and quark-lepton unification*, *JHEP* **0508**, 105 (2005), arXiv: hep-ph/0506297.

- [67] I. MASINA, *A Maximal atmospheric mixing from a maximal CP violating phase*, *Phys. Lett.* **B633**, 134 (2006), arXiv: hep-ph/0508031.
S. ANTUSCH, P. HUBER, S. F. KING, and T. SCHWETZ, *Neutrino mixing sum rules and oscillation experiments*, *JHEP* **0704**, 060 (2007), arXiv: hep-ph/0702286.
- [68] C. JARLSKOG, *A Basis Independent Formulation of the Connection Between Quark Mass Matrices, CP Violation and Experiment*, *Z. Phys.* **C29**, 491 (1985).
- [69] M. BISHAI, E. MCCLUSKEY, A. RUBBIA, and M. THOMSON, *Long-Baseline Neutrino Facility (LBNF) and Deep Underground Neutrino Experiment (DUNE) Conceptual Design Report, Volume 1: The LBNF and DUNE Projects*, (2015), LBNE-doc-10687-v9, <http://http://lbne2-docdb.fnal.gov/cgi-bin/RetrieveFile?docid=10687>.
- [70] G. RACAHA, *On the symmetry of particle and antiparticle*, *Nuovo Cim.* **14**, 322 (1937).
W. H. FURRY, *On transition probabilities in double beta-disintegration*, *Phys. Rev.* **56**, 1184 (1939).
- [71] J. SCHECHTER and J. W. F. VALLE, *Neutrinoless Double beta Decay in $SU(2) \times U(1)$ Theories*, *Phys. Rev.* **D25**, 2951 (1982).
- [72] A. S. BARABASH, *Double beta decay experiments: present status and prospects for the future*, *Phys. Procedia* **74**, 416 (2015).
- [73] S. F. KING and C. LUHN, *On the origin of neutrino flavour symmetry*, *JHEP* **0910**, 093 (2009), arXiv: 0908.1897.
- [74] S. F. KING and N. N. SINGH, *Inverted hierarchy models of neutrino masses*, *Nucl. Phys.* **B596**, 81 (2001), arXiv: hep-ph/0007243.
- [75] C. D. FROGGATT and H. B. NIELSEN, *Hierarchy of Quark Masses, Cabibbo Angles and CP Violation*, *Nucl. Phys.* **B147**, 277 (1979).
- [76] E. MA and G. RAJASEKARAN, *Softly broken $A(4)$ symmetry for nearly degenerate neutrino masses*, *Phys. Rev.* **D64**, 113012 (2001), arXiv: hep-ph/0106291.
- [77] K. S. BABU, E. MA, and J. W. F. VALLE, *Underlying $A(4)$ symmetry for the neutrino mass matrix and the quark mixing matrix*, *Phys. Lett.* **B552**, 207 (2003), arXiv: hep-ph/0206292.
- [78] G. ALTARELLI and F. FERUGLIO, *Tri-bimaximal neutrino mixing from discrete symmetry in extra dimensions*, *Nucl. Phys.* **B720**, 64 (2005), arXiv: hep-ph/0504165.
- [79] H. GEORGI and S. L. GLASHOW, *Unity of All Elementary Particle Forces*, *Phys. Rev. Lett.* **32**, 438 (1974).

- [80] T. P. CHENG and L. F. LI, *Gauge Theory of Elementary Particle Physics*, Oxford University Press, 536, 1984.
- [81] G. SENJANOVIC, *Course on grand unification*, *Springer Proc. Phys.* **118**, 137 (2008).
B. BAJC, *Grand Unification and Proton Decay*, (2011), lecture notes from the 2011 ICTP Summer School on Particle Physics. <http://users.ictp.it/~smr2244/Bajc.pdf>.
- [82] P. NATH and P. FILEVIEZ PEREZ, *Proton stability in grand unified theories, in strings and in branes*, *Phys. Rept.* **441**, 191 (2007).
- [83] S. ANTUSCH and M. SPINRATH, *New GUT predictions for quark and lepton mass ratios confronted with phenomenology*, *Phys. Rev.* **D79**, 095004 (2009), arXiv: 0902.4644 [hep-ph].
- [84] R. FEGER and T. W. KEPHART, *LieART - A Mathematica Application for Lie Algebras and Representation Theory*, *Comput. Phys. Commun.* **192**, 166 (2015), arXiv: 1206.6379.
- [85] R. SLANSKY, *Group Theory for Unified Model Building*, *Phys. Rept.* **79**, 1 (1981).
- [86] M. E. MACHACEK and M. T. VAUGHN, *Two Loop Renormalization Group Equations in a General Quantum Field Theory. 1. Wave Function Renormalization*, *Nucl. Phys.* **B222**, 83 (1983).
- [87] H. GEORGI and C. JARLSKOG, *A New Lepton - Quark Mass Relation In A Unified Theory*, *Phys.Lett.* **B86**, 297 (1979).
- [88] J. C. PATI and A. SALAM, *Unified Lepton-Hadron Symmetry and a Gauge Theory of the Basic Interactions*, *Phys. Rev.* **D8**, 1240 (1973).
- [89] H. GEORGI, *The State of the Art – Gauge Theories*, *AIP Conf. Proc.* **23**, 575 (1975).
H. FRITZSCH and P. MINKOWSKI, *Unified Interactions of Leptons and Hadrons*, *Annals Phys.* **93**, 193 (1975).
- [90] S. M. BARR, *A New Symmetry Breaking Pattern for $SO(10)$ and Proton Decay*, *Phys. Lett.* **B112**, 219 (1982).
- [91] S. ANTUSCH and V. MAURER, *Running quark and lepton parameters at various scales*, *JHEP* **1311**, 115 (2013), arXiv: 1306.6879.
- [92] B. C. ALLANACH, S. F. KING, G. K. LEONTARIS, and S. LOLA, *Yukawa textures in string unified models with $SU(4) \times O(4)$ symmetry*, *Phys. Rev.* **D56**, 2632 (1997), arXiv: hep-ph/9610517.
- [93] S. ANTUSCH, S. F. KING, and M. SPINRATH, *GUT predictions for quark-lepton Yukawa coupling ratios with messenger masses from non-singlets*, *Phys. Rev.* **D89**, 055027 (2014), arXiv: 1311.0877.

- [94] S. J. GATES, M. T. GRISARU, M. ROCEK, and W. SIEGEL, *Superspace Or One Thousand and One Lessons in Supersymmetry*, *Front. Phys.* **58**, 1 (1983), arXiv: hep-th/0108200.
- [95] D. BAILIN and A. LOVE, *Supersymmetric Gauge Field Theory and String Theory*, Taylor & Francis, 322, 1994.
- [96] S. P. MARTIN, *A Supersymmetry primer*, *Adv. Ser. Direct. High Energy Phys* **18**, 1 (1998), arXiv: hep-ph/9709356.
- [97] M. DREES, R. GODBOLE, and P. ROY, *Theory and phenomenology of sparticles: An account of four-dimensional $N=1$ supersymmetry in high energy physics*, World Scientific Publishing, 555, 2004.
- [98] D. J. H. CHUNG, L. L. EVERETT, G. L. KANE, S. F. KING, J. D. LYKKEN, and L.-T. WANG, *The Soft supersymmetry breaking Lagrangian: Theory and applications*, *Phys. Rept.* **407**, 1 (2005), arXiv: hep-ph/0312378.
- [99] M. BERTOLINI, *Lectures on Supersymmetry*, (2015), SISSA lecture notes, <http://people.sissa.it/~bertmat/susycourse.pdf>.
- [100] J. WESS and B. ZUMINO, *Supergauge Transformations in Four-Dimensions*, *Nucl. Phys.* **B70**, 39 (1974).
- [101] J. WESS and B. ZUMINO, *Supergauge Invariant Extension of Quantum Electrodynamics*, *Nucl. Phys.* **B78**, 1 (1974).
- [102] A. SALAM and J. A. STRATHDEE, *Supergauge Transformations*, *Nucl. Phys.* **B76**, 477 (1974).
- [103] P. FAYET and J. ILIOPOULOS, *Spontaneously Broken Supergauge Symmetries and Goldstone Spinors*, *Phys. Lett.* **B51**, 461 (1974).
P. FAYET, *Higgs Model and Supersymmetry*, *Nuovo Cim.* **A31**, 626 (1976).
- [104] R. DELBOURGO, *Superfield Perturbation Theory and Renormalization*, *Nuovo Cim.* **A25**, 646 (1975).
A. SALAM and J. A. STRATHDEE, *Feynman Rules for Superfields*, *Nucl. Phys.* **B86**, 142 (1975).
K. FUJIKAWA and W. LANG, *Perturbation Calculations for the Scalar Multiplet in a Superfield Formulation*, *Nucl. Phys.* **B88**, 61 (1975).
M. T. GRISARU, W. SIEGEL, and M. ROCEK, *Improved Methods for Supergraphs*, *Nucl. Phys.* **B159**, 429 (1979).
- [105] S. ANTUSCH and M. RATZ, *Supergraph techniques and two loop beta functions for renormalizable and nonrenormalizable operators*, *JHEP* **0207**, 059 (2002), arXiv: hep-ph/0203027.

- [106] S. K. SONI and H. A. WELDON, *Analysis of the Supersymmetry Breaking Induced by $N=1$ Supergravity Theories*, *Phys. Lett.* **B126**, 215 (1983).
- [107] S. ANTUSCH, S. F. KING, and M. MALINSKY, *Third Family Corrections to Quark and Lepton Mixing in SUSY Models with non-Abelian Family Symmetry*, *JHEP* **0805**, 066 (2008), arXiv: 0712.3759.
- [108] S. ANTUSCH, S. F. KING, and M. MALINSKY, *Third Family Corrections to Tribimaximal Lepton Mixing and a New Sum Rule*, *Phys. Lett.* **B671**, 263 (2009), arXiv: 0711.4727.
S. ANTUSCH, S. F. KING, and M. MALINSKY, *Perturbative Estimates of Lepton Mixing Angles in Unified Models*, *Nucl. Phys.* **B820**, 32 (2009), arXiv: 0810.3863.
- [109] L. O'RAIFEARTAIGH, *Spontaneous Symmetry Breaking for Chiral Scalar Superfields*, *Nucl. Phys.* **B96**, 331 (1975).
- [110] S. FERRARA, L. GIRARDELLO, and F. PALUMBO, *A General Mass Formula in Broken Supersymmetry*, *Phys. Rev.* **D20**, 403 (1979).
- [111] A. SALAM and J. A. STRATHDEE, *On Goldstone Fermions*, *Phys. Lett.* **B49**, 465 (1974).
- [112] K. HARADA and N. SAKAI, *Softly Broken Supersymmetric Theories*, *Prog. Theor. Phys.* **67**, 1877 (1982).
- [113] D. M. CAPPER, *Explicit Symmetry Breaking in Supersymmetry Theories*, *J. Phys.* **G3**, 731 (1977).
L. GIRARDELLO and M. T. GRISARU, *Soft Breaking of Supersymmetry*, *Nucl. Phys.* **B194**, 65 (1982).
- [114] I. JACK and D. R. T. JONES, *Nonstandard soft supersymmetry breaking*, *Phys. Lett.* **B457**, 101 (1999), arXiv: hep-ph/9903365.
- [115] H. P. NILLES, *Dynamically Broken Supergravity and the Hierarchy Problem*, *Phys. Lett.* **B115**, 193 (1982).
H. P. NILLES, *Supergravity Generates Hierarchies*, *Nucl. Phys.* **B217**, 366 (1983).
- [116] S. DESER and B. ZUMINO, *Broken Supersymmetry and Supergravity*, *Phys. Rev. Lett.* **38**, 1433 (1977).
- [117] R. BARBIERI, S. FERRARA, and C. A. SAVOY, *Gauge Models with Spontaneously Broken Local Supersymmetry*, *Phys. Lett.* **B119**, 343 (1982).
A. H. CHAMSEDDINE, R. L. ARNOWITT, and P. NATH, *Locally Supersymmetric Grand Unification*, *Phys. Rev. Lett.* **49**, 970 (1982).
L. J. HALL, J. D. LYKKEN, and S. WEINBERG, *Supergravity as the Messenger of Supersymmetry Breaking*, *Phys. Rev.* **D27**, 2359 (1983).

- [118] M. DINE and A. E. NELSON, *Dynamical supersymmetry breaking at low-energies*, *Phys. Rev.* **D48**, 1277 (1993), arXiv: hep-ph/9303230.
M. DINE, A. E. NELSON, and Y. SHIRMAN, *Low-energy dynamical supersymmetry breaking simplified*, *Phys. Rev.* **D51**, 1362 (1995), arXiv: hep-ph/9408384.
M. DINE, A. E. NELSON, Y. NIR, and Y. SHIRMAN, *New tools for low-energy dynamical supersymmetry breaking*, *Phys. Rev.* **D53**, 2658 (1996), arXiv: hep-ph/9507378.
G. F. GIUDICE and R. RATTAZZI, *Theories with gauge mediated supersymmetry breaking*, *Phys. Rept.* **322**, 419 (1999), arXiv: hep-ph/9801271.
- [119] L. RANDALL and R. SUNDRUM, *Out of this world supersymmetry breaking*, *Nucl. Phys.* **B557**, 79 (1999), arXiv: hep-th/9810155.
G. F. GIUDICE, M. A. LUTY, H. MURAYAMA, and R. RATTAZZI, *Gaugino mass without singlets*, *JHEP* **9812**, 027 (1998), arXiv: hep-ph/9810442.
T. GHERGHETTA, G. F. GIUDICE, and J. D. WELLS, *Phenomenological consequences of supersymmetry with anomaly induced masses*, *Nucl. Phys.* **B559**, 27 (1999), arXiv: hep-ph/9904378.
- [120] H. P. NILLES, *Supersymmetry, Supergravity and Particle Physics*, *Phys. Rept.* **110**, 1 (1984).
H. E. HABER and G. L. KANE, *The Search for Supersymmetry: Probing Physics Beyond the Standard Model*, *Phys. Rept.* **117**, 75 (1985).
R. BARBIERI, *Looking Beyond the Standard Model: The Supersymmetric Option*, *Riv. Nuovo Cim.* **11N4**, 1 (1988).
- [121] A. SALAM and J. A. STRATHDEE, *Supersymmetry and Fermion Number Conservation*, *Nucl. Phys.* **B87**, 85 (1975).
P. FAYET, *Supergauge Invariant Extension of the Higgs Mechanism and a Model for the electron and Its Neutrino*, *Nucl. Phys.* **B90**, 104 (1975).
G. R. FARRAR and P. FAYET, *Phenomenology of the Production, Decay, and Detection of New Hadronic States Associated with Supersymmetry*, *Phys. Lett.* **B76**, 575 (1978).
- [122] S. WEINBERG, *Supersymmetry at Ordinary Energies. 1. Masses and Conservation Laws*, *Phys. Rev.* **D26**, 287 (1982).
N. SAKAI and T. YANAGIDA, *Proton Decay in a Class of Supersymmetric Grand Unified Models*, *Nucl. Phys.* **B197**, 533 (1982).
- [123] B. C. ALLANACH et al., *SUSY Les Houches Accord 2*, *Comput. Phys. Commun.* **180**, 8 (2009), arXiv: 0801.0045.

- [124] S. DIMOPOULOS and S. D. THOMAS, *Dynamical relaxation of the supersymmetric CP violating phases*, *Nucl. Phys.* **B465**, 23 (1996), arXiv: hep-ph/9510220.
- [125] M. FRANK, T. HAHN, S. HEINEMEYER, W. HOLLIK, H. RZEHAK, and G. WEIGLEIN, *The Higgs Boson Masses and Mixings of the Complex MSSM in the Feynman-Diagrammatic Approach*, *JHEP* **0702**, 047 (2007), arXiv: hep-ph/0611326.
- [126] H. E. HABER and R. HEMPFLING, *Can the mass of the lightest Higgs boson of the minimal supersymmetric model be larger than $m(Z)$?*, *Phys. Rev. Lett.* **66**, 1815 (1991).
- Y. OKADA, M. YAMAGUCHI, and T. YANAGIDA, *Upper bound of the lightest Higgs boson mass in the minimal supersymmetric standard model*, *Prog. Theor. Phys.* **85**, 1 (1991).
- J. R. ELLIS, G. RIDOLFI, and F. ZWIRNER, *Radiative corrections to the masses of supersymmetric Higgs bosons*, *Phys. Lett.* **B257**, 83 (1991).
- [127] S. HEINEMEYER, W. HOLLIK, and G. WEIGLEIN, *FeynHiggs: A Program for the calculation of the masses of the neutral CP even Higgs bosons in the MSSM*, *Comput. Phys. Commun.* **124**, 76 (2000), arXiv: hep-ph/9812320.
- S. HEINEMEYER, W. HOLLIK, and G. WEIGLEIN, *The Masses of the neutral CP - even Higgs bosons in the MSSM: Accurate analysis at the two loop level*, *Eur. Phys. J.* **C9**, 343 (1999), arXiv: hep-ph/9812472.
- G. DEGRASSI, S. HEINEMEYER, W. HOLLIK, P. SLAVICH, and G. WEIGLEIN, *Towards high precision predictions for the MSSM Higgs sector*, *Eur. Phys. J.* **C28**, 133 (2003), arXiv: hep-ph/0212020.
- T. HAHN, S. HEINEMEYER, W. HOLLIK, H. RZEHAK, and G. WEIGLEIN, *High-Precision Predictions for the Light CP-Even Higgs Boson Mass of the Minimal Supersymmetric Standard Model*, *Phys. Rev. Lett.* **112**, 141801 (2014), arXiv: 1312.4937.
- [128] S. BOROWKA, T. HAHN, S. HEINEMEYER, G. HEINRICH, and W. HOLLIK, *Momentum-dependent two-loop QCD corrections to the neutral Higgs-boson masses in the MSSM*, *Eur. Phys. J.* **C74**, 2994 (2014), arXiv: 1404.7074.
- [129] W. HOLLIK and S. PASSEHR, *Higgs boson masses and mixings in the complex MSSM with two-loop top-Yukawa-coupling corrections*, *JHEP* **1410**, 171 (2014), arXiv: 1409.1687.
- W. HOLLIK and S. PASSEHR, *Two-loop top-Yukawa-coupling corrections to the charged Higgs-boson mass in the MSSM*, *Eur. Phys. J.* **C75**, 336 (2015), arXiv: 1502.02394.
- [130] S. P. MARTIN, *Complete two loop effective potential approximation to the lightest Higgs scalar boson mass in supersymmetry*, *Phys. Rev.* **D67**, 095012 (2003), arXiv: hep-ph/0211366.

- [131] L. J. HALL, R. RATTAZZI, and U. SARID, *The Top quark mass in supersymmetric $SO(10)$ unification*, *Phys. Rev.* **D50**, 7048 (1994), arXiv: hep-ph/9306309.
M. CARENA, M. OLECHOWSKI, S. POKORSKI, and C. E. M. WAGNER, *Electroweak symmetry breaking and bottom - top Yukawa unification*, *Nucl. Phys.* **B426**, 269 (1994), arXiv: hep-ph/9402253.
R. HEMPFLING, *Yukawa coupling unification with supersymmetric threshold corrections*, *Phys. Rev.* **D49**, 6168 (1994).
- [132] T. BLAZEK, S. RABY, and S. POKORSKI, *Finite supersymmetric threshold corrections to CKM matrix elements in the large $\tan \beta$ regime*, *Phys. Rev.* **D52**, 4151 (1995), arXiv: hep-ph/9504364.
- [133] S. ANTUSCH and M. SPINRATH, *Quark and lepton masses at the GUT scale including SUSY threshold corrections*, *Phys. Rev.* **D78**, 075020 (2008), arXiv: 0804.0717.
- [134] J. A. CASAS, A. LLEYDA, and C. MUNOZ, *Strong constraints on the parameter space of the MSSM from charge and color breaking minima*, *Nucl. Phys.* **B471**, 3 (1996), arXiv: hep-ph/9507294.
- [135] J. A. CASAS and S. DIMOPOULOS, *Stability bounds on flavor violating trilinear soft terms in the MSSM*, *Phys. Lett.* **B387**, 107 (1996), arXiv: hep-ph/9606237.
- [136] S. P. MARTIN and M. T. VAUGHN, *Two loop renormalization group equations for soft supersymmetry breaking couplings*, *Phys. Rev.* **D50**, 2282 (1994), [Erratum: *Phys. Rev.* **D78**, 039903 (2008)], arXiv: hep-ph/9311340.
- [137] R. BARBIERI and L. J. HALL, *Grand unification and the supersymmetric threshold*, *Phys. Rev. Lett.* **68**, 752 (1992).
Y. YAMADA, *SUSY and GUT threshold effects in SUSY $SU(5)$ models*, *Z. Phys.* **C60**, 83 (1993).
- [138] S. DIMOPOULOS and H. GEORGI, *Softly Broken Supersymmetry and $SU(5)$* , *Nucl. Phys.* **B193**, 150 (1981).
- [139] S. DIMOPOULOS, S. RABY, and F. WILCZEK, *Proton Decay in Supersymmetric Models*, *Phys. Lett.* **B112**, 133 (1982).
- [140] P. NATH, A. H. CHAMSEDDINE, and R. L. ARNOWITT, *Nucleon Decay in Supergravity Unified Theories*, *Phys. Rev.* **D32**, 2348 (1985).
- [141] J. R. ELLIS, D. V. NANOPOULOS, and S. RUDAZ, *A phenomenological comparison of conventional and supersymmetric guts*, *Nucl. Phys.* **B202**, 43 (1982).
R. L. ARNOWITT, A. H. CHAMSEDDINE, and P. NATH, *Nucleon decay branching ratios in supergravity $SU(5)$ GUTs*, *Phys. Lett.* **B156**, 215 (1985).

- [142] J. HISANO, H. MURAYAMA, and T. YANAGIDA, *Nucleon decay in the minimal supersymmetric SU(5) grand unification*, *Nucl. Phys.* **B402**, 46 (1993), arXiv: hep-ph/9207279.
- [143] T. GOTO and T. NIHEI, *Effect of RRRR dimension five operator on the proton decay in the minimal SU(5) SUGRA GUT model*, *Phys. Rev.* **D59**, 115009 (1999), arXiv: hep-ph/9808255.
- [144] A. MASIERO, D. V. NANOPOULOS, K. TAMVAKIS, and T. YANAGIDA, *Naturally Massless Higgs Doublets in Supersymmetric SU(5)*, *Phys. Lett.* **B115**, 380 (1982).
B. GRINSTEIN, *A Supersymmetric SU(5) Gauge Theory with No Gauge Hierarchy Problem*, *Nucl. Phys.* **B206**, 387 (1982).
- [145] H. MURAYAMA and A. PIERCE, *Not even decoupling can save minimal supersymmetric SU(5)*, *Phys. Rev.* **D65**, 055009 (2002), arXiv: hep-ph/0108104.
- [146] B. BAJC, P. FILEVIEZ PEREZ, and G. SENJANOVIC, *Minimal supersymmetric SU(5) theory and proton decay: Where do we stand?*, in *Beyond the desert: Accelerator, non-accelerator and space approaches into the next millennium. Proceedings, 3rd International Conference on particle physics beyond the standard model, Oulu, Finland, June 2-7, 2002*, pp. 131–139, 2002, arXiv: hep-ph/0210374.
- [147] T. SCHWETZ, M. TORTOLA, and J. W. F. VALLE, *Where we are on θ_{13} : addendum to 'Global neutrino data and recent reactor fluxes: status of three-flavour oscillation parameters'*, *New J.Phys.* **13**, 109401 (2011), arXiv: 1108.1376 [hep-ph].
- [148] S. ANTUSCH and V. MAURER, *Large neutrino mixing angle θ_{13}^{MNS} and quark-lepton mass ratios in unified flavour models*, *Phys.Rev.* **D84**, 117301 (2011), arXiv: 1107.3728 [hep-ph].
- [149] D. MARZOCCA, S. T. PETCOV, A. ROMANINO, and M. SPINRATH, *Sizeable θ_{13} from the Charged Lepton Sector in SU(5), (Tri-)Bimaximal Neutrino Mixing and Dirac CP Violation*, *JHEP* **1111**, 009 (2011), arXiv: 1108.0614 [hep-ph].
- [150] G. L. FOGLI, A. M. E. LISI, A. PALAZZO, and A. M. ROTUNNO, *Evidence of $\theta_{13} > 0$ from global neutrino data analysis*, *Phys.Rev.* **D84**, 053007 (2011), arXiv: 1106.6028 [hep-ph].
- [151] P. ADAMSON et al., *First measurement of muon-neutrino disappearance in NOvA*, (2016), arXiv: 1601.05037.
- [152] A. DATTA, L. EVERETT, and P. RAMOND, *Cabibbo haze in lepton mixing*, *Phys.Lett.* **B620**, 42 (2005), arXiv: hep-ph/0503222.
L. L. EVERETT, *Viewing lepton mixing through the Cabibbo haze*, *Phys.Rev.* **D73**, 013011 (2006), arXiv: hep-ph/0510256.

- [153] F. VISSANI, *Large mixing, family structure, and dominant block in the neutrino mass matrix*, *JHEP* **9811**, 025 (1998), arXiv: hep-ph/9810435.
F. VISSANI, *Expected properties of massive neutrinos for mass matrices with a dominant block and random coefficients order unity*, *Phys.Lett.* **B508**, 79 (2001), arXiv: hep-ph/0102236.
P. RAMOND, *Chasing CHOOZ*, *Int.J.Mod.Phys.* **A20**, 1234 (2005), arXiv: hep-ph/0405176.
Y. L. WU, *SU(3) Gauge Family Symmetry and Prediction for the Lepton-Flavor Mixing and Neutrino Masses with Maximal Spontaneous CP Violation*, *Phys.Lett.* **B714**, 286 (2012), arXiv: 1203.2382 [hep-ph].
- [154] A. YU. SMIRNOV, Neutrinos: '...Annus mirabilis', in *Proceedings of the 2nd NO-VE International Workshop on Neutrino Oscillations*, pp. 1–21, 2004, arXiv: hep-ph/0402264.
- [155] H. MINAKATA and A. Y. SMIRNOV, *Neutrino mixing and quark-lepton complementarity*, *Phys.Rev.* **D70**, 073009 (2004), arXiv: hep-ph/0405088.
- [156] S. F. KING, *Tri-bimaximal-Cabibbo Mixing*, *Phys. Lett.* **B718**, 136 (2012).
- [157] S. ANTUSCH, S. F. KING, M. MALINSKY, and M. SPINRATH, *Quark mixing sum rules and the right unitarity triangle*, *Phys.Rev.* **D81**, 033008 (2010), arXiv: 0910.5127 [hep-ph].
- [158] V. K. M. MAURER, *Insights into Grand Unified Theories from Current Experimental Data*, PhD thesis, Basel U., 2015, http://edoc.unibas.ch/diss/DissB_11268.
- [159] R. GATTO, G. SARTORI, and M. TONIN, *Weak Selfmasses, Cabibbo Angle, and Broken SU(2) × SU(2)*, *Phys. Lett.* **B28**, 128 (1968).
N. CABIBBO and L. MAIANI, *Dynamical interrelation of weak, electromagnetic and strong interactions and the value of theta*, *Phys. Lett.* **B28**, 131 (1968).
- [160] S. WEINBERG, *The Problem of Mass*, *Trans. New York Acad. Sci.* **38**, 185 (1977).
F. WILCZEK and A. ZEE, *Discrete Flavor Symmetries and a Formula for the Cabibbo Angle*, *Phys. Lett.* **B70**, 418 (1977), [Erratum: *Phys. Lett.* 72B,504(1978)].
H. FRITZSCH, *Calculating the Cabibbo Angle*, *Phys. Lett.* **B70**, 436 (1977).
- [161] L. J. HALL and A. RASIN, *On the generality of certain predictions for quark mixing*, *Phys. Lett.* **B315**, 164 (1993), arXiv: hep-ph/9303303.
- [162] S. ANTUSCH, J. KERSTEN, M. LINDNER, and M. RATZ, *Running neutrino masses, mixings and CP phases: Analytical results and phenomenological consequences*, *Nucl.Phys.* **B674**, 401 (2003), arXiv: hep-ph/0305273.

- [163] S. ANTUSCH, J. KERSTEN, M. LINDNER, M. RATZ, and M. A. SCHMIDT, *Running neutrino mass parameters in see-saw scenarios*, *JHEP* **0503**, 024 (2005), arXiv: hep-ph/0501272.
- [164] S. BOUDJEMAA and S. F. KING, *Deviations from Tri-bimaximal Mixing: Charged Lepton Corrections and Renormalization Group Running*, *Phys.Rev.* **D 79**, 033001 (2009), arXiv: 0808.2782 [hep-ph].
- [165] S. ANTUSCH, S. F. KING, C. LUHN, and M. SPINRATH, *Right unitarity triangles and tri-bimaximal mixing from discrete symmetries and unification*, *Nucl.Phys.* **B850**, 477 (2011), arXiv: 1103.5930 [hep-ph].
- [166] F. FERUGLIO, C. HAGEDORN, and R. ZIEGLER, *Lepton Mixing Parameters from Discrete and CP Symmetries*, *JHEP* **1307**, 027 (2013), arXiv: 1211.5560.
M. HOLTHAUSEN, M. LINDNER, and M. A. SCHMIDT, *CP and Discrete Flavour Symmetries*, *JHEP* **1304**, 122 (2013), arXiv: 1211.6953.
- [167] Z.-Z. XING, H. ZHANG, and S. ZHOU, *Updated Values of Running Quark and Lepton Masses*, *Phys. Rev.* **D77**, 113016 (2008), arXiv: 0712.1419.
- [168] M. BONA et al., *The 2004 UTfit collaboration report on the status of the unitarity triangle in the standard model*, *JHEP* **0507**, 028 (2005), arXiv: hep-ph/0501199, Winter 2013 fit results available at <http://www.utfit.org/UTfit/ResultsWinter2013PreMoriond>.
- [169] M. C. GONZALEZ-GARCIA, M. MALTONI, J. SALVADO, and T. SCHWETZ, *Global fit to three neutrino mixing: critical look at present precision*, *JHEP* **1212**, 123 (2012), arXiv:1209.3023, NuFIT 1.1 (2013) available at www.nu-fit.org.
- [170] J. H. CHOI et al., *Observation of Energy and Baseline Dependent Reactor Antineutrino Disappearance in the RENO Experiment*, (2015), arXiv: 1511.05849.
- [171] F. P. AN et al., *New Measurement of Antineutrino Oscillation with the Full Detector Configuration at Daya Bay*, *Phys. Rev. Lett.* **115**, 111802 (2015), arXiv: 1505.03456.
- [172] C. H. ALBRIGHT, *Overview of Neutrino Mixing Models and Ways to Differentiate among Them*, in *Proceedings, 13th International Workshop on Neutrino telescopes*, pp. 91–109, 2009, arXiv: 0905.0146.
- [173] R. BARBIERI, L. J. HALL, D. TUCKER-SMITH, A. STRUMIA, and N. WEINER, *Oscillations of solar and atmospheric neutrinos*, *JHEP* **9812**, 017 (1998), arXiv: hep-ph/9807235.
- [174] S. ANTUSCH, S. F. KING, and R. N. MOHAPATRA, *Quark-lepton complementarity in unified theories*, *Phys. Lett.* **B618**, 150 (2005), arXiv: hep-ph/0504007.

- [175] Z. TAVARTKILADZE, *Three Family $SU(5)$ GUT and Inverted Neutrino Mass Hierarchy*, *Phys. Rev.* **D87**, 075026 (2013), arXiv: 1303.1211.
- [176] A. POCAR [ON BEHALF OF THE EXO COLLABORATION], *Searching for neutrinoless double beta decay with EXO-200 and nEXO*, *Nuclear and Particle Physics Proceedings* **265 - 266**, 42 (2015), Proceedings of the 16th International Workshop on Neutrino Telescopes (Neutel 2015).
- [177] V. ALENKOV et al., *Technical Design Report for the AMoRE $0\nu\beta\beta$ Decay Search Experiment*, (2015), arXiv: 1512.05957.
- [178] H. MINAKATA, H. NUNOKAWA, W. J. C. TEVES, and R. ZUKANOVICH FUNCHAL, *Reactor measurement of θ_{12} : Principles, accuracies and physics potentials*, *Phys. Rev.* **D71**, 013005 (2005), arXiv: hep-ph/0407326.
- [179] J. HISANO, T. MOROI, K. TOBE, and T. YANAGIDA, *Suppression of proton decay in the missing partner model for supersymmetric $SU(5)$ GUT*, *Phys. Lett.* **B342**, 138 (1995), arXiv: hep-ph/9406417.
- [180] Y. KAWAMURA, *Triplet doublet splitting, proton stability and extra dimension*, *Prog. Theor. Phys.* **105**, 999 (2001), arXiv: hep-ph/0012125.
- [181] Z. BEREZHIANI and Z. TAVARTKILADZE, *Anomalous $U(1)$ symmetry and missing doublet $SU(5)$ model*, *Phys. Lett.* **B396**, 150 (1997), arXiv: hep-ph/9611277.
- [182] H. MURAYAMA, Y. OKADA, and T. YANAGIDA, *The Georgi-Jarlskog mass relation in a supersymmetric grand unified model*, *Prog. Theor. Phys.* **88**, 791 (1992).
- [183] D.-X. ZHANG and J.-H. ZHENG, *A Missing Partner Model With 24-plet Breaking $SU(5)$* , *JHEP* **1212**, 087 (2012), arXiv: 1212.5852.
- [184] H.-S. TSAO, *$M_W = M_Z \cos \theta_W$ in $SU(5)$* , *Phys. Rev.* **D24**, 791 (1981).
- [185] H. GEORGI, *An almost realistic gauge hierarchy*, *Phys. Lett.* **B108**, 283 (1982).
- [186] M. FALLBACHER, M. RATZ, and P. K. S. VAUDREVANGE, *No-go theorems for R symmetries in four-dimensional GUTs*, *Phys. Lett.* **B705**, 503 (2011), arXiv: 1109.4797.
- [187] S. ANTUSCH, L. CALIBBI, V. MAURER, and M. SPINRATH, *From Flavour to SUSY Flavour Models*, *Nucl. Phys.* **B852**, 108 (2011), arXiv: 1104.3040.
- [188] S. F. KING, *A model of quark and lepton mixing*, *JHEP* **1401**, 119 (2014), arXiv: 1311.3295.

- [189] D. EMMANUEL-COSTA and S. WIESENFELDT, *Proton decay in a consistent supersymmetric $SU(5)$ GUT model*, *Nucl. Phys.* **B661**, 62 (2003), arXiv: hep-ph/0302272.
S. WIESENFELDT, *Proton decay in supersymmetric GUT models*, *Mod. Phys. Lett.* **A19**, 2155 (2004), arXiv: hep-ph/0407173.
- [190] P. NATH, *Hierarchies and textures in supergravity unification*, *Phys. Rev. Lett.* **76**, 2218 (1996), arXiv: hep-ph/9512415.
- [191] V. LUCAS and S. RABY, *Nucleon decay in a realistic $SO(10)$ SUSY GUT*, *Phys. Rev.* **D55**, 6986 (1997), arXiv: hep-ph/9610293.
- [192] L. E. IBANEZ and G. G. ROSS, *Low-Energy Predictions in Supersymmetric Grand Unified Theories*, *Phys. Lett.* **B105**, 439 (1981).
M. B. EINHORN and D. R. T. JONES, *The Weak Mixing Angle and Unification Mass in Supersymmetric $SU(5)$* , *Nucl. Phys.* **B196**, 475 (1982).
- [193] G. AAD et al., *Observation of a new particle in the search for the Standard Model Higgs boson with the ATLAS detector at the LHC*, *Phys. Lett.* **B716**, 1 (2012), arXiv: 1207.7214.
S. CHATRCHYAN et al., *Observation of a new boson at a mass of 125 GeV with the CMS experiment at the LHC*, *Phys. Lett.* **B716**, 30 (2012), arXiv: 1207.7235.
- [194] P. Z. SKANDS et al., *SUSY Les Houches accord: Interfacing SUSY spectrum calculators, decay packages, and event generators*, *JHEP* **0407**, 036 (2004), arXiv: hep-ph/0311123.
- [195] H. BAER, F. E. PAIGE, S. D. PROTOPODESCU, and X. TATA, *Simulating Supersymmetry with ISAJET 7.0 / ISASUSY 1.0*, in *Workshop on Physics at Current Accelerators and the Supercollider Argonne, Illinois, June 2-5, 1993*, 1993, arXiv: hep-ph/9305342.
- [196] B. C. ALLANACH, *SOFTSUSY: a program for calculating supersymmetric spectra*, *Comput. Phys. Commun.* **143**, 305 (2002), arXiv: hep-ph/0104145.
- [197] A. DJOUADI, J.-L. KNEUR, and G. MOULTAKA, *SuSpect: A Fortran code for the supersymmetric and Higgs particle spectrum in the MSSM*, *Comput. Phys. Commun.* **176**, 426 (2007), arXiv: hep-ph/0211331.
- [198] W. POROD, *SPheno, a program for calculating supersymmetric spectra, SUSY particle decays and SUSY particle production at $e^+ e^-$ colliders*, *Comput. Phys. Commun.* **153**, 275 (2003), arXiv: hep-ph/0301101.
- [199] A. DJOUADI, *SUSY calculation tools*, in *Supersymmetry and unification of fundamental interactions. Proceedings of 10th International Conference SUSY'02*, p. 227, 2002, arXiv: hep-ph/0211357.

- [200] S. ANTUSCH and E. CAZZATO, *One-Loop Right-Handed Neutrino Threshold Corrections for Two-Loop Running in Supersymmetric Type I Seesaw Models*, *JHEP* **1512**, 066 (2015), arXiv: 1509.05604.
- [201] D. M. PIERCE, J. A. BAGGER, K. T. MATCHEV, and R.-J. ZHANG, *Precision corrections in the minimal supersymmetric standard model*, *Nucl. Phys.* **B491**, 3 (1997), arXiv: hep-ph/9606211.
- [202] N. ARKANI-HAMED and S. DIMOPOULOS, *Supersymmetric unification without low energy supersymmetry and signatures for fine-tuning at the LHC*, *JHEP* **0506**, 073 (2005), arXiv: hep-th/0405159.
G. F. GIUDICE and A. ROMANINO, *Split supersymmetry*, *Nucl. Phys.* **B699**, 65 (2004), [Erratum: *Nucl. Phys.*B706,65(2005)], arXiv: hep-ph/0406088.
- [203] J. GEHRLEIN, J. P. OPPERMANN, D. SCHÄFER, and M. SPINRATH, *An $SU(5) \times A_5$ golden ratio flavour model*, *Nucl. Phys.* **B890**, 539 (2014), arXiv: 1410.2057.
- [204] A. MERONI, S. T. PETCOV, and M. SPINRATH, *A SUSY $SU(5) \times T'$ Unified Model of Flavour with large θ_{13}* , *Phys. Rev.* **D86**, 113003 (2012), arXiv: 1205.5241.
- [205] H. BAHL, *Update on large-log resummation in FeynHiggs*, (2016), workshop “Precision SUSY Higgs Mass Calculation Initiative”, Heidelberg, <https://sites.google.com/site/kutsmh/home>.
J. PARDO VEGA and G. VILLADORO, *Update on the EFT calculation of the MSSM Higgs mass*, (2016), workshop “Precision SUSY Higgs Mass Calculation Initiative”, Heidelberg, <https://sites.google.com/site/kutsmh/home>.
- [206] G. JUNGMAN, M. KAMIONKOWSKI, and K. GRIEST, *Supersymmetric dark matter*, *Phys. Rept.* **267**, 195 (1996), arXiv: hep-ph/9506380.
- [207] S. R. COLEMAN, *The Fate of the False Vacuum. 1. Semiclassical Theory*, *Phys. Rev.* **D15**, 2929 (1977), [Erratum: *Phys. Rev.*D16,1248(1977)].
C. G. CALLAN, JR. and S. R. COLEMAN, *The Fate of the False Vacuum. 2. First Quantum Corrections*, *Phys. Rev.* **D16**, 1762 (1977).
- [208] I. DASGUPTA, *Estimating vacuum tunneling rates*, *Phys. Lett.* **B394**, 116 (1997), arXiv: hep-ph/9610403.
- [209] B. BAJC, S. LAVIGNAC, and T. MEDE, *Resurrecting the minimal renormalizable supersymmetric $SU(5)$ model*, *JHEP* **1601**, 044 (2016), arXiv: 1509.06680.
- [210] U. SARID, *Tools for tunneling*, *Phys. Rev.* **D58**, 085017 (1998), arXiv: hep-ph/9804308.

- [211] O. BUCHMUELLER, M. CITRON, J. ELLIS, S. GUHA, J. MARROUCHE, K. A. OLIVE, K. DE VRIES, and J. ZHENG, *Collider Interplay for Supersymmetry, Higgs and Dark Matter*, *Eur. Phys. J.* **C75**, 469 (2015), arXiv: 1505.04702.
CEPC-SPPC STUDY GROUP, *CEPC-SPPC Preliminary Conceptual Design Report. 1. Physics and Detector*, (2015), IHEP-CEPC-DR-2015-01, http://cepc.ihep.ac.cn/preCDR/main_preCDR.pdf.
- [212] H. GEORGI, *Lie algebras in particle physics*, Frontiers in Physics, Perseus Books, 320, 1999.
- [213] H. ISHIMORI, T. KOBAYASHI, H. OHKI, Y. SHIMIZU, H. OKADA, and M. TANIMOTO, *Non-Abelian Discrete Symmetries in Particle Physics*, *Prog. Theor. Phys. Suppl.* **183**, 1 (2010), arXiv: 1003.3552.
- [214] P. RAMOND, *Group theory: A physicist's survey*, Cambridge University Press, 310, 2010.
- [215] G. ECKER, W. GRIMUS, and H. NEUFELD, *Spontaneous CP Violation in Left-right Symmetric Gauge Theories*, *Nucl. Phys.* **B247**, 70 (1984).
G. ECKER, W. GRIMUS, and H. NEUFELD, *A Standard Form for Generalized CP Transformations*, *J. Phys.* **A20**, L807 (1987).
H. NEUFELD, W. GRIMUS, and G. ECKER, *Generalized CP Invariance, Neutral Flavor Conservation and the Structure of the Mixing Matrix*, *Int. J. Mod. Phys.* **A3**, 603 (1988).
- [216] M.-C. CHEN, M. FALLBACHER, K. T. MAHANTHAPPA, M. RATZ, and A. TRAUTNER, *CP Violation from Finite Groups*, *Nucl. Phys.* **B883**, 267 (2014), arXiv: 1402.0507.
- [217] B. WALSH, *Markov Chain Monte Carlo and Gibbs Sampling*, 2004.
P. LAM, *MCMC Methods: Gibbs Sampling and the Metropolis-Hastings Algorithm*, (2008), lecture notes, http://www.people.fas.harvard.edu/~plam/teaching/methods/mcmc/mcmc_print.pdf.
P. LAM, *Convergence Diagnostics*, (2008), lecture notes, http://www.people.fas.harvard.edu/~plam/teaching/methods/convergence/convergence_print.pdf.
- [218] N. METROPOLIS and S. ULAM, *The Monte Carlo method*, *Journal of the American statistical association* **44**, 335 (1949).
N. METROPOLIS, A. W. ROSENBLUTH, M. N. ROSENBLUTH, A. H. TELLER, and E. TELLER, *Equation of state calculations by fast computing machines*, *The journal of chemical physics* **21**, 1087 (1953).
- [219] S. P. BROOKS and A. GELMAN, *General methods for monitoring convergence of iterative simulations*, *Journal of computational and graphical statistics* **7**, 434 (1998).

- [220] G. 'T HOOFT and M. J. G. VELTMAN, *Scalar One Loop Integrals*, *Nucl. Phys.* **B153**, 365 (1979).

Curriculum Vitae

Name Constantin Alexander Sluka

Date of birth 10 October 1987

Place of birth Oberndorf, Austria

Nationality Austrian

Address Davidsbodenstrasse 42, CH-4056 Basel, Switzerland

Telephone +41 (0)78 842 18 96

E-Mail Constantin.Sluka@googlemail.com



Education

April 2012 - May 2016

PhD in Theoretical Physics
Universität Basel, Switzerland

October 2009 - February 2012

Master of Science in Theoretical und Mathematical Physics
passed with high distinction (final grade 1.2)
Elite Graduate Program of the Elite Network of Bavaria
Ludwig-Maximilians-Universität München and
Technische Universität München, Germany

October 2006 - October 2009

Bachelor of Science in Physics, average grade 1.25
Leopold-Franzens-Universität Innsbruck, Austria

June 2006

Matura
passed with high distinction (average grade 1.0)
Bundesrealgymnasium Salzburg, Austria

September 1994 - July 1998

Volksschule Elsbethen, Austria

Awards and Recognitions

2015 Participant of the 65th Lindau Nobel Laureate Meeting

2014 Finalist of the Swiss final of FameLab (international science communication competition)

2012 Award for Best Teaching Assistance of the Physics Department's student's council

2007-2009 Merit scholarships of the Leopold-Franzens-Universität Innsbruck

Research Experience

July & August 2009

Summer student at CERN, ATLAS Data Processing Group
CERN, Geneva, Switzerland

July & August 2008

Research internship at the Institute for Astro- and Particle Physics
Leopold-Franzens-Universität Innsbruck, Austria

July - September 2007

Research internship at the Institute for Biomedical Ageing Research
Austrian Academy of Science, Innsbruck, Austria

Professional Training

10 June - 22 June 2013

ICTP Summer School on Particle Physics
ICTP, Trieste, Italy

8 August - 11 August 2012

PreSUSY Summer School
Peking University, Beijing, China

6 June - 17 June 2011

ICTP Summer School on Particle Physics
ICTP, Trieste, Italy

27 February - 3 March 2010

Schladming Winter School on Theoretical Physics "Masses and Constants"
Karl-Franzens-Universität Graz, Schladming, Austria

1 July - 7 August 2009

CERN Summer Student lectures
CERN, Geneva, Switzerland

Public Outreach

Science Slam contributions

Public Outreach talks at Science Slam competitions (in German)
30 April & 5 September 2015

How unlikely is a doomsday catastrophe?

Public Outreach talk on safety of particle physics experiments
29 April 2015

Universität Basel Kids@Science Week 2015

Introducing the importance and aims of Theoretical Physics to 18 pupils aged 10-11.
Preparation of Mathematica Notebook for the pupils to analyse their own data.
January 2015

An Introduction to Theoretical Particle Physics

Public Outreach talk presented at CERN
attended by physics students of the University of Innsbruck on an excursion
25 September 2014

FameLab Switzerland 2014

Finalist of the Swiss heat of the international science communication competition
FameLab

Assistant at the open nights of astronomy

Winter term 2008/09 & Summer term 2009
Leopold-Franzens-Universität Innsbruck, Austria

List of talks

10 July 2014

Flavour GUT models with $\theta_{13}^{PMNS} = \theta_C/\sqrt{2}$, Sinergia Swiss neutrino strategy meeting, University of Bern, Switzerland

29 May 2014

Towards predictive flavour models in SUSY SU(5) GUTs with doublet-triplet splitting, 17. International Conference From the Planck Scale to the Electroweak Scale (Planck 2014), Institut des Cordeliers, Paris, France

5 September 2013

Flavour GUT models with $\theta_{13}^{PMNS} = \theta_C/\sqrt{2}$, Joint annual meeting of the Austrian and Swiss Physical Societies, Johannes Kepler University Linz, Austria

2 July 2013

An inverse neutrino mass hierarchy in an SU(5) \times A₄ GUT, Third Workshop on Flavor Symmetries (FLASY13), Niigata University, Japan

14 August 2012

GUT relations and the lepton mixing matrix, 20. International Conference on Supersymmetry and Unification of Fundamental Interactions (SUSY 2012), Peking University, China

List of publications

- S. Antusch and C. Sluka, *Testable SUSY spectra from GUTs at a 100 TeV pp collider*, <http://arxiv.org/abs/1604.00212>
- S. Antusch and C. Sluka, *Predicting the Sparticle Spectrum from GUTs via SUSY Threshold Corrections with SusyTC*, <http://arxiv.org/abs/1512.06727>
- S. Antusch, I. d. M. Varzielas, V. Maurer, C. Sluka, and M. Spinrath, *Towards predictive flavour models in SUSY SU(5) GUTs with doublet-triplet splitting*, JHEP 1409 (2014) 141, <http://arxiv.org/abs/1405.6962>
- S. Antusch, C. Gross, V. Maurer, and C. Sluka, *Inverse neutrino mass hierarchy in a flavour GUT model*, Nucl. Phys. B 879 (2014) 19, <http://arxiv.org/abs/1306.3984>
- S. Antusch, C. Gross, V. Maurer, and C. Sluka, *A flavour GUT model with $\theta_{13}^{PMNS} = \theta_C/\sqrt{2}$* , Nucl. Phys. B 877 (2013) 772, <http://arxiv.org/abs/1305.6612>
- S. Antusch, C. Gross, V. Maurer, and C. Sluka, *$\theta_{13}^{PMNS} = \theta_C/\sqrt{2}$ from GUTs*, Nucl. Phys. B 866 (2013) 255, <http://arxiv.org/abs/1205.1051>
- M. Flory, R.C. Helling, and C. Sluka, *How I Learned to Stop Worrying and Love QFT*. <http://arxiv.org/abs/1201.2714>
- W. Kapferer, C. Sluka, S. Schindler, C. Ferrari, and B. Ziegler, *The effect of ram pressure on the star formation, mass distribution and morphology of galaxies*, Astron. Astrophys. 499 (2009) 87, <http://arxiv.org/abs/0903.3818>